Final Project Report: Marine Species Density Data Gap Assessments and Update for the AFTT Study Area, 2017-2018 (Opt. Year 2)

Cooperative Agreement Number N62470-15-2-8003

Jason J. Roberts, Laura Mannocci, Robert S. Schick, and Patrick N. Halpin

Marine Geospatial Ecology Lab (MGEL), Duke University

Document Version 1.2 – 2018-09-21

This document should be cited:

Roberts JJ, Mannocci L, Schick RS, Halpin PN (2018) Final Project Report: Marine Species Density Data Gap Assessments and Update for the AFTT Study Area, 2017-2018 (Opt. Year 2). Document version 1.2. Report prepared for Naval Facilities Engineering Command, Atlantic by the Duke University Marine Geospatial Ecology Lab, Durham, NC.

1. Introduction

In the United States, national laws protect cetaceans. The Marine Mammal Protection Act (MMPA) prohibits intentional or incidental killing, injuring, or disturbance of marine mammals and specifies the circumstances and rules under which permits may be issued for activities that have the potential to incidentally injure or disturb marine mammals. The Endangered Species Act (ESA) prohibits harm to species threatened with extinction and requires conservation of their habitat. The National Environmental Policy Act (NEPA) specifies a process by which U.S. federal government agencies must evaluate the potential environmental effects of their actions, consider alternatives, and conduct public reviews. For certain actions this may culminate in the development of an Environmental Impact Statement (EIS). Agency actions that involve decisions to issue permits under the MMPA or ESA are often subject to this process.

The US Navy is responsible for compliance with a suite of federal environmental and natural resources laws and regulations that apply to the marine environment, including MMPA, ESA, the Magnuson-Stevens Fishery Conservation and Management Act, the Marine Protection, Research and Sanctuaries Act (MPRSA), the Clean Water Act (CWA), Executive Order 13089 on Coral Reef Protection, and NEPA/Executive Order 12114 (EO 12114). Additionally, Federal Activities that have the potential to affect the state coastal zone are required to be consistent with respective state coastal zone management plans mandated by the Coastal Zone Management Act (CZMA).

To evaluate the potential effects of proposed training, testing, and marine construction activities on marine mammal populations, the Navy requires a detailed understanding of the spatiotemporal distributions of these populations. To facilitate development of the Navy's Atlantic Fleet Training and Testing (AFTT) Phase III EIS, the Navy funded us (the Duke Marine Geospatial Ecology Lab, or MGEL) to develop density surface models (Hedley & Buckland 2004; Miller et al. 2013) for all cetacean species sighted in the AFTT Study Area (Figure 1) during scientific surveys conducted with protocols compatible with density surface modeling methodology. This culminated in the development and publication of regional models for the U.S. Atlantic coast and northern Gulf of Mexico (Roberts et al. 2016a) and the wider AFTT Study Area (Mannocci et al. 2017). From these results, we prepared a new version of the Navy Marine Species Density Database (NMSDD), the authoritative source of marine species density data maintained by the Navy, for the AFTT Phase III EIS (Roberts 2015; Roberts et al. 2015; U.S. Department of the Navy 2017).

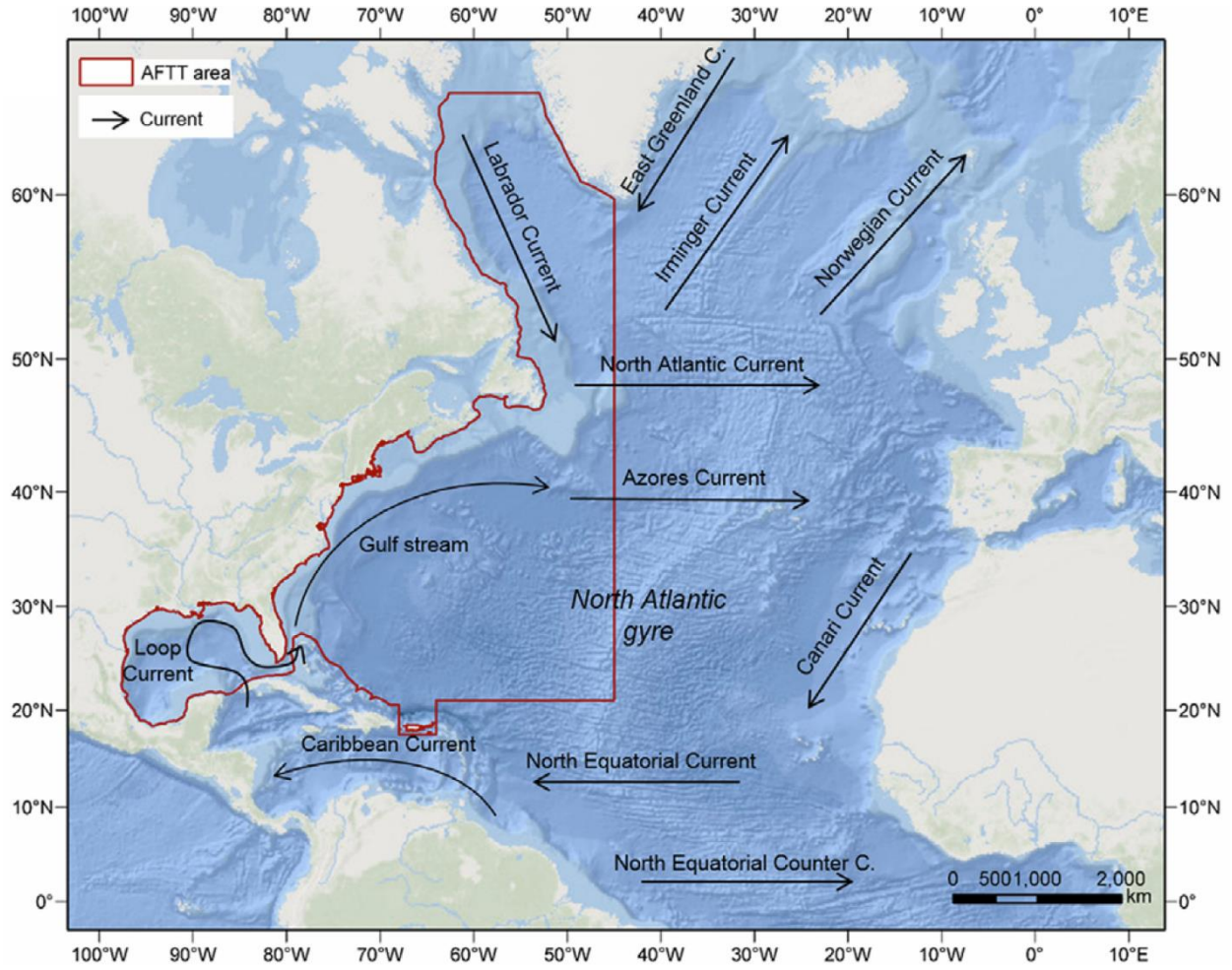

Figure 1. U.S. Navy AFTT Study Area with major current systems. Reproduced from Mannocci et al. (2017).

The regional Phase III models (Roberts et al. 2016a) spanned areas adjacent to the continental U.S. for which sufficient survey data were available to avoid large geographic extrapolations, while the AFTT-wide models (Mannocci et al. 2017) addressed the broad unsurveyed areas of the AFTT Study Area where extrapolations were required. In 2015, after the Phase III models were complete, the Navy initiated the project "Marine Mammal Density Gap Assessments and Update for the AFTT Study Area", a Cooperative Agreement (#N62470-15-2-8003) with us to prepare revised models using newly available data and methodology; these "second generation" models would replace those used in the AFTT Phase III EIS. In the Base Year (2015-2016) of the project, the Navy designated the East Coast (EC) regional models (Figure 2) as the first to be updated. During the Base Year, we acquired and integrated a large quantity of additional survey data in preparation for the update (Roberts et al. 2016b). In Option Year 1 (2016-2017), we updated the EC models for five baleen whale species (fin, humpback, minke, sei, and North Atlantic right whales) and six odontocete species and guilds (harbor porpoise, sperm whale, pilot whale, and Cuvier's, Mesoplodont, and unidentified beaked whales). In Option Year 2 (2017-2018), as documented in this report, we updated the EC models for an additional ten small odontocetes as well as the phocid seals guild, and prepared an accompanying update to the NMSDD and associated web services. The following sections describe these tasks in detail.

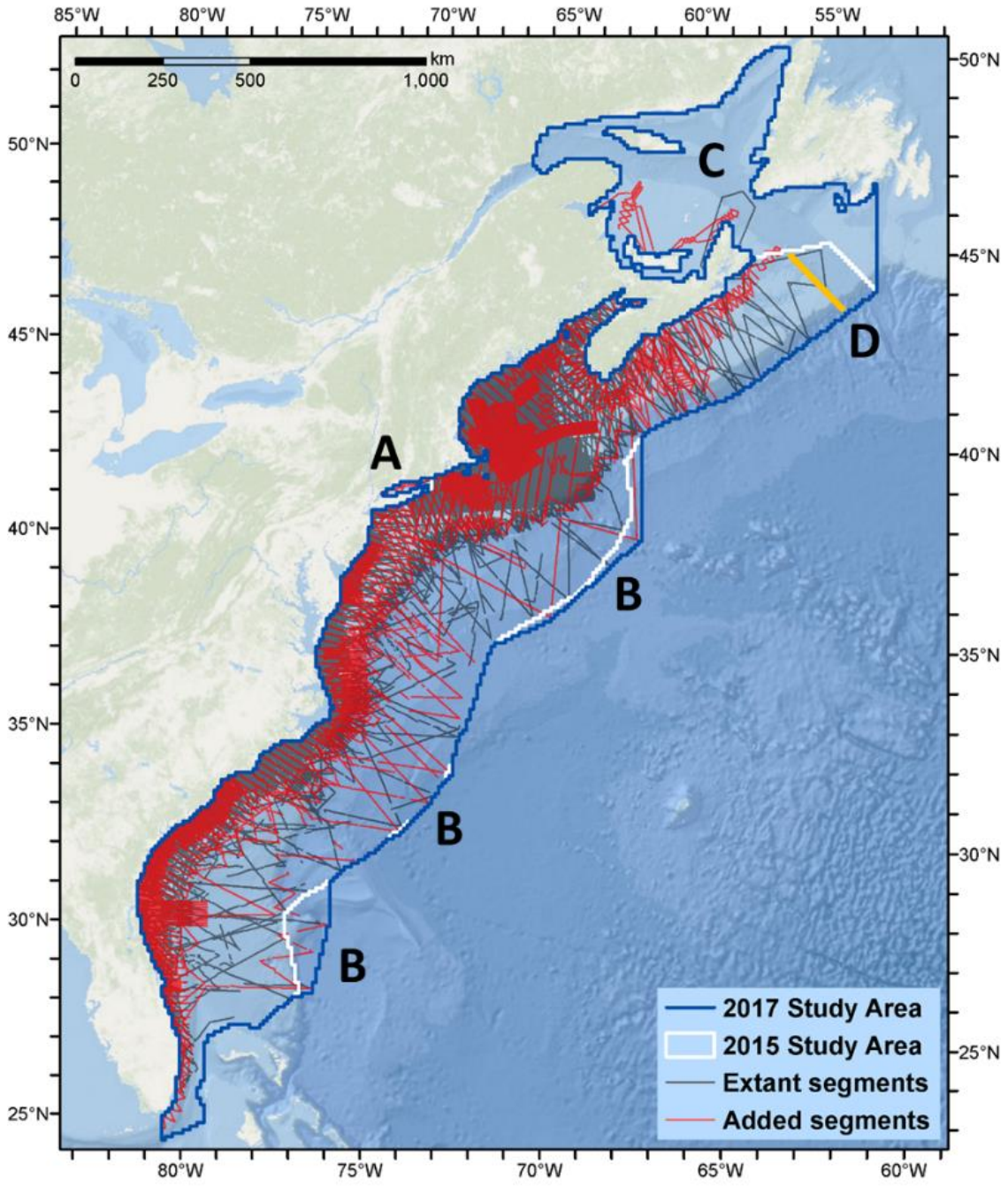

Figure 2. East Coast (EC) model study area. After completing and publishing the original Phase III models (white line) (Roberts et al. 2015, 2016b), we added additional survey data during the Base Year and Option Year 1 of this Cooperative Agreement (Roberts et al. 2016b, 2017) that allowed us to expand the study area (blue line) for the updated models at several locations. Surveys from the first phase of the Atlantic Marine Assessment Program for Protected Species (AMAPPS I) program allowed us to include Long Island Sound (A) and several areas far offshore (B). The North Atlantic Right Whale Sighting Survey expanded coverage into parts of the Gulf of St. Lawrence (C), reflecting increasing use of this area by right whales, but we lacked sufficient survey effort to confidently predict models over this region and truncated the predictions at the southern edge of the Laurentian Channel (D, yellow line). This figure is reproduced from Roberts et al. (2017).

2. Updated Density Surface Models

2.1. Summary of work performed

In Option Year 2, we updated EC regional density models for 13 taxa:

- 9 dolphins: Atlantic spotted, Atlantic white-sided, Clymene, common bottlenose, pantropical spotted, Risso's, rough-toothed, short-beaked common, and striped. In Phase III we modeled three of these (Clymene, pantropical, and rough-toothed) with stratified models. Additional surveys incorporated from collaborators since Phase III boosted sightings counts sufficiently to allow us to replace them with parsimonious habitat-based density surface models. Also, for Atlantic spotted dolphin, we enhanced the temporal resolution of predictions relative to Phase III by predicting the on-shelf subregion at monthly resolution while keeping the off-shelf subregion a static year-round mean.

- Dwarf and pygmy sperm whales (*Kogia* spp.), a two-species guild: In Phase III we modeled this as a stratified model, but surveys added since Phase III allowed us to replace it with a habitat-based density surface model. While the added surveys included a number of sightings with definitive species identifications, there were still too many ambiguous sightings (only resolved to the *Kogia* genus) and too much overlap between the two species to facilitate breaking the guild into species-specific models.

- Phocid seals, a guild of mainly two species, harbor seals and gray seals: In Phase III we modeled this guild with two seasonal habitat-based density surface models, then offered predictions as two static seasonal means. The combination of additional survey data as well as new publications and other results provided sufficient information to predict at a monthly time step and qualitatively validate those predictions. While this model would benefit from additional methodological refinements in the future, we and our collaborators believe the monthly predictions are plausible enough to utilize them for species management purposes.

- Fin whales and sei whales: We first updated these in Option Year 1 (Roberts et al. 2016b), but while developing the Option Year 2 updates, we discovered an error: we had erroneously omitted from the updated models some of the ambiguous "fin or sei whale" sightings that had been classified as one species or the other. We fixed this problem and refitted the models, and included the corrected predictions in our NMSDD update for Option Year 2. The resulting spatial distributions were similar to the Option Year 1 models, but abundance of fin whales increased 14%, while sei whales increased 1%.

2.2. Summary of surveys available for analysis

To keep the models developed in Option Year 2 (this past year) consistent with the first batch of updates developed in Option Year 1, and facilitate the publication of all updated models together in Option Year 3, we did not introduce additional surveys (e.g., AMAPPS II) for the Option Year 2 updates. Roberts et al. (2016b) documented the surveys utilized in both Option Years 1 and 2.

Table 1 enumerates the surveys that were used for modeling in Option Year 2. The surveys added in the Base Year and Option Year 1 boosted the survey effort available for small cetaceans and seals by 32% (aerial surveys) and 47% (shipboard surveys) over that available for the Phase III models. The added surveys filled critical seasonal gaps throughout the study area, yielding complete coverage of the continental shelf (0-200m) from southern Florida to the Bay of Fundy, and much of the continental slope (200-2000m) from Cape Hatteras to Georges Bank, in all seasons (Figure 3). However, off the shelf, nearly all additional effort occurred in summer and remained sparse in other seasons. In addition to filling seasonal gaps, the added surveys boosted coverage sufficiently that we could consider excluding surveys conducted prior to the launch of the SeaWiFS ocean color sensor in mid-1997. By excluding these surveys, we could ensure that biological covariates derived from ocean color observations would be available for all survey transects in contemporaneous form (i.e. for the date each transect was conducted) rather than only climatological form. We discuss this further in Section 2.3.5 below.

There are two important differences in the surveys used for model updates completed in Option Years 1 and 2. First, many of the Option Year 1 models utilized the Southeast U.S. North Atlantic Right Whale (SEUS NARW) surveys. These surveys systematically logged sightings only of large whales and were not usable for other species. Because all of Option Year 2 models were of small delphinids or seals, we did not use the SEUS NARW surveys in Option Year 2.

Table 1. Survey effort available for use in the Option Year 2 models. "Extant" effort was used in the Phase III regional models (Roberts et al. 2016a). "Added" effort was incorporated during the Base Year and Option Year 1 for the updated models. Not all of this effort was utilized in every model; please see the documentation for the individual models in Section 2.3.5 below for per-model specifications of the surveys used. Survey providers: NEFSC: NOAA Northeast Marine Fisheries Science Center; NJDEP: New Jersey Department of Environmental Protection; SEFSC: NOAA Southeast Fisheries Science Center; UNCW: University of North Carolina, Wilmington; VAMSC: Virginia Aquarium & Marine Science Center.

			Survey Effort (1000 km)			
Platform	Provider	Program	Extant	Added	Total	% Increase
Aerial	NEFSC	Marine mammal abundance surveys	70	41	112	59
		NARWSS harbor porpoise survey	6		6	
		NARWSS right whale surveys	432	87	520	20
	SEFSC	Marine mammal abundance surveys	43	66	108	154
	UNCW	Cape Hatteras Navy Surveys	19	16	35	86
		Jacksonville Navy Surveys	65	22	87	34
		Marine mammal surveys, 2002	18		18	
		Norfolk Canyon Navy Surveys		12	12	
		Onslow Bay Navy Surveys	49		49	
		Right whale surveys, 2005-2008	114		114	
	VAMSC	MD Wind Energy Area surveys		16	16	
		VA Wind Energy Area surveys	17	5	21	28
	All		832	264	1097	32
Shipboard	NEFSC	Marine mammal abundance surveys	16	12	28	76
	NJDEP	New Jersey Ecological Baseline Study	14		14	
	SEFSC	Marine mammal abundance surveys	28	15	43	52
	All		58	27	85	47

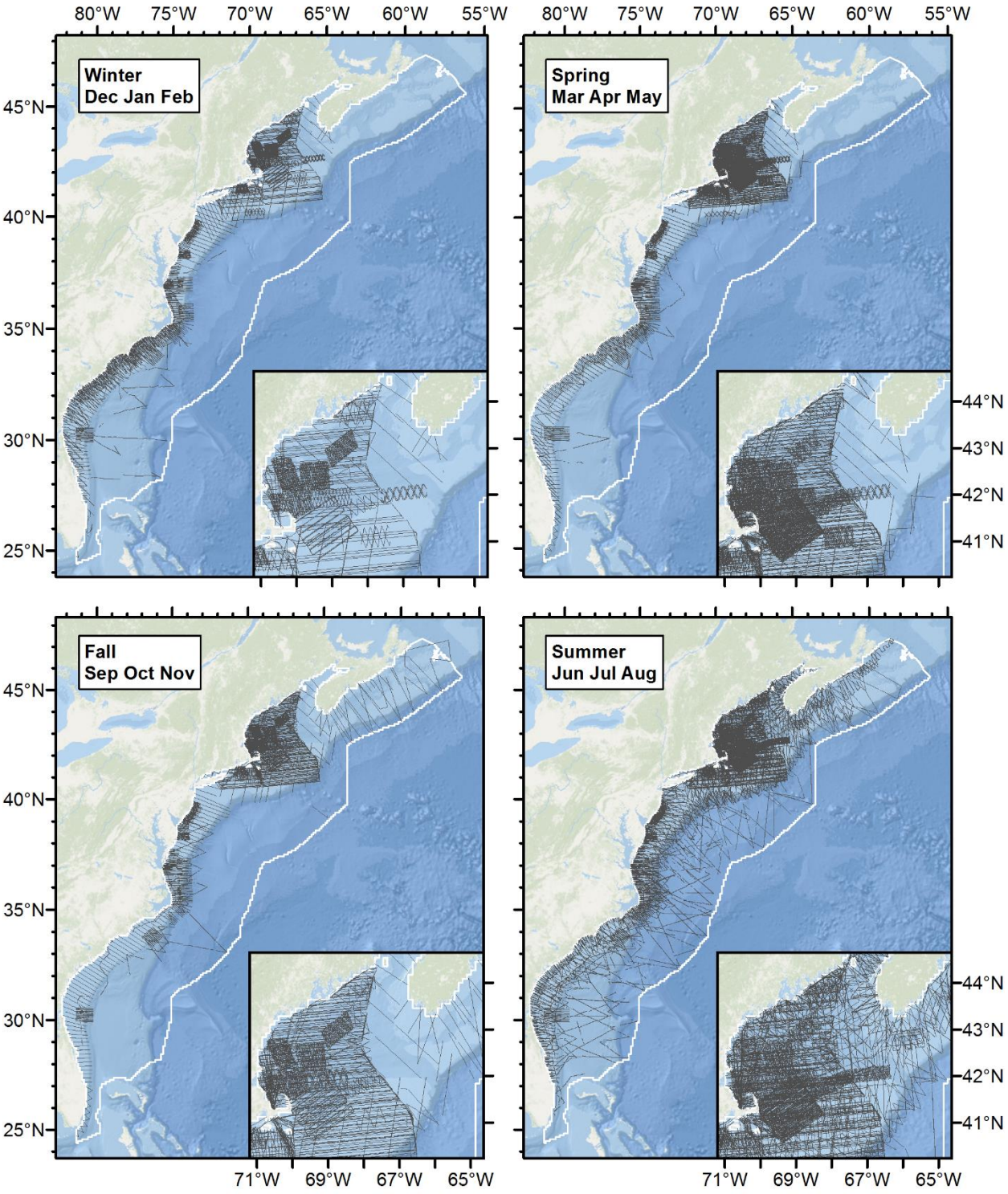

Figure 3. Seasonal maps of survey effort available for use in the Option Year 2 models.

Second, we excluded the NJDEP aerial surveys from the Option Year 2 models. The only Option Year 2 species sighted on these surveys were bottlenose dolphins (sighted frequently), short-beaked common dolphins (sighted rarely), and an unidentified seal (sighted once). Modeling detectability of delphinids for the NJDEP aerial surveys was problematic because in the aerial data we received from NJDEP, the vertical angles of delphinid sightings were

binned into just four possible values. In the Phase III models, for which the NJDEP surveys were the only recent aerial data available to us that covered that region and spanned all seasons, we dealt with this problem by pooling the NJDEP aerial surveys with a set of SEFSC surveys. Although both the NJDEP and SEFSC surveys were conducted at 750 ft. altitude and used two observers without a belly port, the NJDEP surveys used flat windows while the SEFSC surveys used bubble windows. Also, most of these SEFSC sightings were from the Gulf of Mexico. These incompatibilities introduced an unknown degree of error into our treatment of the NJDEP aerial surveys in Phase III, but we judged this as a reasonable tradeoff for obtaining 4-season aerial coverage of this region. In Option Year 1 we incorporated the AMAPPS I surveys, providing a new source of 4-season aerial coverage spanning the entire shelf, including New Jersey. Having that, we opted to drop the NJDEP aerial surveys from the Option Year 2 models. (We retained them for the Option Year 1 models, as they were not problematic to use for baleen whales or harbor porpoises, and sightings of those species are rare and very helpful for modeling in the mid-Atlantic area).

2.3. New and updated East Coast (EC) models

Here, we discuss the production of the 11 new or updated EC density models we are delivering in our NMSDD update for Option Year 2. These models used the same methodology as the published Phase III models (Roberts et al. 2016a) with the updates and improvements developed in Option Year 1 (Roberts et al. 2017), plus several additional improvements. (We omit discussion of the corrected fin and sei whale models; please see the Option Year 1 report for details.) These models are intended to eventually replace the corresponding Phase III models published by Roberts et al. (2016a). We met with and reviewed all of these models with peer modelers and species experts, including colleagues at the NOAA Northeast, Southeast, and Southwest Fisheries Science Centers (NEFSC, SEFSC, and SWFSC), the University of North Carolina, Wilmington (UNCW), the Virginia Aquarium & Marine Science Center (VAMSC), and the Atlantic Marine Conservation Society (AMCS).

Although we believe, at the time of this writing, that these models have reached final publishable formulations, we will continue to examine them and discuss them with additional experts, in preparation for submitting a publication. It is possible these examinations and discussions will lead us to further adjust some models. If this happens we will make any changes available to the Navy as additional NMSDD updates. As we prepare the publication, the results that appear here and other diagnostics will be consolidated and placed in species-specific reports designed as supplementary information for the publication. As was done with the original Phase III density models, we will provide these reports to the Navy as they are produced.

2.3.1. Detection functions

As with the models updated in Option Year 1, we fitted new detection functions for all species updated in Option Year 2 using the methodology described by Roberts et al. (2016a) with the improvements documented by Roberts et al. (2017). We reviewed the detection functions and related diagnostics with project collaborators and species experts but omit them from this report for brevity. Complete details of the detection functions will appear in taxon-specific supplementary reports that will accompany a manuscript we will submit to a peer-reviewed scientific journal, as was done with the Phase III models produced by Roberts et al. (Roberts et al. 2016a).

In the remainder of this section, we document one important change from the methodology noted above. This change concerns detection modeling for shipboard surveys, particularly those conducted by SEFSC. In the Phase III modeling timeframe, we organized the shipboard detection hierarchy according to survey vessel, to account for different ships having different heights for observation platforms. While building those models, we encountered a paradoxical result: detection probability at far distances sometimes was lower on the highest platform—SEFSC's R/V Gordon Gunter—than on the lower platforms, such as NEFSC's R/V Endeavor and R/V Abel-J. For example, at 2000 m, for bottlenose dolphins, hazard rate detection functions with no adjustments or covariates yielded a detection probability of less than 0.1 for the Gordon Gunter (Figure 4) but about 0.4 for the Endeavor and 0.2 for the Abel-J (Figure 5).

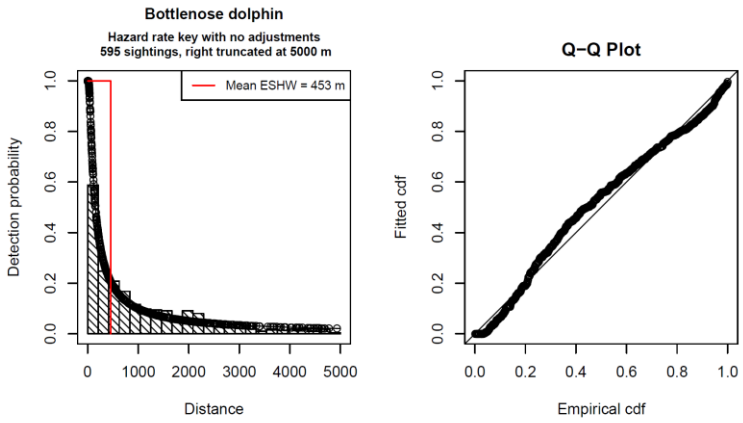

Figure 4. Candidate detection function from Phase III modeling project (left) for bottlenose dolphins sighted by SEFSC's R/V Gordon Gunter and the associated Q-Q plot (right) showing a systematic bias. This candidate was not selected as the best, but more clearly shows the problem than the one that was selected. (Please see the supplementary bottlenose dolphin report from Roberts et al. (2016a) for the final function.)

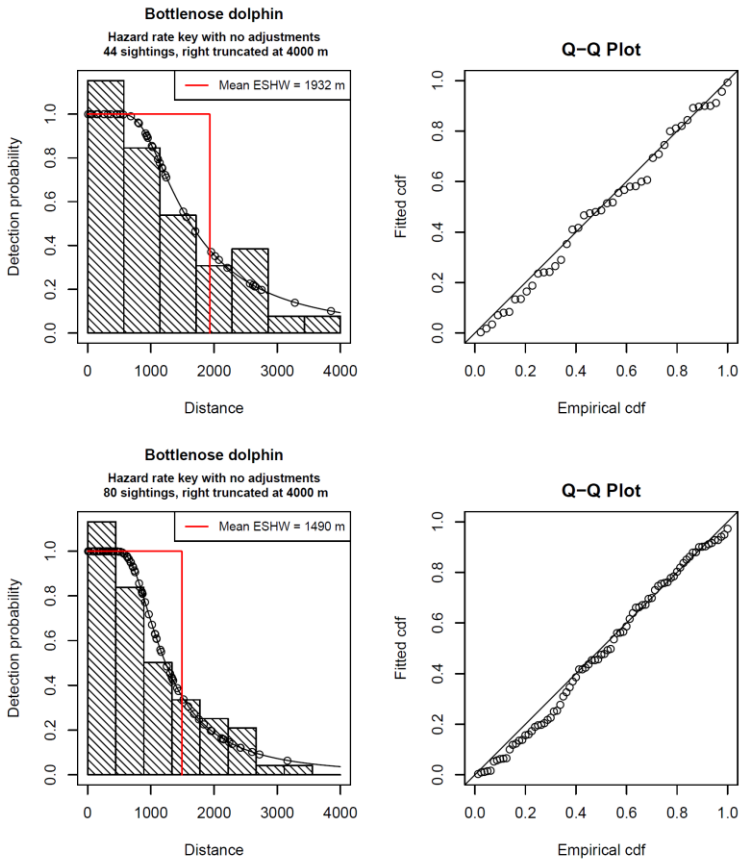

Figure 5. Candidate detection functions from the Phase III modeling project (left column) for bottlenose dolphins sighted by NEFSC's R/V Endeavor (top row) and R/V Abel-J (bottom row), and the associated Q-Q plots (right column). Although the Q-Q plots show some deviation from the diagonal, such deviations are common for detection functions with only 50-100 sightings and do not indicate a systematic bias. (These candidates were not selected as best but are shown to provide an appropriate contrast to Figure 4 by using the same key function with no covariates.)

This was contradictory—in general, higher platforms should have higher detection probabilities at far distances. We only noticed the problem with detection functions for dolphins, but it did not happen for all species, and the surveys were spread across six vessels, making it hard to obtain enough sightings to do systematic comparisons with per-vessel detection functions. We lacked the time to investigate this fully for the Phase III models and proceeded with detection functions fitted with our usual procedure.

In Option Year 2, which focused on updating density models for dolphins, we revisited this problem, investigated it fully, and crafted a solution. This section documents our findings and solution.

2.3.1.1. The "spike" at the trackline in SEFSC shipboard surveys

In Phase III, our modeling infrastructure lacked the ability to include categorical covariates in detection functions. Thus, to address differences between ships or species, our only choice was to separate sightings by ship or species into independent detection functions, resulting in a loss of statistical power compared to a single detection function in which the difference could be addressed by a categorical covariate. In Option Year 1, we added this capability. After experimenting with different combinations of surveys and covariates, we discovered that the biased detection functions only happened on SEFSC ships (Figure 6), and that it happened on both of them: the higher-platformed R/V Gordon Gunter and the lower-platformed R/V Oregon II. For the updated detection functions, we reorganized the shipboard detection hierarchy to separate the surveys by organization (NEFSC, SEFSC, and NJ-DEP) and then treated per-vessel effects within each organization with a covariate. This isolated the problem to SEFSC and allowed all organizations to have larger counts of sightings.

We investigated the SEFSC shipboard sightings further and discovered that the problem in fitting the detection function resulted from a "spike" of a very large number of sightings occurring close to the trackline (Figure 7). A detailed examination showed that there were 133 dolphin sightings with perpendicular distances less than 5m, and less than 50 sightings in every other 5m bin beyond that.

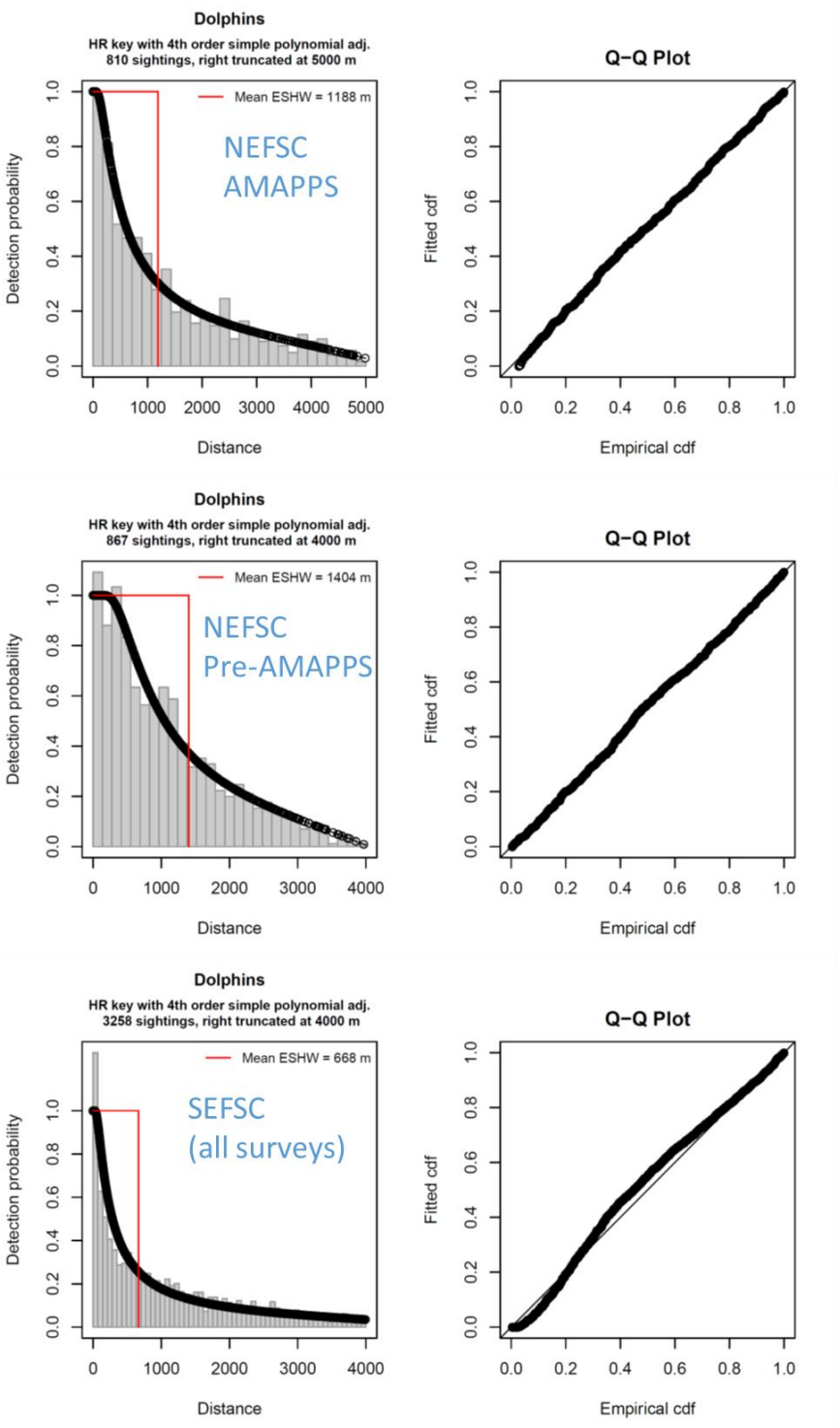

Figure 6. Experimental detection functions fitted in Option Year 2 for all delphinids (pooled) that were sighted on NEFSC and SEFSC shipboard surveys, 1992-2016, in the U.S. Atlantic and Gulf of Mexico. Note how the SEFSC histogram shows many more sightings close to the trackline relative to the NEFSC histograms, and a biased Q-Q plot.

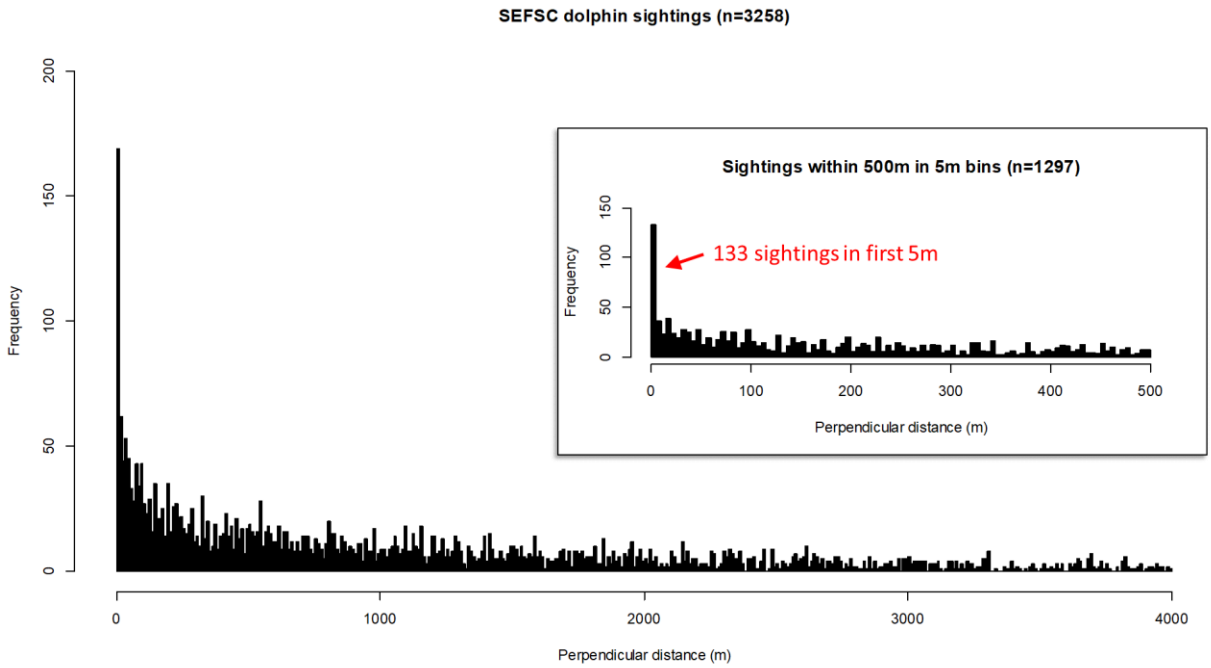

Figure 7. Histogram of perpendicular distances of all delphinids (pooled) sighted on SEFSC shipboard surveys, 1992-2016, in the U.S. Atlantic and Gulf of Mexico. Note the "spike" in detections in the first histogram bin.

2.3.1.2. Would smearing the sighting bearings help?

Our first thought was that perhaps the "spike" resulted from too many distant sightings reported with a bearing of exactly 0°. When the bearing is exactly 0°, it does not matter how far (radially) the animals are from the observer; the perpendicular distance will always be exactly 0. We examined the sighting bearings and noted distinct heaping at 5° increments (Figure 8). In itself, this degree of heaping is not necessarily problematic but we wondered if by smearing the bearings at exactly 0° by 5° (i.e. to range between 2.5° to the left and 2.5° to the right), the detection function would improve. While smearing reduced the number of sightings with perpendicular distances of exactly 0 (Figure 9), it yielded virtually no improvement when we fitted a new detection function (Figure 10).

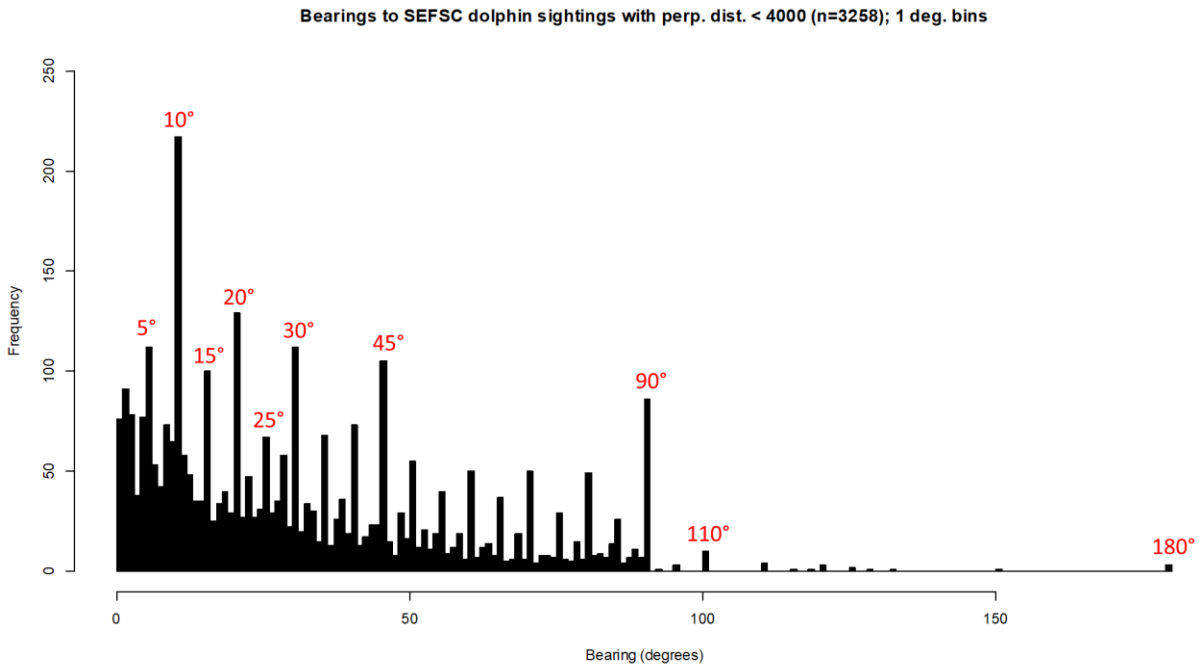

Figure 8. Histogram of sighting bearings for all delphinids (pooled) sighted on SEFSC shipboard surveys, 1992-2016, in the U.S. Atlantic and Gulf of Mexico. Sightings from both sides of the vessel have been collapsed into a 0-180° scale. Note heaping at 5° increments.

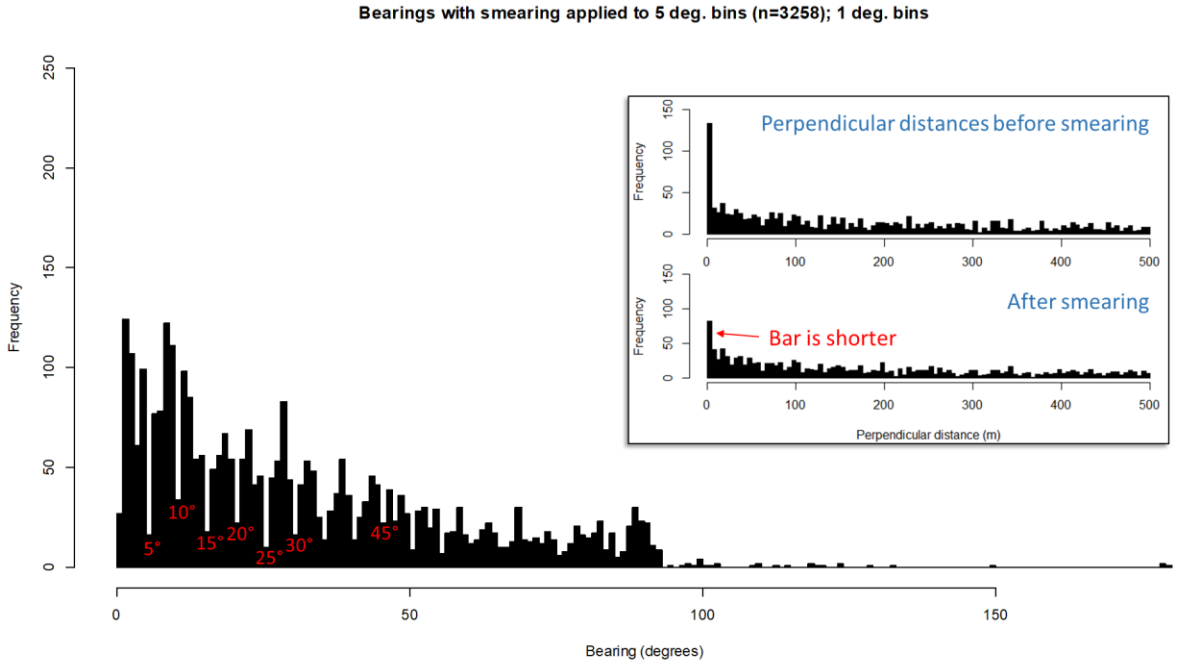

Figure 9. Histogram from Figure 8 after sightings at 5° increments were smeared by +/- 2.5°. The smearing reduced the number of sightings between 0-5m perpendicular distance by half.

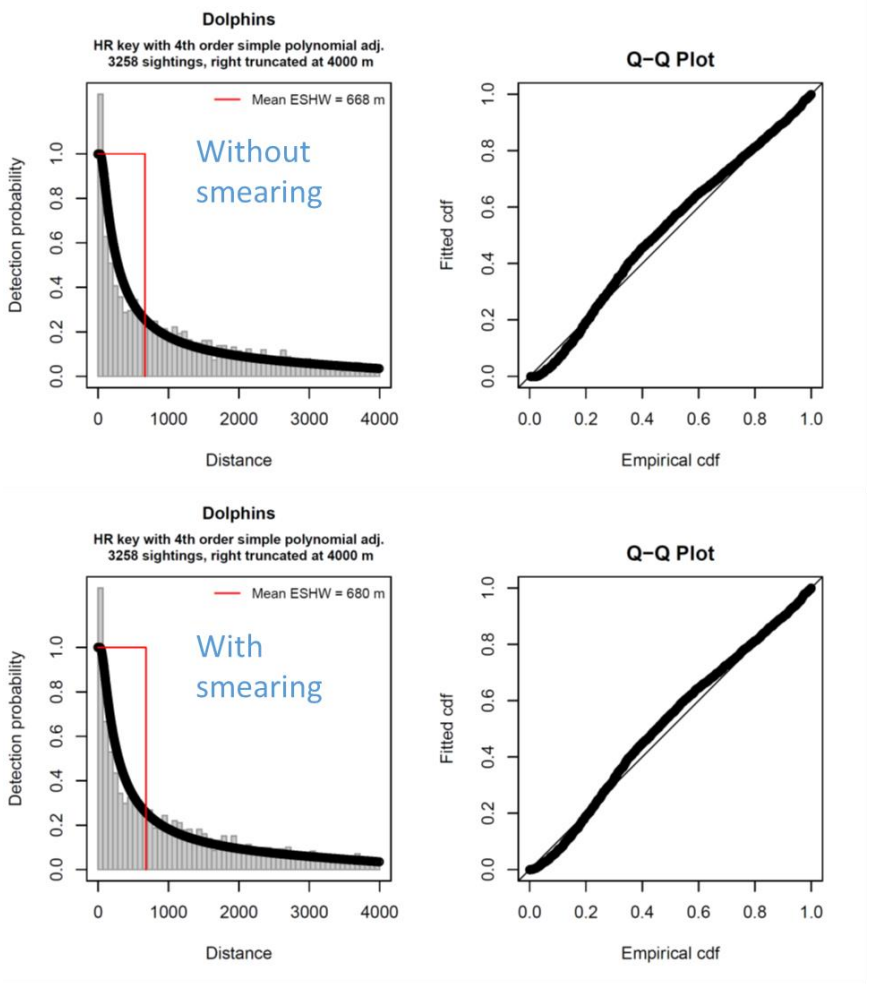

Figure 10. Detection functions fitted with and without smearing the sighting bearings at 5° increments by +/- 2.5°, for all delphinids (pooled) sighted on SEFSC shipboard surveys, 1992-2016, in the U.S. Atlantic and Gulf of Mexico. Note that smearing did not improve the detection function.

2.3.1.3. Would right truncation help?

Fitting detection functions with a long "tail" is known to be problematic, and the recommended solution is to right-truncate the sightings, removing sparse distant sightings that contribute little to the final abundance estimate (Thomas et al. 2010), so that the optimizer can focus on fitting the function to the bulk of the sightings made close to the trackline. To test this idea here, we truncated the SEFSC dolphin sightings at progressively closer distances to see whether good-fitting detection functions could be obtained. This approach did not work. Even truncating as close as 400m, which resulted in a loss of 67% of the sightings (which would be intolerable in practice), still produced a biased detection function, with the "spike" strongly evident (Figure 11).

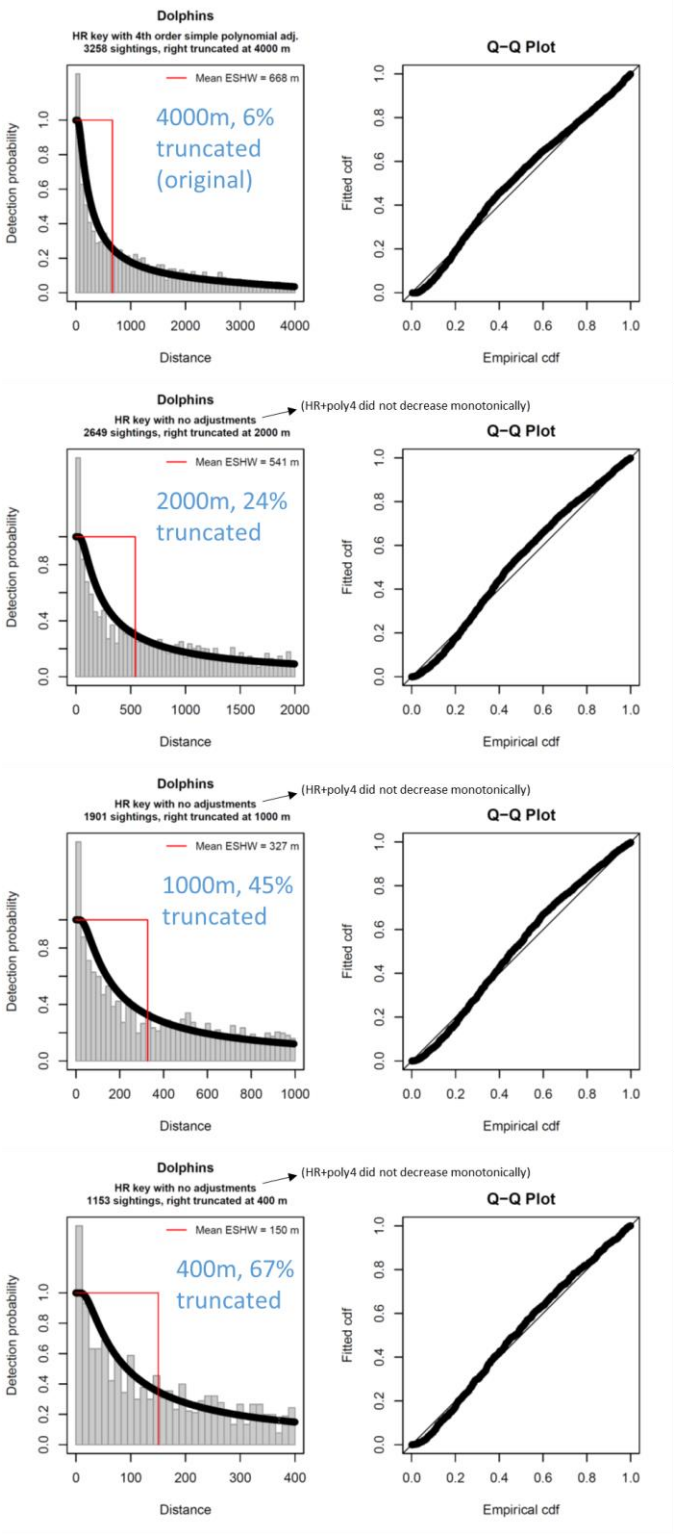

Figure 11. Detection functions fitted with increasingly extreme right truncation distances, for all delphinids (pooled) sighted on SEFSC shipboard surveys, 1992-2016, in the U.S. Atlantic and Gulf of Mexico. Note that detection functions still showed biases even with very extreme truncation that resulted in the loss of most of the sightings.

2.3.1.4. Would left truncation help?

The right-truncation experiments suggested that the spike of detections close to the trackline was the problem. The smearing experiments showed that the detections at bearings of exactly 0° were not the problem. For our third experiment, we applied left truncation to remove the spike of sightings close to the trackline. This experiment showed that a relatively small degree of left truncation yielded much better detection functions (Figure 12), confirming that the spike was causing the problem. When we left-truncated the spike, the SEFSC detection functions began to resemble the better-behaved detection functions of NEFSC. Left truncation looked like a possible solution, but first we wanted to try to isolate the spike, to figure out what might be causing it.

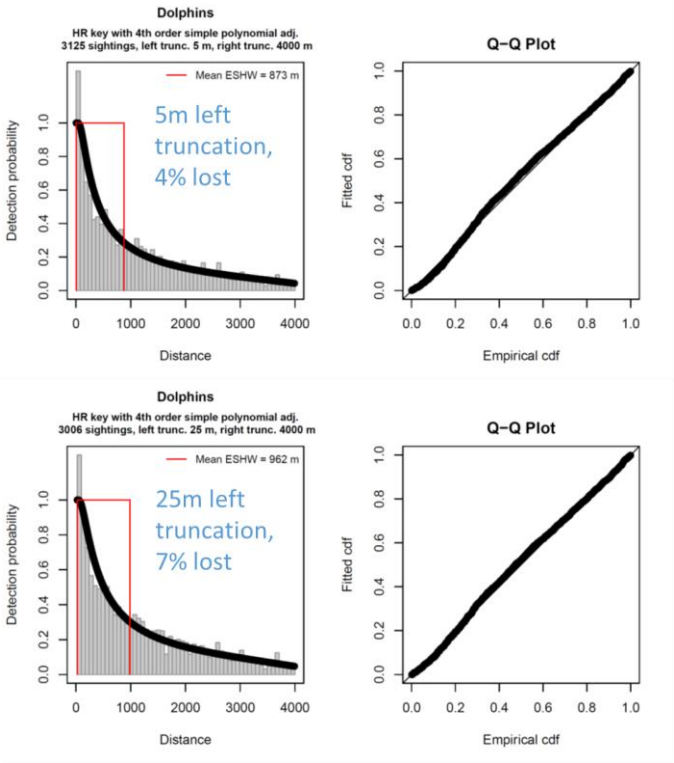

Figure 12. Detection functions fitted with relatively minor left truncation distances. Compare these to the top detection function of Figure 11. Note how a relatively small degree of left truncation greatly improves the shape of the detection function, boosts the effective strip half width (ESHW) to values similar to NEFSC shipboard surveys (Figure 6), and yields a straight Q-Q plot.

2.3.1.5. Was the spike caused by dolphins approaching the ship?

A common problem with shipboard surveys for small cetaceans is that some species are known to be attracted to vessels or to avoid them. If cetaceans detect the vessel and move toward it before observers detect them, detection distances will be biased low and detectability will be underestimated (and abundance potentially overestimated). Conversely, if cetaceans move away from the vessel before observers detect them, detection distances will be biased high and detectability will be overestimated (and abundance potentially underestimated).

Würsig et al. (1998) examined the behavioral reactions of cetaceans to SEFSC ships and aircraft in the Gulf of Mexico and found that many of them were attracted to vessels. The spike of dolphin sightings close to the trackline that we noted in the surveys were suggestive of an attraction problem: perhaps the dolphins noticed and approached the ship before they were detected by observers. To investigate this further, we fitted species-specific detection functions for the eight species for which we had at least 50 sightings (Figure 13). Six of these were species reported

by Würsig et al. (1998) to approach ships and bowride at least 75% of the time: Atlantic spotted dolphin, common bottlenose dolphin, Clymene dolphin, pantropical spotted dolphin, rough-toothed dolphin, and spinner dolphin. Two others, Risso's dolphin and striped dolphin, were reported to avoid ships and bowride less frequently. We found that four of the six ship-attracted species exhibited spikes in detections close to the trackline and problematic detection functions, while two of them and the two ship-avoiding species did not. Finally, we fitted a ninth detection function to the ambiguous "Atlantic spotted or bottlenose dolphin" sightings. We found that these did not show a spike and were detectable at greater distances, consistent with the assumption that animals that approached the ship were more likely to be fully identified to the species level.

This experiment isolated the "spike" problem to the species reported to be attracted to ships, and suggested that the ship-attracted dolphins were moving towards the ship before being detected by the observers. But before devising a solution we examined other factors to see if they could be contributing to the problem, including the sea state, vessel, region, and time period or survey program.

2.3.1.6. Other possible influences

In general, as sea state increases, distant animals become harder to detect. It was possible that high sea states severely limited the number of distant detections, causing distant detections only to occur in low sea states. In the Phase III detection functions, we added Beaufort sea state as a covariate and it improved their fit. We tried this again, including all of the additional dolphin sightings added after Phase III. We also tried detection functions that excluded sightings with Beaufort > 4 and Beaufort > 2.

The results (Figure 14) indicated that neither approach was effective at fixing the problem. ESHW, a measure of integrated probability of detection for the detection function, remained below 1000 m with or without the Beaufort sea state covariate unless we excluded sightings with Beaufort > 2, resulting in a loss of 47% of the sightings, which we considered too extreme for practical use. And even with that exclusion, there was still a spike in detections close to the trackline (Figure 15) and the Q-Q plots still showed some bias (Figure 14). This suggested that, if dolphins were approaching the ship before detection, it was less of a problem at low sea states (e.g. observers were detecting them farther away), but filtering by sea state did not completely solve it and was also impractical.

To check whether the spike was associated with a particular vessel, we fitted a detection function that utilized vessel as a covariate (Figure 16). It did not help. Histograms of perpendicular distances by vessel showed the spike was present for both of them (Figure 17).

Both NEFSC and SEFSC appeared to have long-term staff supporting the protected species surveys and to have maintained very consistent, high-quality survey protocols since the surveys started. However, we considered it plausible that different regions, time periods, or survey programs would exert biases that could be related to the "spike" of close detections problem. To examine this, we split the surveys into six groups according to region (Atlantic or Gulf of Mexico) and NMFS survey program (AMAPPS, Shelf CetShip, Oceanic CetShip, and so on).

The results revealed the spike existed in the five earliest survey programs but not in the Atlantic AMAPPS surveys (Figure 18). Consequently, detection functions for the five earlier programs exhibited poor fit, low ESHW, and the characteristic bias, while the AMAPPS detection function exhibited good fit and an ESHW as high as NEFSC surveys. We examined the AMAPPS sightings closely to determine whether there was something that would explain this. In aggregate, the AMAPPS sightings had a similar composition and distribution of species, sea states, etc. as the Atlantic pre-AMAPPS surveys (results not shown). We could not identify a factor that differentiated the AMAPPS sightings from the Atlantic pre-AMAPPS sightings, other than that they were different programs from different time periods (AMAPPS: 2011-2013 (years with shipboard surveys), Atlantic pre-AMAPPS: 1998-2006). As far as we could tell, the difference between AMAPPS and the other programs was real, with one caveat: AMAPPS reported the fewest number of sightings (226), as it only comprised two years of shipboard surveys. In future modeling cycles, as additional AMAPPS shipboard surveys are made available to us by SEFSC, we can see whether a spike is revealed.

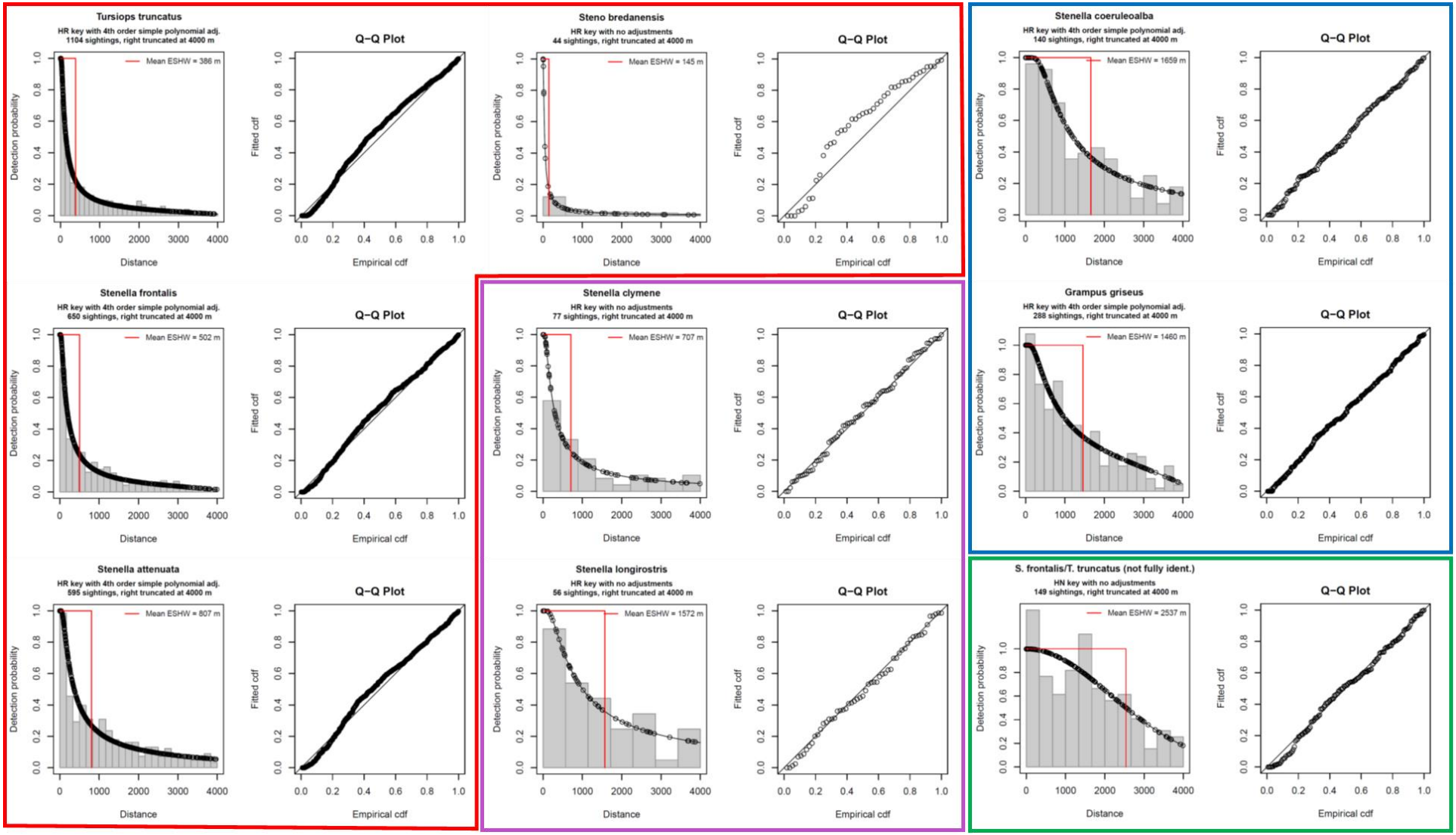

Figure 13**.** Species-specific detection functions for dolphin species having at least 50 sightings on SEFSC shipboard surveys, 1992-2016, in the U.S. Atlantic and Gulf of Mexico. Four species (red box) were reported by Würsig et al. (1998) to approach ships and yielded problematic detection functions with a large "spike" of sightings close to the trackline. Two more species (purple box) were reported to approach ships but did not display as problematic of a detection function (although the number of sightings were lower). The two species (blue box) reported to avoid ships did not yield problematic detection functions, nor did ambiguous "Atlantic spotted or bottlenose dolphin" sightings (green box).

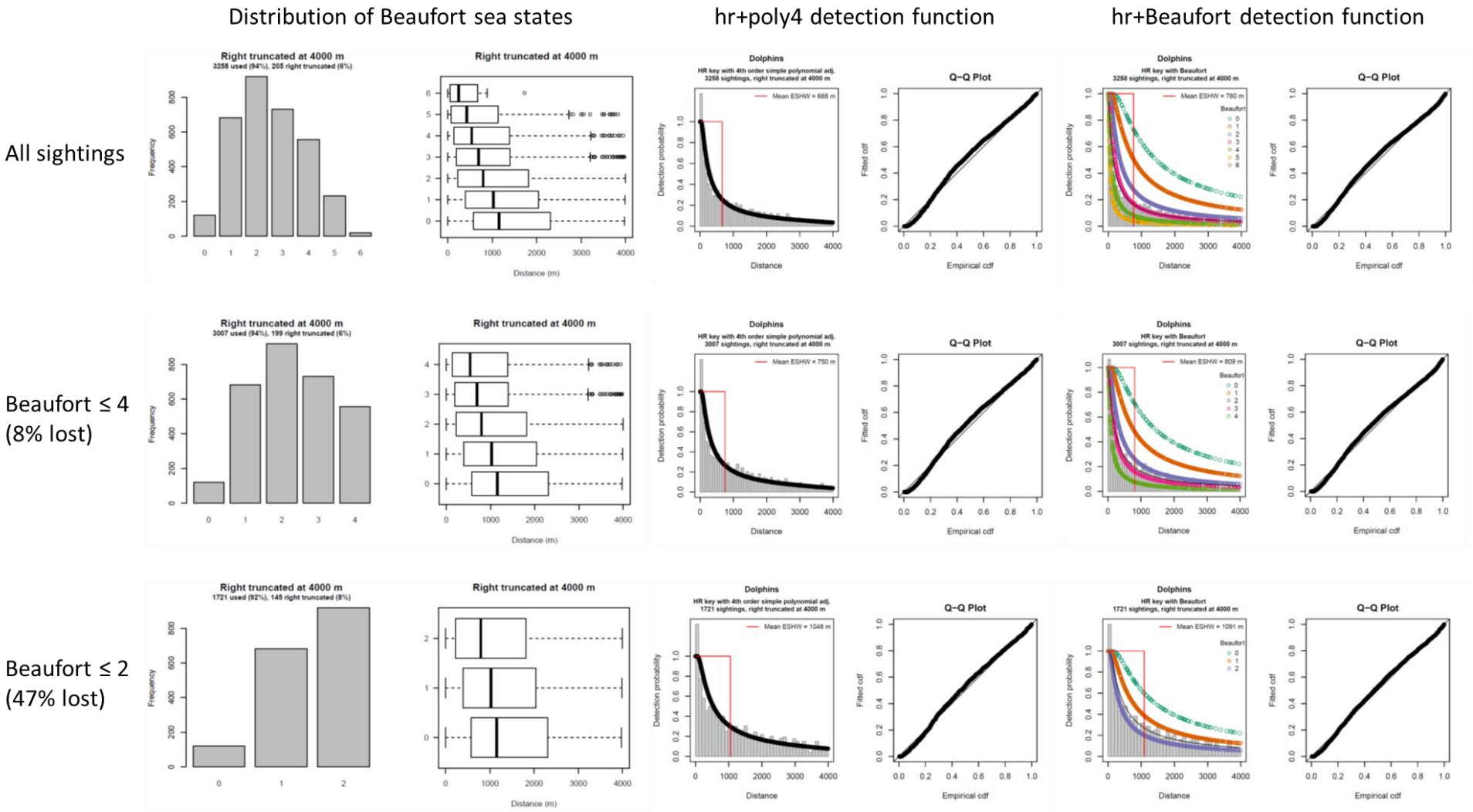

Figure 14. Influence of sea state on detection functions for all delphinids (pooled) sighted on SEFSC shipboard surveys, 1992-2016, in the U.S. Atlantic and Gulf of Mexico. The three rows of plots show results for three subsets of data: all sightings (top), those with Beaufort sea state ≤ 4 (middle), and those with Beaufort sea state ≤ 2 (bottom). The middle column shows a simple hazard rate detection function with a 4th order polynomial adjustment and no covariates. The right column shows a detection function that uses Beaufort sea state as a categorical covariate. Note that excluding sightings made in high sea states or adding a sea state covariate improved the detection function only marginally.

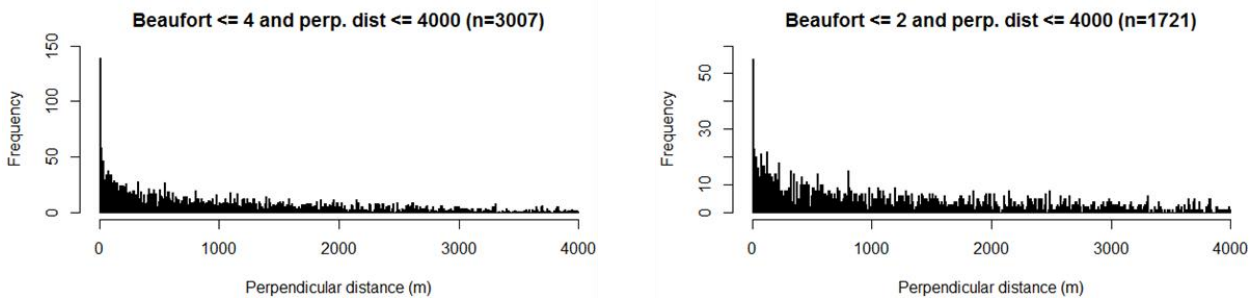

Figure 15. Histograms of perpendicular distances of SEFSC delphinid sightings, showing that excluding sightings with high sea state does not eliminate the "spike" of sightings close to the trackline.

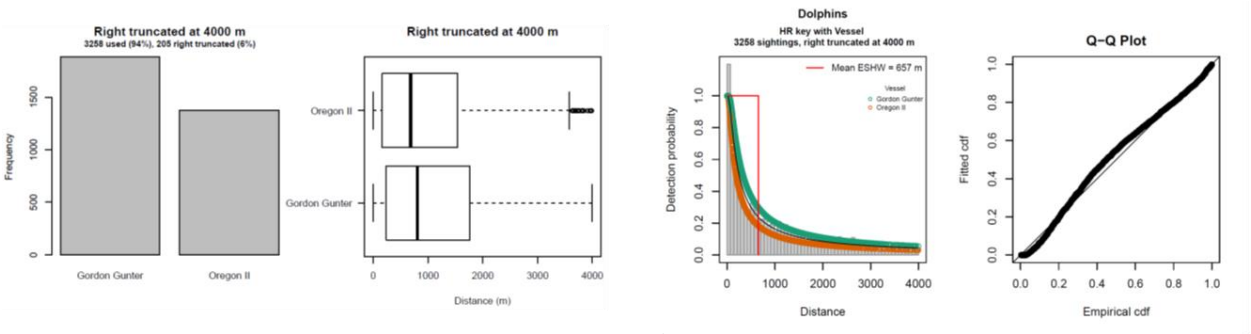

Figure 16. Detection function that uses vessel as a covariate. Note that this yielded the expected effect—that sightings were made at greater distances from the ship with the higher observation platform, the R/V Gordon Gunter—but that it did not fix the detection function.

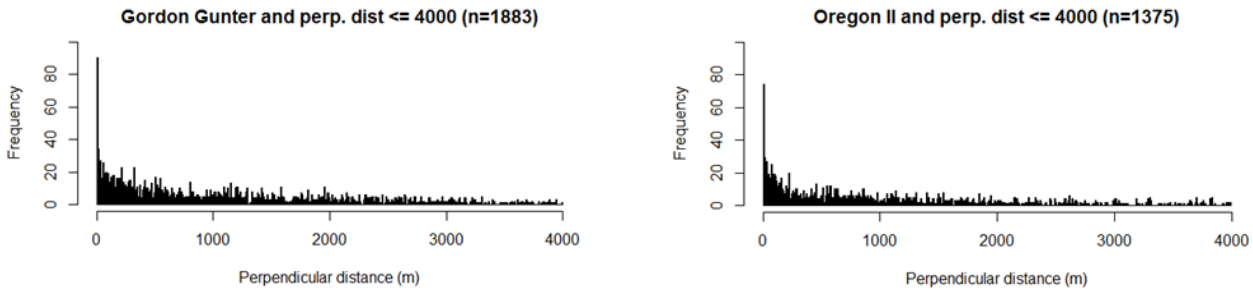

Figure 17. Histograms of perpendicular distances of SEFSC delphinid sightings, showing that the spike was present for both of SEFSC's survey vessels.

Atlantic Pre-AMAPPS

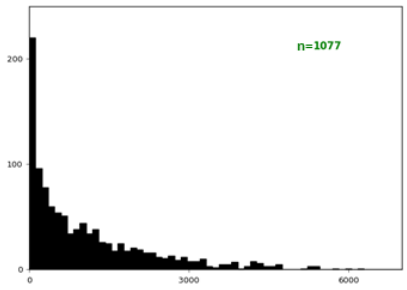

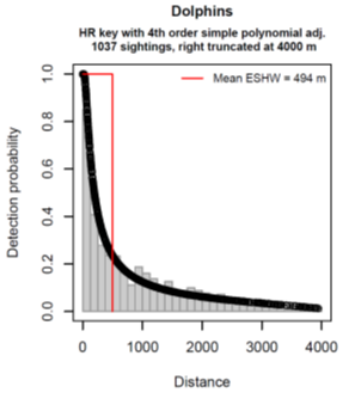

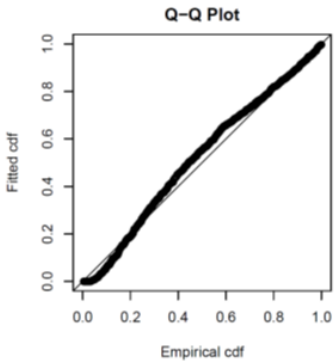

Atlantic AMAPPS

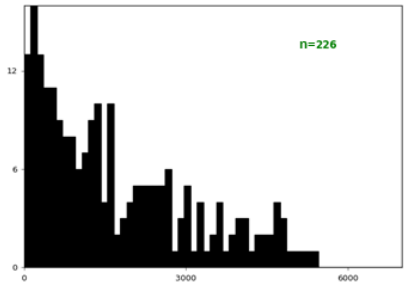

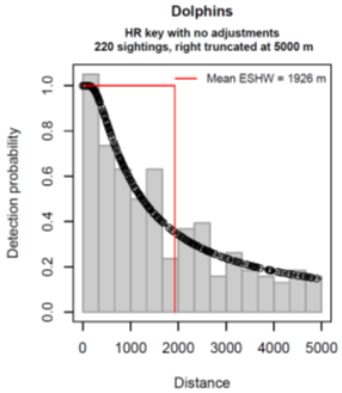

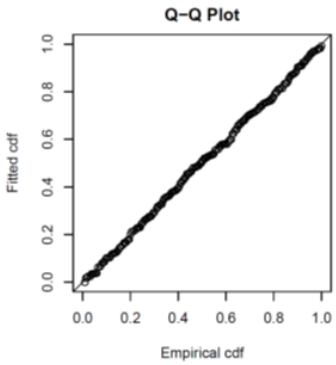

GoMex Oceanic CetShip 1992-1994

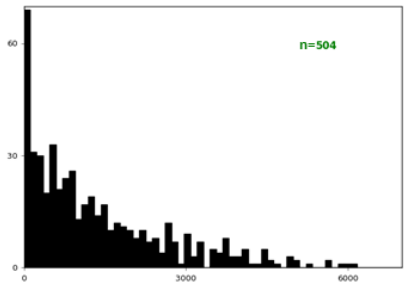

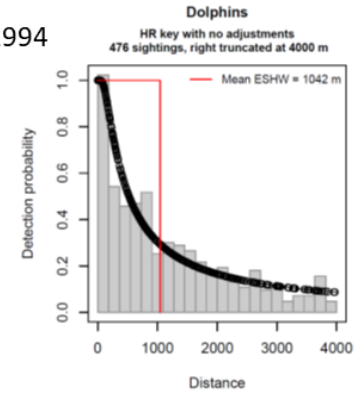

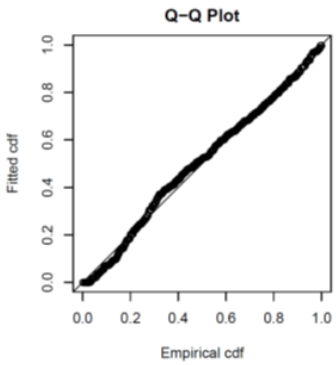

GoMex Oceanic CetShip 1996-2001

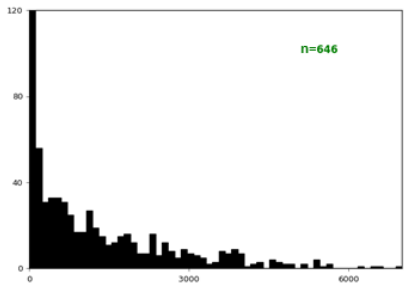

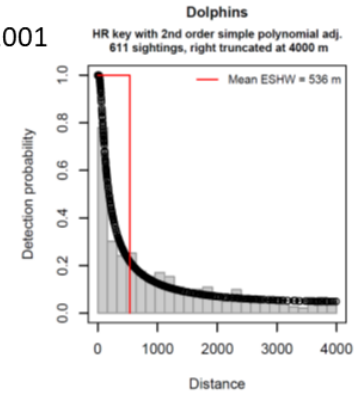

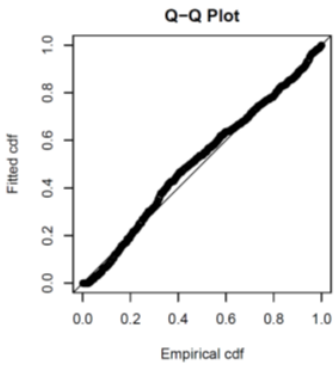

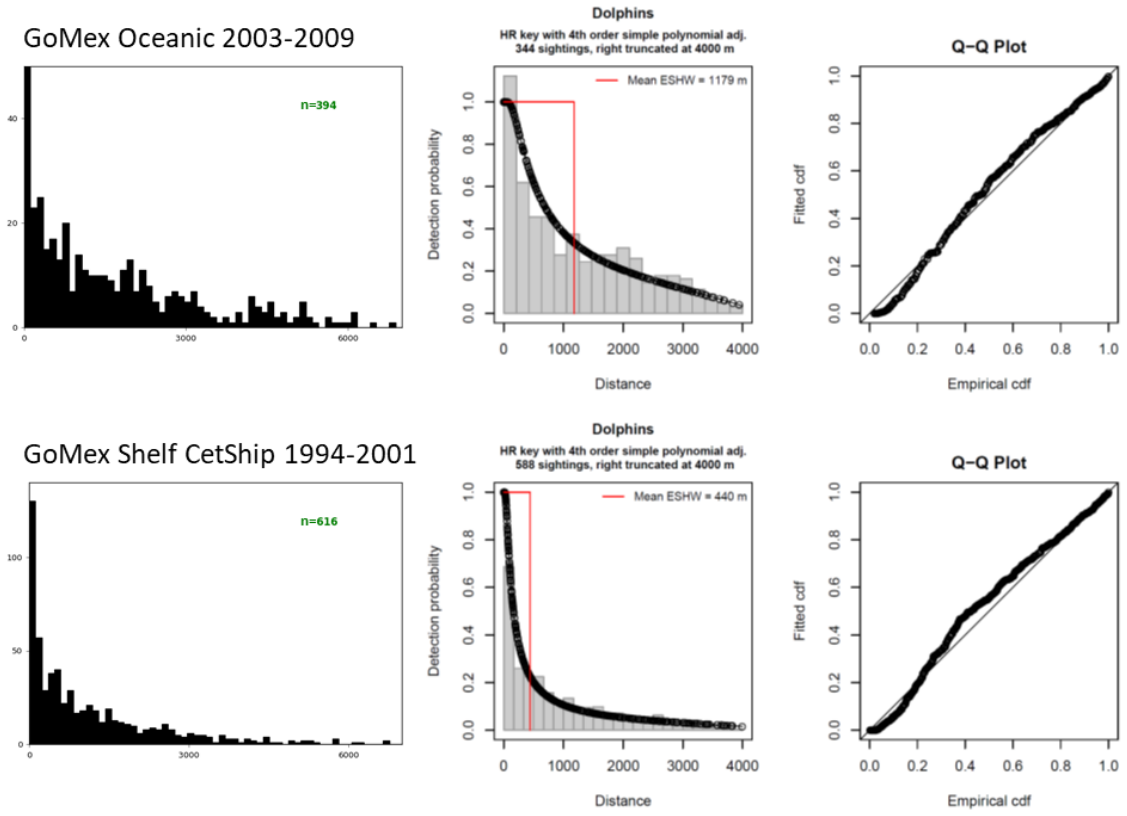

Figure 18. Histograms of perpendicular distances, delphinid detection functions, and detection function Q-Q plots for the six groups of SEFSC shipboard surveys. Note that for five of the six groups (excepting the Atlantic AMAPPS group), the "spike" of detections close to the trackline is present and the Q-Q plots show the characteristic bias.

2.3.1.7. The solution

The experiments recounted above demonstrated that for SEFSC shipboard surveys there is a problematic "spike" in sightings close to the trackline for species known to be attracted to ships, that this occurred across SEFSC survey programs in the Atlantic and Gulf of Mexico going back to the 1990s except for the most recent AMAPPS surveys, and that the problem was not related to sea state or survey vessel. When we reviewed these results with survey team leaders from SEFSC, L. Garrison and K. Mullin, they agreed with our diagnosis. Garrison noted that there was a tendency for the ship-attracted species to "sneak in under the 25x binoculars" and be sighted by the data recorder who relies on naked eyes or handheld binoculars. They described their own past attempts to solve this problem, e.g. drop all sightings not made from the 25x binoculars, or model the 25x binoculars and naked-eye sightings separately, or truncate all sightings within certain radial distance. Similar to these ideas, we implemented the following strategy.

1. We split out the non-problematic species—Risso's, striped, and spinner dolphins (we presume the latter was easy to detect because of its showy behavior)—and fitted a detection function for them alone. We pooled all species and surveys to maximize the utility of observation covariates. This detection function selected visibility, species ID, swell height, vessel, and the base-10 logarithm of group size as covariates, and yielded a mean ESHW of 1979m (Figure 19).

2. For the problematic species—Atlantic spotted, Clymene, common bottlenose, pantropical, rough-toothed, and short-beaked common dolphins (which were sighted infrequently but we assumed would be problematic because of its reputation for bowriding)—we split the AMAPPS surveys out and fitted a detection function for them alone, which selected sea state as its only covariate and yielded a mean ESHW of 2589m (Figure 20).

3. Finally, for the problematic species sighted on non-AMAPPS surveys, we left truncated the sightings at 200m (Figure 21) and fitted a detection function. (We discuss the choice of 200m below.) As above, we pooled all species and surveys to maximize the utility of observation covariates. This detection function selected vessel, swell height, sea state, and the base-10 logarithm of group size as covariates and yielded a mean ESHW of 1709m (Figure 22). We applied this detection function to the sightings with distance ≥ 200m. For sightings with distance < 200m, we assumed that detectability was 1 rather than discarding them from the analysis, effectively treating the 0-200m zone along the trackline as a strip transect, similar to one of SEFSC's previous solutions to this problem (Mullin & Fulling 2003). This boosted the ESHW to 1909m, which was fairly similar to what we obtained above for the non-problematic species.

In adopting the 200m strip-transect approach for the problematic species, our reasoning was two-fold. First, the 200m distance was within the shoulder of hazard rate detection functions for dolphins in non-problematic scenarios (e.g. the non-problematic species, the problematic species on AMAPPS, and on NEFSC surveys). Had observers detected the dolphins before they moved toward the ship, it would have been within shoulder—the zone of distances where detection probability is 1. Second, 200m was sufficient to chop out enough of the spike to yield a well-behaved detection function. SEFSC team leaders reviewed these results and approved the choice of 200m for truncation.

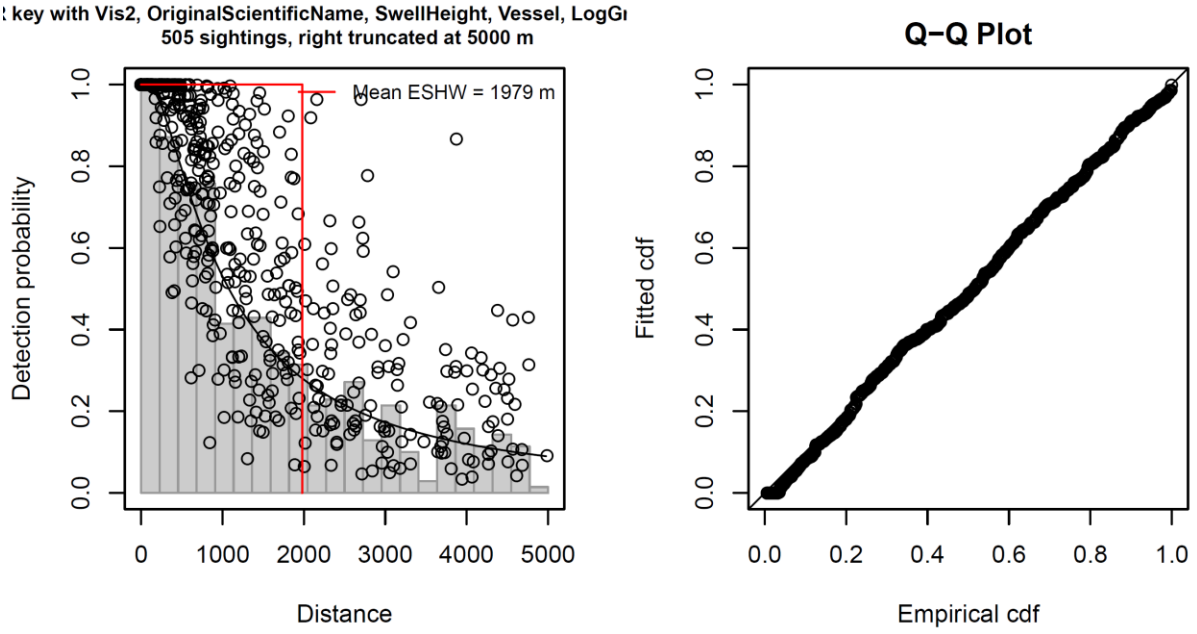

Figure 19. Detection function for non-problematic dolphin species (Risso's, striped, and spinner dolphins) sighted on all SEFSC shipboard surveys, 1992-2016, in the U.S. Atlantic and Gulf of Mexico.

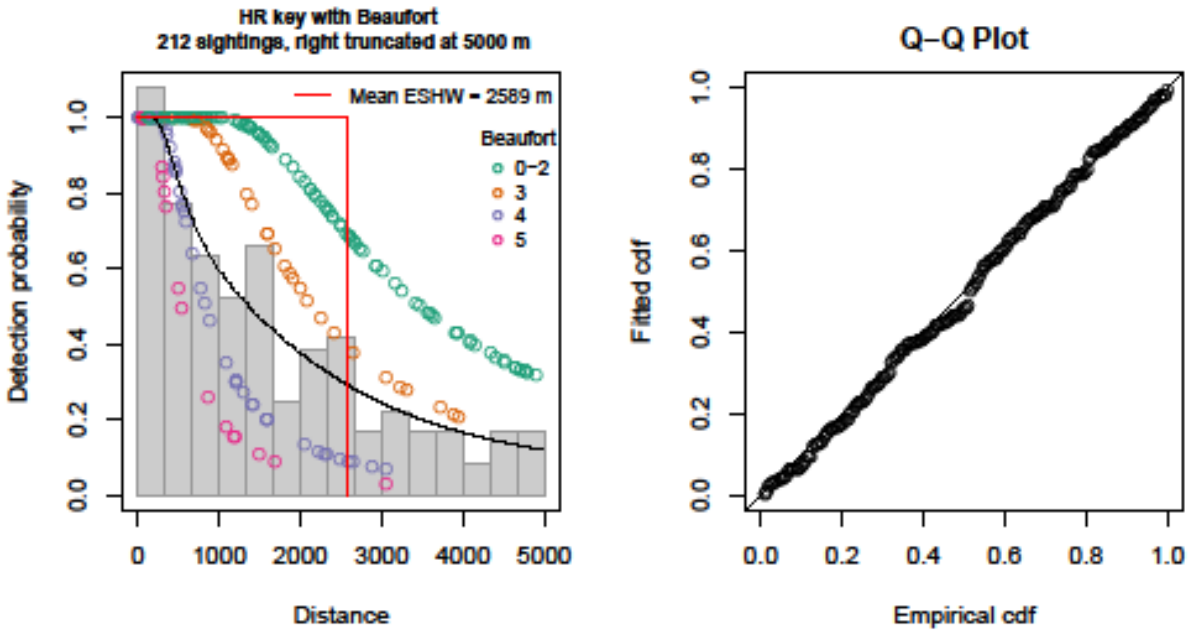

Figure 20. Detection function for problematic dolphin species (Atlantic spotted, Clymene, common bottlenose, pantropical, rough-toothed, and short-beaked common dolphins) sighted on SEFSC AMAPPS surveys in 2011 and 2013.

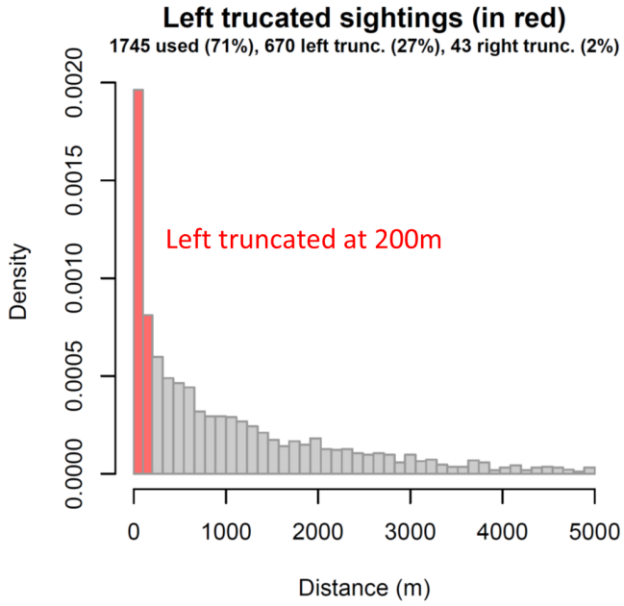

Figure 21. Histogram of perpendicular distances of problematic dolphin species (Atlantic spotted, Clymene, common bottlenose, pantropical, rough-toothed, and short-beaked common dolphins) sighted on all non-AMAPPS SEFSC shipboard surveys, 1992-2016, in the U.S. Atlantic and Gulf of Mexico.

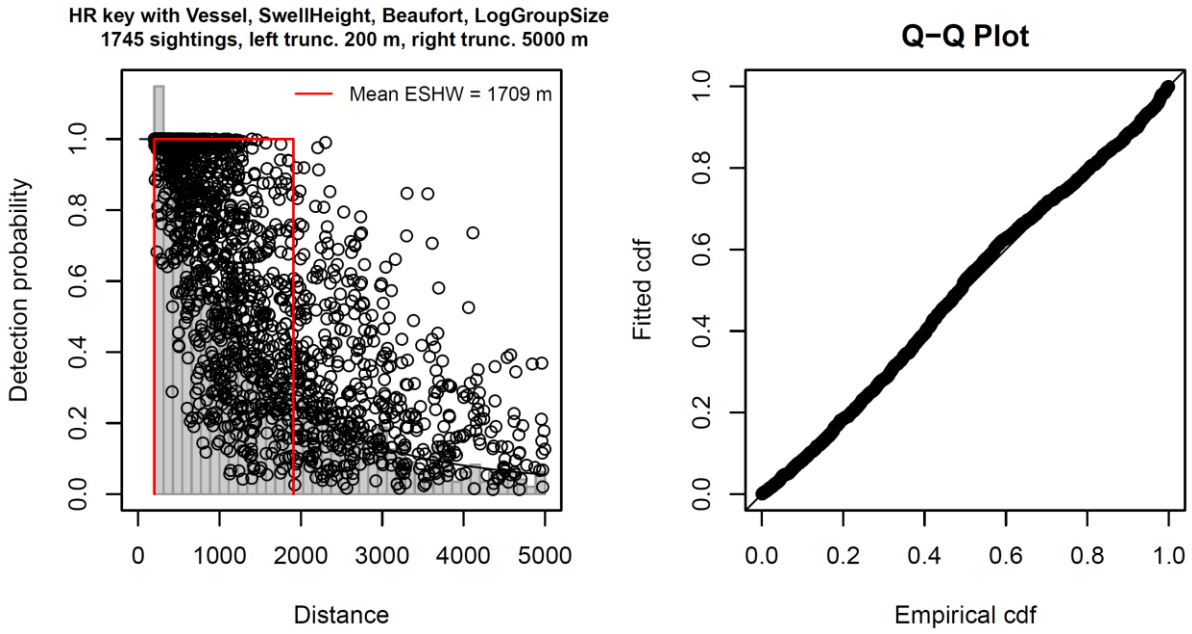

Figure 22. Detection function for problematic dolphin species (Atlantic spotted, Clymene, common bottlenose, pantropical, rough-toothed, and short-beaked common dolphins) sighted on all non-AMAPPS SEFSC shipboard surveys, 1992-2016, in the U.S. Atlantic and Gulf of Mexico.

2.3.2. Availability and perception bias corrections

Through Option Year 1, we relied on availability and perception bias corrections from sources identified during the Phase III modeling cycle. To correct sightings reported on shipboard surveys, for most species we used corrections from Palka's (2006) analysis for the NEFSC surveys analyzed therein, and otherwise used corrections from Barlow and Forney (2007), who drew from a much larger quantity of data, albeit from surveys of the Pacific. For aerial surveys, for small dolphins we largely relied on Palka's (2006) species-generic small cetacean $g(0)$ correction, made from four years of NEFSC aerial surveys. For more information about these estimates, please see Roberts et al. (2016a), especially the supplementary species-specific reports.

At the end of Option Year 1, NEFSC and SEFSC jointly published new availability and perception bias corrections (Palka et al. 2017) derived from AMAPPS surveys from 2010-2013. These researchers derived species-specific availability bias corrections from tagging studies, when available, or from the literature. They derived perception bias corrections specific to species, platform (shipboard or aerial), and team (NEFSC or SEFSC) by conducting AMAPPS surveys with two simultaneously-operating independent observer teams and applying mark-recapture distance sampling (MRDS) methodology (Borchers et al. 1998; Laake & Borchers 2004; Burt et al. 2014).

After discussing these new estimates with model collaborators, principally Debra Palka, who led development of the new estimates, we decided to use them for the Option Year 2 model updates, as they were likely to be both more accurate and more precise than what we used in Phase III. To apply them, we calculated new $g(0)$ corrections, i.e. the probability of observers detecting an animal directly on the survey trackline, corrected for both availability and perception biases, as:

$$g(0) = availability \times p(0)$$

where *availability* for aerial surveys was obtained from Table 5-16 of Palka et al. (2017) and for shipboard surveys was assumed to be 1, following Palka et al. (2017), i.e., small dolphins were assumed to be always available to shipboard observers because of their short dive times. $p(0)$, the perception bias correction, was taken from species-specific tables of MRDS parameter estimates reported in Appendix I of Palka et al. (2017).

We applied the AMAPPS-derived, SEFSC-specific $g(0)$ corrections to all surveys conducted by SEFSC and also to aerial surveys conducted south of Maryland by UNCW and VAMSC. The UNCW and VAMSC surveys were conducted at a higher altitude (1000 ft. vs. 600 ft.) with flat windows and no belly observer. Most likely, the AMAPPS-derived $g(0)$ corrections underestimated perception bias for the UNCW and VAMSC surveys, at least for the bias components relating to altitude and platform configuration. We used a similar approach for the Phase III and Option Year 1 models, in which we applied a correction that Palka (2006) previously derived from earlier NEFSC aerial surveys conducted with AMAPPS-compatible protocols.

We applied the AMAPPS-derived, NEFSC-specific $g(0)$ corrections to all surveys conducted by NEFSC except for the AJ 99-02 survey conducted with naked eye observations (for this we used the AJ 99-02 survey-specific estimates from Palka (2006)). We also applied the AMAPPS-derived, NEFSC-specific corrections to the VAMSC aerial surveys of Maryland, which were conducted using NEFSC's protocol. Finally, we applied the NEFSC corrections to shipboard surveys conducted by NJ-DEP, which used a protocol similar to the NEFSC shipboard 25x binocular surveys. (As noted previously, we did not use the NJ-DEP aerial surveys in the Option Year 2 models.)

2.3.3. Spatial covariates

For the spatial models in our workflow—classification models for ambiguous sightings (Section 2.3.4) and density surface models (Section 2.3.5)—we utilized the same spatial covariates as in Option Year 1, plus one additional covariate (Table 2). To help distinguish the more saline waters within and south of the Gulf Stream with the fresher waters north of Cape Hatteras along the continental shelf, we added a salinity covariate taken from the Hybrid Coordinate Ocean Model (HYCOM) at 0.08° resolution. (The time series consisted of the 1993-2012 reanalysis followed by the ongoing near-real-time model that started in 2012.) This covariate was often selected in density surface models for species that inhabit off-shelf waters north of Cape Hatteras, but not on-shelf waters, such as striped dolphin. Salinity can provide a better distinction between these habitats throughout all seasons than other covariates, such as sea surface temperature (SST) or primary productivity, that are more influenced by insolation.

2.3.4. Classification of ambiguous sightings

Certain marine mammal species look and behave similarly, and unless observers are afforded an opportunity for careful examination, they cannot distinguish between them. In such cases, observers record sightings with ambiguous taxonomic identifications, such as "fin or sei whale". As with the Phase III models, we did not want to exclude these ambiguous sightings from the analysis, as they would represent a significant number of animals that were sighted but not accounted for by the models, potentially biasing abundance low. We handled these sightings specially, based on their degree of ambiguity, with a classification model using the methodology described by Roberts et al. (2016a, 2017). Here, we summarize the results of applying this approach to the odontocete and pinniped species modeled during Option Year 2. Please see the aforementioned documents for details of the methodology.

2.3.4.1. Ambiguous "Short-beaked common or Atlantic white-sided dolphin" sightings

Short-beaked common dolphins (*Delphinus delphis*) and Atlantic white-sided dolphins (*Lagenorhynchus acutus*) can be difficult to distinguish during aerial surveys. The Atlantic white-sided dolphin is a cold-water species; ambiguous "common or white-sided dolphin" sightings were only reported in the northern half of the study area, and only by NEFSC aerial surveys (Table 3). On these surveys, the number of ambiguous sightings reported was nearly twice the number of fully-resolved common dolphin sightings, and about two-thirds the number of fully-resolved white-sided dolphin sightings (Table 3).

For all surveys in aggregate, the seasonal rate of ambiguous sightings ranged from 24-38% (Table 4, Figure 23), with the lowest rate in summer (24%) and the highest in fall (38%). The variation in this rate mainly reflected the ratio of NEFSC NARWSS effort to that of other surveys. The NARWSS program surveyed mainly north of 40°N, where both species are present, maintained some level of surveying throughout the year, and contributed the most sightings of any program. The other programs were most active in summer, resulting in a large number of common dolphin sightings in this season (Table 4) spread down the shelf break (Figure 23).

Table 2. Candidate covariates for the spatial models. All covariates were rescaled to the 10 km Albers equal area map projection used for the analysis. Each model only considered the covariates that were appropriate for the modeled region and known ecology of the taxon. All covariates were available in contemporaneous and climatological formulations; in later sections of this report, covariates prefaced by "Clim" refer to the climatological formulation.

Type	Covariates	Resolution	Time range	Description
Static	Depth, Slope	30 arc sec		Seafloor depth and slope, derived from SRTM30-PLUS global bathymetry (Becker et al. 2009)
	DistToShore, DistTo125m, DistTo300m, DistTo1500m	30 arc sec		Distance to the closest shoreline, excluding Bermuda and Sable Island, and various ecologically-relevant isobaths, derived from SRTM30-PLUS (Becker et al. 2009)
	DistToCan, DistToCanOrSmt	30 arc sec		Distance to the closest submarine canyon, and to the closest canyon or seamount, derived from Harris et al. (2014)
Physical oceanographic	SST, DistToFront	0.2°, daily	1991-2016	Foundation sea surface temperature (SST), from GHRSST Level 4 CMC SST (Brasnett 2008), and distance to the closest SST front identified with Canny's (1986) algorithm
	TKE, EKE	0.25°, daily	1993-2016	Total kinetic energy (TKE) and eddy kinetic energy (EKE), from Aviso 1/4° DT-MADT/MSLA geostrophic currents
	DistToEddy, DistToAEddy, DistToCEddy	0.25°, weekly	1993-2016	Distance to the ring of the closest geostrophic eddy having any (DistToEddy), anticyclonic (DistToAEddy), or cyclonic (DistToCEddy) polarity, from Aviso 1/4° DT-MADT using a revision of Chelton et al.'s (2011) algorithm; we tested eddies at least 9, 4, and 0 weeks old
	FSLE	0.04°, 5-day	1994-2015	Backward-in-time Finite Size Lyapunov Exponents (FSLE) (d'Ovidio et al. 2004) from AVISO 1/4° sea surface altimetry
	Salinity	0.08°, daily	1993-2016	Sea surface salinity from the HYCOM model (Bleck 2002)
	WindSpeed	0.25°, 6-hour	1991-2016	Wind speed from L3.0 Cross-Calibrated Multi-Platform (CCMP) Version 2.0 gridded surface vector winds (Atlas et al. 2011); we tested 1, 5, 15, and 30-day running means
Biological	Chl	9 km, daily	1997-2014	GSM merged SeaWiFS/Aqua/MERIS/VIIRS chlorophyll (Chl) *a* concentration (Maritorena et al. 2010), smoothed with a 3D Gaussian smoother to reduce data loss to < 10%
	VGPM, CumVGPM45, CumVGPM90	9 km, 8 days	1997-2014	Net primary production (mg C m^{-2} day^{-1}) derived from SeaWiFS and Aqua using the Vertically Generalized Production Model (VPGM) (Behrenfeld & Falkowski 1997); we tested the original 8 day estimates as well as 45 and 90 day running accumulations
	PkPP, PkPB	0.25°, weekly	1997-2013	Zooplankton production (PkPP; g m^{-2} day^{-1}) and biomass (PkPB; g m^{-2}) from the SEAPODYM model (Lehodey et al. 2010)
	EpiMnkPP, EpiMnkPB	0.25°, weekly	1997-2013	Epipelagic micronekton production (EpiMnkPP; g m^{-2} day^{-1}) and biomass (EpiMnkPB; g m^{-2}) from the SEAPODYM model (Lehodey et al. 2010)

Table 3. Summary of short-beaked common dolphin and Atlantic white-sided dolphin sightings, 1992-2016, available for the updated models. "Extant" sightings were used in the Phase III regional model (Roberts et al. 2016a). "Added" sightings were incorporated during the Base Year and Option Year 1 for the updated model.

			Common dolphin			White-sided dolphin			Ambiguous		
Platform	Provider	Program	Extant	Added	Total	Extant	Added	Total	Extant	Added	Total
Aerial	NEFSC	Marine mammal abundance surveys	304	100	404	218	101	319	9	14	23
		NARWSS harbor porpoise survey	5		5	31		31			
		NARWSS right whale surveys	345	130	475	1456	639	2095	892	641	1533
	NJDEP	New Jersey Ecological Baseline Study	5		5						
	SEFSC	Marine mammal abundance surveys	3	107	110						
	UNCW	Cape Hatteras Navy Surveys	12	10	22						
		Marine mammal surveys, 2002	4		4						
		Norfolk Canyon Navy Surveys		28	28						
		Onslow Bay Navy Surveys	1		1						
		Right whale surveys, 2005-2008	26		26						
	VAMSC	MD Wind Energy Area surveys		22	22						
		VA Wind Energy Area surveys	25		25						
	All		730	397	1127	1705	740	2445	901	655	1556
Shipboard	NEFSC	Marine mammal abundance surveys	173	258	431	42	22	64			
	NJDEP	New Jersey Ecological Baseline Study	19		19						
	SEFSC	Marine mammal abundance surveys	36	7	43						
	All		228	265	493	42	22	64			

Table 4. Seasonal distribution of short-beaked common dolphin (*D. delphis*) and Atlantic white-sided dolphin (*L. acutus*) sightings used in the classification model. (A single model was fitted to all sightings, but we break them out by season here to illustrate seasonal variations.) We trained the model on the fully-resolved sightings (first two rows) and predicted it on the ambiguous sightings (third row). Note that a small number of the fully-resolved sightings listed in Table 3 above were dropped from the model because of missing covariate values. Season definitions used in this table: Winter: Jan-Mar; Spring: Apr-Jun; Summer: Jul-Sep; Fall: Oct-Dec.

Identification	Winter	Spring	Summer	Fall
D. delphis	229	361	868	162
L. acutus	172	793	1271	275
Ambiguous	160	463	662	271
% Ambiguous	29 %	29 %	24 %	38 %

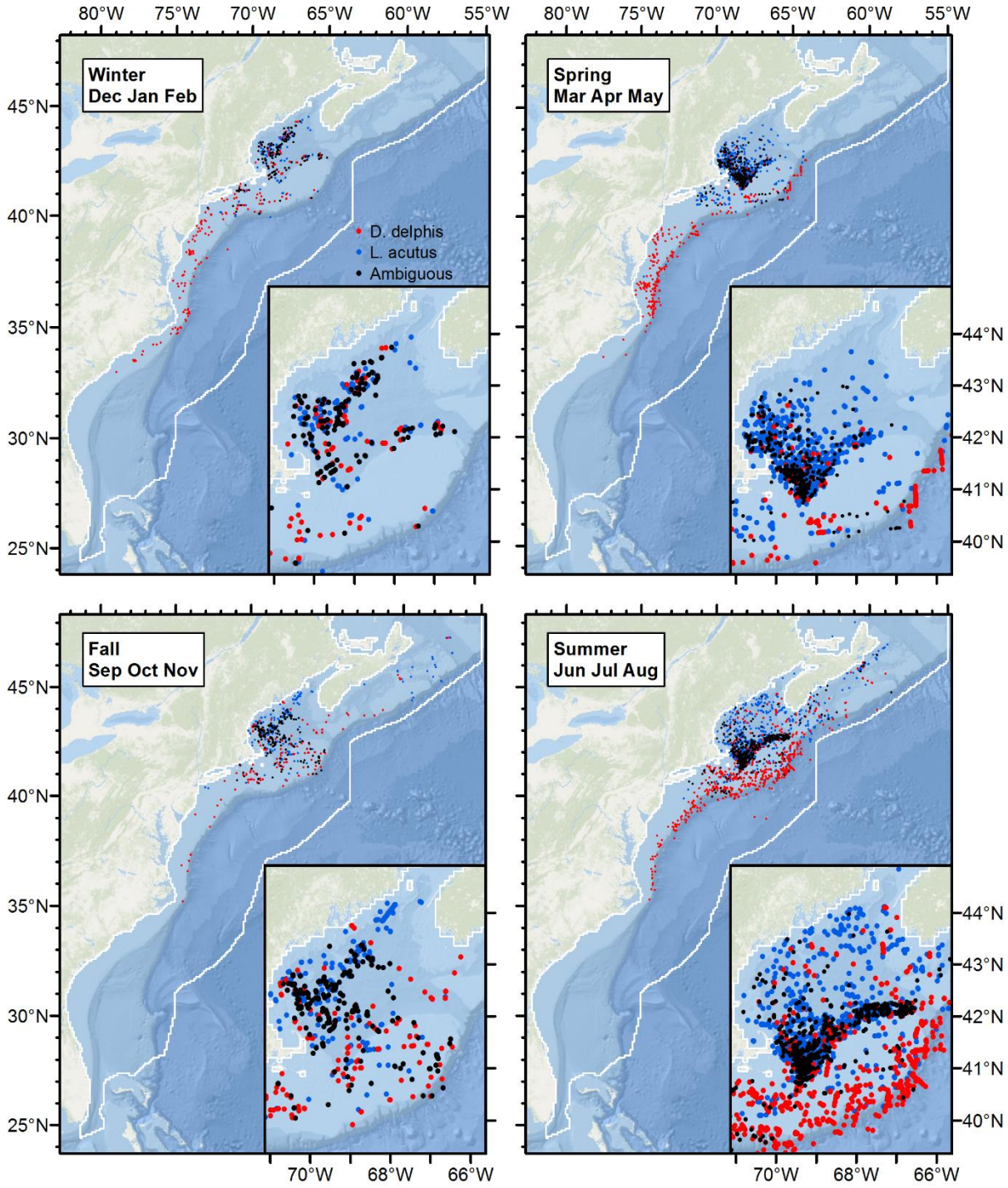

Figure 23. Seasonal maps of the short-beaked common dolphin (*D. delphis*) and Atlantic white sided dolphin (*L. acutus*) sightings summarized in Tables 3 and 4. (A single model was fitted to all sightings, but we break them out by season here to illustrate seasonal variations.)

The most important covariates identified by the classification model were distance to the 300m isobath (representing the continental shelf break), zooplankton biomass, and distance to SST fronts (Figs. 25, 26). Sightings closer to the 300m isobath, in areas of lower zooplankton biomass (e.g. not in the Gulf of Maine basins where zooplankton aggregate), and closer to SST fronts were more likely to be common dolphins (Figure 24). For the training data, the area under the ROC curve (Figure 25) (AUC) statistic was 0.913, slightly higher than what was obtained with the Phase III classification model. At the selected threshold (a.k.a. cutoff) value of 0.597, the misclassification rate for common dolphins was 10.9% and for white-sided dolphins was 7.0%.

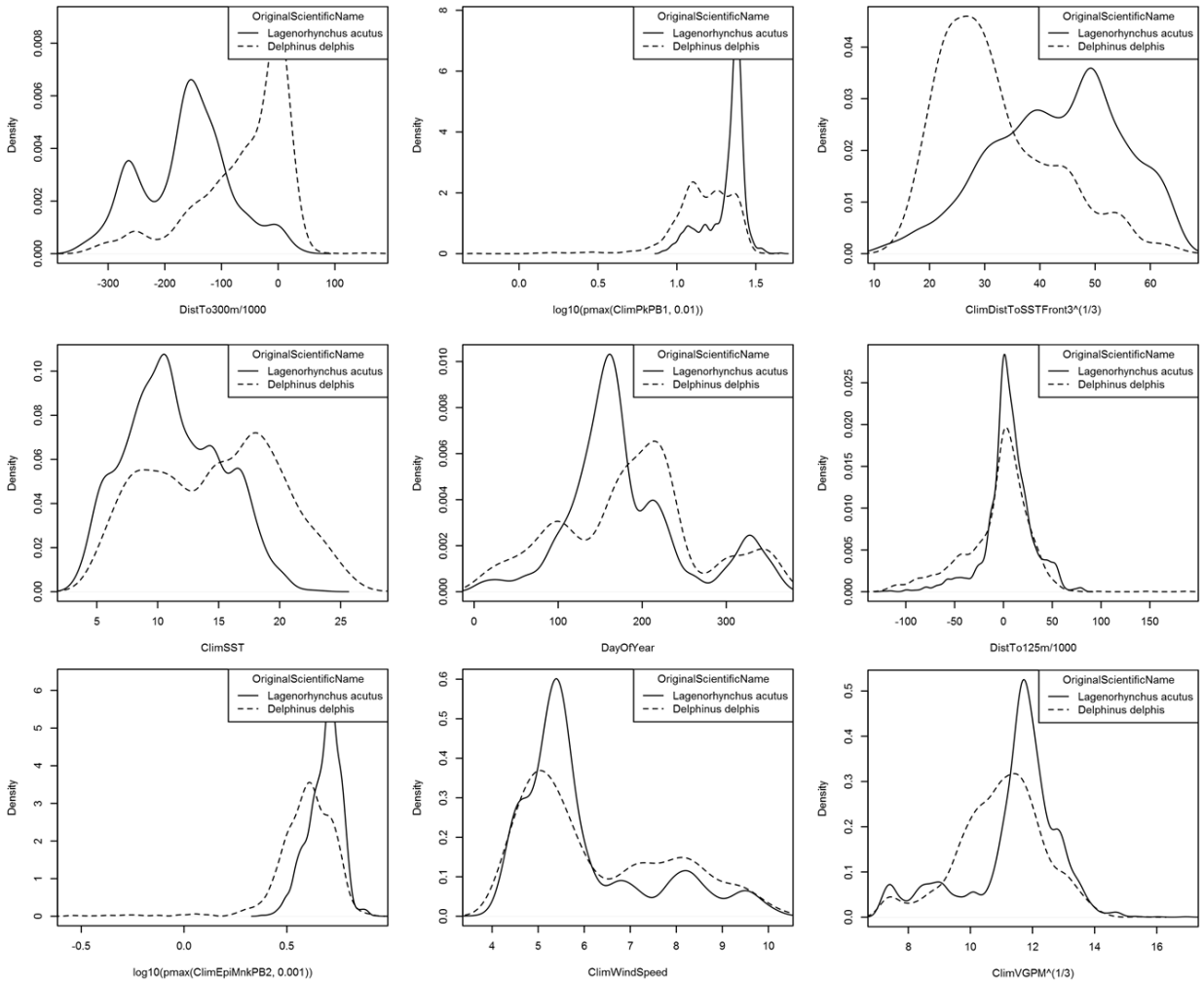

Figure 24. Density histograms for fully-resolved short-beaked common dolphin (*D. delphis*) and Atlantic white-sided dolphin (*L. acutus*) sightings for the nine most important covariates (ranked by the cforest *varimp* function).

```
Random Forest using Conditional Inference Trees
(cforest function from R party package 1.2-3)

Number of trees:  1000

Response:  factor(OriginalScientificName)
Inputs:  ClimChl1, ClimDistToSSTFront3,
ClimEpiMnkPB2, ClimFSLE, ClimPkPB1, ClimSST,
ClimVGPM, ClimWindSpeed, DayOfYear, Depth,
DistTo125m, DistTo300m, Slope
Number of observations:  4131

Number of variables tried at each split: 5

Estimated predictor variable importance
(conditional = FALSE):

                    Importance
DistTo300m              0.1059
ClimPkPB1               0.0585
ClimDistToSSTFront3     0.0469
ClimSST                 0.0304
DayOfYear               0.0275
DistTo125m              0.0201
ClimEpiMnkPB2           0.0195
ClimWindSpeed           0.0184
ClimVGPM                0.0129
ClimFSLE                0.0128
Depth                   0.0112
ClimChl1                0.0109
Slope                   0.0100
```

```
Statistics calculated from the training data.

Area under the ROC curve (auc) = 0.974

User-specified model cutoff = 0.597

L. acutus correct (true positive rate)  = 0.913
L. acutus wrong (false negative rate)   = 0.070
D. delphis correct (true negative rate) = 0.891
D. delphis wrong (false positive rate)  = 0.109

Cohen's kappa (K) = 0.821

                        Actual L. acutus  Actual D. delphis  Total
Predicted L. acutus                 2335                176   2511
Predicted D. delphis                 176               1444   1620
Total                               2511               1620   4131
```

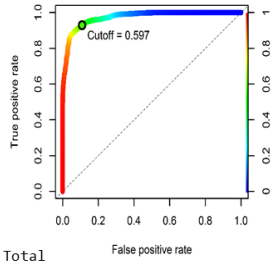

Figure 25. Statistical output from the short-beaked common dolphin (*D. delphis*) and Atlantic white-sided dolphin (*L. acutus*) classification model.

When we applied the classification model to the ambiguous sightings, it predicted 1268 white-sided dolphins and 288 common dolphins, a ratio of 4.40 (Table 5). In the fully-resolved sightings used to train the model, the ratio was only 1.55. By comparison, the Phase III model predicted a ratio of 2.44 for the ambiguous sightings vs. a ratio of 1.96 in that model's training data. For both models, we attribute the differences in ratios between the ambiguous sightings and the fully-resolved sightings to differences in geographical distributions in these sightings. The fully-resolved sightings were more spread out, with large numbers of common dolphins reported along the shelf break and across the shelf in the mid-Atlantic (Figure 26). By contrast, the ambiguous sightings were concentrated in northern colder waters, in the Gulf of Maine and over Georges Bank. Our models and prior analysis (Selzer & Payne 1988) indicated that these colder waters are better habitat for white-sided dolphins, thus it follows that most of the ambiguous sightings would be classified as white-sided dolphins. The increase in the white-sided/common ratio in the new model relative to the Phase III model follows from the large quantity of additional NEFSC aerial surveys (NARWSS and AMAPPS) incorporated for the new model, relative to surveys conducted in more southerly waters.

Table 5. Seasonal distribution of the predictions made by applying the short-beaked common dolphin (*D. delphis*) and Atlantic white-sided dolphin (*L. acutus*) classification model to the ambiguous sightings. Season definitions used in this table: Winter: Jan-Mar; Spring: Apr-Jun; Summer: Jul-Sep; Fall: Oct-Dec.

Identification	Winter	Spring	Summer	Fall	Total
Predicted *L. acutus*	99	439	536	194	1268
Predicted *D. delphis*	61	24	126	77	288
Total	160	463	662	271	1556

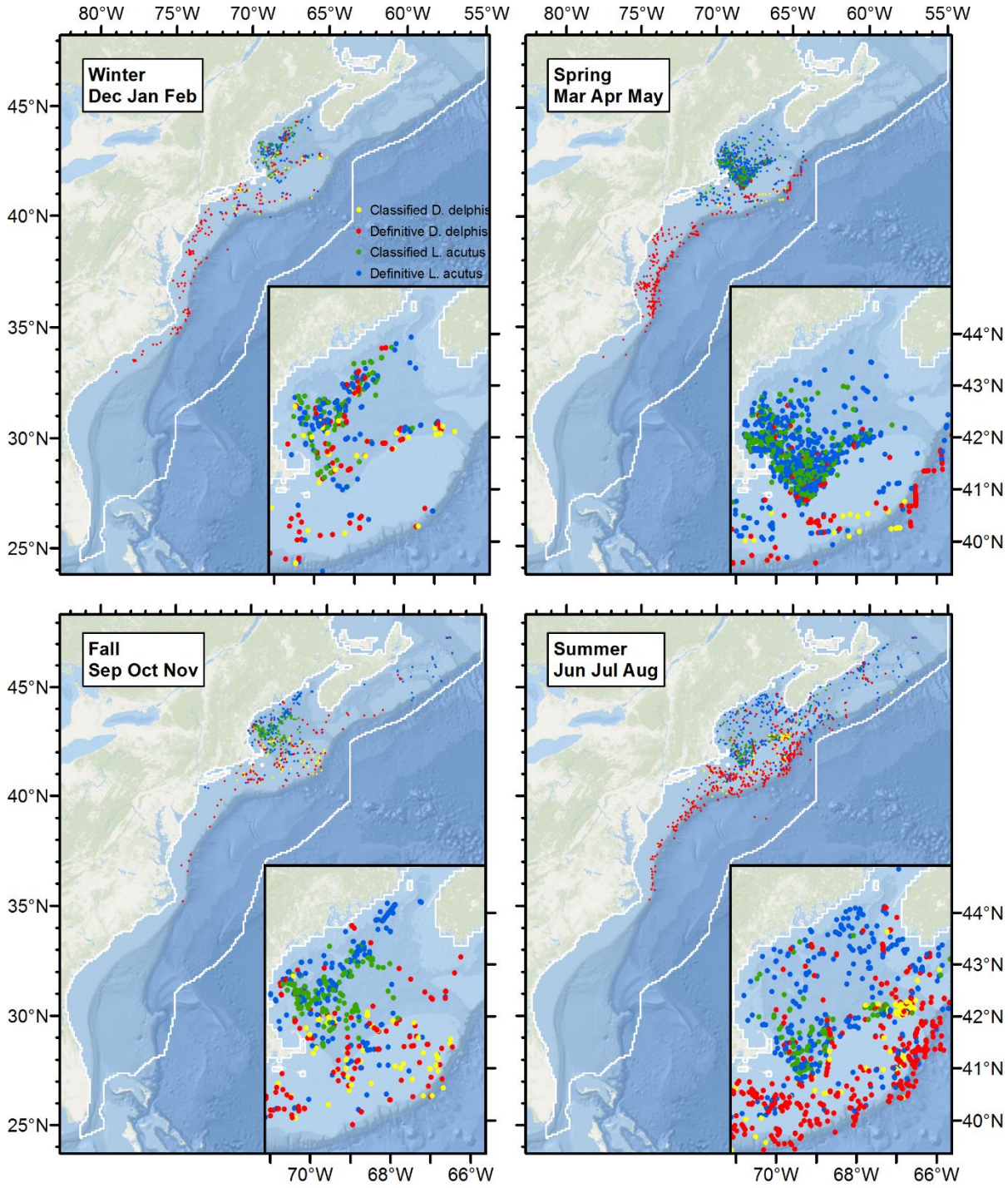

Figure 26. Seasonal maps of fully-resolved sightings of short-beaked common dolphins (*D. delphis*) (red) and Atlantic white-sided dolphins (*L. acutus*) (blue), along with ambiguous sightings classified as short-beaked common dolphins (yellow) and Atlantic white-sided dolphins (green).

2.3.4.2. Ambiguous "Atlantic spotted or common bottlenose dolphin" sightings

Atlantic spotted dolphins (*Stenella frontalis*) and common bottlenose dolphins (*Tursiops truncatus*) can be difficult to distinguish. On the U.S. east coast, Atlantic spotted dolphins tend to avoid colder waters; accordingly, ambiguous "Atlantic spotted or bottlenose dolphin" sightings were only reported in the southern half of the study area, and only by SEFSC surveys (Table 7). South of Cape Hatteras, both species occur year-round in large numbers, with bottlenose dolphins dominating waters close to shore and along the shelf break and slope and Atlantic spotted dolphins "sandwiched" between them over the mid-shelf (Figure 27). It is within this mid-shelf area that most of the ambiguous sightings were reported. North of Cape Hatteras, both species occur seasonally on the mid-Atlantic shelf, with bottlenose dolphins heavily dominating nearshore waters and the shelf-break. Distant off-shelf areas north of Cape Hatteras were only surveyed in summer; here, surveys reported more Atlantic spotted dolphins. This alternating pattern of species dominance by depths—nearshore: bottlenose; mid-shelf: spotted; shelf-break: bottlenose; offshore: spotted—can also be observed in histograms showing the relative density of sightings by depth (Figure 28, bottom right).

For all surveys in aggregate, the seasonal rate of ambiguous sightings ranged from only 1.6-2.6% (Table 7), with the lowest rate in spring (1.6%) and the highest in fall (2.6%). These low rates raised the question of whether it was worth it to build a classification model rather than just ignore these sightings. For bottlenose dolphins, it was probably not worth it. The number of ambiguous sightings was only 2.6% the number of fully-resolved bottlenose dolphin sightings. Thus if all of the ambiguous sightings were bottlenose dolphins, ignoring them would likely bias abundance low by only a few percent, at most. But the number of ambiguous sightings was 12.7% of the number of fully-resolved Atlantic spotted dolphin sightings. We judged that fraction high enough to warrant building a classification model.

The most important covariates identified by the model were chlorophyll concentration, cumulative primary productivity over the last 45 days, and slope (Figs. 29, 30). Bottlenose dolphin sightings occurred more frequently in areas of higher chlorophyll concentration, primary productivity, and slope, reflecting the large number of sightings close to shore (where productivity is high) and the shelf break (where slope is high). For the training data, the AUC statistic was 0.969 (Figure 29), slightly lower than what was obtained with the Phase III classification model. At the selected threshold value of 0.562, the misclassification rate for bottlenose dolphins was 4.3% and for Atlantic spotted dolphins was 22.3%.

The markedly higher misclassification rate for Atlantic spotted dolphins resulted from our strategy of tuning the threshold such that when the model is applied to the training data, the predicted number of sightings for each species is the same as the observed number of sightings, to try to avoid biasing overall abundance when the model is applied to the ambiguous sightings. This differs from the strategy taken in Phase III, which tuned the threshold to minimize overall error in the model. In that model, misclassifications were about twice as high for bottlenose dolphins (8.5%) but only one quarter as high for Atlantic spotted dolphins (5.8%). Although this seemed like a good tradeoff, when the model was applied to the training data, it predicted 1138 Atlantic spotted dolphins when only 804 were sighted. We presume this resulted in a similar bias when the model was applied to the ambiguous sightings in Phase III—i.e. that more ambiguous sightings were classified as Atlantic spotted dolphins than should have been. In the updated model we attempted to reduce this potential bias. For more discussion of this approach, please see Roberts et al. (2017).

Table 6. Summary of Atlantic spotted dolphin and common bottlenose dolphin sightings, 1992-2016, available for the updated models. "Extant" sightings were used in the Phase III regional model (Roberts et al. 2016a). "Added" sightings were incorporated during the Base Year and Option Year 1 for the updated model.

			Atl. spotted dolphin			Bottlenose dolphin			Ambiguous		
Platform	Provider	Program	Extant	Added	Total	Extant	Added	Total	Extant	Added	Total
Aerial	NEFSC	Marine mammal abundance surveys	1		1	99	54	153			
		NARWSS right whale surveys				47	33	80			
	NJDEP	New Jersey Ecological Baseline Study				91		91			
	SEFSC	Marine mammal abundance surveys	110	96	206	859	684	1543	54	51	105
	UNCW	Cape Hatteras Navy Surveys	19	25	44	113	145	258			
		Jacksonville Navy Surveys	267	63	330	325	87	412			
		Marine mammal surveys, 2002	1		1	308		308			
		Norfolk Canyon Navy Surveys		27	27		52	52			
		Onslow Bay Navy Surveys	65		65	149		149			
		Right whale surveys, 2005-2008	5		5	1817		1817			
	VAMSC	MD Wind Energy Area surveys		1	1		270	270			
		VA Wind Energy Area surveys	1	2	3	118	30	148			
	All		469	214	683	3926	1355	5281	54	51	105
Shipboard	NEFSC	Marine mammal abundance surveys	16	42	58	177	177	354			
	NJDEP	New Jersey Ecological Baseline Study				160		160			
	SEFSC	Marine mammal abundance surveys	319	114	433	356	154	510	33	11	44
	All		335	156	491	693	331	1024	33	11	44

Table 7. Seasonal distribution of Atlantic spotted dolphin (*S. frontalis*) and common bottlenose dolphin (*T. truncatus*) sightings used in the classification model. (A single model was fitted to all sightings, but we break them out by season here to illustrate seasonal variations.) We trained the model on the fully-resolved sightings (first two rows) and predicted it on the ambiguous sightings (third row). Note that a small number of the fully-resolved sightings listed in Table 6 above were dropped from the model because of missing covariate values. Season definitions used in this table: Winter: Jan-Mar; Spring: Apr-Jun; Summer: Jul-Sep; Fall: Oct-Dec.

Identification	Winter	Spring	Summer	Fall
T. truncatus	1685	1855	2094	514
S. frontalis	186	238	588	172
Ambiguous	43	33	55	18
% Ambiguous	2.2 %	1.6 %	2.0 %	2.6 %

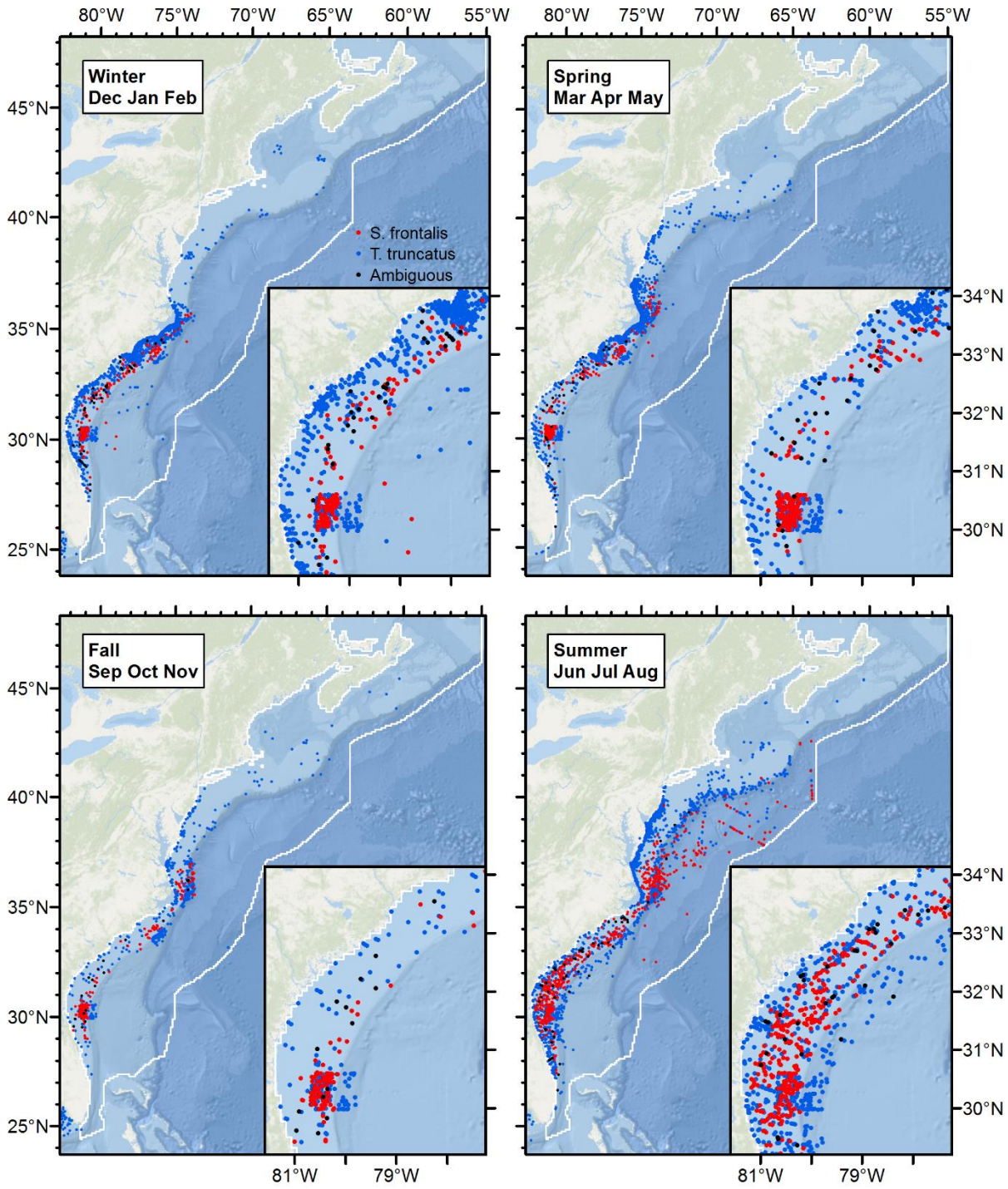

Figure 27. Seasonal maps of the Atlantic spotted dolphin (*S. frontalis*) and common bottlenose dolphin (*T. truncatus*) sightings summarized in Tables 6 and 7. (A single model was fitted to all sightings, but we break them out by season here to illustrate seasonal variations.)

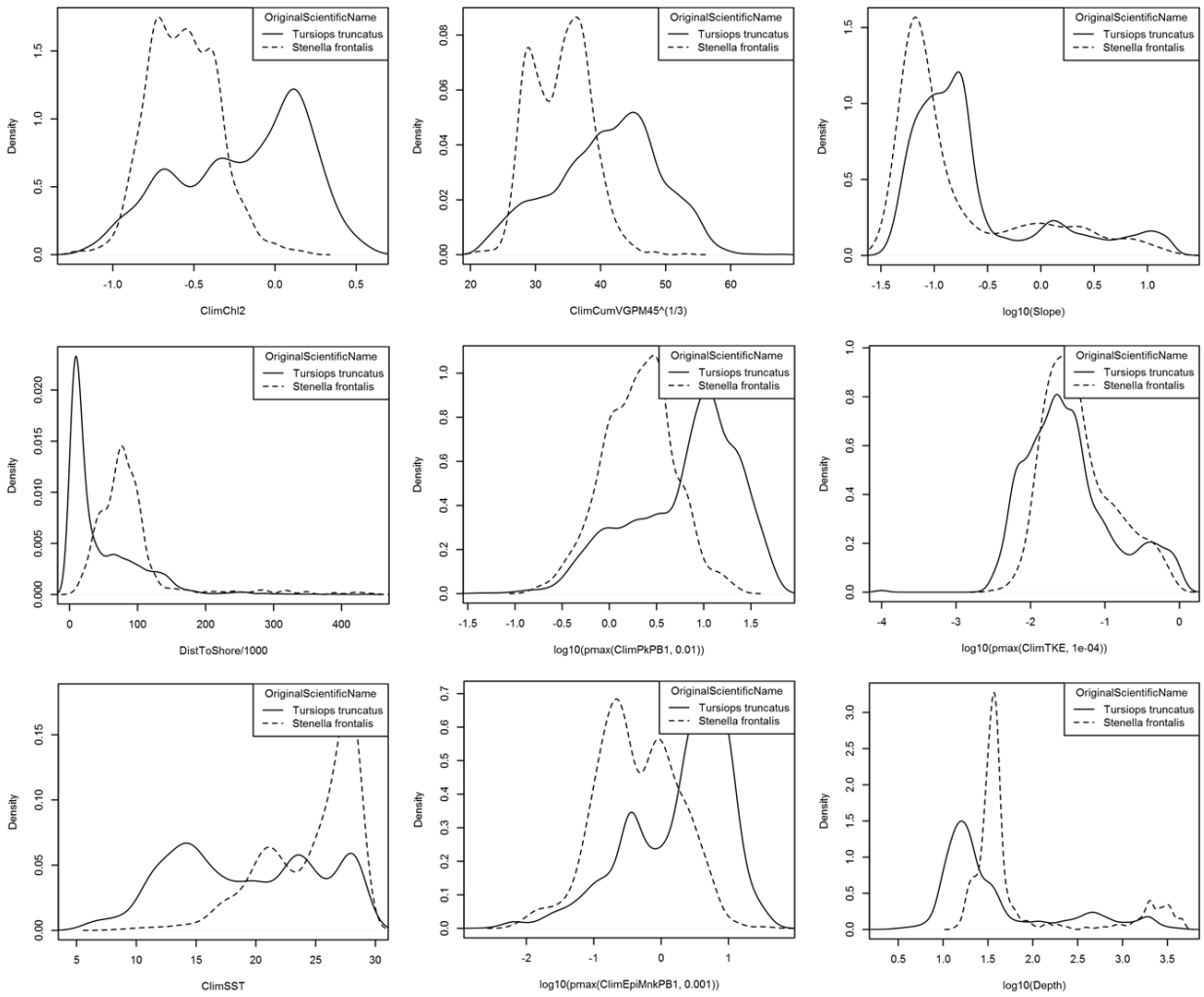

Figure 28. Density histograms for fully-resolved Atlantic spotted dolphin (*S. frontalis*) and common bottlenose dolphin (*T. truncatus*) sightings for the nine most important covariates (ranked by the cforest *varimp* function).

```
Random Forest using Conditional Inference Trees
(cforest function from R party package 1.2-3)

Number of trees:  900

Response:  factor(OriginalScientificName)
Inputs:  ClimChl2, ClimCumVGPM45, ClimDistToAEddy,
ClimDistToCEddy, ClimDistToSSTFront1, ClimEpiMnkPB1, ClimFSLE,
ClimPkPB1, ClimSST, ClimTKE, ClimWindSpeed30Day, Depth,
DistTo125m, DistTo300m, DistToShore, Slope
Number of observations:  7322

Number of variables tried at each split: 5

Estimated predictor variable importance (conditional = FALSE):

                  Importance
ClimChl2             0.01917
ClimCumVGPM45        0.01584
Slope                0.01548
DistToShore          0.01387
ClimPkPB1            0.01345
ClimTKE              0.01328
ClimSST              0.01111
ClimEpiMnkPB1        0.00929
Depth                0.00703
DistTo125m           0.00608
DistTo300m           0.00584
ClimDistToAEddy      0.00508
ClimDistToCEddy      0.00443
ClimDistToSSTFront1  0.00397
ClimWindSpeed30Day   0.00378
ClimFSLE             0.00339
```

```
Statistics calculated from the training data.

Area under the ROC curve (auc) = 0.969

User-specified model cutoff = 0.562

T. truncatus correct (true positive rate) = 0.957
T. truncatus wrong (false negative rate)  = 0.043
S. frontalis correct (true negative rate) = 0.777
S. frontalis wrong (false positive rate)  = 0.223

Cohen's kappa (K) = 0.734

                         Actual T. truncatus  Actual S. frontalis  Total
Predicted T. truncatus                  5886                  262   6148
Predicted S. frontalis                   262                  912   1174
Total                                   6148                 1174   7322
```

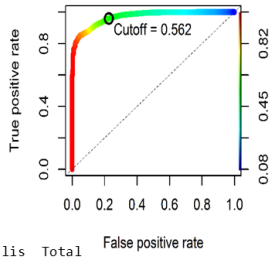

Figure 29. Statistical output from the Atlantic spotted dolphin (*S. frontalis*) and common bottlenose dolphin (*T. truncatus*) classification model.

When we applied the classification model to the ambiguous sightings, it predicted 109 bottlenose dolphins and 40 Atlantic spotted dolphins, a ratio of 2.73 (Table 8). In the fully-resolved sightings used to train the model, the ratio was 5.24. By comparison, the Phase III model predicted a ratio of 1.96 vs. a ratio of 5.55 in that model's training data. For both models, we attributed the differences in ratios between the ambiguous sightings and the fully-resolved sightings to differences in geographical distributions in these sightings. The fully-resolved sightings concentrated in areas where habitat characteristics strongly favored one species over the other, such as areas close to shore, where bottlenose dolphins predominate, or far offshore, where Atlantic spotted dolphins are more likely to occur in large groups. By contrast, the ambiguous sightings mostly occurred over the mid-shelf of the southeast (Figure 30, inset maps), where the species' habitats overlap and Atlantic spotted dolphins are more comparable in size to the bottlenose dolphins occurring there, and often occur in smaller groups, making group size less reliable for distinguishing the species. The increase in the bottlenose/Atlantic spotted ratio with the new model resulted from our change in strategy in selecting the classification threshold, with the new approach yielding more bottlenose dolphins than the Phase III approach.

Table 8. Seasonal distribution of the predictions made by applying the Atlantic spotted dolphin (*S. frontalis*) and common bottlenose dolphin (*T. truncatus*) classification model to the ambiguous sightings. Season definitions used in this table: Winter: Jan-Mar; Spring: Apr-Jun; Summer: Jul-Sep; Fall: Oct-Dec.

Identification	Winter	Spring	Summer	Fall	Total
Predicted *T. truncatus*	36	26	37	10	109
Predicted *S. frontalis*	7	7	18	8	40
Total	43	33	55	18	149

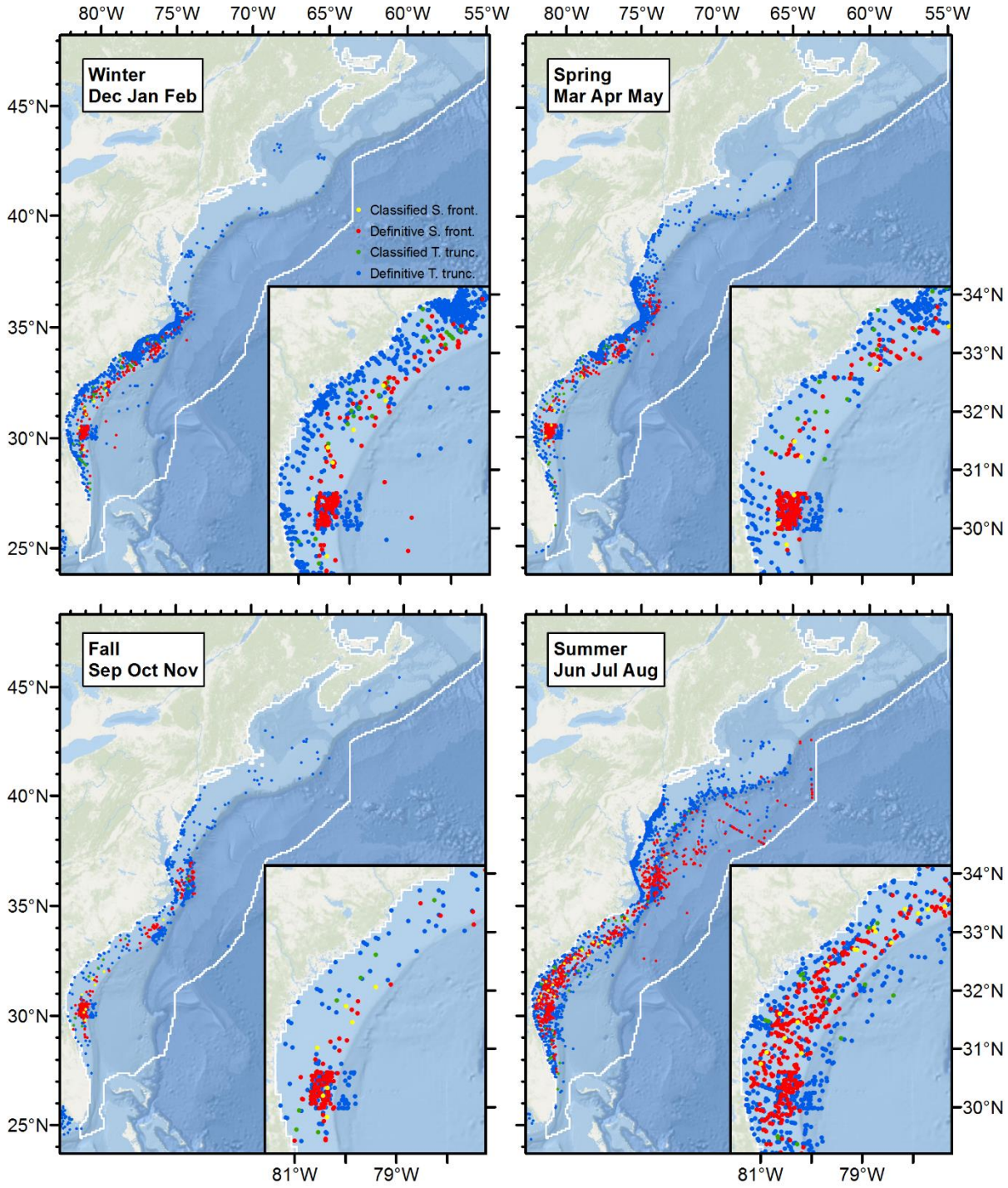

Figure 30. Seasonal maps of fully-resolved sightings of Atlantic spotted dolphins (red) and common bottlenose dolphins (blue), along with ambiguous sightings classified as Atlantic spotted (yellow) and common bottlenose dolphins (green).

2.3.4.3. *Ambiguous "Dwarf or pygmy sperm whale" (Kogia spp.) sightings*

The two extant species of *Kogia*, the dwarf sperm whale (*Kogia sima*) and the pygmy sperm whale (*Kogia breviceps*), are very difficult for observers to distinguish at sea (Jefferson & Schiro 1997). In the surveys available for modeling in Phase III, very few were reported with identifications fully-resolved to the species level. Instead, most were either reported as "*Kogia spp.*" or, during NEFSC surveys, occasionally as "unidentified small whale" (D. Palka, pers. comm.). The number of fully-resolved sightings was too low to attempt a classification so we modeled the density of the two *Kogia* species together as a guild.

After the Phase III models were complete, NEFSC and SEFSC contributed the 2010-2015 surveys from the AMAPPS I program, which we incorporated during the Base Year and Option Year 1. During AMAPPS I, NEFSC undertook a special effort to fully identify all *Kogia* using new techniques (D. Palka, pers. comm.), resulting in an increased number of fully-resolved sightings (Table 9). This raised the prospect of building a classification model in Option Year 2 but we declined to do so, for several reasons.

Despite the increase in fully-resolved sightings, the majority of sightings were still ambiguous identifications. In total, there were less than 50 fully-resolved sightings, which we judged was only enough to fit a classification model of one or two variables. Although the fully-resolved sightings showed the possibility of a difference in habitat between the two species, with more pygmy sperm whales (*K. breviceps*) appearing in the north and dwarf sperm whales (*K. sima*) appearing in the south of NEFSC's survey area, there was also substantial overlap. In several cases, the two species were sighted on the same day within 10 km of each other, making them virtually indistinguishable geographically, temporally, and in covariate space. Finally, while SEFSC's AMAPPS surveys reported *Kogia* at a higher rate than previous SEFSC surveys (more sightings per kilometer surveyed), virtually all SEFSC sightings were ambiguous, both before and during AMAPPS I (Table 9). Because NEFSC and SEFSC survey different areas, this led to a geographic bias in the availability of fully-resolved sightings, with almost none available south of Chesapeake Bay (Figure 31).

Given these complications, we did not try to classify ambiguous *Kogia* sightings but instead modeled the ambiguous and fully-resolved sightings together as a guild, as we did for Phase III. Please see Section 2.3.5.11 below for details. Perhaps as more fully-resolved sightings are collected in future surveys, a classification model may become possible. To facilitate this, we urge additional collaboration between NEFSC and SEFSC, so that techniques for fully-identifying *Kogia*, such as those suggested by Keenan-Bateman et al. (2016), may be shared across teams.

Table 9. Dwarf and pygmy sperm whale (*Kogia spp.*) sightings, 1992-2016. "Extant" sightings were used in the Phase III regional model (Roberts et al. 2016a). "Added" sightings were incorporated during the Base Year and Option Year 1 for the updated model.

			Dwarf sperm whale			Pygmy sperm whale			Ambiguous		
Platform	Provider	Program	Extant	Added	Total	Extant	Added	Total	Extant	Added	Total
Aerial	NEFSC	Marine mammal abundance surveys							1		1
	UNCW	Cape Hatteras Navy Surveys							1	3	4
		Jacksonville Navy Surveys							1		1
	All								3	3	6
Shipboard	NEFSC	Marine mammal abundance surveys	1	19	20	3	20	23	7	8	15
	SEFSC	Marine mammal abundance surveys	3	2	5				14	29	43
	All		4	21	25	3	20	23	21	37	58

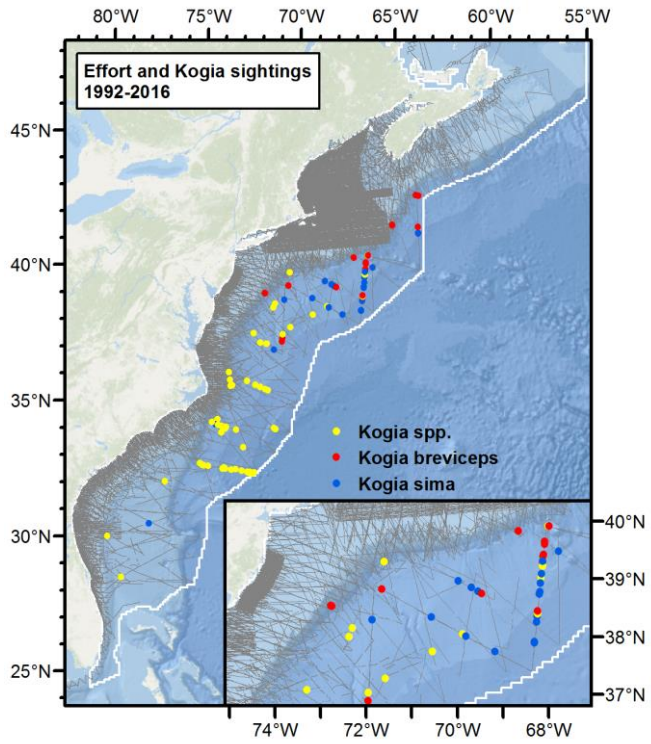

Figure 31. Dwarf (*K. sima*) and pygmy sperm whale (*K. breviceps*) sightings, 1992-2016, color coded by taxonomic identification.

2.3.4.4. Ambiguous "Unidentified seal" sightings

Seals in the water are very difficult for aerial observers to identify. In the Phase III analysis, only 22% of seal sightings were fully identified to the species level, while the remaining 78% were "unidentified seal" (Table 10). The surveys added after the Phase III contributed a large number of additional "unidentified seal" sightings, reducing the fraction that were fully identified to 15%. With so few fully identified sightings, we did not try to classify ambiguous seal sightings but instead modeled the ambiguous and fully-resolved sightings together as a guild, as we did for Phase III. Please see Section 2.3.5.12 below for details.

Table 10. Seal sightings, 1992-2016. "Extant" sightings were used in the Phase III regional model (Roberts et al. 2016a). "Added" sightings were incorporated during the Base Year and Option Year 1 for the updated model. Only a subset of these were used for the updated model (see Section 2.3.5.12 below).

			Harbor seal			Gray seal			Unidentified seal		
Platform	Provider	Program	Extant	Added	Total	Extant	Added	Total	Extant	Added	Total
Aerial	NEFSC	Marine mammal abundance surveys	145	4	149	3	7	10	20	180	200
		NARWSS harbor porpoise survey							22		22
		NARWSS right whale surveys				2	2	4	848	449	1297
	All		145	4	149	5	9	14	890	629	1519
Shipboard	NEFSC	Marine mammal abundance surveys	80	4	84	21	8	29	1	1	2
	NJDEP	New Jersey Ecological Baseline Study	1		1				2		2
	All		81	4	85	21	8	29	3	1	4

2.3.5. Density surface models

Here, we discuss the 11 density surface models we newly introduced or substantially revised during Option Year 2. (As noted previously, we omit discussion of the corrected fin and sei whale models; please see the Option Year 1 report (Roberts et al. 2017) for details of those models.) We start by describing general methodological improvements that applied to all models, then discuss each model in detail.

2.3.5.1. General methodological improvements

2.3.5.1.1 Salinity covariate

To help distinguish the more saline waters within and south of the Gulf Stream with the fresher waters north of Cape Hatteras along the continental shelf, we added a salinity covariate taken from the Hybrid Coordinate Ocean Model (HYCOM) at 0.08° resolution. (The time series consisted of the 1993-2012 reanalysis followed by the ongoing near-real-time model that started in 2012.) This covariate was often selected in models of species such as striped dolphin that inhabit off-shelf waters north of Cape Hatteras, but not on-shelf waters. Salinity can provide a better distinction between these habitats throughout all seasons than other covariates, such as sea surface temperature (SST) or primary productivity, that are more influenced by insolation.

2.3.5.1.2 Increased flexibility with subregional models

To better model species that switch habitat preferences during different seasons or subregions of the study area (e.g. right whales breeding at calving grounds or overwintering at feeding grounds), our modeling framework allows the year to be split into arbitrary "seasons" at monthly boundaries, the study area to be subdivided into subregions, and independent models to be fitted to each season-subregion combination. Then, when predictions are made and summarized into climatologies of density, for each season we can choose between models fitted with contemporaneous or climatological habitat covariates and whether the predictions should be summarized into monthly density surfaces or a single, season-long density surface. For the models produced through Option Year 1, our framework limited these choices to the season; all subregions defined for a season were required to be predicted and summarized the same way. In Option Year 2, we enhanced the framework to allow these choices to be made on a per-subregion basis as well. This was done to allow the on-shelf and oceanic populations of Atlantic spotted dolphins, which have been shown to be genetically distinct, to be modeled, predicted, and summarized differently. Please see the discussion of the Atlantic spotted dolphin models below for more details.

2.3.5.2. Striped dolphin model

Striped dolphins (*Stenella coeruleoalba*) are found throughout the world in tropical and warm-temperate waters (Archer 2009). In the western North Atlantic and Gulf of Mexico, they occur almost exclusively in oceanic waters. In the surveys available to us (Figure 32), most sightings occurred in deep waters over the continental slope and abyssal plain with a few over the continental shelf. Most occurred in relatively cool waters north of the Gulf Stream, while a few occurred within the Gulf Stream itself, yielding a wide range of sea surface temperatures (SSTs) in which the species was sighted.

Shipboard surveys added after the Phase III models roughly doubled the number of sightings available in the core habitat area (Table 11, Figure 33). As with the models updated in Option Year 1, we reviewed the available literature and data to assess the feasibility of excluding the surveys from 1992-1997 from the updated spatial model, as this period predated the launch of the SeaWiFS ocean color sensor needed for contemporaneous biological covariates. Surveys from 1992-1997 reported 32 sightings, all but one of which were in areas where the 1998-2016 surveys reported many sightings (Figure 32). The one exception occurred on 9 February 1995, when the SEFSC Southeast Cetacean Aerial Survey (SECAS) sighted one group near South Carolina on the shallow side of the 125 m isobath. While this unusual sighting gave us pause, we ultimately excluded the 1992-1997 surveys, as species experts considered this sighting extralimital, and we noted its inclusion in the Phase III model did not yield an appreciable boost in density in the southeast on-shelf region. This resulted in a net loss of less than 10% of the sightings available in the full 1992-2016 period, with 339 remaining for use in the updated spatial model.

For the updated model, we applied $g(0)$ estimates (Table 12) derived from availability and perception bias corrections developed by Palka et al. (2017).

Table 11. Striped dolphin sightings from 1998-2016, available for the Option Year 2 spatial model. "Extant" sightings were used in the Phase III regional model (Roberts et al. 2016a). "Added" sightings were incorporated during the Base Year and Option Year 1 for the updated model.

			Striped dolphin		
Platform	Provider	Program	Extant	Added	Total
Aerial	NEFSC	Marine mammal abundance surveys	1	10	11
		NARWSS right whale surveys	5		5
	SEFSC	Marine mammal abundance surveys		1	1
	UNCW	Cape Hatteras Navy Surveys	4	1	5
		Norfolk Canyon Navy Surveys		7	7
	All		10	19	29
Shipboard	NEFSC	Marine mammal abundance surveys	107	124	231
	SEFSC	Marine mammal abundance surveys	48	31	79
	All		155	155	310

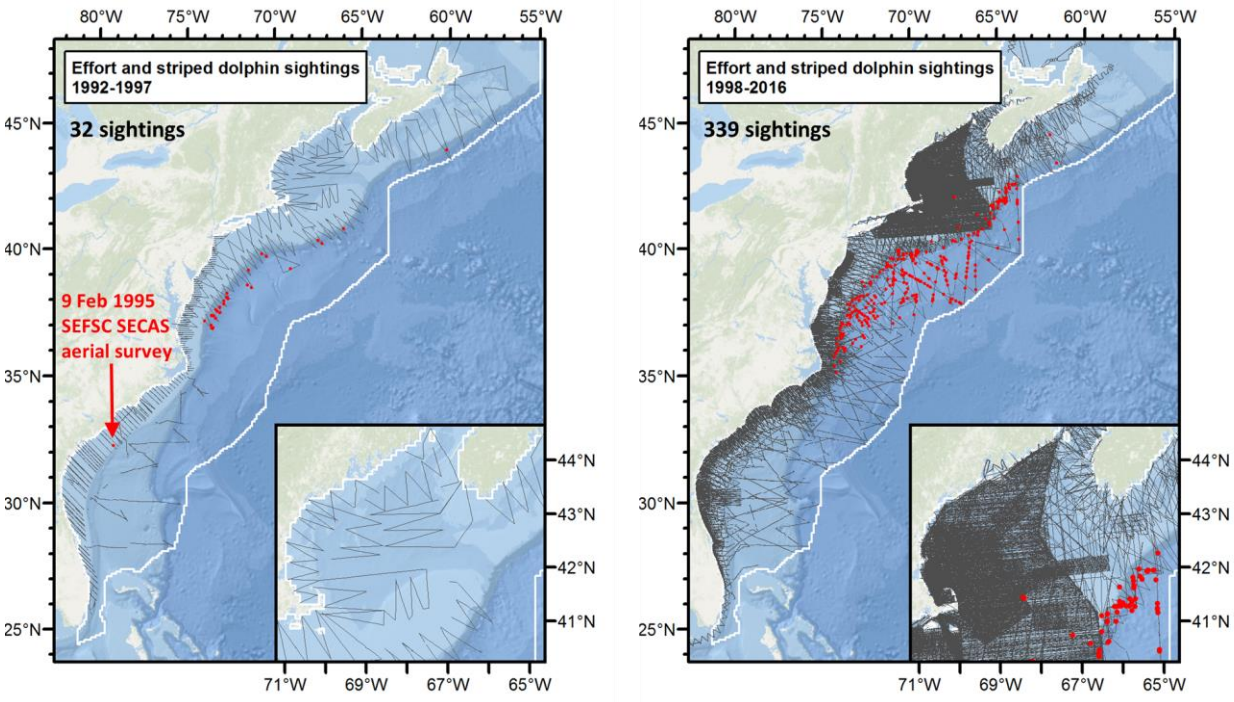

Figure 32. Survey effort and striped dolphin sightings from the 1992-1997 period (left), excluded from the updated model, and the 1998-2016 period (right), available for the updated model.

Table 12. *g*(0) estimates used in the updated striped dolphin model.

Platform	Region	Perception Bias	Availability Bias	*g*(0)	Source (all Palka et al. 2017)
Shipboard	Northeast	0.764	1	0.764	Striped dolphin shipboard NE
	Southeast	0.722	1	0.722	Striped dolphin shipboard SE
Aerial	Northeast	0.706	1	0.706	Striped dolphin aerial NE
	Southeast	0.856	1	0.856	Striped dolphin aerial SE

Detailed accounts of this species off the U.S. east coast are sparse. Lacking evidence that it would exhibit different behaviors in different seasons or subregions of the study area, we grouped all of the surveys into a single spatial model. Candidate models fitted to climatological environmental covariates yielded slightly better restricted maximum likelihood (REML) scores and lower coefficients of variation (CVs) than models fitted to contemporaneous environmental covariates, so we selected the climatological-covariates model fitted to all survey segments as the best (Figure 33, Figure 35). The model indicated higher densities of striped dolphins in deep, saline waters, in areas of higher slopes and epipelagic micronekton productivity, away from the shelf, close to submarine canyons and seamounts, close to anticyclonic (warm-core) eddies, and away from cyclonic (cold-core) eddies. Although the model was complex, retaining eight covariates, these relationships were reasonable for this species. Notably, SST was dropped from the final model, possibly reflecting the wide range of water temperatures within which the species was sighted.

The resulting predictions showed relatively uniform densities throughout the off-shelf region north of Cape Hatteras, both within and north of the Gulf Stream (Figure 34). The literature offered no information about seasonal movements of striped dolphins in the region and nearly all surveying of the predicted off-shelf habitat occurred in summer months. Because of this lack of knowledge of wintertime distributions, we recommend that the year-round mean density surface be used for management of this species.

The year-round mean abundance predicted by the model was very close to that of the Roberts et al. (2016a) model used for Phase III (Table 13), with a lower CV (because of the additional survey data). It also showed less seasonal variability, with peak abundance still occurring in spring but at a lower absolute value, with higher abundances for fall and winter than the Phase III model. In summer, where the bulk of distant off-shelf sampling occurred, abundance differed by 1% from the Phase III model and 3% from Palka et al.'s (2017) estimate for these months from data collected in 2010-2013. It also fell about halfway between the 2004 and 2011 SAR estimates (Table 13). The general agreement between all of these models suggests confidence in the predicted abundance estimate, with the important caveat that most sampling of the core habitat area occurred in summer. To better characterize the species' distribution throughout the year, we recommend additional surveying of offshore waters in other seasons (acknowledging the logistical difficulties and safety risks of performing distant offshore surveys in seasons with poor weather).

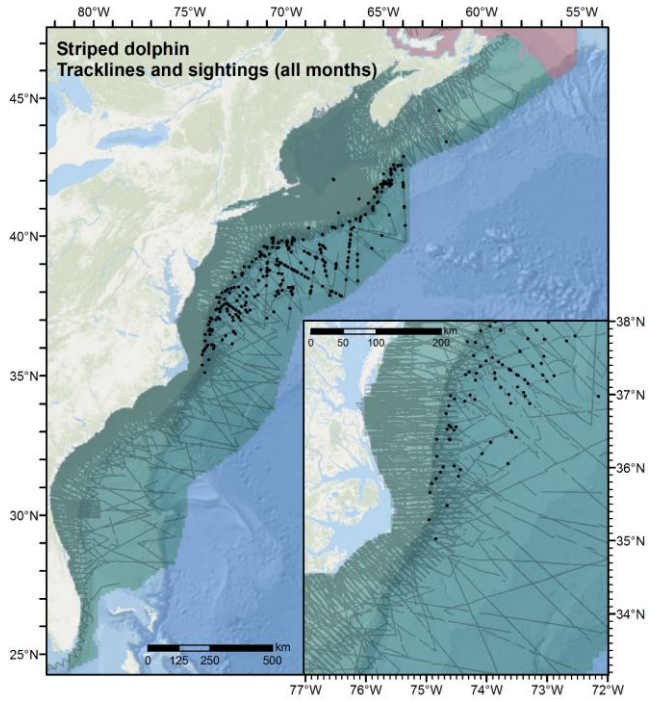

Figure 33. Striped dolphin model's tracklines, sightings, and prediction area (green).

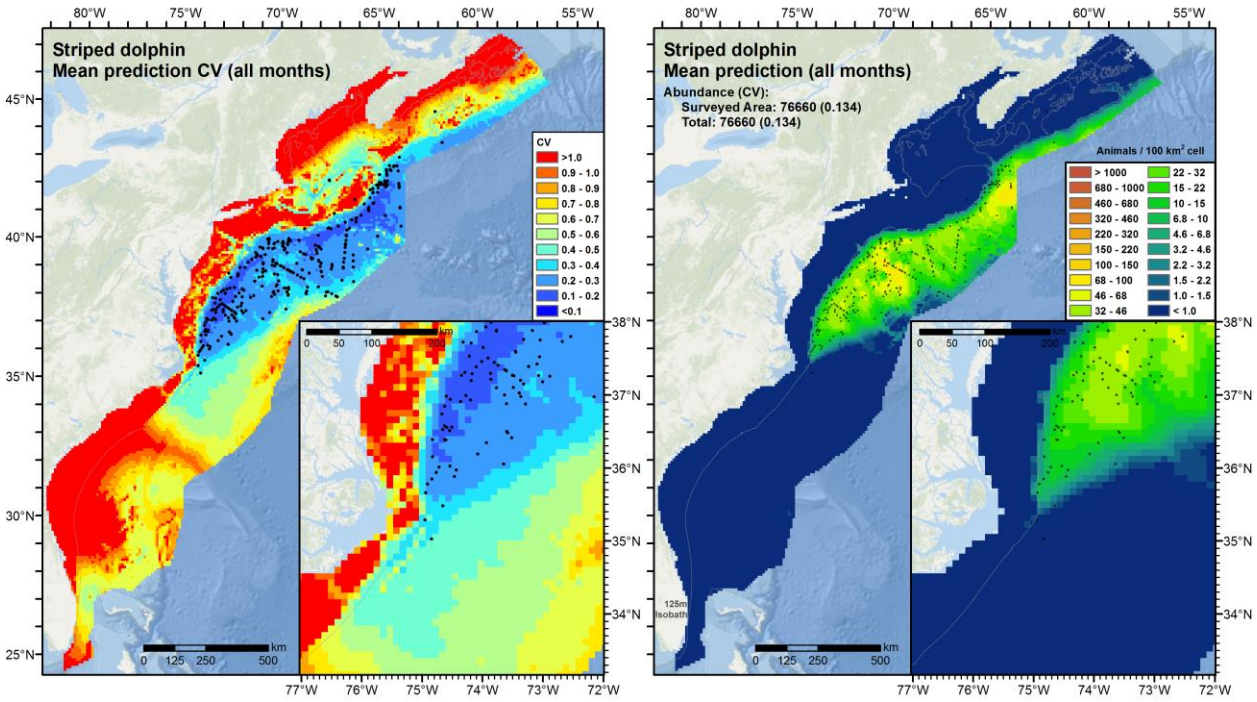

Figure 34. Predicted year-round mean density and total abundance (right) and coefficient of variation (left) for striped dolphin, with sightings overlaid.

```
Family: Tweedie(p=1.31)
Link function: log

Formula:
Abundance ~ offset(log(Area)) + s(log10(Depth), bs = "ts") + s(log10(Slope), bs = "ts") +
    s(I(DistTo125m/1000), bs = "ts") + s(I(DistToCanOrSmt/1000), bs = "ts") + s(ClimSalinity, bs = "ts") +
    s(log10(pmax(ClimEpiMnkPP1, 1e-06)), bs = "ts") + s(I(ClimDistToAEddy4/1000), bs = "ts") +
    s(I(ClimDistToCEddy4/1000), bs = "ts")

Parametric coefficients:
            Estimate Std. Error t value Pr(>|t|)
(Intercept) -12.7312     0.7877  -16.16   <2e-16 ***
---
Signif. codes:  0 '***' 0.001 '**' 0.01 '*' 0.05 '.' 0.1 ' ' 1

Approximate significance of smooth terms:
                                       edf Ref.df     F  p-value
s(log10(Depth))                     1.0115      9 2.256 1.84e-06 ***
s(log10(Slope))                     4.3523      9 2.795 1.35e-05 ***
s(I(DistTo125m/1000))               0.9850      9 1.842 1.06e-05 ***
s(I(DistToCanOrSmt/1000))           1.0258      9 1.796 1.92e-05 ***
s(ClimSalinity)                     5.3927      9 9.510  < 2e-16 ***
s(log10(pmax(ClimEpiMnkPP1, 1e-06))) 0.9763      9 2.728 3.75e-07 ***
s(I(ClimDistToAEddy4/1000))         3.1908      9 2.958 9.12e-07 ***
s(I(ClimDistToCEddy4/1000))         1.0061      9 1.539 9.29e-05 ***
---
Signif. codes:  0 '***' 0.001 '**' 0.01 '*' 0.05 '.' 0.1 ' ' 1

R-sq.(adj) =  0.0609   Deviance explained = 74.3%
-REML = 2766.8  Scale est. = 139.37    n = 134614
```

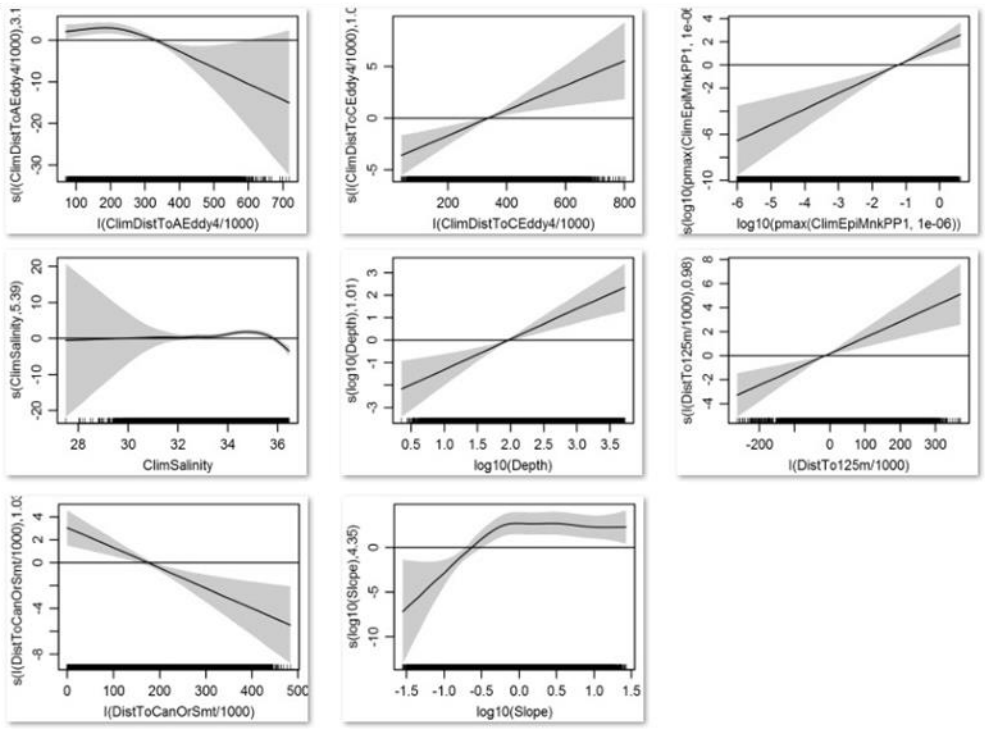

Figure 35. Striped dolphin model's statistical output and covariate functional plots.

Table 13. Comparison of abundance estimates (with CV in parentheses) for striped dolphin, obtained from recent NMFS Stock Assessment Reports (SARs) and density surface models. "Updated model" refers to the model presented here. For this and the preceding Roberts et al. (2016) model, we recommend a single, year-round density surface for management purposes but show seasonal estimates (brown text) to facilitate more granular comparison to the SARs and Palka et al. (2017) estimates, which were made only for the June-August season.

	Years	Dec-Feb	Mar-May	Jun-Aug	Sep-Nov	Year-round
NMFS SARs	2004			94,462 (0.40)		
	2011			54,807 (0.30)		
Roberts et al. (2016) [1,2]	1998-2013	50,240	123,523	79,991	48,239	75,657 (0.21)
Palka et al. (2017) [1]	2010-2013			81,512 (0.121)		
Updated model [1,2]	1998-2016	69,643	96,604	79,100	60,904	76,660 (0.134)

[1] CV is underestimated; it only accounts for uncertainty in spatial model parameters, not detection functions or $g(0)$.
[2] 3-month mean abundance shown for comparison, but we recommend the year-round average be used for management.

2.3.5.3. Risso's dolphin model

A recent comprehensive review of the global distribution of Risso's dolphin (*Grampus griseus*) reported that they "occur in all habitats from coastal to oceanic [but] show a strong preference for the mid-temperate waters of the continental shelf and slope between 30-45 degrees latitude" (Jefferson et al. 2014). This description is consistent with the sightings reported by the surveys we utilized: the highest concentrations of sightings occurred over the continental slope close to the shelf break, especially north of Cape Hatteras, North Carolina (Figure 36). The association of Risso's dolphins with the continental slope off the U.S. east coast has also been observed in tracking studies (Wells et al. 2009; Baird et al. 2017) and bycatch records (Garrison 2007). In deeper waters, sightings occurred less frequently, mainly in the Gulf Stream and cooler waters to the north. On the continental shelf, sightings occurred only sporadically, mainly north of the New York Bight, especially in the deeper waters of the Gulf of Maine basin.

Surveys added after the Phase III models increased the number of sightings available by about 60% (Table 14, Figure 36). Most of these were reported in the northern half of the study area. As with the models updated in Option Year 1, we reviewed the available literature and data to assess the feasibility of excluding surveys from 1992-1997 from the updated spatial model, as this period predated the launch of the SeaWiFS ocean color sensor needed for contemporaneous biological covariates. Surveys from 1992-1997 reported 79 sightings, all along the continental slope north of Cape Hatteras. This area was heavily sampled in the 1998-2016 period, with many sightings reported. We elected to exclude the 1992-1997 surveys, resulting in a net loss of less than 8% of the sightings available in the full 1992-2016 period, with over 1000 remaining for use in the updated spatial model.

For the updated model, we applied $g(0)$ estimates (Table 15) derived from availability and perception bias corrections developed by Palka et al. (2017).

Table 14. Risso's dolphin sightings from 1998-2016, available for the Option Year 2 spatial model. "Extant" sightings were used in the Phase III regional model (Roberts et al. 2016a). "Added" sightings were incorporated during the Base Year and Option Year 1 for the updated model.

			Risso's dolphin		
Platform	Provider	Program	Extant	Added	Total
Aerial	NEFSC	Marine mammal abundance surveys	148	49	197
		NARWSS harbor porpoise survey	2		2
		NARWSS right whale surveys	86	51	137
	SEFSC	Marine mammal abundance surveys		34	34
	UNCW	Cape Hatteras Navy Surveys	10	10	20
		Jacksonville Navy Surveys	43	5	48
		Norfolk Canyon Navy Surveys		10	10
		Onslow Bay Navy Surveys	6		6
	All		295	159	454
Shipboard	NEFSC	Marine mammal abundance surveys	273	190	463
	SEFSC	Marine mammal abundance surveys	77	31	108
	All		350	221	571

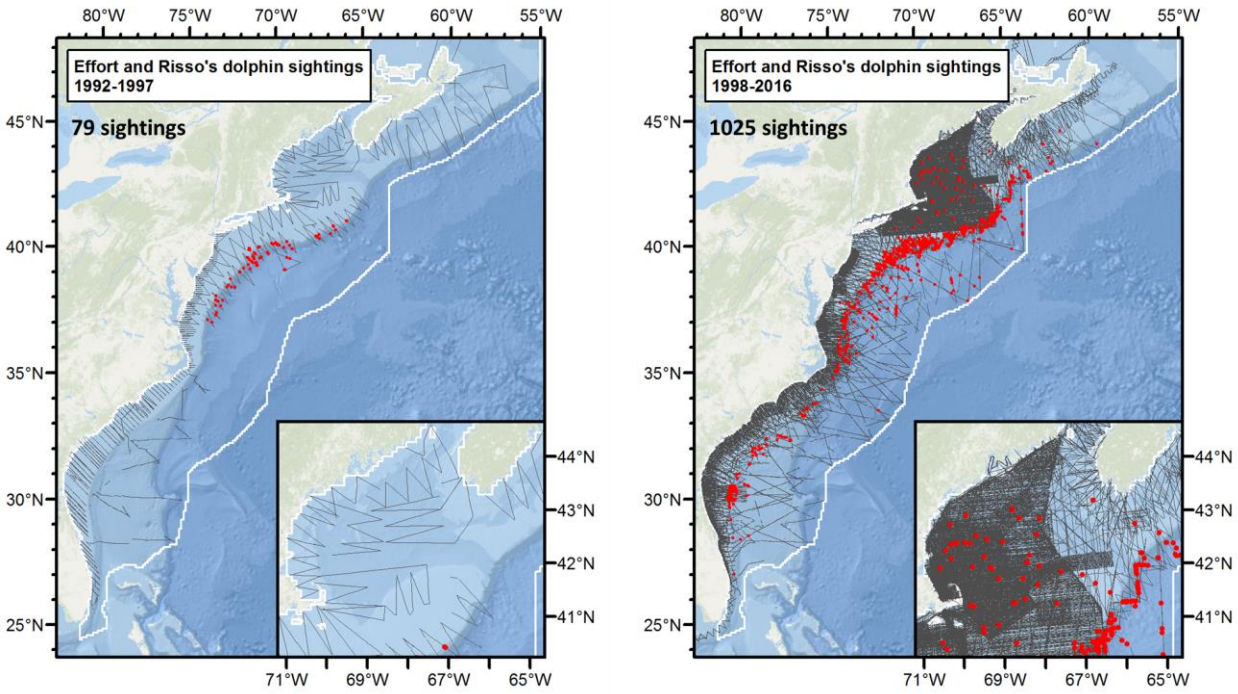

Figure 36. Survey effort and Risso's dolphin sightings from the 1992-1997 period (left), excluded from the updated model, and the 1998-2016 period (right), available for the updated model.

Table 15. *g*(0) estimates used in the updated Risso's dolphin model.

Platform	Region	Perception Bias	Availability Bias	*g*(0)	Source (all Palka et al. 2017)
Shipboard	Northeast	0.674	1	0.674	Risso's dolphin shipboard NE
	Southeast	0.671	1	0.671	Risso's dolphin shipboard SE
Aerial	Northeast	0.647	0.850	0.550	Risso's dolphin aerial NE
	Southeast	0.712	0.850	0.605	Risso's dolphin aerial SE

Detailed accounts of this species off the U.S. east coast are sparse. The population is reported to occupy the mid-Atlantic continental shelf edge year round, and expand northward onto the shelf of Georges Bank and into the Gulf of Maine during spring, summer and fall, contracting southward in winter (Winn 1982; Waring et al. 2016). Given the species' presence both north and south of the Gulf Stream, and lacking evidence that the species would exhibit distinctly different behaviors in different seasons or subregions of the study area, we grouped all of the surveys into a single spatial model. Candidate models fitted to climatological environmental covariates yielded better REML scores and explained more deviance than models fitted to contemporaneous environmental covariates, so we selected the climatological-covariates model fitted to all survey segments as the best (Figure 37, Figure 39). The model indicated higher densities of Risso's dolphins in deep, zooplankton-rich waters (zooplankton are likely a proxy for their prey), and close to SST fronts, anticyclonic (warm-core) eddies, and submarine canyons. It also indicated higher densities at high SST and far from canyons, and exhibited a complex relationship with distance to shore. These latter relationships likely reflect seasonal movements correlated with water temperature and the occasional use of additional habitats beyond the core area along the continental slope.

Consistent with the literature, the model predicted highest densities along the continental slope from Chesapeake Bay to the Scotian Shelf (Figure 38) and in patches along the Scotian Slope, although the Scotian Slope was surveyed relatively sparsely. Monthly predictions showed a late-spring expansion north onto the shelf and into the Gulf of Maine, with a retreat at the onset of winter (Figure 40). Given the agreement of these patterns with the literature, we recommend monthly mean density surfaces be used for management of this species.

Total abundance predicted by the model was higher in all seasons than that predicted by the Roberts et al. (2016a) model used for Phase III (Table 16). We attribute most of this difference to the lower *g*(0) estimates used for shipboard surveys by the updated model (density and abundance scale inversely with *g*(0)). The summer abundance estimate was slightly higher than those of the SARs, and closer to them than the Phase III model. The spring estimate was close to that of Palka et al.'s (2017) model, but much lower than Palka et al.'s (2017) summer and fall model. These large differences are an item for future investigation between the modeling teams.

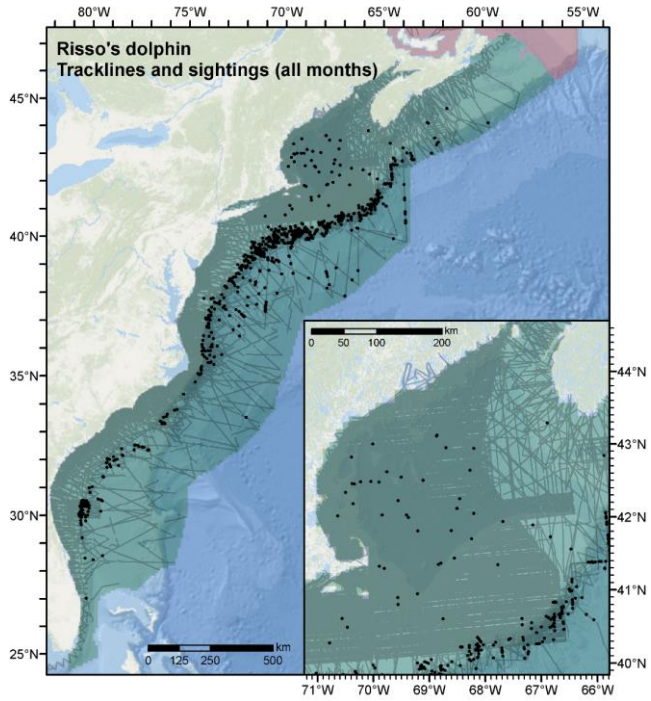

Figure 37. Risso's dolphin model's tracklines, sightings, and prediction area (green).

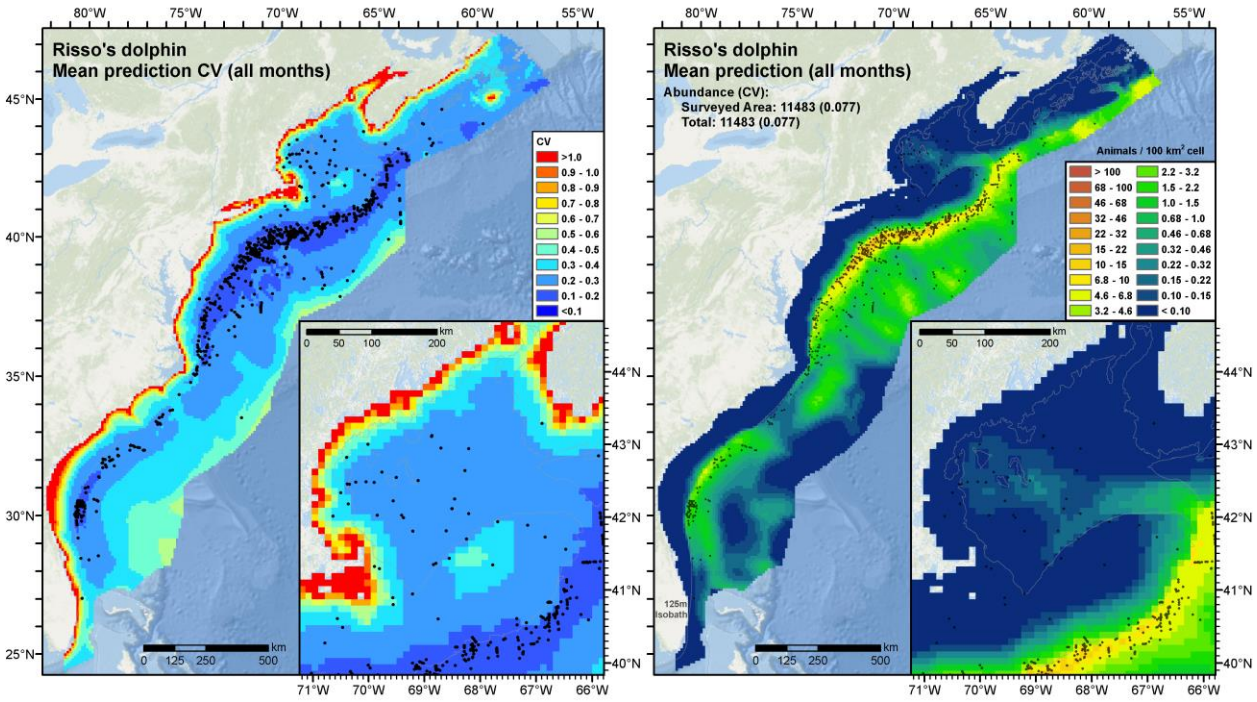

Figure 38. Predicted year-round mean density and total abundance (right) and coefficient of variation (left) for Risso's dolphin, with sightings overlaid. Note: We recommend that monthly mean predictions be used for management purposes (see text).

```
Family: Tweedie(p=1.301)
Link function: log

Formula:
Abundance ~ offset(log(Area)) + s(log10(Depth), bs = "ts") + s(sqrt(DistToShore/1000), bs = "ts") +
    s(I(DistToCan/1000), bs = "ts") + s(ClimSST, bs = "ts") + s(I(ClimDistToSSTFront2^(1/3)), bs = "ts") +
    s(log10(pmax(ClimPkPB1, 0.01)), bs = "ts") + s(I(ClimDistToAEddy/1000), bs = "ts")

Parametric coefficients:
            Estimate Std. Error t value Pr(>|t|)
(Intercept)  -7.9811     0.1757  -45.43   <2e-16 ***
---
Signif. codes:  0 '***' 0.001 '**' 0.01 '*' 0.05 '.' 0.1 ' ' 1

Approximate significance of smooth terms:
                                edf Ref.df      F  p-value
s(log10(Depth))               4.174      9 13.694  < 2e-16 ***
s(sqrt(DistToShore/1000))     5.263      9  5.221 1.67e-10 ***
s(I(DistToCan/1000))          4.836      9 10.706  < 2e-16 ***
s(ClimSST)                    5.340      9 15.018  < 2e-16 ***
s(I(ClimDistToSSTFront2^(1/3))) 4.238      9  4.767 2.78e-10 ***
s(log10(pmax(ClimPkPB1, 0.01))) 5.404      9 13.586  < 2e-16 ***
s(I(ClimDistToAEddy/1000))    1.136      9  2.076 6.68e-06 ***
---
Signif. codes:  0 '***' 0.001 '**' 0.01 '*' 0.05 '.' 0.1 ' ' 1

R-sq.(adj) =  0.0755   Deviance explained = 58.2%
-REML = 5839.1  Scale est. = 55.562    n = 134614
```

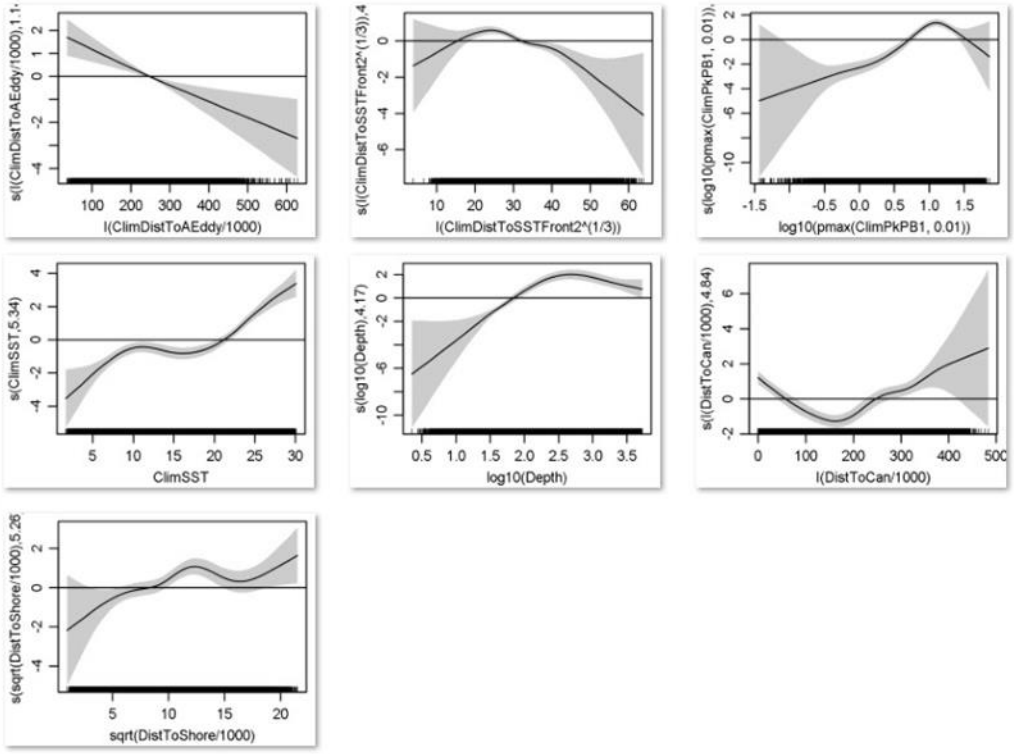

Figure 39. Risso's dolphin model's statistical output and covariate functional plots.

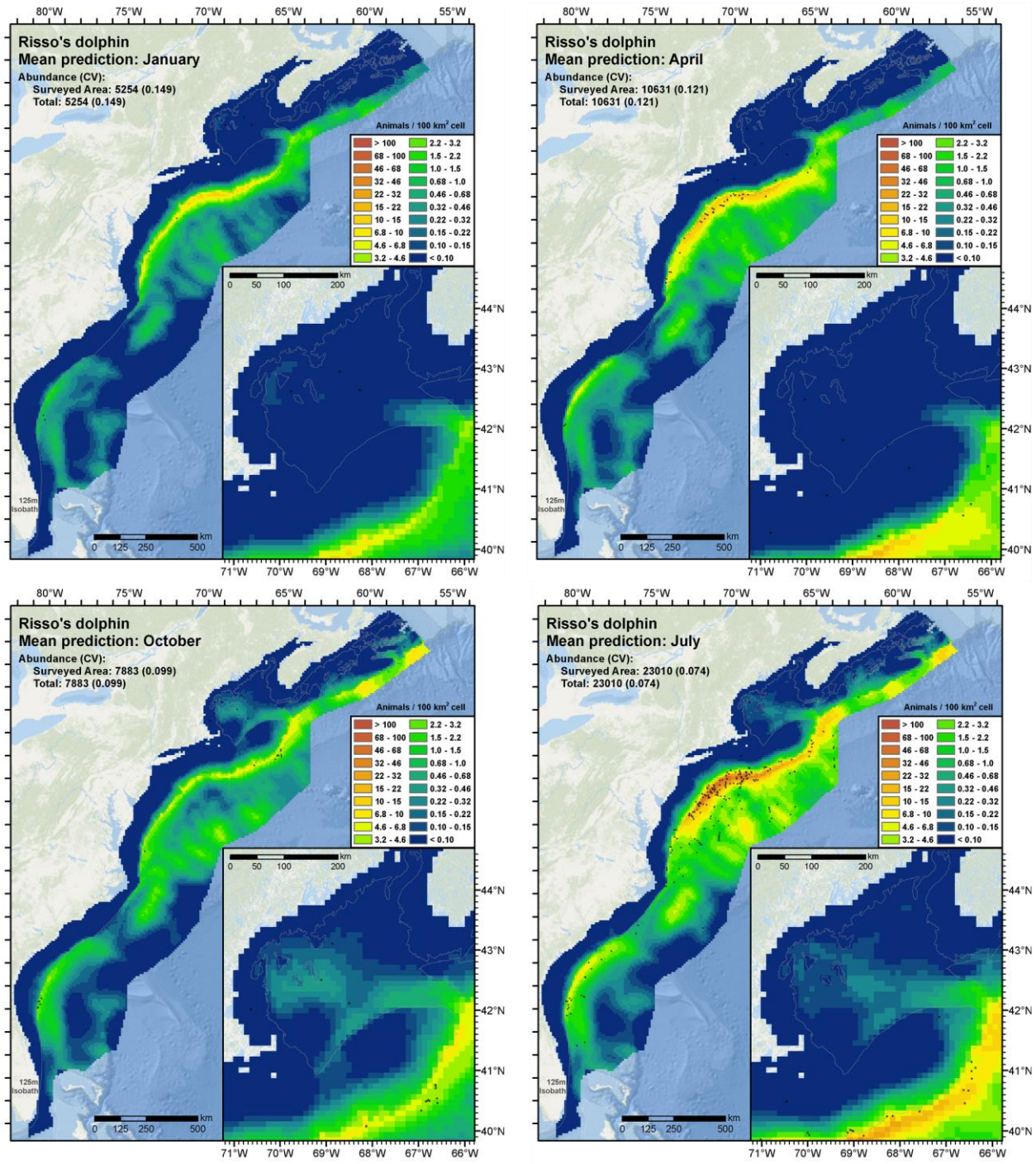

Figure 40. Four monthly predictions for the middle month of each season, with sightings overlaid. Clockwise from upper-left: winter (January), spring (April), summer (July), fall (October). Note that because survey effort was not uniform across months, a lack of sightings in an area should not be taken as evidence that the species was absent (there might have been no surveying done there during that month).

Table 16. Comparison of abundance estimates (with CV in parentheses) for Risso's dolphin, obtained from recent NMFS Stock Assessment Reports (SARs) and density surface models. "Updated model" refers to the model presented here.

	Years	Dec-Feb	Mar-May	Jun-Aug	Sep-Nov	Year-round
NMFS SARs	2004			20,479 (0.59)		
	2011			18,250 (0.46)		
Roberts et al. (2016) [1,2]	1992-2014	2,963	4,672	15,578	7,222	7,732 (0.09)
Palka et al. (2017) [1]	2010-2013		12,759 (0.207)	36,785 (0.205)	29,093 (0.205)	
Updated model [1,2]	1998-2016	5,804	10,307	20,960	9,352	11,483 (0.077)

[1] CV is underestimated; it only accounts for uncertainty in spatial model parameters, not detection functions or $g(0)$.
[2] 3-month mean abundance shown for comparison, but we recommend monthly averages be used for management.

2.3.5.4. Atlantic white-sided dolphin model

Atlantic white-sided dolphins (*Lagenorhynchus acutus*) occur in temperate and sub-polar waters of the North Atlantic (Waring et al. 2016). In the western North Atlantic they occur mainly over the shelf, from central West Greenland as far south as North Carolina. Although stranding records have been reported as far south as Georgia (Powell et al. 2012; Byrd et al. 2014; Waring et al. 2016), the southernmost two sightings reported by the surveys contributed by our collaborators were off Virginia and Maryland; all others were from New York and waters to the north. Palka et al. (1997) reported that spatiotemporal patterns in sightings and strandings indicate seasonal shifts in Atlantic white-sided dolphin distribution, suggesting a more northerly distribution in summer and southerly in winter. Consistent with this view, strandings in North Carolina for the period 1997-2008 all occurred in the months of February, March, and April (Byrd et al. 2014).

Surveys added after the Phase III models increased the number of sightings available by about 60% (Table 17, Figure 41). As with the models updated in Option Year 1, we reviewed the available literature and data to assess the feasibility of excluding surveys from 1992-1997 from the updated spatial model, as this period predated the launch of the SeaWiFS ocean color sensor needed for contemporaneous biological covariates. Surveys from 1992-1997 reported 47 sightings, all within or north of the Gulf of Maine (Figure 41). These represented only 1.3% of the total reported during the 1998-2016 period, and the areas surveyed in 1992-1997 were covered well in 1998-2016, with the exception of the northeast corner of the Scotian Shelf (Figure 41), where a number of sightings were reported in a 1995 aerial survey. This area was only lightly surveyed in 1998-2016, so we initially thought to retain the 1992-1997 surveys for our analysis. However, exploratory modeling (not shown here) indicated that retaining these surveys made little difference in the resulting model predictions—moderate density was predicted across that part of the Scotian Shelf in either case—so we limited the final models to the 1998-2016 period.

All Atlantic white-sided dolphins were sighted by NEFSC. Almost all sightings occurred on aerial surveys, with most of the rest on the AJ 99-02 shipboard naked eye survey of the northern Gulf of Maine, and a handful on AMAPPS shipboard 25x binocular surveys. In the updated model, for aerial surveys we applied a $g(0)$ estimate (Table 18) derived from availability and perception bias corrections developed by Palka et al. (2017), covering the bulk of the sightings. For the AJ 99-02 survey, we applied Palka's (2006) survey-specific estimate, as we did with the Phase III model. For the NEFSC surveys with 25x binoculars, we derived an estimate from Palka et al.'s (2017) bias corrections for short-beaked common dolphin, as a proxy.

Table 17. Atlantic white-sided dolphin sightings from 1998-2016, available for the Option Year 2 spatial model. "Extant" sightings were used in the Phase III regional model (Roberts et al. 2016a). "Added" sightings were incorporated during the Base Year and Option Year 1 for the updated model. Counts include both sightings with fully-resolved species identifications and ambiguous sightings reclassified as Atlantic white-sided dolphins.

			White-sided dolphin		
Platform	Provider	Program	Extant	Added	Total
Aerial	NEFSC	Marine mammal abundance surveys	172	106	278
		NARWSS harbor porpoise survey	31		31
		NARWSS right whale surveys	2093	1207	3300
	All		2296	1313	3609
Shipboard	NEFSC	Marine mammal abundance surveys	42	22	64
	All		42	22	64

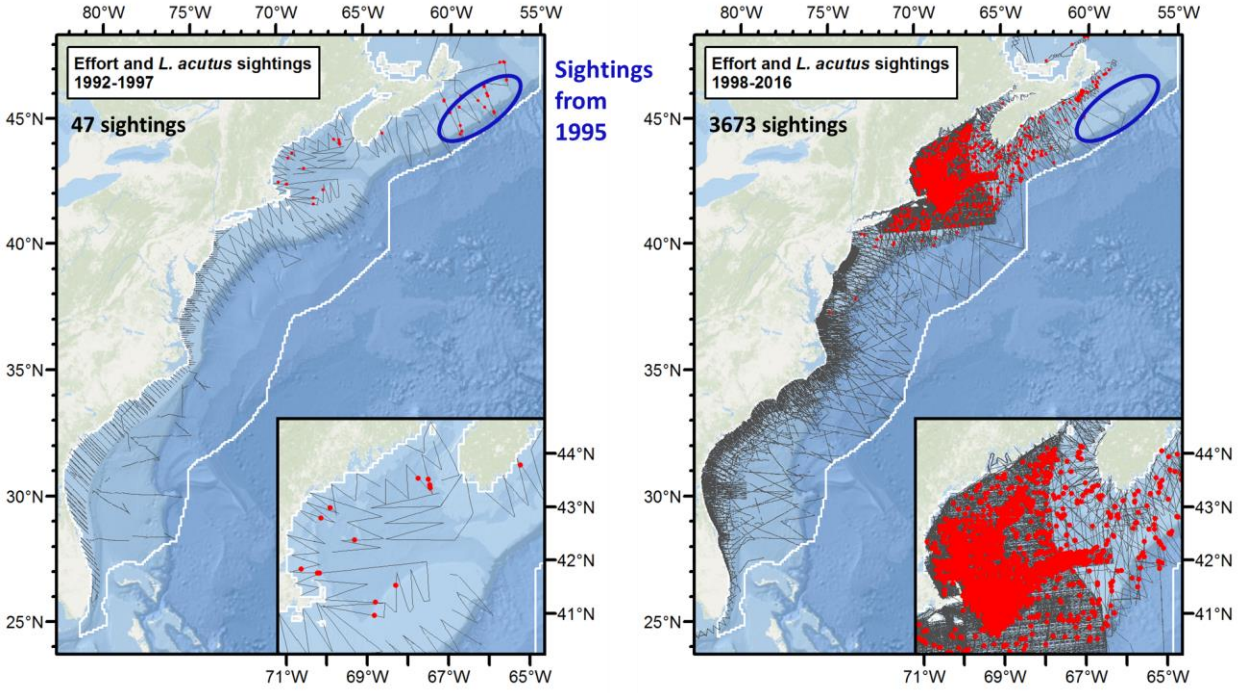

Figure 41. Survey effort and Atlantic white-sided dolphin sightings from the 1992-1997 period (left), excluded from the updated model, and the 1998-2016 period (right), available for the updated model. Circled sightings from 1995 (left) were made in an area that was not substantially surveyed in later years (right). Nevertheless, the resulting model, fitted to surveys from 1998-2016, did predict density in this area (Figure 43).

Table 18. *g*(0) estimates used in the updated Atlantic white-sided dolphin model.

Platform	Region	Perception Bias	Availability Bias	*g*(0)	Source (all Palka et al. 2017 except first row)
Ship. naked eye	Northeast	0.270	1	0.270	Palka (2006) Atlantic white-sided dolphin
Ship. 25x binocs	Northeast	0.600	1	0.600	Short-beaked common dolphin NE
Aerial	Northeast	0.600	0.890	0.534	Atlantic white-sided dolphin NE

Given the species' reported cool-water distribution, the lack of sightings south of Virginia, and that only 14 strandings were reported in North Carolina over a 12-year period (1997-2008), we concluded the species does not regularly inhabit waters south of Cape Hatteras. We split the study area there, fit a model to survey segments collected north of the Gulf Stream, and assumed the species was absent in the south (Figure 42). Lacking evidence that the species would exhibit distinctly different behaviors in different seasons, we grouped all of the northern segments into a single model.

Candidate models fitted to climatological environmental covariates yielded better REML scores and explained more deviance than models fitted to contemporaneous environmental covariates, so we selected the climatological-covariates model fitted to all survey segments as the best (Figure 42, Figure 44). The resulting model was complex, with nine covariates retained, reflecting the large number of segments and sightings used to fit the model. The model retained all five static covariates, which we suspect were used to distribute density across the deeper waters of the continental shelf, with reduced density close to shore and as the continental slope deepens. Dynamic relationships indicated higher density in areas of high zooplankton biomass (e.g. the Gulf of Maine), low kinetic energy, and between 8-22 °C SST, with the highest between about 10-15 °C. This is a higher range of SST than that reported by Selzer and Payne (1988), however we urge caution in drawing firm ecological conclusions from individual functional relationships of such a complex multivariate model.

Consistent with the literature, the model predicted highest densities in the cool, productive waters of the Gulf of Maine and the Scotian Shelf (Figure 43). Monthly predictions showed a late-spring expansion north into the Gulf of Maine and Canada, with a winter retreat south into the mid-shelf and slope waters of the mid-Atlantic (Figure 45). Given the agreement of these patterns with the literature, we recommend monthly mean density surfaces be used for management of this species.

Year-round total abundance predicted by the model was 57% higher than that predicted by the Roberts et al. (2016a) model used for Phase III (Table 19). Abundance increased in all seasons. We attribute this difference to the lower $g(0)$ estimate used for aerial surveys. Roughly two-thirds of the sightings were of groups of five or more individuals. In the Phase III model, we used Carretta et al.'s (2000) estimate of $g(0)=0.960$ for large groups, made from sightings made from surveys of the U.S. west coast. In the new model, we applied Palka et al.'s (2017) bias corrections, which did not differentiate by group size, yielding a $g(0)$ of 0.534 for groups of any size. Thus, because density and abundance scale inversely with $g(0)$, it is not surprising that they increased substantially when $g(0)$ dropped from 0.960 to 0.534 for the two-thirds of the sightings with the largest group sizes.

The resulting abundance predictions were markedly higher than both the 2011 SAR and Palka et al.'s (2017) model. These large differences are an item for future investigation between the modeling teams, however we note that those predictions had relatively high CVs (being based on a far smaller number of sightings) and were predicted over a smaller study area (about halfway up the Scotian Shelf).

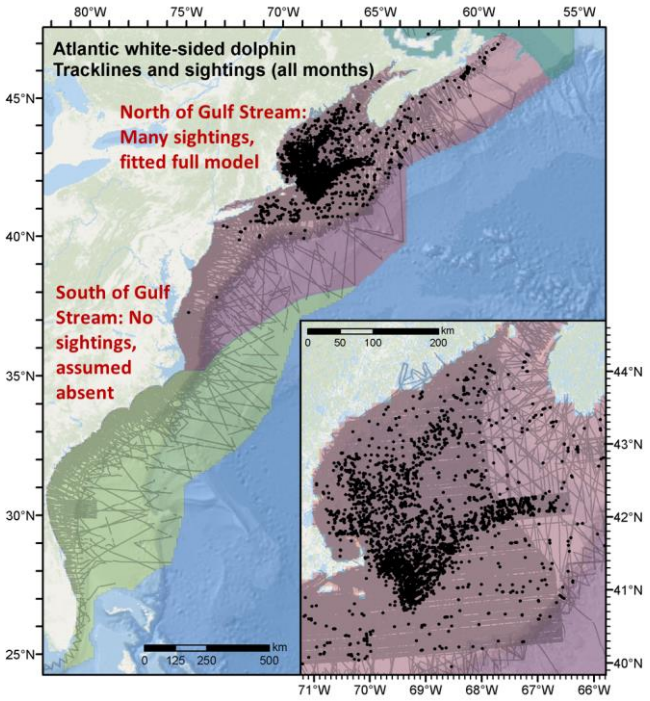

Figure 42. Atlantic white-sided dolphin's tracklines, sightings, and prediction areas. North of the Gulf Stream (red) we fitted a full density model. South of the Gulf Stream (light green), we assumed the species was absent (see text).

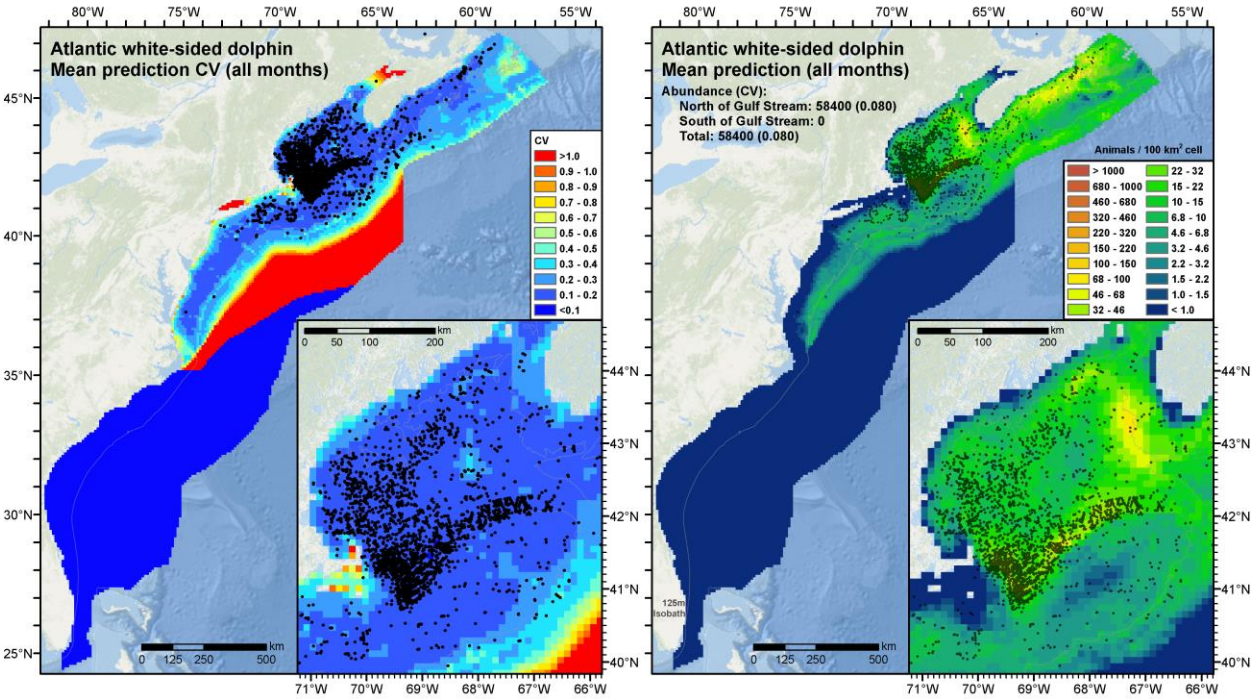

Figure 43. Predicted year-round mean density and total abundance (right) and coefficient of variation (left) for Atlantic white-sided dolphin, with sightings overlaid. Note: We recommend that monthly mean predictions be used for management purposes (see text).

```
Family: Tweedie(p=1.482)
Link function: log

Formula:
Abundance ~ offset(log(Area)) + s(log10(Depth), bs = "ts") + s(sqrt(DistToShore/1000), bs = "ts") +
    s(log10(Slope), bs = "ts") + s(I(DistTo125m/1000), bs = "ts") + s(I(DistTo300m/1000), bs = "ts") +
    s(ClimSST, bs = "ts") + s(I(ClimDistToSSTFront1^(1/3)), bs = "ts") +
    s(log10(pmax(ClimPkPB1, 0.01)), bs = "ts") + s(log10(pmax(ClimTKE, 1e-04)), bs = "ts")

Parametric coefficients:
            Estimate Std. Error t value Pr(>|t|)
(Intercept)  -5.1799     0.3835  -13.51   <2e-16 ***
---
Signif. codes:  0 '***' 0.001 '**' 0.01 '*' 0.05 '.' 0.1 ' ' 1

Approximate significance of smooth terms:
                                edf Ref.df      F  p-value
s(log10(Depth))               4.452      9 14.679  < 2e-16 ***
s(sqrt(DistToShore/1000))     4.569      9  3.483 3.28e-07 ***
s(log10(Slope))               4.926      9  3.784 6.16e-08 ***
s(I(DistTo125m/1000))         4.099      9 11.478  < 2e-16 ***
s(I(DistTo300m/1000))         5.556      9 21.914  < 2e-16 ***
s(ClimSST)                    6.569      9 13.099  < 2e-16 ***
s(I(ClimDistToSSTFront1^(1/3))) 4.388      9  4.400 3.78e-09 ***
s(log10(pmax(ClimPkPB1, 0.01))) 4.818      9 11.642  < 2e-16 ***
s(log10(pmax(ClimTKE, 1e-04)))  5.108      9  4.083 1.11e-07 ***
---
Signif. codes:  0 '***' 0.001 '**' 0.01 '*' 0.05 '.' 0.1 ' ' 1

R-sq.(adj) =  0.0164   Deviance explained = 27.4%
-REML =  20177  Scale est. = 106.31    n = 88141
```

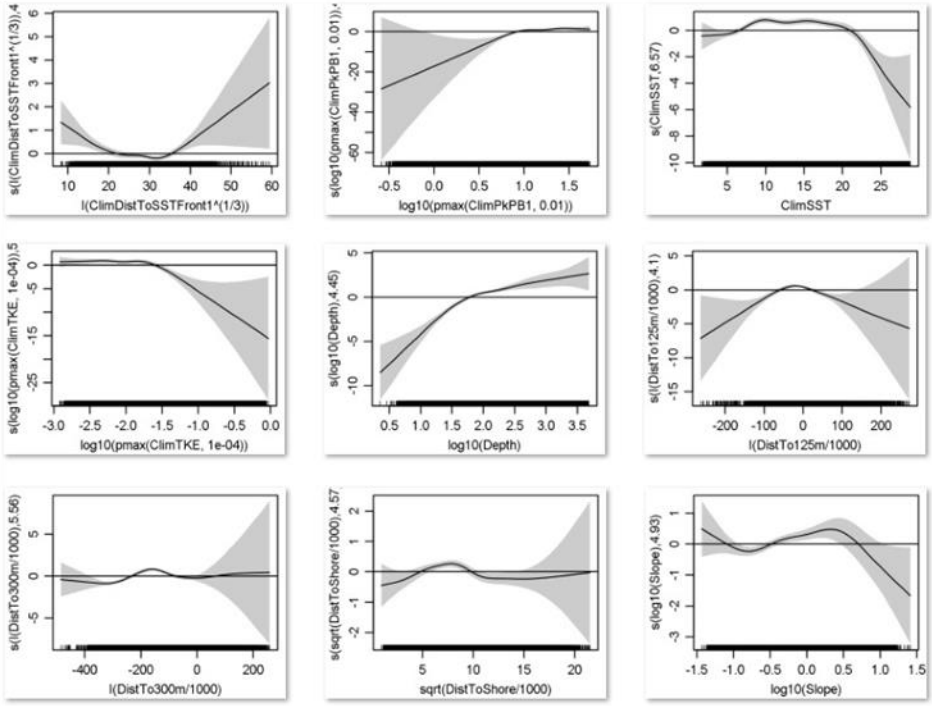

Figure 44. Atlantic white-sided dolphin model's statistical output and covariate functional plots.

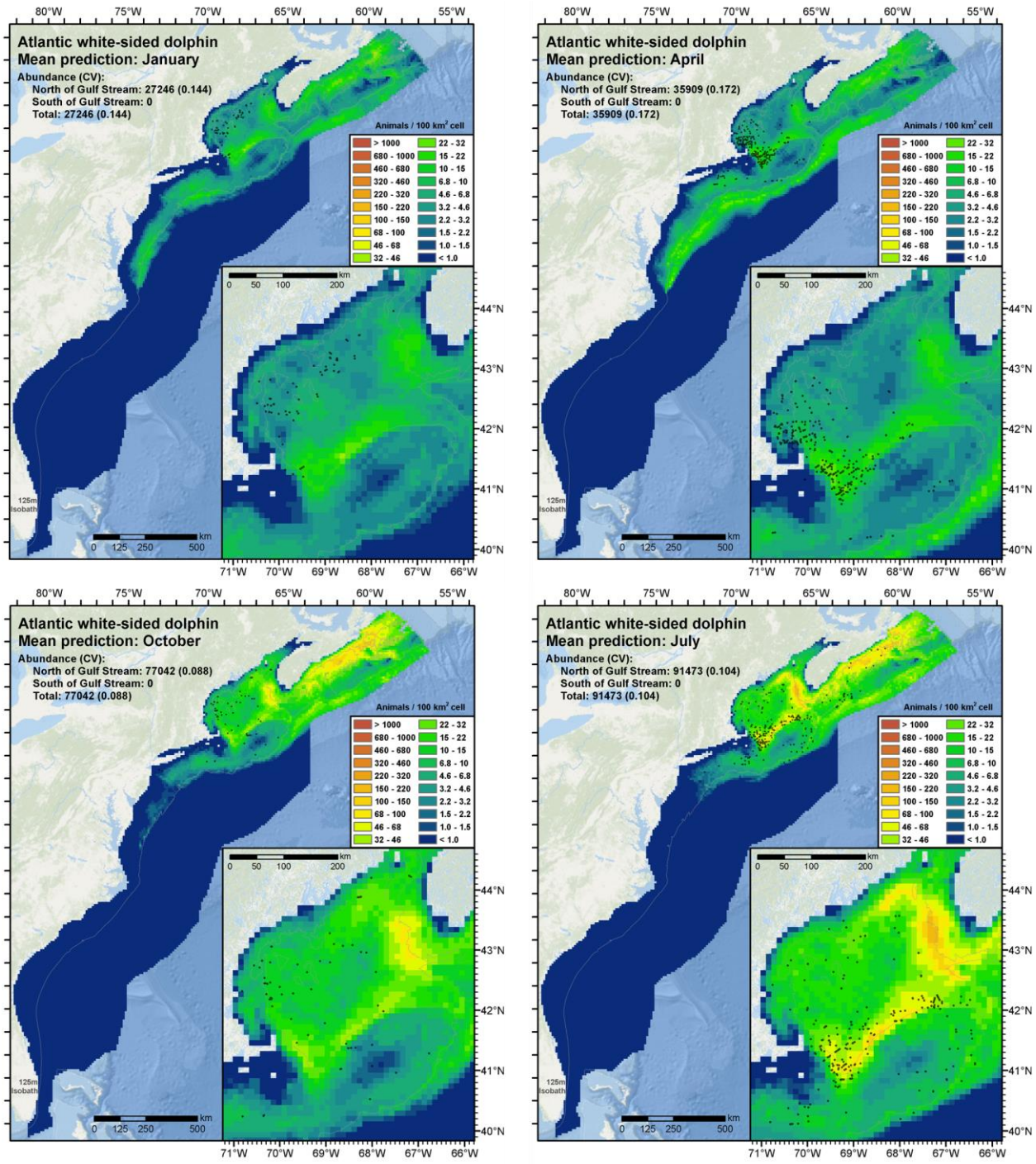

Figure 45. Four monthly predictions for the middle month of each season, with sightings overlaid. Clockwise from upper-left: winter (January), spring (April), summer (July), fall (October). Note that because survey effort was not uniform across months, a lack of sightings in an area should not be taken as evidence that the species was absent (there might have been no surveying done there during that month).

Table 19. Comparison of abundance estimates (with CV in parentheses) for Atlantic white-sided dolphin, obtained from recent NMFS Stock Assessment Reports (SARs) and density surface models. "Updated model" refers to the model presented here.

	Years	Dec-Feb	Mar-May	Jun-Aug	Sep-Nov	Year-round
NMFS SARs	2011			48,819 (0.61)		
Roberts et al. (2016) [1,2]	1995-2014	23,694	19,996	50,828	55,224	37,180 (0.07)
Palka et al. (2017) [1]	2010-2013		47,370 (0.666)	42,895 (0.463)	44,276 (0.394)	
Updated model [1,2]	1998-2016	30,103	40,798	88,068	74,446	58,400 (0.080)

[1] CV is underestimated; it only accounts for uncertainty in spatial model parameters, not detection functions or $g(0)$.
[2] 3-month mean abundance shown for comparison, but we recommend monthly averages be used for management.

2.3.5.5. Short-beaked common dolphin model

Short-beaked common dolphins (*Delphinus delphis*) are widely distributed in temperate and sub-tropical waters (Waring et al. 2016). At the time of this writing, Jefferson et al. (2009) provided the most recent comprehensive review of the species' distribution in the western North Atlantic. According to this study, in recent decades off the North American east coast, short-beaked common dolphins were found mainly in cooler waters, ranging between the 200m and 2000m isobaths, as far south as the Georgia/South Carolina border but mainly extending north from Cape Hatteras to 47-50 °N off the Canadian coast. This may be a change from the first half of the 20th century, in which short-beaked common dolphins were believed to occur in the waters of the southeast U.S more frequently than today, ranging as far south as Florida. The shift may be related to changes in water temperature, or prey distributions resulting from oceanographic changes, or displacement by Stenella species (Jefferson et al. 2009).

Jefferson et al. (2009) described seasonal movements in our study area as follows. From January to May, short-beaked common dolphins regularly range north only as far as Georges Bank, then shift northwards in summer as waters warm, moving into the Gulf of Maine, Scotian Shelf, and prominent bottom escarpments such as the Flemish Cap. They are extremely rare in the Bay of Fundy at all times but are common in slope waters of Nova Scotia in late summer and autumn and are frequently seen near the "Gully" canyon at this time. Concurrent with Jefferson et al.'s review but not considered by it, Lawson and Gosselin (2009) reported 198 sightings of short-beaked common dolphins in a survey of the Scotian Shelf in July-August 2007, and 2 more near Cape Breton, and ultimately estimated the abundance for this area during the survey to be 171,680, the most of any cetacean they sighted (Lawson & Gosselin 2011).

Surveys added after the Phase III models increased the number of sightings available for our model by about 65% (Table 20, Figure 46). As with the models updated in Option Year 1, we reviewed the available literature and data to assess the feasibility of excluding surveys from 1992-1997 from the updated spatial model, as this period predated the launch of the SeaWiFS ocean color sensor needed for contemporaneous biological covariates. Surveys from 1992-1997 reported 35 sightings, mostly along the outer edge of Georges Bank (Figure 46). These represented only 1.9% of the total reported during the 1998-2016 period, and the areas surveyed in 1992-1997 were covered well in 1998-2016 (Figure 46). Accordingly, we excluded the 1992-1997 surveys from our new model.

For the updated model, we applied $g(0)$ estimates (Table 21) derived from availability and perception bias corrections developed by Palka et al. (2017).

Table 20. Short-beaked common dolphin sightings from 1998-2016, available for the Option Year 2 spatial model. "Extant" sightings were used in the Phase III regional model (Roberts et al. 2016a). "Added" sightings were incorporated during the Base Year and Option Year 1 for the updated model. Counts include both sightings with fully-resolved species identifications and ambiguous sightings reclassified as short-beaked common dolphins.

			Common dolphin		
Platform	Provider	Program	Extant	Added	Total
Aerial	NEFSC	Marine mammal abundance surveys	307	109	416
		NARWSS harbor porpoise survey	5		5
		NARWSS right whale surveys	543	203	746
	SEFSC	Marine mammal abundance surveys	3	107	110
	UNCW	Cape Hatteras Navy Surveys	12	10	22
		Marine mammal surveys, 2002	4		4
		Norfolk Canyon Navy Surveys		28	28
		Onslow Bay Navy Surveys	1		1
		Right whale surveys, 2005-2008	26		26
	VAMSC	MD Wind Energy Area surveys		22	22
		VA Wind Energy Area surveys	25		25
	All		926	479	1405
Shipboard	NEFSC	Marine mammal abundance surveys	143	258	401
	NJDEP	New Jersey Ecological Baseline Study	19		19
	SEFSC	Marine mammal abundance surveys	36	7	43
	All		198	265	463

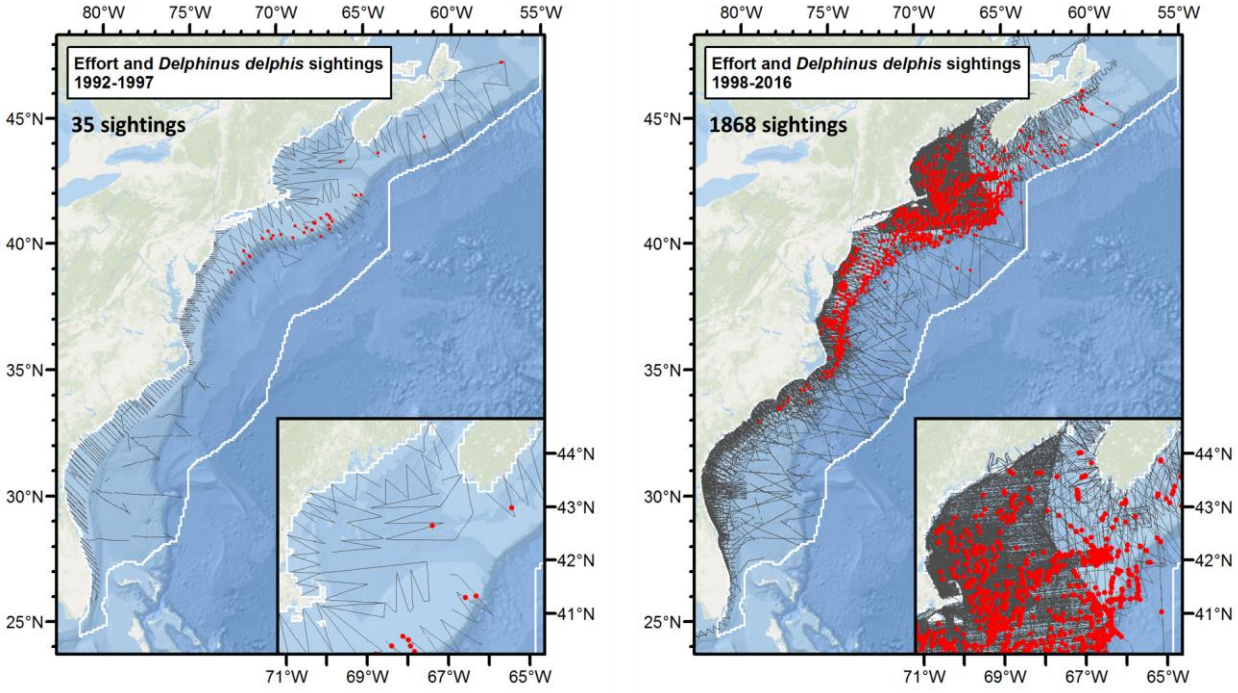

Figure 46. Survey effort and short-beaked common dolphin sightings from the 1992-1997 period (left), excluded from the updated model, and the 1998-2016 period (right), available for the updated model.

Table 21. *g*(0) estimates used in the updated short-beaked common dolphin model.

Platform	Region	Perception Bias	Availability Bias	*g*(0)	Source (all Palka et al. 2017)
Shipboard	Northeast	0.600	1	0.600	Common dolphin shipboard NE
	Southeast	0.722	1	0.722	Common dolphin shipboard SE
Aerial	Northeast	0.706	0.930	0.657	Common dolphin aerial NE
	Southeast	0.859	0.930	0.799	Common dolphin aerial SE

Given the species' presence both north and south of the Gulf Stream, and lacking evidence that it would exhibit different behaviors in different seasons or subregions of the study area, we grouped all of the surveys into a single spatial model. Candidate models fitted to climatological environmental covariates yielded slightly better REML scores and explained more deviance than models fitted to contemporaneous environmental covariates, so we selected the climatological-covariates model fitted to all survey segments as the best (Figure 47, Figure 49). The resulting model was complex, with nine covariates retained, reflecting the large number of segments and sightings used to fit the model. Functional relationships indicated higher density near the shelf break (close to submarine canyons, over areas of high slope, and depths of 100-1000m) and in dynamic and productive waters (close to SST fronts and cyclonic (cold-core) eddies, and areas of high zooplankton biomass). The relationship with SST was complex, but indicated decreasing density as temperatures fell below 8 °C.

Consistent with the literature, the model predicted highest densities along the continental shelf break and shallower portions of the continental slope, mainly north of Cape Hatteras (Figure 48). Monthly predictions showed highest densities in the mid-Atlantic in winter and spring, with density shifting north to the Gulf of Maine and Canadian waters in summer and fall (Figure 50). Given the overall agreement of these patterns with the literature, we recommend monthly mean density surfaces be used for management of this species. We note that the surveys used in our models reported sightings in the Gulf of Maine all months of the year, and our models predict some density there in every month, suggesting the wintertime distribution ranges farther north than reported by Jefferson et al. (2009).

The new model also predicted very little abundance south of Cape Hatteras, in contrast with the Roberts et al. (2016a) model used for Phase III, which predicted a band of low density down the shallow side of the shelf break south to Miami. While the old model was not implausible, given that short-beaked common dolphins were known to inhabit this area in the 20th century (Jefferson et al. 2009), we believed the new model better reflected the present-day distribution. We suspected the addition of the AMAPPS I aerial surveys conducted by SEFSC over several years and seasons provided the absence data that influenced the new model to predict lower density here.

Year-round total abundance predicted by the model was about 20% higher than that predicted by the Roberts et al. (2016a) model (Table 22). Abundance increased in all seasons and peaked in summer rather than fall. As with Atlantic white-sided dolphin, we attribute the increased abundance to the lower *g*(0) estimates used in the new models. For common dolphins, *g*(0) decreased both for large groups sighted on aerial surveys and for both small and large groups sighted on shipboard surveys. (Please see the Atlantic white-sided dolphin section for further discussion.)

The resulting abundance predictions were markedly higher than the 2011 SAR but relatively close to Palka et al.'s (2017) spring and summer predictions. Palka et al.'s (2017) fall predictions were about 50% higher than both their predictions for the other two seasons and our predictions for all seasons. The difference between these models remain an item for future investigation between the modeling teams.

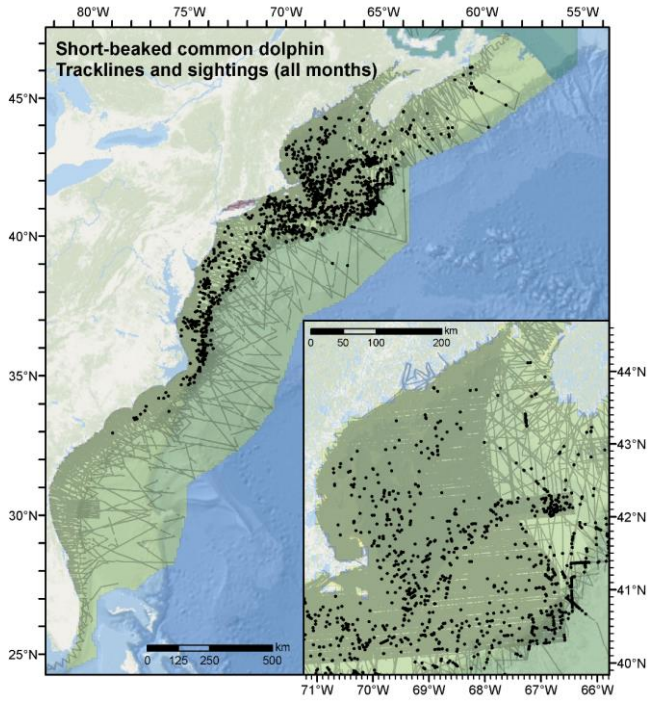

Figure 47. Short-beaked common dolphin model's tracklines, sightings, and prediction area (light green).

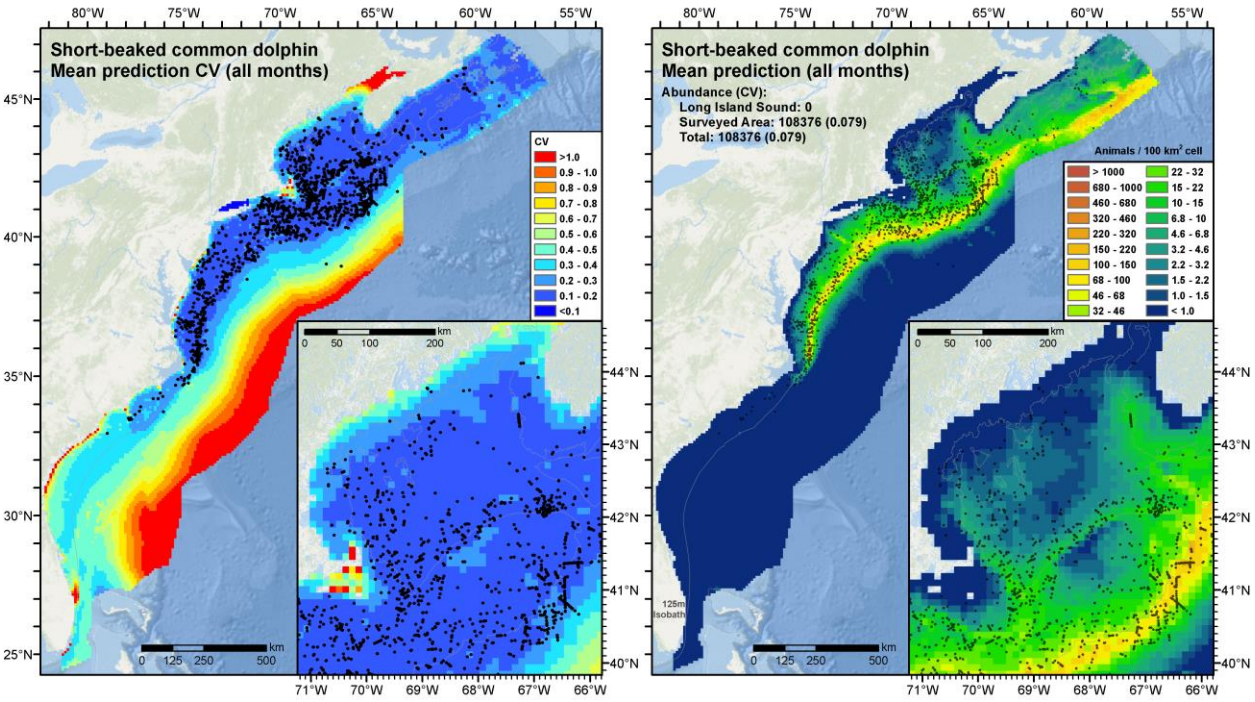

Figure 48. Predicted year-round mean density and total abundance (right) and coefficient of variation (left) for short-beaked common dolphin, with sightings overlaid. Note: We recommend that monthly mean predictions be used for management purposes (see text).

```
Family: Tweedie(p=1.447)
Link function: log

Formula:
Abundance ~ offset(log(Area)) + s(log10(Depth), bs = "ts") + s(log10(Slope), bs = "ts") +
    s(sqrt(DistToShore/1000), bs = "ts") + s(I(DistTo125m/1000), bs = "ts") + s(I(DistToCan/1000), bs = "ts") +
    s(ClimSST, bs = "ts") + s(I(ClimDistToSSTFront3^(1/3)), bs = "ts") +
    s(log10(pmax(ClimPkPB1, 0.01)), bs = "ts") + s(I(ClimDistToCEddy4/1000), bs = "ts")

Parametric coefficients:
            Estimate Std. Error t value Pr(>|t|)
(Intercept) -5.50007    0.09202  -59.77   <2e-16 ***
---
Signif. codes:  0 '***' 0.001 '**' 0.01 '*' 0.05 '.' 0.1 ' ' 1

Approximate significance of smooth terms:
                                edf Ref.df      F  p-value
s(log10(Depth))               6.006      9 15.709  < 2e-16 ***
s(log10(Slope))               3.485      9  7.662  < 2e-16 ***
s(sqrt(DistToShore/1000))     3.571      9  2.359 3.00e-05 ***
s(I(DistTo125m/1000))         1.031      9  3.125 2.15e-08 ***
s(I(DistToCan/1000))          1.433      9 12.669  < 2e-16 ***
s(ClimSST)                    7.579      9 13.129  < 2e-16 ***
s(I(ClimDistToSSTFront3^(1/3))) 1.214      9  7.213  < 2e-16 ***
s(log10(pmax(ClimPkPB1, 0.01))) 6.105      9 22.596  < 2e-16 ***
s(I(ClimDistToCEddy4/1000))   6.568      9  5.035 2.46e-09 ***
---
Signif. codes:  0 '***' 0.001 '**' 0.01 '*' 0.05 '.' 0.1 ' ' 1

R-sq.(adj) =  0.022   Deviance explained = 47.6%
-REML =  12652  Scale est. = 142.06    n = 134516
```

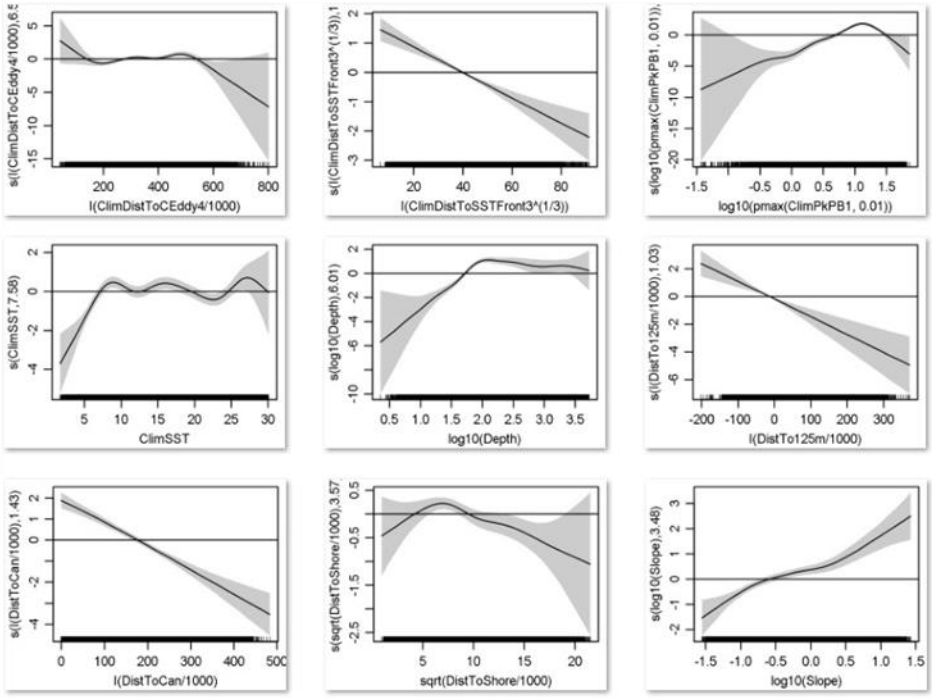

Figure 49. Short-beaked common dolphin model's statistical output and covariate functional plots.

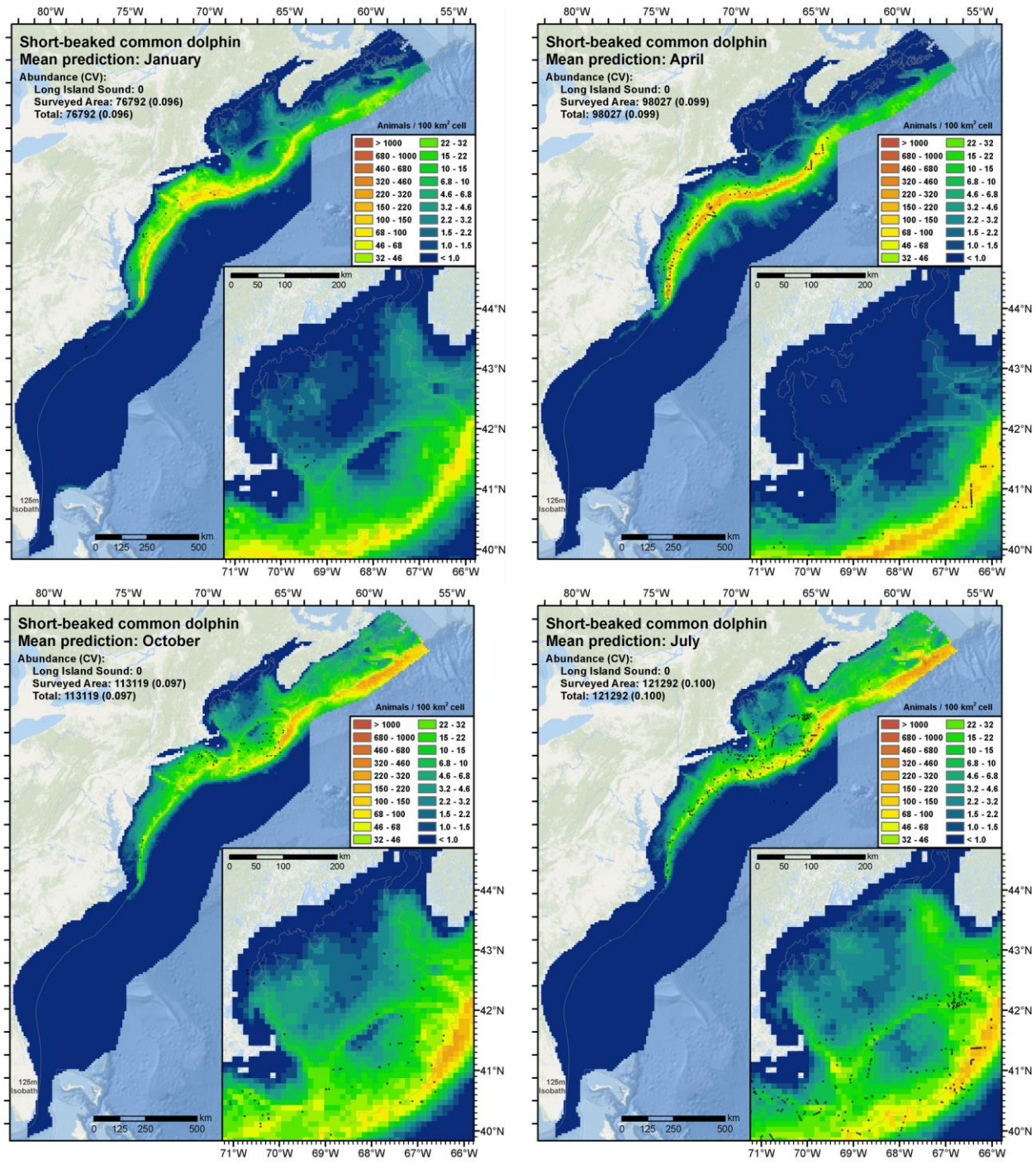

Figure 50. Four monthly predictions for the middle month of each season, with sightings overlaid. Clockwise from upper-left: winter (January), spring (April), summer (July), fall (October). Note that because survey effort was not uniform across months, a lack of sightings in an area should not be taken as evidence that the species was absent (there might have been no surveying done there during that month).

Table 22. Comparison of abundance estimates (with CV in parentheses) for short-beaked common dolphin, obtained from recent NMFS Stock Assessment Reports (SARs) and density surface models. "Updated model" refers to the model presented here.

	Years	Dec-Feb	Mar-May	Jun-Aug	Sep-Nov	Year-round
NMFS SARs	2011			70,184 (0.28)		
Roberts et al. (2016) [1,2]	1998-2013	78,420	66,821	87,179	108,431	86,098 (0.12)
Palka et al. (2017) [1]	2010-2013		111,041 (0.216)	118,695 (0.213)	183,509 (0.185)	
Updated model [1,2]	1998-2016	85,587	104,340	125,027	115,737	108,376 (0.079)

[1] CV is underestimated; it only accounts for uncertainty in spatial model parameters, not detection functions or $g(0)$.
[2] 3-month mean abundance shown for comparison, but we recommend monthly averages be used for management.

2.3.5.6. Atlantic spotted dolphin model

The Atlantic spotted dolphin (*Stenella frontalis*) occurs in tropical and temperate waters of the Atlantic Ocean. In the North Atlantic, two ecotypes occur: a large, heavily-spotted form that inhabits the continental shelf and a smaller, less-spotted form that occurs offshore and around islands (Waring et al. 2014). A recent genetic analysis of samples collected in the Gulf of Mexico, the western North Atlantic, and the Azores, confirmed genetic differentiation between the ecotypes (Viricel & Rosel 2014), and an analysis of Atlantic spotted dolphin whistles reported statistically significant differences in several whistle characteristics between the ecotypes (Baron et al. 2008). The offshore form can be difficult for observers to distinguish from pantropical spotted dolphin (*Stenella attenuata*), and prior to 1999, NOAA reported a combined abundance estimate for the two species for the western North Atlantic (Waring et al. 2014). It has since been shown that full identifications can confidently be made south of Cape Hatteras (Waring et al. 2014). All of the spotted dolphin sightings that we have south of Cape Hatteras, going back to the earliest survey from 1992, were fully-resolved to the species level. In contrast, the more northerly offshore surveys we have prior to 1998 all reported the ambiguous identification "spotted dolphin" (although the surveys from 1998 were fully-resolved to the species level).

Surveys added after the Phase III models increased the number of sightings available for our model by about 50% (Table 23, Figure 51). As with the models updated in Option Year 1, we reviewed the available literature and data to assess the feasibility of excluding surveys from 1992-1997 from the updated spatial model, as this period predated the launch of the SeaWiFS ocean color sensor needed for contemporaneous biological covariates. Excluding surveys from 1992-1997 would also obviate the need to address the ambiguous "spotted dolphin" sightings reported by NEFSC surveys from this period. (In the Roberts et al. (2016a) model used for Phase III, we assumed the "spotted dolphin" sightings were all Atlantic spotted dolphins, based on the much higher abundance of that species in this area, and its more temperate distribution.) However, the 1992-1997 surveys from SEFSC reported important sightings in two areas. First, the R/V Oregon II 1992 shipboard survey, conducted in winter, reported several sightings of Atlantic spotted dolphins over the Blake Plateau, far beyond the shallow portion of the shelf where the species is usually sighted. These are the only sightings in this area across the entire 1992-2016 period. Second, the SEFSC MATS 1995 aerial survey reported two mid-shelf sightings outside Chesapeake Bay. (Although these were north of Cape Hatteras, they are undoubtedly of the coastal form, which is readily differentiable from pantropical spotted dolphin.) These two were not as remarkable as the Blake Plateau sightings, but were desirable to help define seasonal shifts in density north of Cape Hatteras. Considering all of these concerns, we decided to retain SEFSC surveys from the 1992-1997 period but exclude the NEFSC surveys (Figure 51).

For the updated model, we applied $g(0)$ estimates (Table 24) derived from availability and perception bias corrections developed by Palka et al. (2017).

Table 23. Atlantic spotted dolphin sightings from 1992-2016, available for the Option Year 2 spatial model. "Extant" sightings were used in the Phase III regional model (Roberts et al. 2016a). "Added" sightings were incorporated during the Base Year and Option Year 1 for the updated model. Counts include both sightings with fully-resolved species identifications and ambiguous sightings reclassified as Atlantic spotted dolphins.

			Atl. spotted dolphin		
Platform	Provider	Program	Extant	Added	Total
Aerial	NEFSC	Marine mammal abundance surveys	2		2
	SEFSC	Marine mammal abundance surveys	121	112	233
	UNCW	Cape Hatteras Navy Surveys	19	25	44
		Jacksonville Navy Surveys	267	63	330
		Marine mammal surveys, 2002	1		1
		Norfolk Canyon Navy Surveys		27	27
		Onslow Bay Navy Surveys	65		65
		Right whale surveys, 2005-2008	5		5
	VAMSC	MD Wind Energy Area surveys		1	1
		VA Wind Energy Area surveys	1	2	3
	All		481	230	711
Shipboard	NEFSC	Marine mammal abundance surveys	19	42	61
	SEFSC	Marine mammal abundance surveys	328	118	446
	All		347	160	507

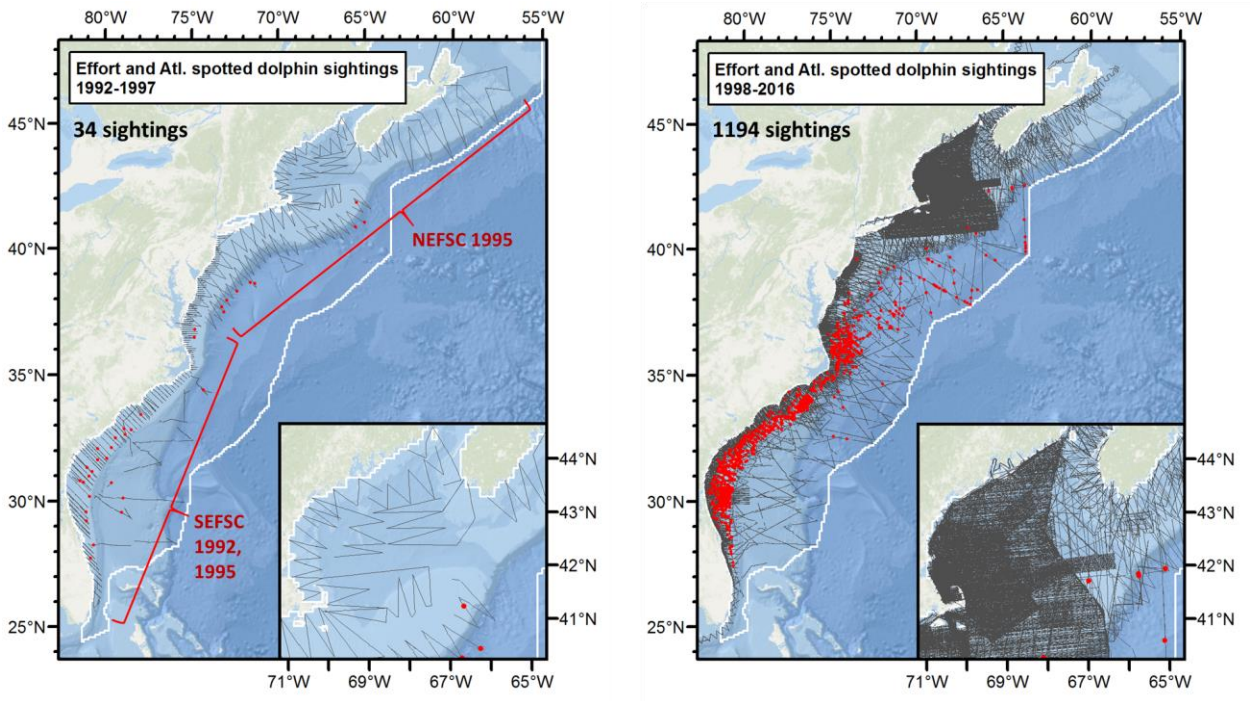

Figure 51. Survey effort and Atlantic spotted dolphin sightings. Not all surveys shown were used in the updated model (see text).

Table 24. *g*(0) estimates used in the updated Atlantic spotted dolphin model.

Platform	Region	Perception Bias	Availability Bias	*g*(0)	Source (all Palka et al. 2017)
Shipboard	Northeast	0.924	1	0.924	Atl. spotted dolphin shipboard NE
	Southeast	0.722	1	0.722	Atl. spotted dolphin shipboard SE
Aerial	Northeast	0.843	1	0.843	Atl. spotted dolphin aerial SE
	Southeast	0.843	1	0.843	Atl. spotted dolphin aerial SE

Given that genetic, morphometric, and behavioral analysis showed a geographic boundary between the coastal and offshore ecotypes at the shelf break at Cape Hatteras (Baron et al. 2008; Viricel & Rosel 2014), and that the offshore ecotype was found most frequently in a very different ecosystem (i.e. within and north of the Gulf Stream) than the coastal ecotype, we split the study area into subregions at the 125m isobath and modeled them separately (Figure 52). For the on-shelf subregion, candidate models fitted to climatological environmental covariates yielded better REML scores and explained more deviance than models fitted to contemporaneous environmental covariates, so we selected the climatological-covariates model fitted to all survey segments as the best (Figure 52, Figure 54). (For brevity, we omit discussion of the functional relationships.)

For the off-shelf region, contemporaneous covariates clearly performed better but the best contemporaneous model retained a biological covariate derived from ocean color observations (Figure 55). These data were not available prior to late 1997, which meant the surveys prior to this period, such as the Oregon II winter survey of the Blake Plateau, were excluded from the model by virtue of not having values for the biological covariates. Nevertheless the resulting model did predict low density across the portion of the Blake Plateau where the species was sighted in 1992 (Figure 53). This assuaged our main concern with the contemporaneous model and we selected it as best.

As occurred with the Roberts et al. (2016a) model used for Phase III, the aggregate predictions of the two subregional models showed a thin band of low density along the shelf break, where the two models met (Figure 53). Concerned that this could be an "edge effect" resulting from splitting the surveys into two models there, we fitted an experimental model that grouped all surveys into a single model. The "dip" in density along the shelf break occurred in that model as well, and functional relationships for the depth and distance to 125m isobath covariates clearly showed this effect (Figure 56). Confident that the dip was real, we retained the subregional models. The dip provides additional evidence that the two ecotypes are geographically distinct.

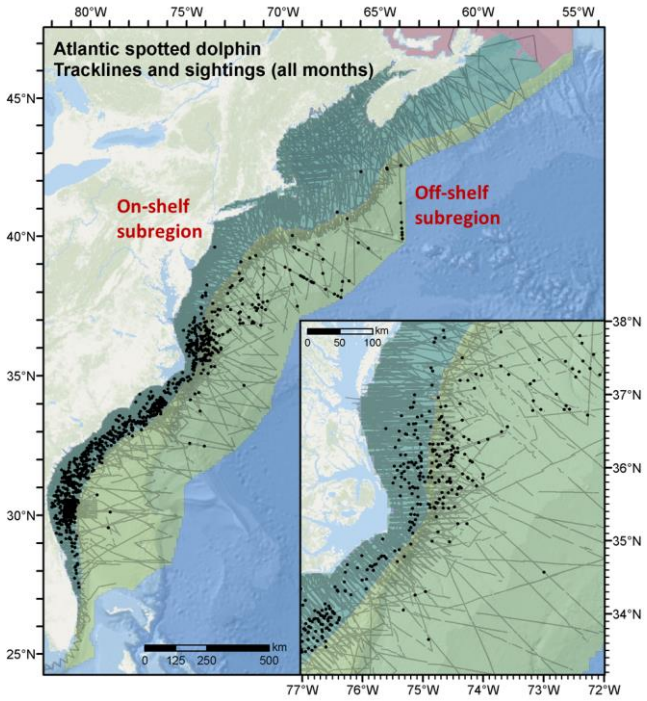

Figure 52. Atlantic spotted dolphin model's tracklines, sightings, and subregions (dark green, light green). We fitted and predicted independent models for each subregion (see text).

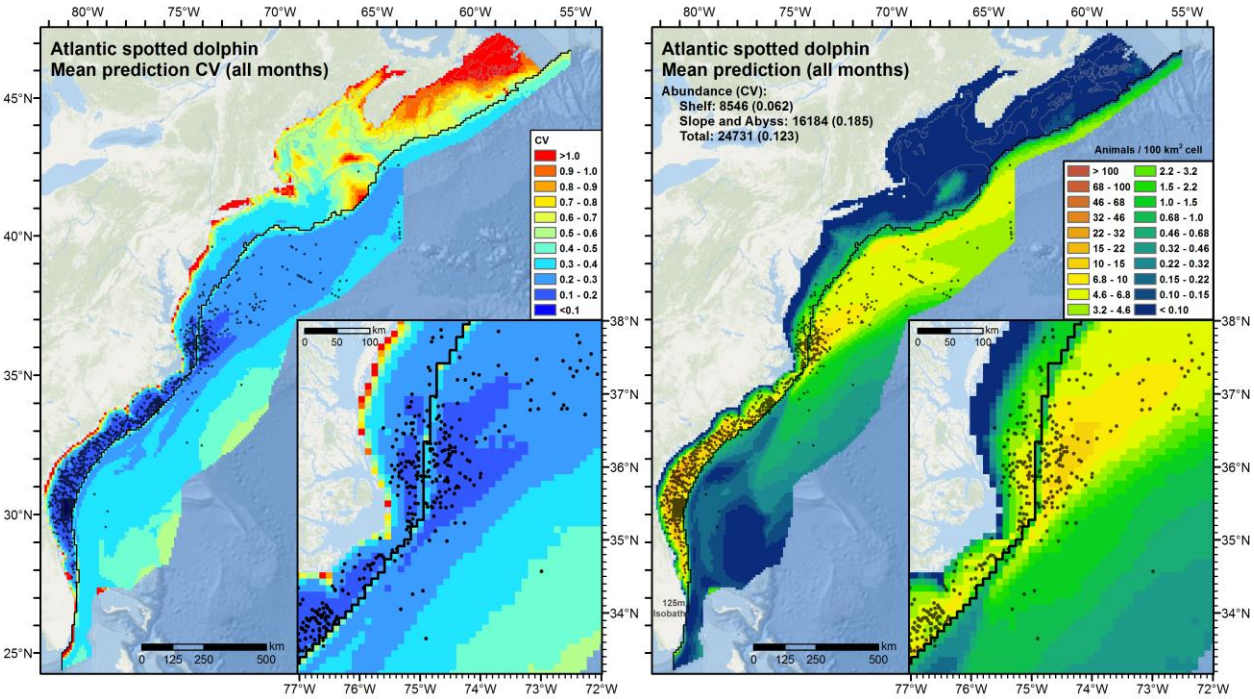

Figure 53. Predicted year-round mean density and total abundance (right) and coefficient of variation (left) for Atlantic spotted dolphin, with sightings overlaid. Heavy black line shows the boundary between the subregional models. Note: We recommend that monthly mean predictions be used for management purposes (see text).

```
Family: Tweedie(p=1.395)
Link function: log

Formula:
Abundance ~ offset(log(Area)) + s(log10(Depth), bs = "ts") + s(log10(Slope), bs = "ts") +
    s(sqrt(DistToShore/1000), bs = "ts") + s(ClimSST, bs = "ts") + s(ClimSalinity, bs = "ts") +
    s(I(ClimDistToSSTFront3^(1/3)), bs = "ts") + s(log10(pmax(ClimPkPP1, 0.1)), bs = "ts") +
    s(log10(pmax(ClimTKE, 1e-04)), bs = "ts")

Parametric coefficients:
            Estimate Std. Error t value Pr(>|t|)
(Intercept)  -5.7287     0.1488  -38.51   <2e-16 ***
---
Signif. codes:  0 '***' 0.001 '**' 0.01 '*' 0.05 '.' 0.1 ' ' 1

Approximate significance of smooth terms:
                                edf Ref.df      F  p-value
s(log10(Depth))               4.6502      9  5.721 1.63e-12 ***
s(log10(Slope))               0.9744      9  1.283 0.000243 ***
s(sqrt(DistToShore/1000))     3.7655      9  4.284 1.14e-09 ***
s(ClimSST)                    3.7490      9  9.966  < 2e-16 ***
s(ClimSalinity)               4.7753      9 14.098  < 2e-16 ***
s(I(ClimDistToSSTFront3^(1/3))) 1.0833      9  2.132 1.26e-06 ***
s(log10(pmax(ClimPkPP1, 0.1)))  4.3361      9 13.664  < 2e-16 ***
s(log10(pmax(ClimTKE, 1e-04)))  7.2794      9  4.809 3.70e-08 ***
---
Signif. codes:  0 '***' 0.001 '**' 0.01 '*' 0.05 '.' 0.1 ' ' 1

R-sq.(adj) =  0.0492   Deviance explained = 40.2%
-REML = 8050.8  Scale est. = 64.54     n = 60249
```

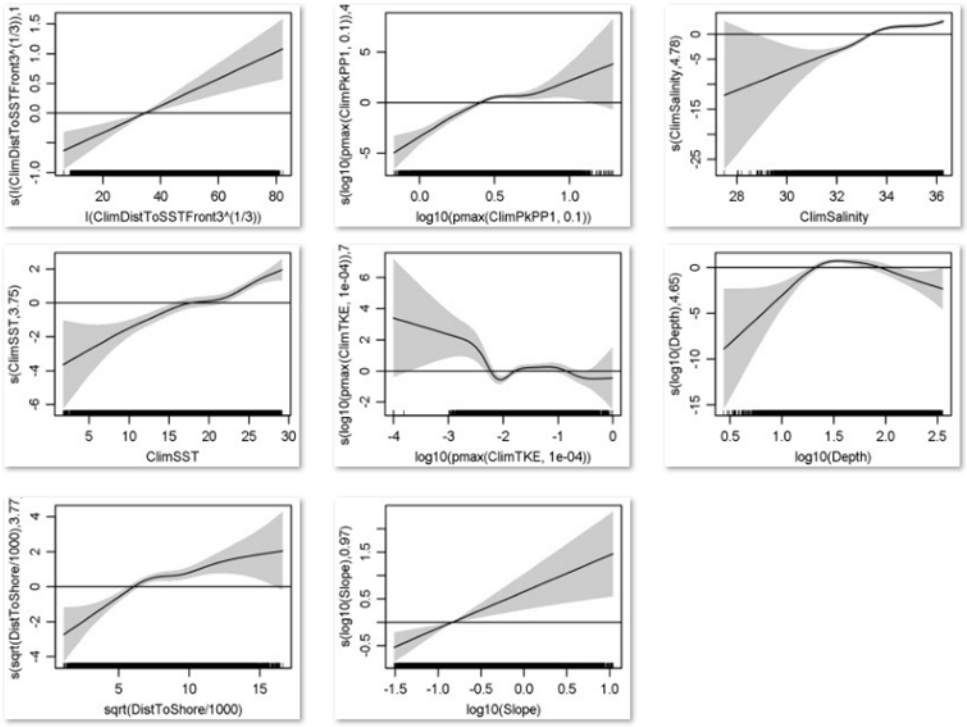

Figure 54. Atlantic spotted dolphin's "on-shelf subregion" model's statistical output and covariate term plots.

```
Family: Tweedie(p=1.33)
Link function: log

Formula:
Abundance ~ offset(log(Area)) + s(log10(Depth), bs = "ts") + s(ClimSST, bs = "ts") + s(ClimSalinity, bs = "ts") +
    s(I(ClimDistToSSTFront1^(1/3)), bs = "ts") + s(log10(pmax(ClimPkPP1, 0.1)), bs = "ts") +
    s(log10(pmax(ClimTKE, 1e-04)), bs = "ts")

Parametric coefficients:
            Estimate Std. Error t value Pr(>|t|)
(Intercept)  -5.1934     0.1688  -30.77   <2e-16 ***
---
Signif. codes:  0 '***' 0.001 '**' 0.01 '*' 0.05 '.' 0.1 ' ' 1

Approximate significance of smooth terms:
                                   edf Ref.df     F  p-value
s(log10(Depth))                 1.9058      9 8.618  < 2e-16 ***
s(ClimSST)                      7.0543      9 7.488 6.06e-14 ***
s(ClimSalinity)                 0.9100      9 0.778 0.003230 **
s(I(ClimDistToSSTFront1^(1/3))) 3.0359      9 2.525 6.62e-06 ***
s(log10(pmax(ClimPkPP1, 0.1)))  2.6888      9 6.165 1.84e-15 ***
s(log10(pmax(ClimTKE, 1e-04)))  0.9683      9 1.161 0.000296 ***
---
Signif. codes:  0 '***' 0.001 '**' 0.01 '*' 0.05 '.' 0.1 ' ' 1

R-sq.(adj) =  0.0449   Deviance explained = 44.1%
-REML = 2023.7  Scale est. = 124.86    n = 24679
```

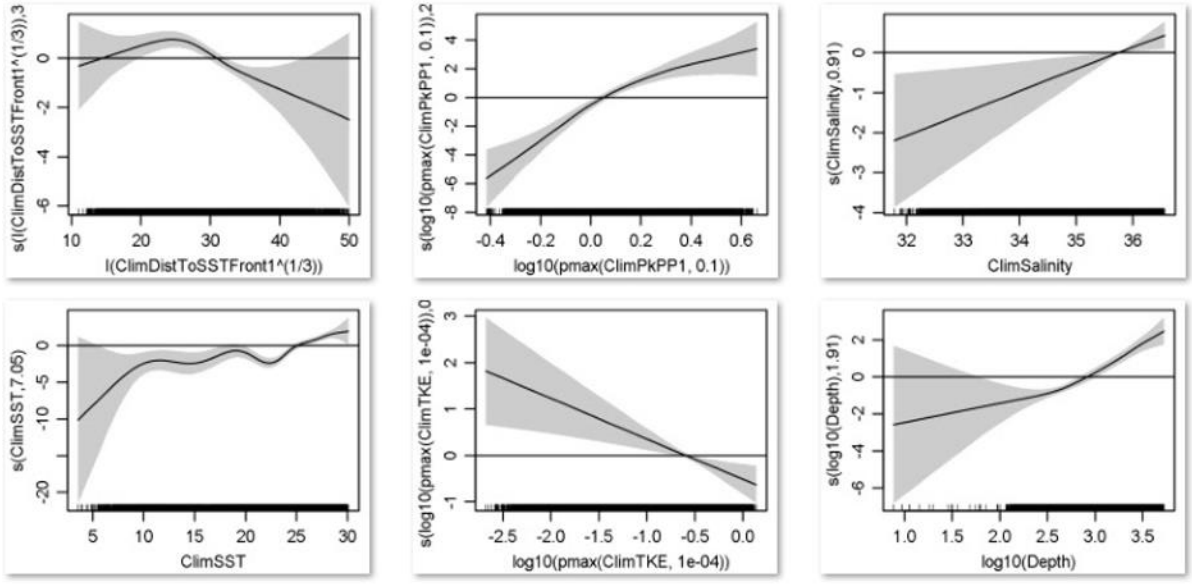

Figure 55. Atlantic spotted dolphin's "off-shelf subregion" model's statistical output and covariate functional plots.

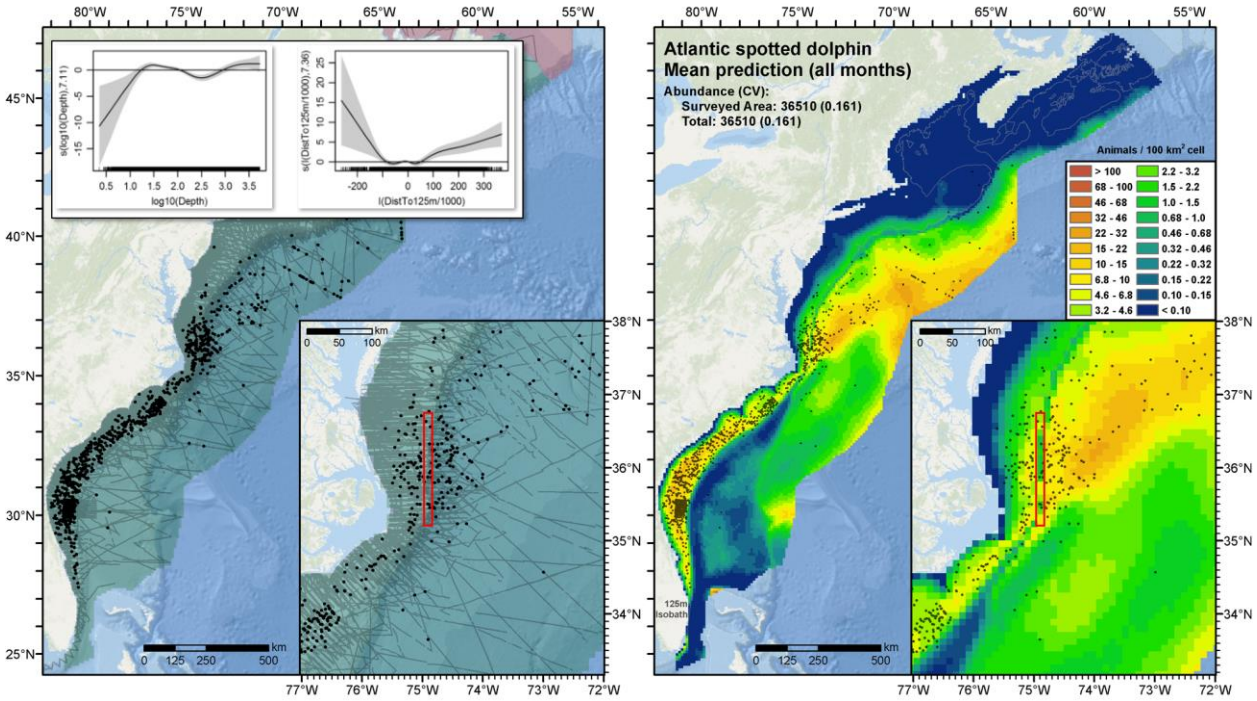

Figure 56. Density surface (right) predicted from an experimental model that grouped all surveys in a single model (left). This shows that the "dip" in density at the shelf break (red boxes) occurs both when the surveys are split into two independent subregional models (as in Figure 52) and when they are grouped into a single model (as here). Insets (upper left) show fitted relationships for static covariates that captured the dip (other covariates not shown).

Little has been reported about seasonal movements of Atlantic spotted dolphins. Read et al. (2014) conducted several years of aerial surveys at Onslow Bay, NC, spanning the shallow and deep sides of the 125m shelf break. (These are included in our models.) They sighted only the continental shelf ecotype of Atlantic spotted dolphin and reported "some indication of an effect of season and/or water temperature on the probability of the presence of spotted dolphins, but this effect was small compared to the overriding effect of water depth." Normally, without further published evidence of seasonal movements, we recommend that year-round (static) density predictions be used for species management, as we did with Atlantic spotted dolphins in Roberts et al. (2016a). However, the AMAPPS, UNCW, and VAMSC surveys of the continental shelf north of Cape Hatteras that were added after Phase III provided year-round coverage of this area. The survey data showed a clear pattern of relative absence in winter and early spring and high presence in summer and fall. In addition, acoustic monitoring of the Maryland Wind Energy Area with C-PODs by H. Bailey and A. Rice showed a drop in dolphin acoustic detections from January-April (H. Bailey, unpublished data). (This acoustic survey did not differentiate between dolphin species, but most likely all of the detections were either of common bottlenose dolphins or Atlantic spotted dolphins.) Monthly predictions from our models reproduced this pattern (Figure 57). After reviewing this new evidence and model results with collaborators, we agreed to recommend monthly density predictions for management of Atlantic spotted dolphins on the continental shelf. Off the shelf, we recommend the year-round prediction be used, similar to striped dolphin, because of the seasonal bias in survey effort. For the NMSDD and other model users, we are providing 12 monthly maps that show density varying from month-to-month on the shelf while remaining constant off-shelf (Figure 57).

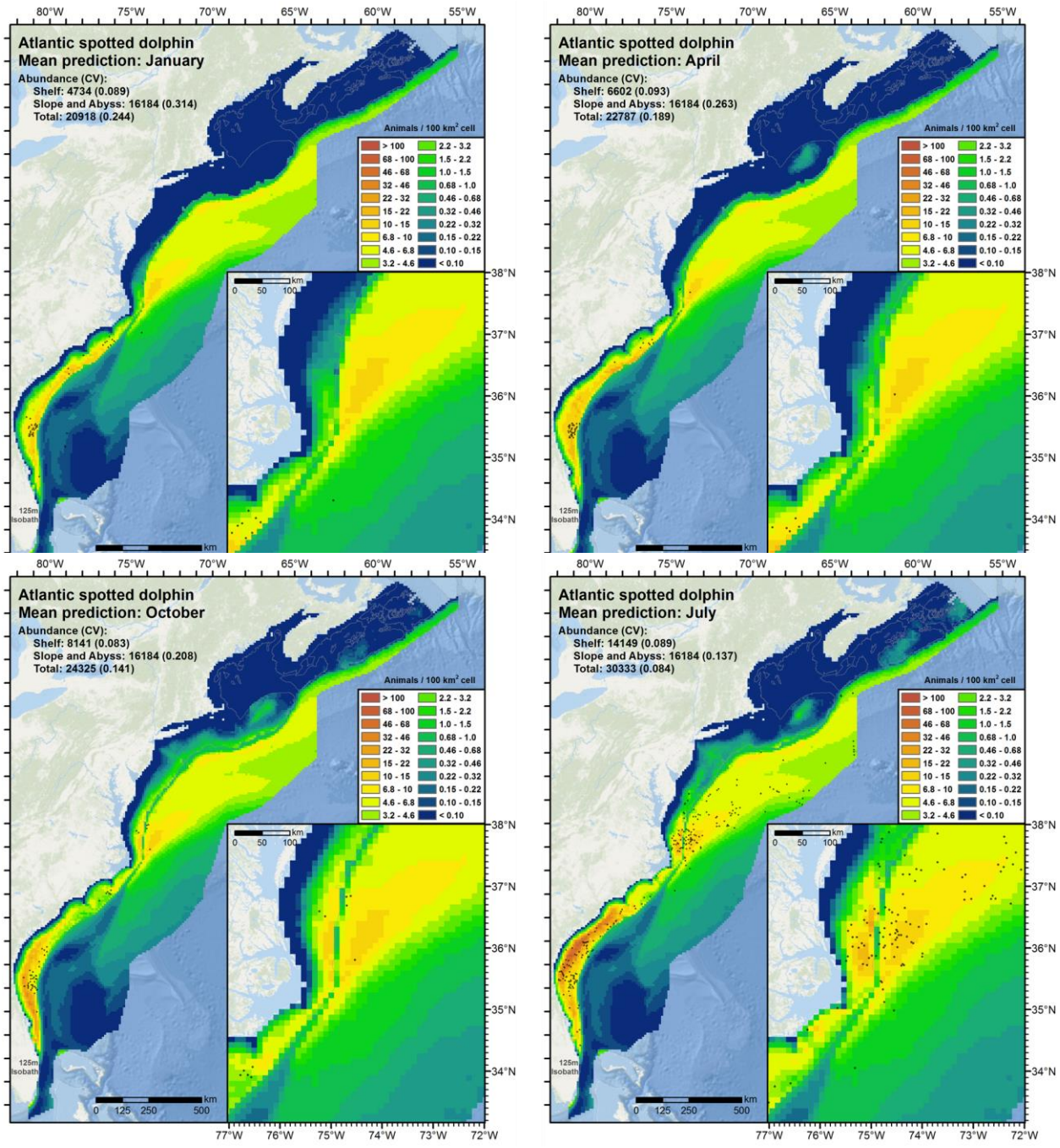

Figure 57. Four monthly predictions for the middle month of each season, with sightings overlaid. Clockwise from upper-left: winter (January), spring (April), summer (July), fall (October). Note that because survey effort was not uniform across months, a lack of sightings in an area should not be taken as evidence that the species was absent (there might have been no surveying done there during that month).

Year-round total abundance predicted by the updated model was less than half of that predicted by the Roberts et al. (2016a) model (Table 25) used for Phase III. We attribute much of this difference to the new SEFSC shipboard detection function that addressed the "spike" in detections close to the trackline (see Section 2.3.1 above). The new detection function estimated a much higher probability of detection than the Phase III detection function, resulting in a much smaller correction for dolphins that were "missed" by observers.

Abundance predictions from the updated model were lower than those of Phase III for all seasons except winter, which were markedly higher (Table 25). When predictions were summarized seasonally, the updated model showed less variation by season, ranging from about 21,000 to 30,000, while the Phase III model ranged from 12,000 to 94,000. We believe the lower seasonal variation is more realistic, as it seems unlikely that the species would be migrating in and out of the study area in such high numbers.

The updated model's abundance predictions were also substantially lower than the SAR estimates and Palka et al.'s (2017) predictions. For the 2004 SAR, this difference might be attributable to our detection function correcting for the "spike" in shipboard detections on SEFSC surveys. But the 2011 SAR and Palka et al. (2017) models relied on AMAPPS surveys alone, and these did not exhibit the "spike" seen on earlier surveys, so the difference between their detection functions and ours would not be as pronounced. The differences between the models remain an item for future investigation between the modeling teams.

Table 25. Comparison of abundance estimates (with CV in parentheses) for Atlantic spotted dolphin, obtained from recent NMFS Stock Assessment Reports (SARs) and density surface models. "Updated model" refers to the model presented here. For the preceding Roberts et al. (2016) model, we recommend a single, year-round density surface for management purposes but show seasonal estimates (brown text) to facilitate more granular comparison to the SARs and other models.

	Years	Dec-Feb	Mar-May	Jun-Aug	Sep-Nov	Year-round
NMFS SARs	2004			50,978 (0.42)		
	2011			44,715 (0.43)		
Roberts et al. (2016) [1,2]	1992-2014	12,217	94,485	80,913	34,969	55,436 (0.32)
Palka et al. (2017) [1]	2010-2013		65,948 (0.156)	54,731 (0.153)	56,372 (0.165)	
Updated model [1,2]	1992-2016	20,952	22,594	30,232	25,368	24,731 (0.123)

[1] CV is underestimated; it only accounts for uncertainty in spatial model parameters, not detection functions or $g(0)$.
[2] 3-month mean abundance shown for comparison. In Roberts et al. (2016), we recommend the year-round average be used for management, while for the updated model, we recommend monthly averages.

2.3.5.7. Common bottlenose dolphin model

The common bottlenose dolphin (*Tursiops truncatus*) is the most abundant cetacean along the U.S. east coast, with the possible exception of the short-beaked common dolphin. Owing to its high abundance and its distribution close to shore, the surveys used in our analysis reported more than 6000 sightings of bottlenose dolphin (Table 26), which was more than any other species.

Bottlenose dolphins exhibit the most complex population structure yet documented for any cetacean in the U.S. Atlantic or Gulf of Mexico. The MMPA requires that cetaceans be managed on a per-"stock" basis, and defines a stock as "a group of marine mammals of the same species or smaller taxa in a common spatial arrangement, that interbreed when mature". NMFS is responsible for defining stocks and estimating their abundance, and periodically issues stock assessment reports that summarize the latest research and promulgate stock definitions and abundance estimates. At the time that NMFS last revised the stock assessment reports for many of the east coast stocks (Hayes et al. 2018), the reports described the western North Atlantic stocks as follows:

Two morphologically and genetically distinct morphotypes of bottlenose dolphins, known as the coastal and offshore forms, inhabit the western North Atlantic. The offshore form is larger and more robust, and consists of a single stock, which inhabits off-shelf, slope, and shelf-break waters, as well as outer portions of the continental shelf.

The spatiotemporal extent and dynamics of its on-shelf distribution (e.g. how close it comes to shore) are a topic of active research and appear to vary spatially and seasonally. The coastal morphotype consists of multiple "coastal" and "estuarine" stocks. At the time of this writing, NMFS defined five coastal stocks for the east coast, each genetically distinct. They generally inhabit the inner portions of the continental shelf, and some migrate north along the shelf in summer and return south in winter. NMFS also defined 10 estuarine stocks for the east coast. These inhabit particular bays, sounds, rivers, and other estuarine systems and may be genetically distinct from each other as well as the other coastal stocks. They generally do not migrate.

There is spatiotemporal overlap between many of these stocks–between the offshore and coastal stocks, among the coastal stocks, between the estuarine and coastal stocks, and among the estuarine stocks. At present, we lack the information necessary to model each stock individually. The core problem is that there is no reliable and comprehensive way to determine which stock a given sighting belongs to. Some surveys in our study reported "coastal bottlenose dolphin" or "offshore bottlenose dolphin", but most did not, and none reported more precise detail than that.

NMFS stock assessment reports and the literature (e.g. Torres et al. 2003) discussed potential methods for classifying sightings based on geographic location, distance to shore, depth, and other variables, but these proposals did not cover all of the stocks or definitively address the overlaps between them, and there was no widespread agreement among the research community on the efficacy of proposed approaches. At the present time, the only foolproof method of classifying a sighting into a stock is through genetics. Therefore we have made no attempt to model bottlenose dolphins on a per-stock basis from the visual sightings, and have instead modeled all stocks in a single model. Prior to fitting our spatial model, we discarded all estuarine survey transects, thus it is probably reasonable to assume that our model estimates the aggregate density of the offshore and coastal stocks and excludes the estuarine stocks (although some estuarine stocks are known to range into coastal areas beyond their home estuaries; presumably some of these were sighted and we failed to discard them).

Surveys added after the Phase III models increased the number of sightings available for our model by about 58% (Table 26, Figure 58). As with the models updated in Option Year 1, we reviewed the available literature and data to assess the feasibility of excluding surveys from 1992-1997 from the updated spatial model, as this period predated the launch of the SeaWiFS ocean color sensor needed for contemporaneous biological covariates. However, unlike many of the other models we updated in Option Years 1 and 2, for bottlenose dolphins we decided not to exclude the surveys from 1992-1997, for two reasons. First, as with Atlantic spotted dolphins, the R/V Oregon II 1992 wintertime shipboard survey reported several sightings of bottlenose dolphins over the Blake Plateau, far beyond the shelf and shelf-break waters where the species is more frequently sighted. Second, east coast bottlenose dolphins are known to suffer recurrent cetacean morbillivirus epizootics (Duignan et al. 2006) that can kill large fractions of affected stocks. During one such event in 1987-88, more than half of the inshore population between Florida and New Jersey may have died (Taubenberger et al. 1996). A similar event occurred from July 1, 2013 through March 1, 2015. As far as we know, mortality estimates for this event have not been published in the peer-reviewed literature yet—analysis by NMFS is ongoing—but the total number of known strandings (over 1600) more than doubled that of the 1987-88 event (about 740) (https://www.fisheries.noaa.gov/national/marine-life-distress/2013-2015-bottlenose-dolphin-unusual-mortality-event-mid-atlantic). Populations are believed to have recovered somewhat in the years after such events (L. Garrison, pers. comm.). Given this pattern of high cyclic interdecadal variability in population sizes, and that our results might be utilized for take estimation for time periods relatively far in the future (e.g. the Navy AFTT Phase IV EIS, which would cover the 2025-2032 period), SEFSC species experts recommended we utilize all available data for the 1992-2016 period, so that model predictions would characterize the long-term average.

For the updated model, we applied $g(0)$ estimates (Table 27) derived from availability and perception bias corrections developed by Palka et al. (2017).

Table 26. Common bottlenose dolphin sightings from 1992-2016, available for the Option Year 2 spatial model. "Extant" sightings were used in the Phase III regional model (Roberts et al. 2016a). "Added" sightings were incorporated during the Base Year and Option Year 1 for the updated model. Counts include both sightings with fully-resolved species identifications and ambiguous sightings reclassified as common bottlenose dolphins.

			Bottlenose dolphin		
Platform	Provider	Program	Extant	Added	Total
Aerial	NEFSC	Marine mammal abundance surveys	99	54	153
		NARWSS right whale surveys	47	33	80
	SEFSC	Marine mammal abundance surveys	902	719	1621
	UNCW	Cape Hatteras Navy Surveys	113	145	258
		Jacksonville Navy Surveys	325	87	412
		Marine mammal surveys, 2002	308		308
		Norfolk Canyon Navy Surveys		52	52
		Onslow Bay Navy Surveys	149		149
		Right whale surveys, 2005-2008	1817		1817
	VAMSC	MD Wind Energy Area surveys		270	270
		VA Wind Energy Area surveys	118	30	148
	All		3878	1390	5268
Shipboard	NEFSC	Marine mammal abundance surveys	177	177	354
	NJDEP	New Jersey Ecological Baseline Study	160		160
	SEFSC	Marine mammal abundance surveys	380	161	541
	All		717	338	1055

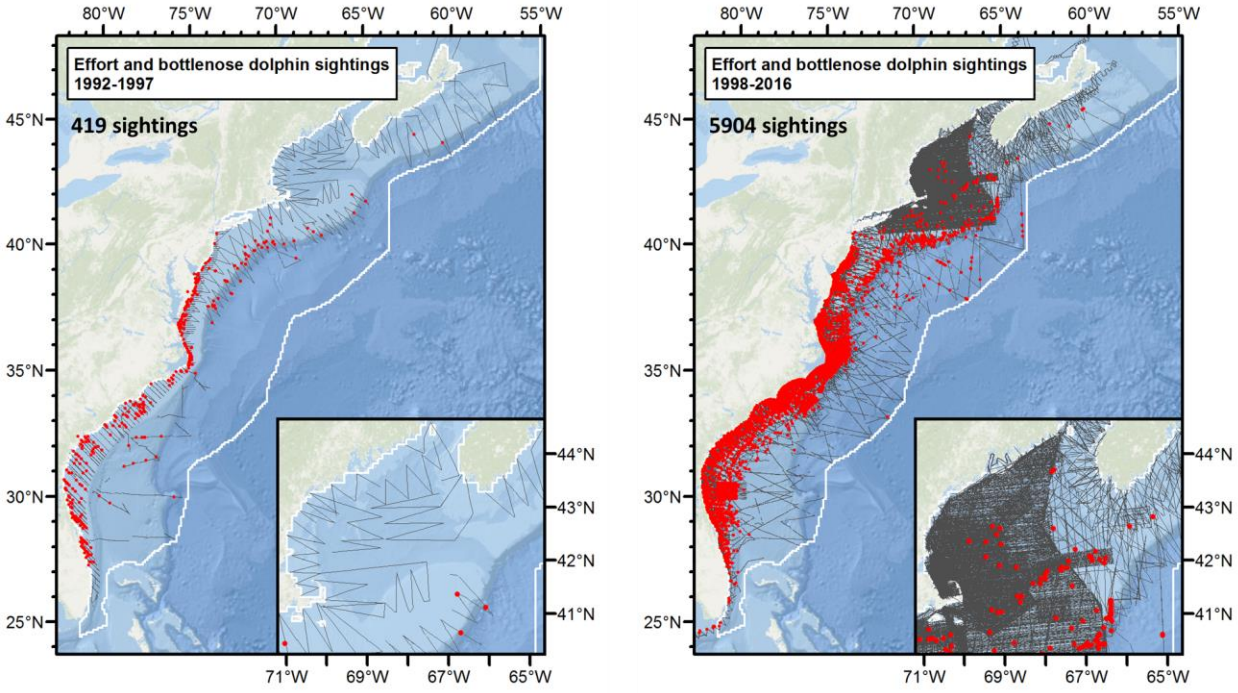

Figure 58. Survey effort and common bottlenose dolphin sightings available for the updated model. Unlike several other models, we did not exclude the 1992-1997 period from the updated model (see text).

Table 27. *g*(0) estimates used in the updated common bottlenose dolphin model.

Platform	Region	Perception Bias	Availability Bias	*g*(0)	Source (all Palka et al. 2017)
Shipboard	Northeast	0.643	1	0.643	Bottlenose dolphin shipboard NE
	Southeast	0.609	1	0.609	Bottlenose dolphin shipboard SE
Aerial	Northeast	0.657	0.785	0.516	Bottlenose dolphin aerial NE
	Southeast	0.814	0.785	0.634	Bottlenose dolphin aerial SE

As mentioned, some coastal stocks of bottlenose dolphins are known to migrate north in summer and return south in winter. The dynamics may vary by stock and year and are not well understood. NMFS has often described the migratory ranges and dynamics as being influenced or limited by water temperature (Hayes et al. 2018). Our literature review did not reveal evidence of distinct seasonal changes in species-environment relationships, in contrast with other species such as baleen whales. Given the lack of evidence for such changes, we did not split the data into seasonal strata to be modeled separately, and instead relied on dynamic predictors such as SST to reproduce seasonal shifts in density within a single "year-round" model. Given the spatial overlap between stocks, we did not split the data into geographic strata either.

Candidate models fitted to climatological environmental covariates yielded better REML scores and explained more deviance than models fitted to contemporaneous environmental covariates, so we selected the climatological-covariates model fitted to all survey segments as the best (Figure 59, Figure 61). The model was the most complex of all species updated this Option Year, retaining 10 covariates, many of which showed high functional complexity (Figure 61). This result reflects the large number of sightings available to the model, and that multiple stocks with differing environmental preferences were grouped into a single model, rather than being modeled separately. For example, the fitted relationship for the depth covariate was bimodal (Figure 61), with a peak in density at 15 m (or 1.2 in log10 scale) and then again from about 300-2000 m (or 2.5-3.3 in log10 scale), likely corresponding to the habitat preferences of the coastal and offshore morphotypes, respectively. The model also showed a strong fall-off in density as SST fell below 8 °C, which was close to but did not exactly match NMFS' finding that the species' "northern distribution in winter appears to be limited by water temperatures <9.5 ºC" (Hayes et al. 2018). However, given the exceptional complexity of these relationships and the large number of covariates retained, we urge considerable caution in interpreting them.

Consistent with the literature, the model predicted highest densities close to shore, concentrated in the southeast and mid-Atlantic (Figure 60), where the coastal morphotype predominates. On the shelf, density remained high south of Cape Hatteras in all seasons. Monthly predictions showed density moving up the coast as spring progressed, reaching southern New England in summer, persisting through fall, and retreating south in early winter (Figure 62). Another band of elevated density, presumably of the offshore morphotype, occurred over the upper continental slope and spanned the study area (Figure 60), with a peak at Cape Hatteras, and diminishing at the northeast Scotian Shelf, where bottlenose dolphins have been sighted occasionally (Baird et al. 1993; Gowans & Whitehead 1995; Lawson & Gosselin 2009). This band persisted in all seasons as far north as the Northeast Channel of the Gulf of Maine (Figure 62). While sightings of bottlenose dolphins were reported in all seasons around Georges Bank or in the Gulf of Maine in all seasons, most surveys of the continental slope occurred in summer, and we urge caution with model predictions in colder months.

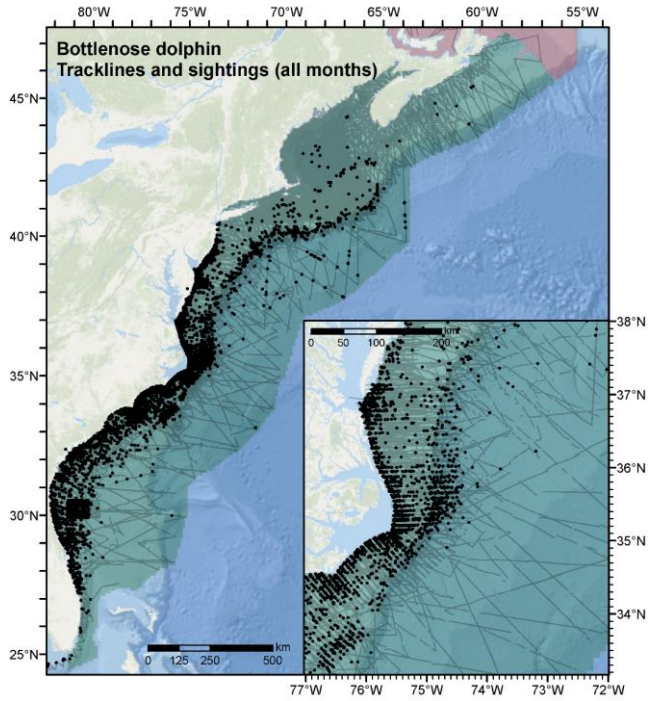

Figure 59. Common bottlenose dolphin model's tracklines, sightings, and prediction area (green).

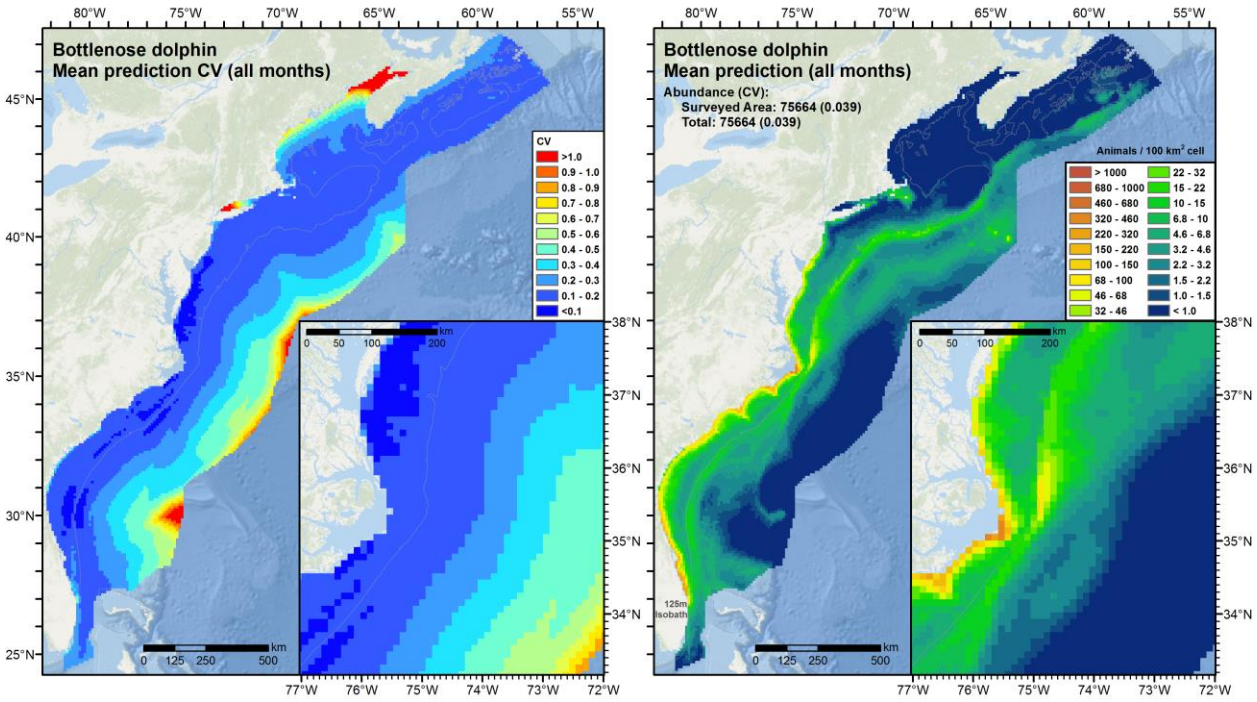

Figure 60. Predicted year-round mean density and total abundance (right) and coefficient of variation (left) for common bottlenose dolphin (sightings omitted to avoid obscuring the density and CV surfaces). Note: We recommend that monthly mean predictions be used for management purposes (see text).

```
Family: Tweedie(p=1.458)
Link function: log

Formula:
Abundance ~ offset(log(Area)) + s(log10(Depth), bs = "ts") + s(log10(Slope), bs = "ts") +
    s(sqrt(DistToShore/1000), bs = "ts") + s(I(DistTo125m/1000), bs = "ts") + s(ClimSST, bs = "ts") +
    s(pmax(ClimSalinity, 31), bs = "ts") + s(I(ClimDistToSSTFront2^(1/3)), bs = "ts") +
    s(log10(pmax(ClimEpiMnkPB3, 0.001)), bs = "ts") + s(I(ClimDistToAEddy4/1000), bs = "ts") +
    s(I(ClimDistToCEddy4/1000), bs = "ts")

Parametric coefficients:
            Estimate Std. Error t value Pr(>|t|)
(Intercept) -4.50689    0.05137  -87.74   <2e-16 ***
---
Signif. codes:  0 '***' 0.001 '**' 0.01 '*' 0.05 '.' 0.1 ' ' 1

Approximate significance of smooth terms:
                                     edf Ref.df      F  p-value
s(log10(Depth))                    8.299      9 26.497  < 2e-16 ***
s(log10(Slope))                    1.134      9  2.632 3.89e-07 ***
s(sqrt(DistToShore/1000))          8.121      9 24.263  < 2e-16 ***
s(I(DistTo125m/1000))              8.120      9  5.879 1.24e-09 ***
s(ClimSST)                         8.749      9 33.065  < 2e-16 ***
s(pmax(ClimSalinity, 31))          8.380      9 31.201  < 2e-16 ***
s(I(ClimDistToSSTFront2^(1/3)))    6.362      9  9.706  < 2e-16 ***
s(log10(pmax(ClimEpiMnkPB3, 0.001))) 8.674    9 21.669  < 2e-16 ***
s(I(ClimDistToAEddy4/1000))        7.164      9  4.746 1.06e-07 ***
s(I(ClimDistToCEddy4/1000))        5.116      9 29.476  < 2e-16 ***
---
Signif. codes:  0 '***' 0.001 '**' 0.01 '*' 0.05 '.' 0.1 ' ' 1

R-sq.(adj) =  0.0342   Deviance explained = 34.3%
-REML =  39605  Scale est. = 49.594    n = 138131
```

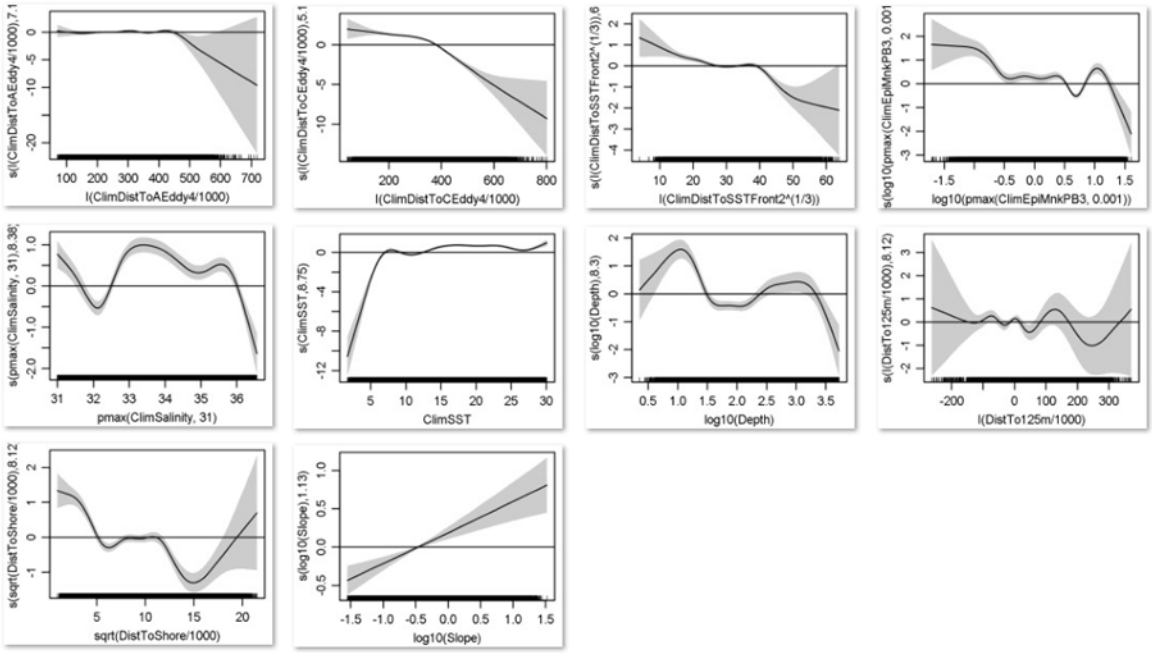

Figure 61. Common bottlenose dolphin model's statistical output and covariate functional plots.

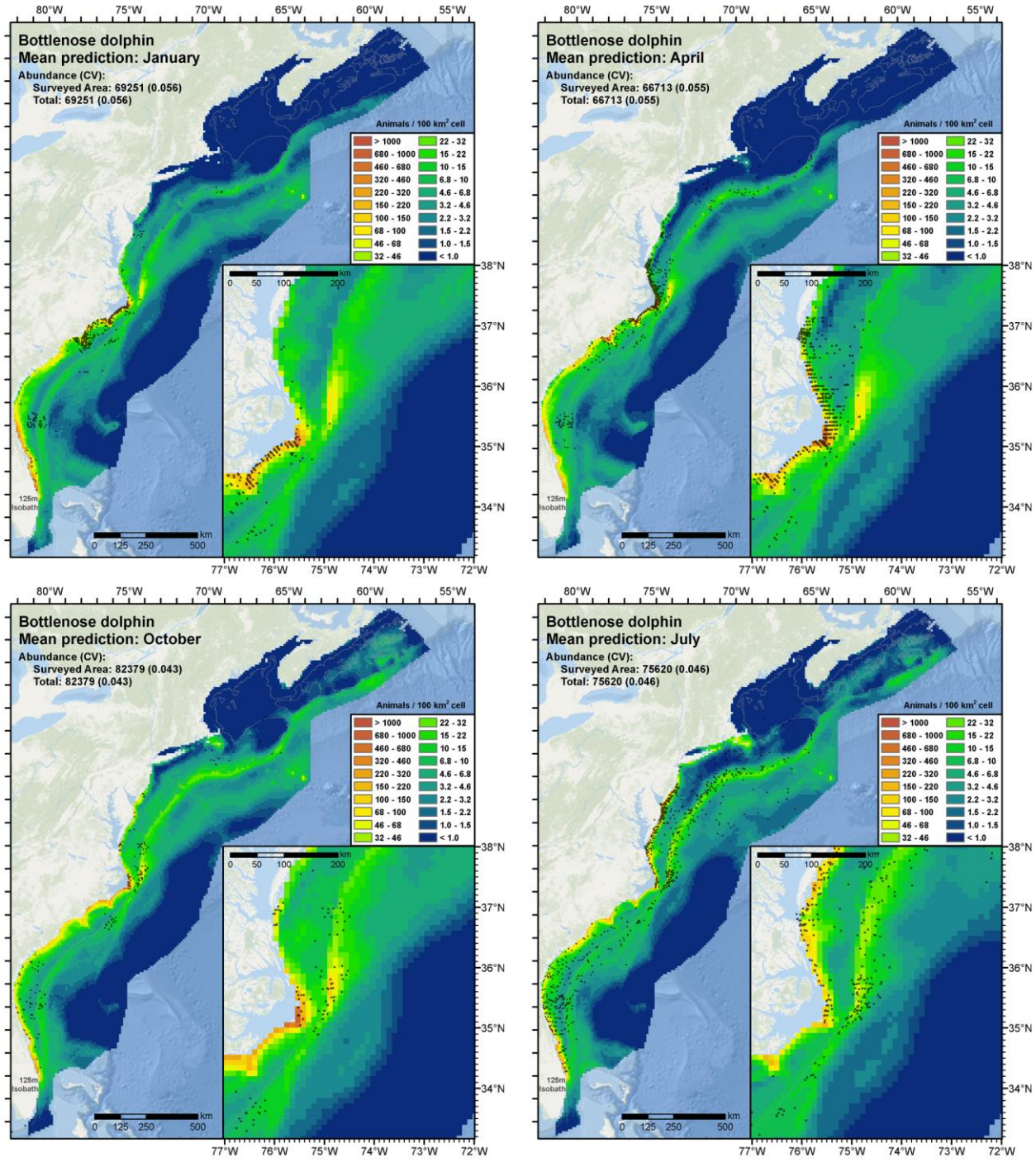

Figure 62. Four monthly predictions for the middle month of each season, with sightings overlaid. Clockwise from upper-left: winter (January), spring (April), summer (July), fall (October). Note that because survey effort was not uniform across months, a lack of sightings in an area should not be taken as evidence that the species was absent (there might have been no surveying done there during that month).

Year-round total abundance predicted by the updated model was about 23% less than that predicted by the Roberts et al. (2016a) model used for Phase III (Table 28). Abundance varied with the same seasonal pattern, with highest abundance in summer and fall. The relative difference in between the seasons of highest and lowest abundance (fall and spring) decreased from 30% to 16%.

We believe several factors contributed to the decrease in abundance relative to the Phase III model. First, as with Atlantic spotted dolphin, the new SEFSC shipboard detection function that addressed the "spike" in detections close to the trackline (see Section 2.3.1 above) resulted in a much smaller correction for dolphins that were "missed" by observers, pushing abundance down. Also contributing to the decrease were many new surveys spanning the 2013-2015 period, when the morbillivirus epizootic killed many animals, and we presume survey transects reported lower sighting rates in habitats that had higher abundance in prior years. Opposed to these were decreases in $g(0)$ for all sightings except of groups of 1-5 individuals sighted by aircraft, for which $g(0)$ increased (compare values in Table 27 to those in the supplementary report for bottlenose dolphin in Roberts et al. (2016a)). Decreases in $g(0)$ influence abundance on the corresponding segments higher, while increases influence it lower. With many factors in play, it is hard to apportion the changes in total abundance between them without a detailed sensitivity analysis.

The updated model's abundance predictions were also substantially lower than the SAR estimates and Palka et al.'s (2017) predictions. The SAR estimate for 2016 appeared to be designed to account for the morbillivirus epizootic and were substantially lower than the estimate for 2011, but still higher than our estimate for the 1992-2016 period. The Palka et al. (2017) predictions were higher than all of the others except the Roberts et al. (2016a) prediction for the September-November period. The higher estimates from Palka et al. (2017) might have resulted from these models being based on surveys that occurred just before the epizootic, when abundance might have peaked. The differences between the models remain an item for future investigation between the modeling teams.

Table 28. Comparison of abundance estimates (with CV in parentheses) for common bottlenose dolphin, obtained from recent NMFS Stock Assessment Reports (SARs) and density surface models. "Updated model" refers to the model presented here.

	Years	Dec-Feb	Mar-May	Jun-Aug	Sep-Nov	Year-round
NMFS SARs [1]	2011			118,987		
	2016			96,044		
Roberts et al. (2016) [2,3]	1992-2014	89,412	78,365	109,679	111,283	97,476 (0.06)
Palka et al. (2017) [2]	2010-2013	110,485 (0.240)	111,720 (0.376)	138,700 (0.364)	104,971 (0.240)	
Updated model [2,3]	1992-2016	71,360	69,492	78,008	82,597	75,664 (0.039)

[1] Offshore stock plus five coastal stocks added together (CV not estimated). All estimates from SAR dated April 2018.
[2] CV is underestimated; it only accounts for uncertainty in spatial model parameters, not detection functions or $g(0)$.
[3] 3-month mean abundance shown for comparison, but we recommend monthly averages be used for management.

2.3.5.8. Pantropical spotted dolphin model

The pantropical spotted dolphin (*Stenella attenuata*) has been described as occurring worldwide in tropical, sub-tropical, and some warm-temperate waters between about 40 °N and °40 S (Perrin 2001). Outside of the Pacific Ocean, its distribution is primarily oceanic (Perrin 2001), and it is the most abundant oceanic (> 200 m depth) delphinid in the Gulf of Mexico (Jefferson & Schiro 1997). In the western North Atlantic, it can be difficult for observers to distinguish from the offshore form of Atlantic spotted dolphin, and prior to 1999, NOAA reported a combined abundance estimate for the two species for this area (Waring et al. 2014). It has since been shown that full identifications can confidently be made south of Cape Hatteras (Waring et al. 2014). All of the spotted dolphin sightings that we have south of Cape Hatteras, going back to the earliest survey from 1992, were fully-resolved to the species level. In contrast, the more northerly offshore surveys we have prior to 1998 all reported the ambiguous identification "spotted dolphin". Beginning in 1998, all sightings of spotted dolphins were fully-resolved to the species level. These included four sightings reported by a shipboard survey on August 16, 1998 at 40.6 °N just off Georges Bank. At our request, E. Josephson at NOAA NEFSC reviewed the original records and reconfirmed that observers'

sketches and written descriptions indicated that these were pantropical spotted dolphins, the most northerly sightings reported by any survey conducted by our collaborators.

As with the updated models for other species, we first assessed the feasibility of excluding surveys from 1992-1997 from the updated spatial model, as this period predated the launch of the SeaWiFS ocean color sensor needed for contemporaneous biological covariates. No surveys reported fully-taxonomically-resolved, on-effort sightings of pantropical spotted dolphins during 1992-1997, thus it was not important to retain surveys from this period to boost sighting counts to help establish habitat relationships. Therefore we limited the updated model to surveys from the 1998-2016 period.

Surveys from 1998-2016 reported only 22 sightings (Table 29). Most were reported over the continental slope or abyssal waters in the southern half of the study area (Figure 63), consistent with the literature's description of the species inhabiting warm, oceanic waters. Given the generally offshore, warm-water distribution of this species, we based the updated model only on NOAA's broad-scale abundance surveys and UNCW's aerial surveys of Navy study areas. (The other surveys did not substantially cover pantropical spotted dolphin habitat and did not report any sightings.) We applied $g(0)$ estimates (Table 30) derived from availability and perception bias corrections developed by Palka et al. (2017) for Atlantic spotted dolphin, as no such corrections were available for pantropical spotted dolphin.

For models with only 20-40 sightings, our methodology was to fit a model with only one covariate (Roberts et al. 2016a). Accordingly, we fitted a series of independent univariate models (one for each covariate available), discarded those that exhibited implausible ecological relationships, and selected from the retained models the one with the best goodness of fit statistics. The best-fitting model used contemporaneous sea surface salinity (see Section 2.3.5.1.1). Density exhibited a positive relationship with salinity (Figure 65), reflecting the species' preference for the relatively warm, saline waters beyond the shelf and, to a lesser degree, the shelf waters of the South Atlantic Bight (Figure 64). Although delphinid distributions often correlate well with SST, salinity performed better in this case because it better distinguished the on-shelf and off-shelf waters north of Cape Hatteras during summer, when higher insolation and increased stratification reduced the temperature difference between surface waters on and off the shelf. The contemporaneous formulation of salinity performed markedly better than the climatological formulation, explaining 5% more deviance, possibly because the northernmost sightings from 1998 occurred within an anticyclonic eddy shed from the Gulf Stream (Figure 66).

Table 29. Pantropical spotted dolphin sightings from 1998-2016, available for the Option Year 2 spatial model. "Extant" sightings were used in the Phase III regional model (Roberts et al. 2016a). "Added" sightings were incorporated during the Base Year and Option Year 1 for the updated model.

			Pantropical spotted dolphin		
Platform	Provider	Program	Extant	Added	Total
Aerial	SEFSC	Marine mammal abundance surveys	2		2
	UNCW	Jacksonville Navy Surveys	1		1
	All		3		3
Shipboard	NEFSC	Marine mammal abundance surveys	4		4
	SEFSC	Marine mammal abundance surveys	10	5	15
	All		14	5	19

Table 30. $g(0)$ estimates used in the updated pantropical spotted dolphin model.

Platform	Region	Perception Bias	Availability Bias	$g(0)$	Source (all Palka et al. 2017)
Shipboard	Northeast	0.924	1	0.924	Atl. spotted dolphin shipboard NE
	Southeast	0.722	1	0.722	Atl. spotted dolphin shipboard SE
Aerial	Northeast	0.843	1	0.843	Atl. spotted dolphin aerial SE
	Southeast	0.843	1	0.843	Atl. spotted dolphin aerial SE

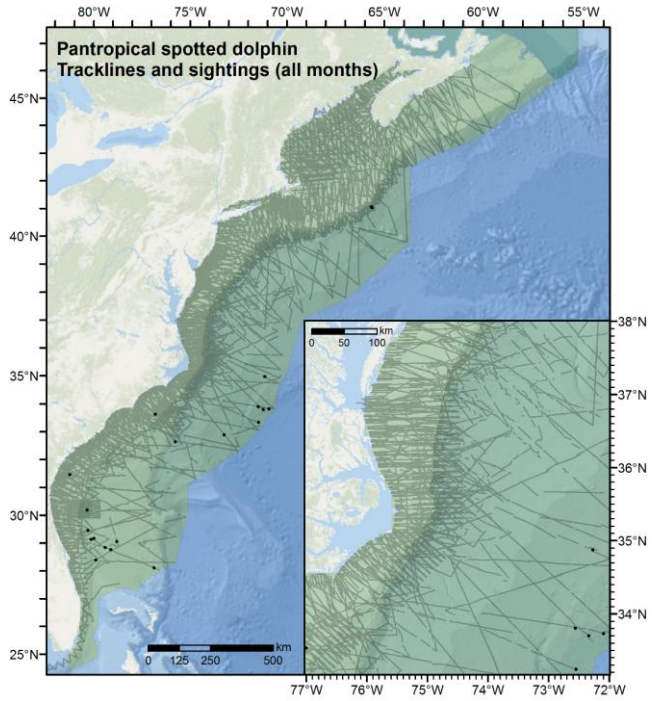

Figure 63. Pantropical spotted dolphin model's tracklines, sightings, and prediction area (light green).

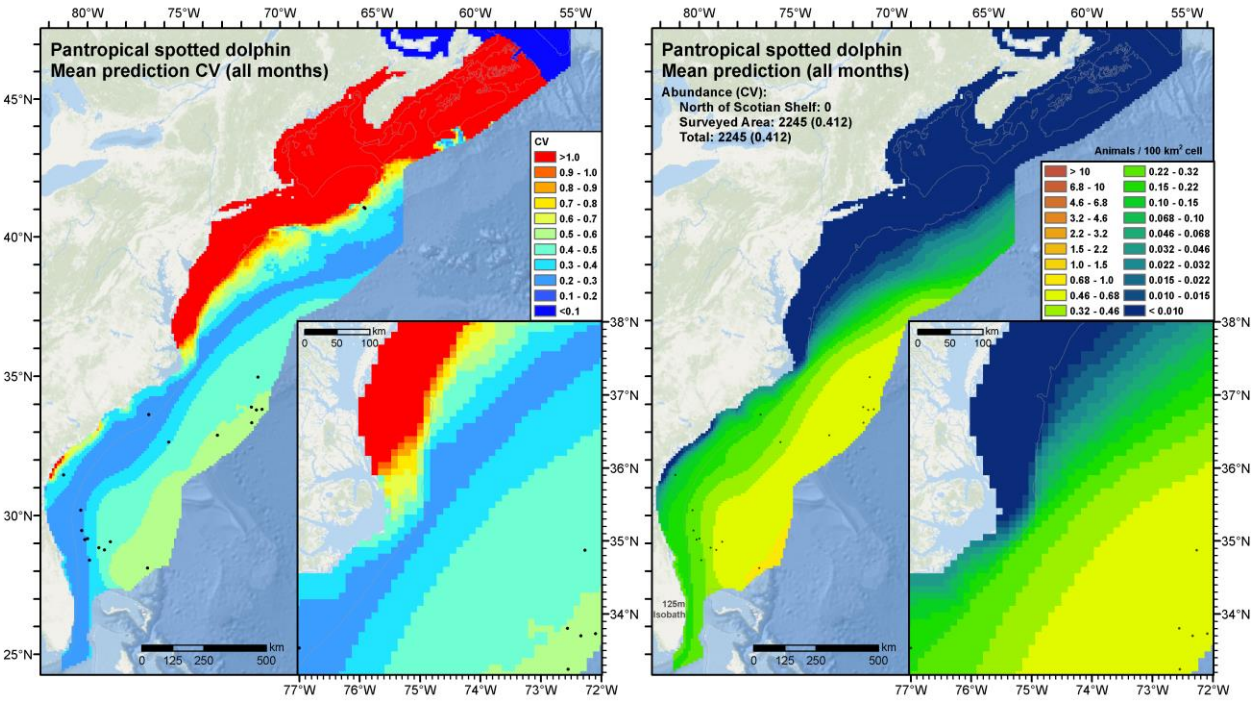

Figure 64. Predicted year-round mean density and total abundance (right) and coefficient of variation (left) for pantropical spotted dolphin, with sightings overlaid.

```
Family: Tweedie(p=1.278)
Link function: log

Formula:
Abundance ~ offset(log(Area)) + s(pmin(Salinity, 36.725), bs = "ts")

Parametric coefficients:
            Estimate Std. Error t value Pr(>|t|)
(Intercept)   -10.52       1.71   -6.15  7.8e-10 ***
---
Signif. codes:  0 '***' 0.001 '**' 0.01 '*' 0.05 '.' 0.1 ' ' 1

Approximate significance of smooth terms:
                               edf Ref.df    F p-value
s(pmin(Salinity, 36.725)) 0.8958      9 0.78 0.00495 **
---
Signif. codes:  0 '***' 0.001 '**' 0.01 '*' 0.05 '.' 0.1 ' ' 1

R-sq.(adj) =  0.00187   Deviance explained =   39%
-REML =    255  Scale est. = 275.99    n = 61617
```

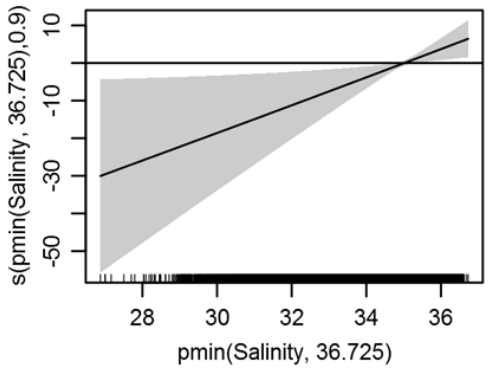

Figure 65. Pantropical spotted dolphin model's statistical output and covariate functional plot.

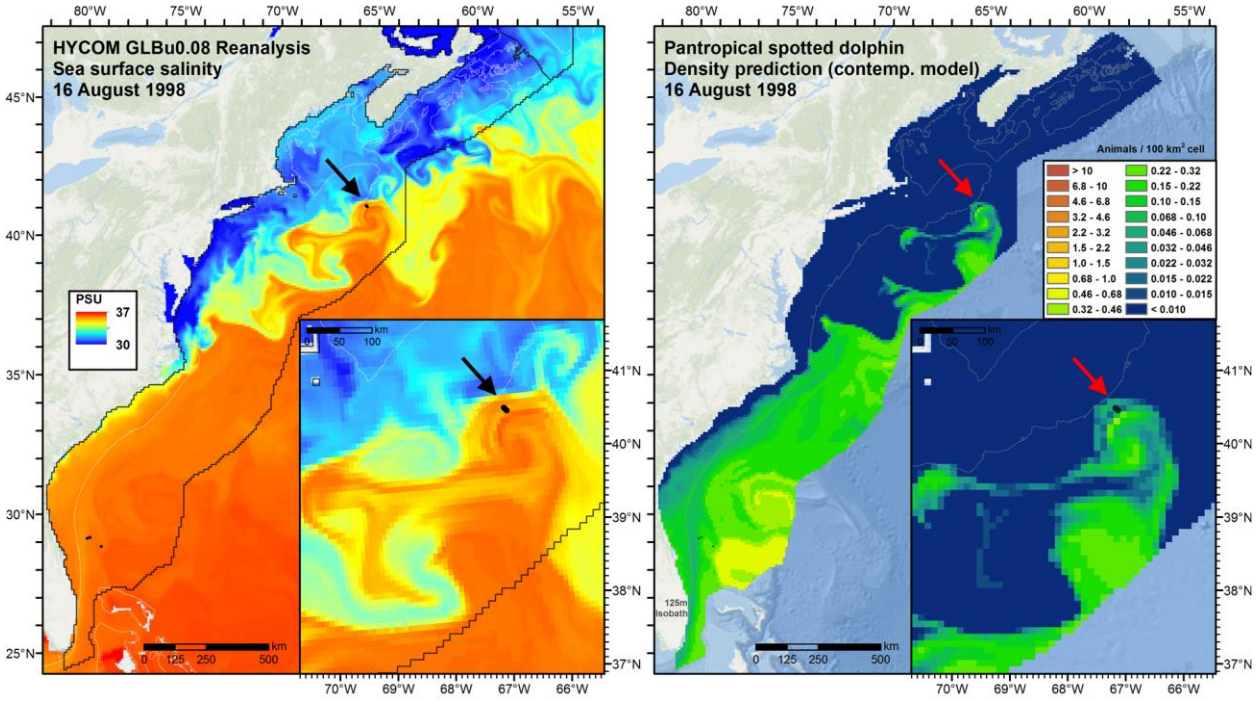

Figure 66. Comparison of sea surface salinity (left), the only covariate used in the pantropical spotted dolphin density model, to predicted density (right) for the day in which the northernmost sightings were reported (black and red arrows), which occurred in an anticyclonic (warm-core) eddy shed from the Gulf Stream.

Year-round total abundance predicted by the updated model was about half of that predicted by the Roberts et al. (2016a) model used for Phase III (Table 31). As with Atlantic spotted dolphin, we attribute this difference largely to the new SEFSC shipboard detection function that addressed the "spike" in detections close to the trackline (see Section 2.3.1 above). The majority of sightings used in both models were from SEFSC shipboard surveys (15 of 22 in the updated model). The new detection function resulted in a much smaller correction for dolphins that were "missed" by observers, pushing abundance down in the updated model. The predicted abundance was also substantially lower than the SAR estimates (Table 31), however all estimates exhibited high CVs and would likely not be significantly different from each other at a 95% confidence level if all sources of uncertainty were accounted for. Estimates with lower CVs may be obtained if additional sightings are made on future surveys. Finally, although we offer this model for year-round use, we urge additional caution applying it in non-summer seasons, as most of sampling of the offshore waters preferred by this species occurred in summer. To better characterize the species' distribution throughout the year, we recommend additional surveying of offshore waters in other seasons (acknowledging the logistical difficulties and safety risks of performing distant offshore surveys in seasons with poor weather).

Table 31. Comparison of abundance estimates (with CV in parentheses) for pantropical spotted dolphin, obtained from recent NMFS Stock Assessment Reports (SARs) and density surface models. "Updated model" refers to the model presented here. For this, we recommend a single, year-round density surface for management purposes but show seasonal estimates (brown text) to facilitate more granular comparison to the SARs' estimates, which were made only for the June-August season. The Roberts et al. (2016) model, for which few sightings were available, did not retain any spatial covariates and thus yielded a uniform density estimate, with constant abundance for all seasons.

	Years	Dec-Feb	Mar-May	Jun-Aug	Sep-Nov	Year-round
NMFS SARs	2004			4,439 (0.49)		
	2011			3,333 (0.91)		
Roberts et al. (2016) [1]	1998-2013					4,436 (0.33)
Updated model [1,2]	1998-2016	2,963	2,632	1,605	1,797	2,245 (0.412)

[1] CV is underestimated; it only accounts for uncertainty in spatial model parameters, not detection functions or $g(0)$.
[2] 3-month mean abundance shown for comparison, but we recommend the year-round average be used for management.

2.3.5.9. Rough-toothed dolphin model

The rough-toothed dolphin (*Steno bredanensis*) is distributed worldwide and generally occurs in warm temperate, subtropical, or tropical waters at a wide range of depths (West et al. 2011; Waring et al. 2014). It has been sighted regularly in the Gulf of Mexico but rarely along the U.S. Atlantic coast (Waring et al. 2014). Surveys of the Atlantic contributed by our collaborators reported only 25 sightings during the period 1998-2016 (Table 32), and none prior. As with the updated models for other species, we assessed the feasibility of excluding surveys from 1992-1997 from the updated spatial model, as this period predated the launch of the SeaWiFS ocean color sensor needed for contemporaneous biological covariates. Because it was not important to retain surveys from this period to boost sighting counts to help establish habitat relationships, we limited the updated model to surveys from the 1998-2016 period.

South of Cape Hatteras, most sightings of rough-toothed dolphin occurred close to the continental shelf break, on both the shallow and deep sides, while one sighting occurred far offshore, east of the Gulf Stream (Figure 67). North of Cape Hatteras, all sightings occurred beyond the shelf break, scattered from the high continental slope out over the abyssal plain. Most sightings occurred in warm water, however on 22 February 2013, an aerial survey of the continental shelf and upper slope by SEFSC reported a sighting near Hudson Canyon with 13.8 °C surface temperature. (At our request, SEFSC reviewed this sighting and reconfirmed the species identification.) Given the generally warm-water distribution of this species, the aforementioned sighting notwithstanding, and lack of on-shelf sightings north of Cape Hatteras, we based the updated model only on NOAA's broad-scale abundance surveys and UNCW's aerial surveys of Navy study areas. (The other surveys predominantly covered the shelf north of Cape Hatteras and did not report any sightings.) We applied $g(0)$ estimates (Table 33) derived from availability and perception bias corrections developed by Palka et al. (2017) for common bottlenose dolphin, as no such corrections were available for rough-toothed dolphin.

Table 32. Rough-toothed dolphin sightings from 1998-2016, available for the Option Year 2 spatial model. "Extant" sightings were used in the Phase III regional model (Roberts et al. 2016a). "Added" sightings were incorporated during the Base Year and Option Year 1 for the updated model.

Platform	Provider	Program	Rough-toothed dolphin Extant	Added	Total
Aerial	SEFSC	Marine mammal abundance surveys		1	1
	UNCW	Cape Hatteras Navy Surveys	1		1
		Jacksonville Navy Surveys	6	3	9
		Onslow Bay Navy Surveys	3		3
	All		10	4	14
Shipboard	NEFSC	Marine mammal abundance surveys		6	6
	SEFSC	Marine mammal abundance surveys	2	3	5
	All		2	9	11

Table 33. *g*(0) estimates used in the updated rough-toothed dolphin model.

Platform	Region	Perception Bias	Availability Bias	*g*(0)	Source (all Palka et al. 2017)
Shipboard	Northeast	0.643	1	0.643	Bottlenose dolphin shipboard NE
	Southeast	0.609	1	0.609	Bottlenose dolphin shipboard SE
Aerial	Northeast	0.657	0.785	0.516	Bottlenose dolphin aerial NE
	Southeast	0.814	0.785	0.634	Bottlenose dolphin aerial SE

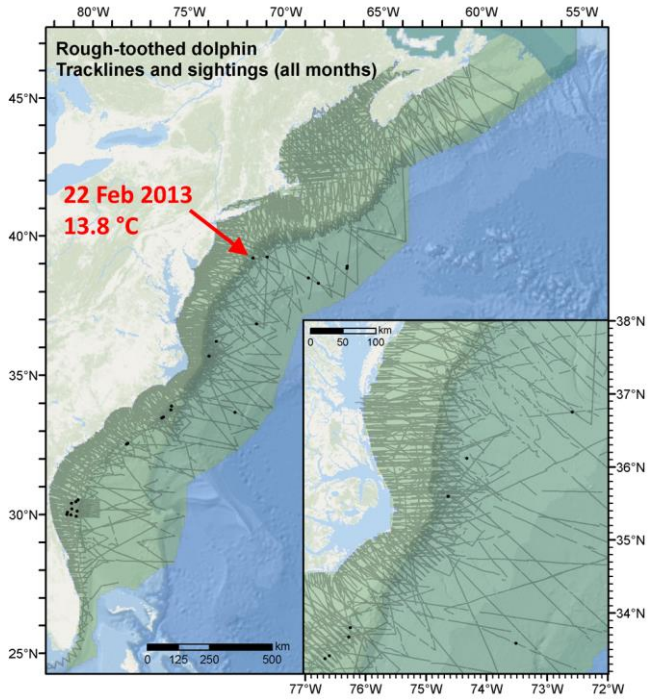

Figure 67. Rough-toothed dolphin model's tracklines, sightings, and prediction area (light green). Red arrow highlights a northerly wintertime sighting in relatively cool water, reported by a SEFSC aerial survey.

For models with only 20-40 sightings, our methodology was to fit a model with only one covariate (Roberts et al. 2016a). Accordingly, we fitted a series of independent univariate models (one for each covariate available), discarded those that exhibited implausible ecological relationships, and selected among the retained models the one with the best goodness of fit statistics. As with pantropical spotted dolphin, the best-fitting model used contemporaneous sea surface salinity (see Section 2.3.5.1.1). Density exhibited a positive relationship with salinity (Figure 69), reflecting the species' preference for the relatively warm, saline waters found over the shelf south of Cape Hatteras and beyond the shelf both south and north of Cape Hatteras (Figure 68). Although delphinid distributions often correlate well with SST, salinity performed better in this case because it better distinguished the on-shelf and off-shelf waters north of Cape Hatteras during summer, when higher insolation and increased stratification reduced the temperature difference between surface waters on and off the shelf.

As with pantropical spotted dolphin, the contemporaneous formulation of salinity performed better than the climatological formulation, explaining 2.4% more deviance. However, this difference was not as great as for pantropical spotted dolphin, for which the contemporaneous formulation explained 5% more, nor did the most unusual northerly sighting occur in a distinct geostrophic feature (Figure 70). Finally, the rough-toothed dolphin model explained much less deviance (8.6%) than the pantropical spotted dolphin model (39%), yielding a flatter covariate relationship (compare Figure 69 to Figure 65) and density prediction (compare Figure 68 to Figure 64). The relative lack of spatial variability for this species and ineffectiveness of our covariates for explaining the variations that did occur accords with our experience modeling the species in the Gulf of Mexico during the Phase III analysis. There, we had twice as many sightings (51) but they were similarly scattered and the only covariate retained by the model was seafloor slope, which explained only 17.3% of the deviance and resulted in a similarly homogeneous prediction of density.

It may be that this species occurs relatively homogenously in low densities throughout its range. However, ongoing analysis has revealed the presence of multiple insular and genetically-distinct populations around islands throughout the Pacific (Baird et al. 2008; Oremus et al. 2012; Albertson et al. 2017) and an apparently relict population in the eastern Mediterranean that is geographically detached from, and showed some genetic divergence from, populations in the Atlantic, and strong genetic separation from populations in the Indian and Pacific Oceans (Kerem et al. 2016). As of this writing, NMFS had recognized two stocks in the Pacific, Hawaii and American Samoa, and was reviewing evidence in Hawaii to see whether further delineation of island-associated stocks was warranted (Hayes et al. 2018).

The sightings available for our model, though sparse, showed a pattern potentially indicating distinct metapopulations with differing habitat preferences. All of the sightings near 30 °N, totaling 9 of the 25 available for our model, occurred in the Navy JAX OPAREA. This area was heavily surveyed by UNCW in all months for multiple years, with transects laid perpendicular to the shelf break (defined here as the 125 m isobath), each extending 30-50 km on either side of it. All of the sightings occurred on the shallow side of the break, suggesting a distinct preference for shallower water, or some related habitat feature. This contrasted with the remaining 16 sightings, which all occurred at least 2° farther north and on the deep side of the 125 m isobath. Given this pattern, and the finding of isolated metapopulations elsewhere that qualify as separate stocks under the MMPA, we urge caution in treating all rough-toothed dolphins in U.S. Atlantic waters as a single stock. NMFS notes that additional morphological, genetic, or behavioral data are needed to provide further information on stock delineation (Waring et al. 2014).

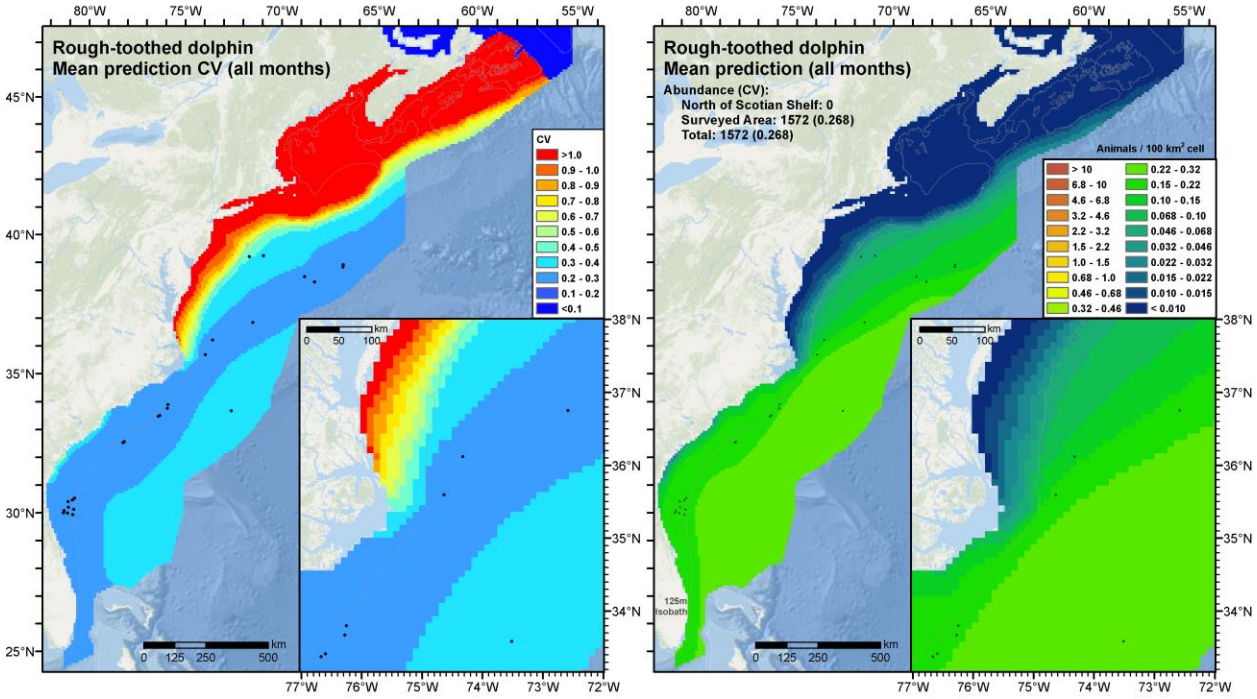

Figure 68. Predicted year-round mean density and total abundance (right) and coefficient of variation (left) for rough-toothed dolphin, with sightings overlaid.

```
Family: Tweedie(p=1.306)
Link function: log

Formula:
Abundance ~ offset(log(Area)) + s(pmin(Salinity, 36.725), bs = "ts")

Parametric coefficients:
            Estimate Std. Error t value Pr(>|t|)
(Intercept)  -7.2453     0.3956  -18.32   <2e-16 ***
---
Signif. codes:  0 '***' 0.001 '**' 0.01 '*' 0.05 '.' 0.1 ' ' 1

Approximate significance of smooth terms:
                              edf Ref.df     F p-value
s(pmin(Salinity, 36.725)) 0.9241      9 0.885 0.00311 **
---
Signif. codes:  0 '***' 0.001 '**' 0.01 '*' 0.05 '.' 0.1 ' ' 1

R-sq.(adj) =  -0.000183   Deviance explained =  8.6%
-REML = 307.68  Scale est. = 319       n = 61617
```

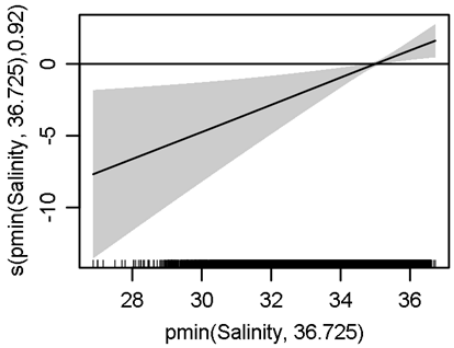

Figure 69. Rough-toothed dolphin model's statistical output and covariate functional plot.

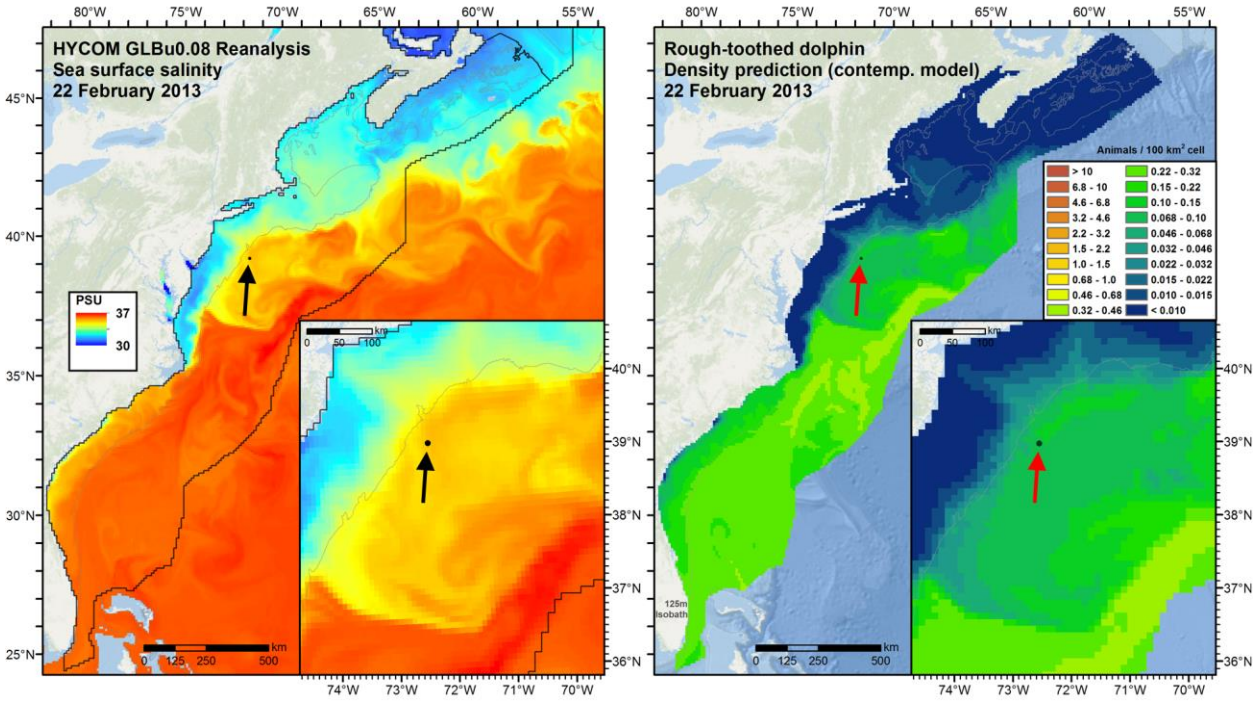

Figure 70. Comparison of sea surface salinity (left), the only covariate used in the rough-toothed dolphin density model, to predicted density (right) for the day in which a rare northerly wintertime sighting in relatively cool water was reported (black and red arrows). This sighting occurred north of the Gulf Stream over the continental slope, where warmer, more-saline water mixes with colder, fresher water on the shelf, but not in a distinct geostrophic feature.

Year-round total abundance predicted by the updated model was about three times that predicted by the Roberts et al. (2016a) model used for Phase III (Table 34). We attribute this change to a different composition of surveys used to fit the models and to the switch from a model that assumed a uniform distribution throughout the presumed species range to a model that utilized a habitat covariate to characterize both species range and density. The Phase III model presumed the on-shelf area north of Cape Hatteras was within the species' range, while the new model indicated low density there. By including that area of species absence in the Phase III model but not accounting for the more intense sampling that occurred there, we believe the Phase III model biased the final uniform density estimate too low. We also note that the exclusion of the sightings from the 1992-1997 period, when no rough-toothed dolphins were sighted, likely boosted density relative to what would have happened had we included the 1992-1997 period. This might suggest an increasing trend in species abundance, however we strongly caution against that conclusion given the very low number of sightings available across the period. Finally, although the mean abundance estimates of the Phase III model and the updated model are significantly different at the 95% confidence level between model generations (Table 34), we note that those CVs do not include all known sources of model uncertainty, e.g. in detection functions and $g(0)$ corrections. Methodological limitations prevented us from accounting for all of these sources of uncertainty. Were they incorporated into the final abundance estimates, it is possible they would no longer be significantly different.

The year-round total abundance predicted by the updated model was also much higher than that from the current SAR (Table 34). The SAR was based on shipboard surveys from 2011, which covered a smaller prediction area than our model and only reported one sighting south of Virginia and four sightings to the north, resulting in a CV of 1.00. Given the differences in prediction areas, methodology, and number of sightings utilized, and the low numbers of sightings available to both models, we are not surprised by the large difference in estimated abundance. The typical way to resolve a more reliable abundance estimate is to conduct more surveys and obtain more sightings; however, this species remains rare enough in the U.S. Atlantic that the effort needed to yield precise estimates may be cost-prohibitive.

Table 34. Comparison of abundance estimates (with CV in parentheses) for rough-toothed dolphin, obtained from the most recent NMFS Stock Assessment Report (SAR) and density surface models. "Updated model" refers to the model presented here. For this, we recommend a single, year-round density surface for management purposes but show seasonal estimates (brown text) to facilitate more granular comparison to the SAR estimate, which was made only for the June-August season. The Roberts et al. (2016) model, for which few sightings were available, did not retain any spatial covariates and thus yielded a uniform density estimate, with constant abundance for all seasons.

	Years	Dec-Feb	Mar-May	Jun-Aug	Sep-Nov	Year-round
NMFS SAR	2011			271 (1.00)		
Roberts et al. (2016) [1]	1992-2014					532 (0.36)
Updated model [1,2]	1998-2016	1,712	1,626	1,426	1,526	1,572 (0.268)

[1] CV is underestimated; it only accounts for uncertainty in spatial model parameters, not detection functions or $g(0)$.
[2] 3-month mean abundance shown for comparison, but we recommend the year-round average be used for management.

2.3.5.10. Clymene dolphin model

The Clymene dolphin (*Stenella clymene*), a hybrid of the striped and spinner dolphins (Amaral et al. 2014), is endemic to tropical to warm temperate waters of the Atlantic Ocean (Jefferson & Curry 2003). It has been sighted regularly in deep, oceanic waters of the northern Gulf of Mexico but more rarely in the western North Atlantic, where it is nonetheless considered to occur routinely (Waring et al. 2014). The northernmost record of Clymene dolphin was a stranding that occurred in June 1976 in New Jersey (Fertl et al. 2003). Surveys of the Atlantic contributed by our collaborators reported only 26 sightings during the period 1998-2016 (Table 35), and none prior. As with the updated models for other species, we assessed the feasibility of excluding surveys from 1992-1997 from the updated spatial model, as this period predated the launch of the SeaWiFS ocean color sensor needed for contemporaneous biological covariates. Because it was not important to retain surveys from this period to boost sighting counts to help establish habitat relationships, we limited the updated model to surveys from the 1998-2016 period.

The Clymene dolphin is believed to be an oceanic species that rarely moves over the continental shelf. Along the Atlantic coast, the available records suggest the Gulf Stream influences Clymene dolphin distribution (Fertl et al. 2003). Most of the sightings reported by the surveys in our database were consistent with these hypotheses: most occurred off North Carolina and Virginia, off the shelf, within the Gulf Stream or slightly north of it (Figure 71). In contrast, one sighting was reported over the continental shelf near Georgia. Given the warm-water, oceanic distribution of this species, we based our updated model only on NOAA's broad-scale abundance surveys and UNCW's aerial surveys of Navy study areas. (The other surveys predominantly covered the shelf north of Cape Hatteras and did not report any sightings.) For shelf waters north of New Jersey, which were beyond the species' reported range, we assumed the species was absent and excluded these transects from our spatial model. We applied $g(0)$ estimates (Table 33) derived from availability and perception bias corrections developed by Palka et al. (2017) for striped dolphin, a parental species (Amaral et al. 2014), as no such corrections were available for Clymene dolphin.

Table 35. Clymene dolphin sightings from 1998-2016, available for the Option Year 2 spatial model. "Extant" sightings were used in the Phase III regional model (Roberts et al. 2016a). "Added" sightings were incorporated during the Base Year and Option Year 1 for the updated model.

			Clymene dolphin		
Platform	Provider	Program	Extant	Added	Total
Aerial	SEFSC	Marine mammal abundance surveys	1		1
	UNCW	Cape Hatteras Navy Surveys	3	8	11
		Norfolk Canyon Navy Surveys		1	1
	All		4	9	13
Shipboard	NEFSC	Marine mammal abundance surveys		1	1
	SEFSC	Marine mammal abundance surveys	7	5	12
	All		7	6	13

Table 36. *g*(0) estimates used in the updated Clymene dolphin model.

Platform	Region	Perception Bias	Availability Bias	*g*(0)	Source (all Palka et al. 2017)
Shipboard	Northeast	0.764	1	0.764	Striped dolphin shipboard NE
	Southeast	0.722	1	0.722	Striped dolphin shipboard SE
Aerial	Northeast	0.706	1	0.706	Striped dolphin aerial NE
	Southeast	0.856	1	0.856	Striped dolphin aerial SE

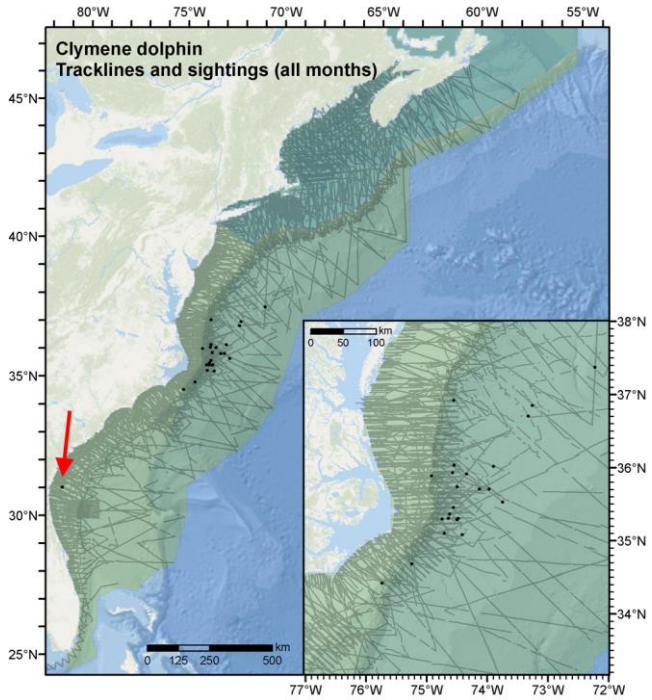

Figure 71. Clymene dolphin model's tracklines, sightings, and prediction areas. In oceanic waters and shelf waters north through New Jersey (light green) we fitted a density model. For the shelf north of New Jersey (dark green), we assumed the species was absent (see text). The sighting (August 2002 by a SEFSC aerial survey) indicated by the red arrow was right-truncated during detection modeling and thus not used in the spatial model.

For models with only 20-40 sightings, our usual methodology was to build a univariate model using the best-fitting, ecologically-plausible covariate, as we did with the pantropical spotted and rough-toothed dolphin models described above. However, when we presented candidate models for several covariates to collaborating species experts at SEFSC, UNCW, and VAMSC, they objected that none of the candidate models sufficiently concentrated density offshore in the vicinity of Cape Hatteras, where all of the sightings except one were reported (Figure 71). For example, the best-fitting ecologically-plausible univariate model used eddy kinetic energy (EKE), with density increasing as EKE increased. This accorded both with the literature's description of the Atlantic coast distribution being influenced by the Gulf Stream (Fertl et al. 2003) and with our Phase III model for Clymene dolphin in the Gulf of Mexico (Roberts et al. 2016a), which retained EKE and distance to the closest cyclonic (cold-core) eddy as the only dynamic covariates. (The EKE relationship there was negative, however the distance-to-eddy relationship indicated increasing density close to eddies; together these suggested density was higher in the cores of cyclonic eddies, where EKE is lower, rather than at the edges, where EKE is higher.) However, the east coast univariate model with EKE predicted high density not only in the area of the Gulf Stream where sightings were concentrated, but several other areas as well, where no sightings were ever reported (Figure 72).

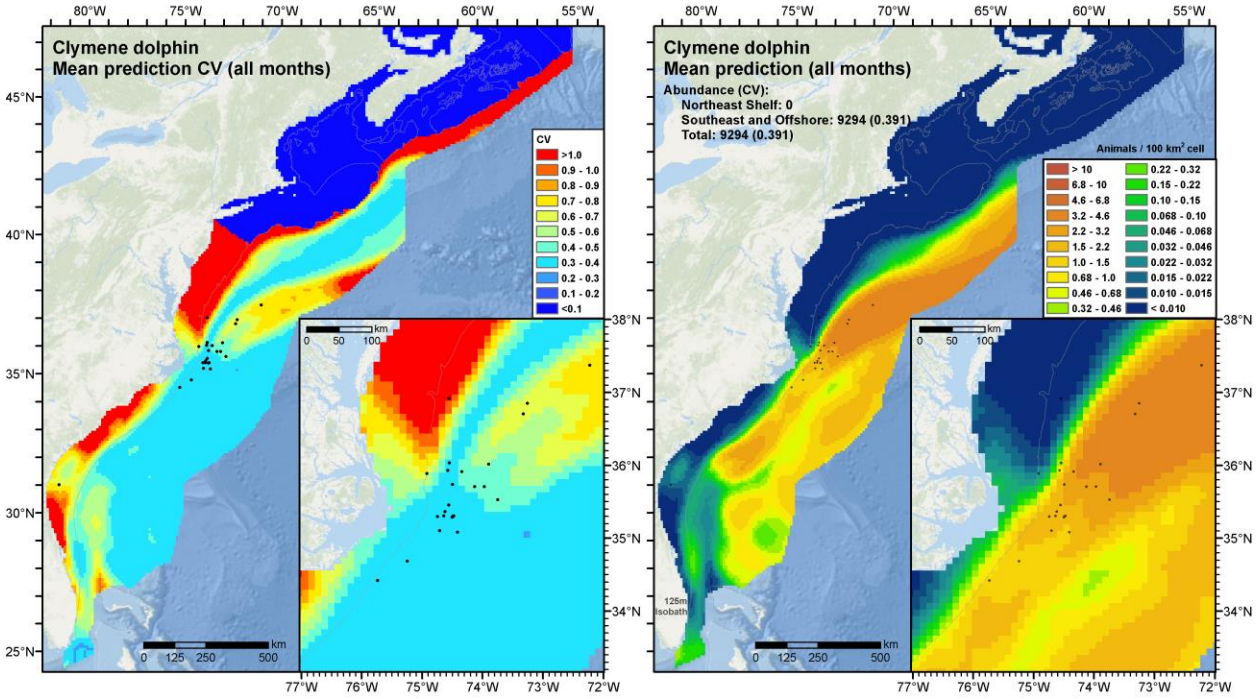

Figure 72. Candidate univariate Clymene dolphin model that exhibited the best fit by REML score. This model used eddy kinetic energy (EKE) as the covariate. We ultimately rejected this model (see text).

As an additional problem, this model predicted increasingly higher density to the east of the area where the sightings were concentrated, as the Gulf Stream departed the continental shelf. This is a prolific eddy-generating region, and when the model was predicted across all seasons, values of EKE during strong eddy activity often exceeded the range of values sampled by the surveys, requiring the model to extrapolate the relationship. The model predicted high density with a high CV (Figure 72), a situation we try to avoid when at all possible.

In the Phase III modeling project, we encountered a similar problem with Bryde's whale in the Gulf of Mexico. This model had a similar number of sightings (22) and our best candidate univariate model used depth as the covariate, fitting a classic envelope relationship that concentrated density within a specific range of depths on the continental slope. When we proposed this model, species experts were satisfied that the depth relationship matched the core habitat for Bryde's whale, but objected that the model predicted a "bathtub ring" of high density around the entire Gulf. They noted that Bryde's whales had not been seen in the western Gulf of Mexico since the early 1990s, and called for modifications to the model that would reflect this. To correct this, we added a second term to the model, a bivariate smooth of spatial location (x and y coordinates in the Albers equal area coordinate system used by the model). While we normally avoid including spatial location terms in our models, and prefer to base the models on habitat relationships that can better interpolate across spatial gaps in sampling, or better extrapolate to poorly sampled areas at the edge of the study area, it is a recommended practice to include such terms in density surface models (Miller et al. 2013). When we added the location term to the Bryde's whale model, both it and depth were retained, the prediction of density in the western Gulf was curtailed, and species experts expressed satisfaction with the result.

The candidate models for Clymene dolphin for the east coast presented a similar situation, and when we added a bivariate smooth of spatial location, it similarly concentrated density in the area of the sightings and mitigated the extrapolation problem. However, the collaborators had also raised a second concern, which was that they were unsure which ecological relationships were driving the occurrence of Clymene dolphins near Cape Hatteras and not elsewhere in the study area, and were much less comfortable simply choosing the model with the best goodness-of-fit statistics. To address this uncertainty about model selection, we built a model for each covariate, selected the five with the lowest AIC (Table 37, Figure 73), computed Akaike weights (Burnham & Anderson 2002; Wagenmakers & Farrell 2004), predicted the models (Figure 74-75), and computed the Akaike-weighted density surface as our final prediction of Clymene dolphin density (Figure 77).

Table 37. Five best Clymene dolphin models, ranked by AIC (lower indicates better model fit), with summary statistics. Abund. is the total abundance predicted by the model for the study area, with associated CV (coefficient of variation).

Model	REML	AIC	ΔAIC	Akaike Weight	% Dev. Expl.	Abund.	CV
xy + TKE	325.3	52983.93	0.00	0.7247	71.3	4,039	0.50
xy + DistToAEddy	325.6	52988.09	4.16	0.0904	75.8	6,638	0.59
xy + Salinity	327.6	52988.39	4.46	0.0780	71.9	11,063	0.65
xy + EpiMnkPB3	328.2	52988.63	4.71	0.0689	71.3	4,772	0.50
xy + CumVGPM90	328.3	52989.83	5.90	0.0380	73.9	5,326	0.54

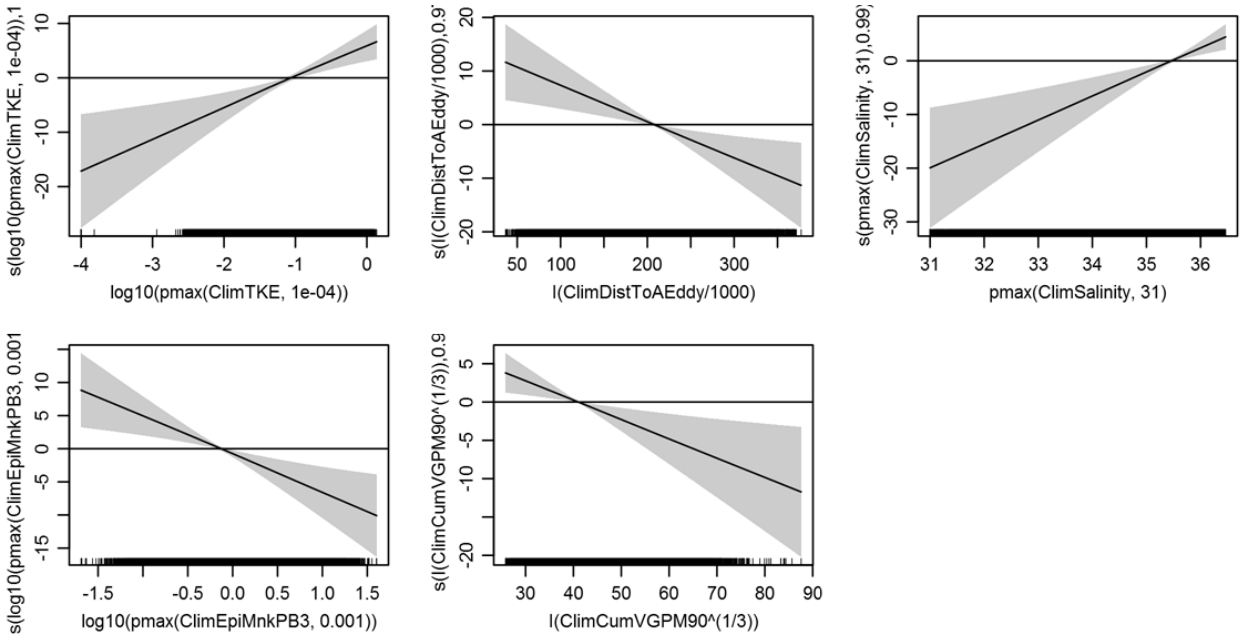

Figure 73. Covariate functional plots for each of the five best Clymene dolphin models.

All five models retained both the bivariate smooth of location ("xy") and their habitat covariate (Table 37). The best two models included total kinetic energy (TKE) and distance to closest anticyclonic (warm-core) eddy, respectively, indicating higher density at higher kinetic energies and closer to eddies (Figure 73). The strong performance of these hydrodynamic covariates accorded with the Phase III Clymene dolphin model for the Gulf of Mexico (Roberts et al. 2016a), which retained EKE and distance to the closest cyclonic (cold-core) eddy as dynamic covariates, along with three static covariates. The third best model included salinity, indicating higher density at higher salinity, corresponding to the more saline, tropical waters of the Gulf Stream. The fourth and fifth best models included biomass of epipelagic micronekton and cumulative primary productivity over the last 90 days, respectively, indicating decreasing density as those covariates increased. These relationships, while contrary to the expectation that a mobile predator would be found more frequently in biologically productive waters, serve to concentrate in the vicinity of the Gulf Stream, away both from the shelf and from northerly offshore waters, where productivity is high but the shallow depths or cold waters are unsuitable for this oceanic warm-water species. All models exhibited relatively high CVs, owing to the low sample size and the use of the bivariate smooth.

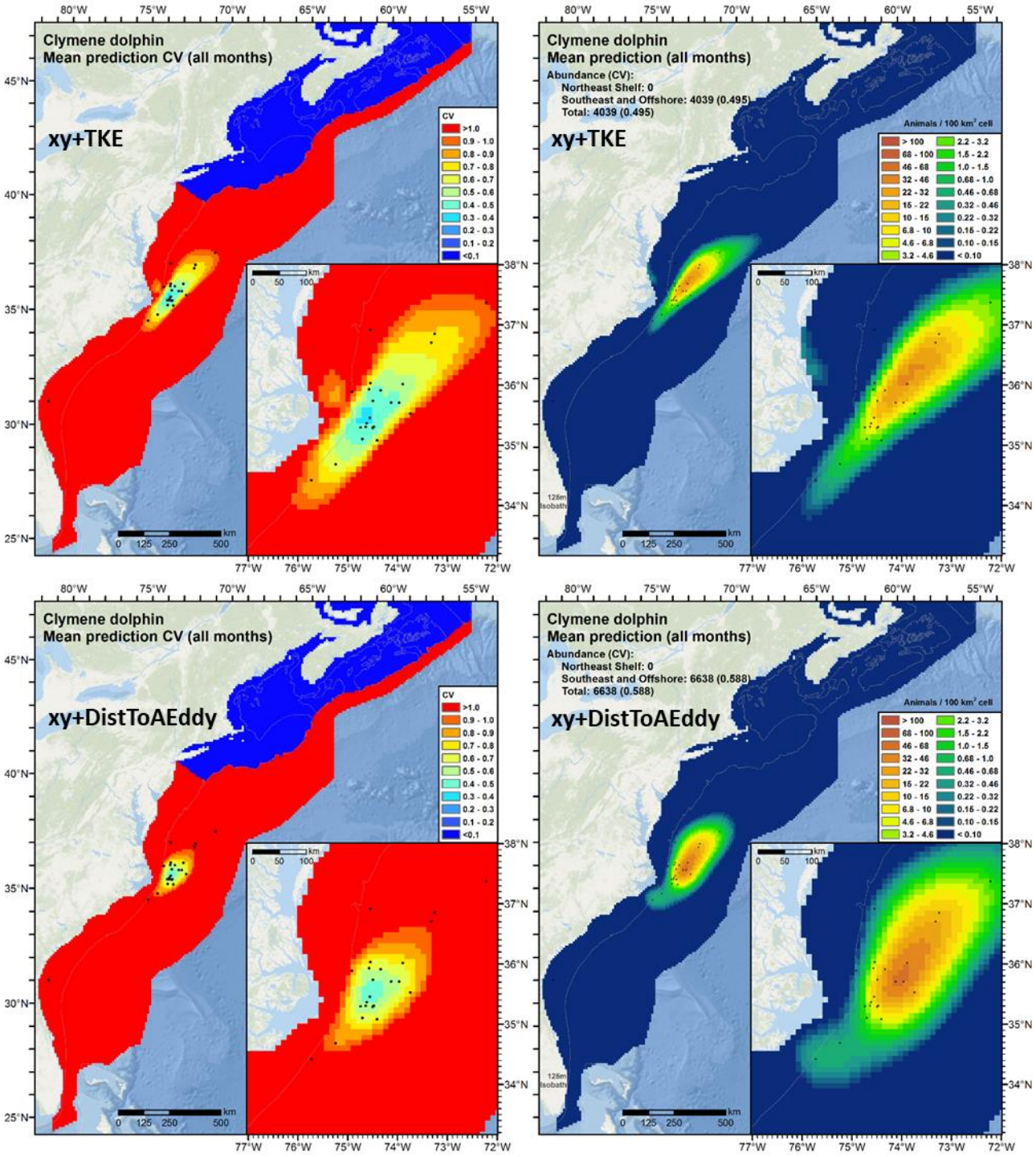

Figure 74. Predicted year-round mean density and total abundance (right column) and coefficient of variation (left column) for the first (top row) and second (bottom row) best Cymene dolphin models, with sightings overlaid.

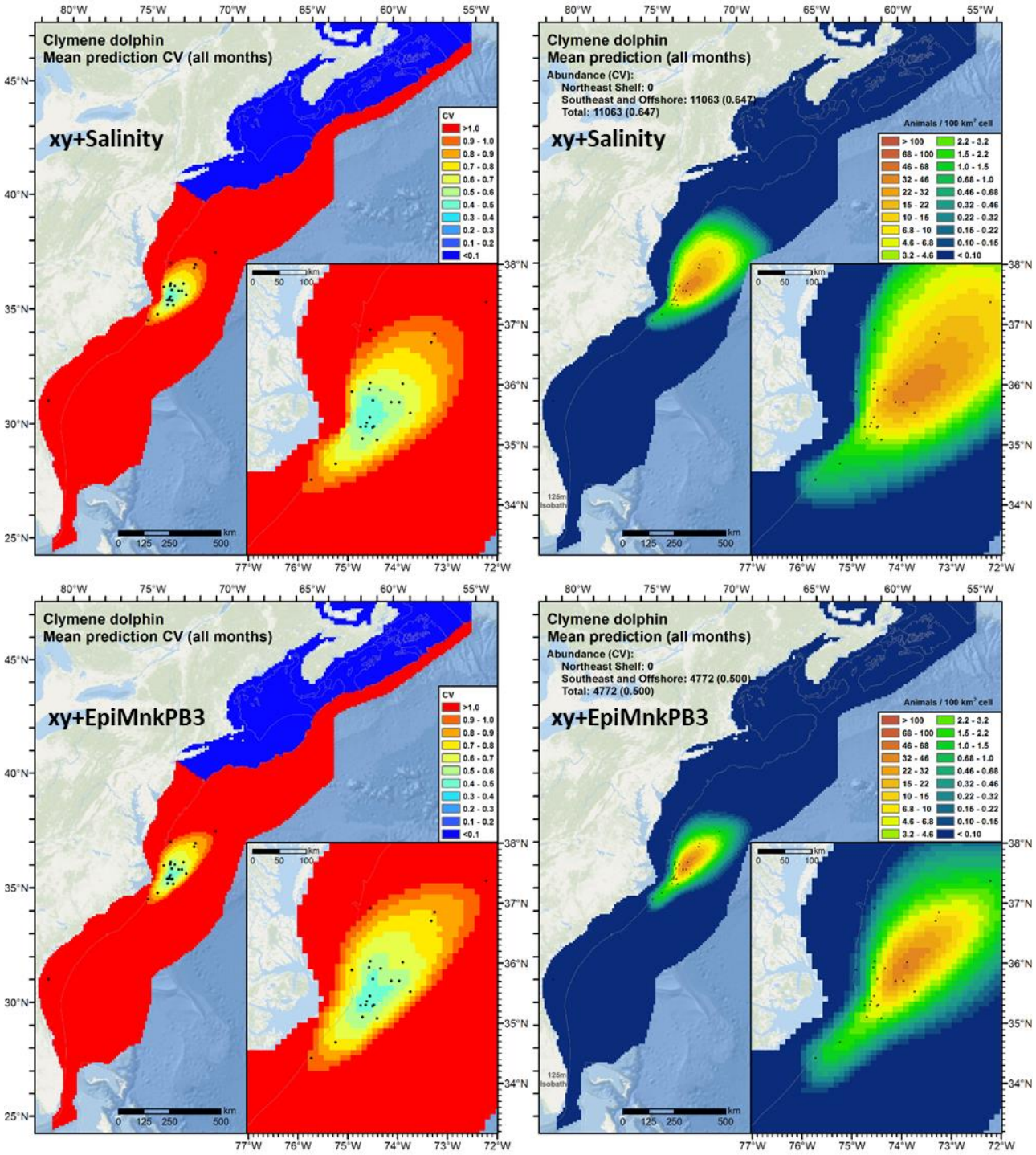

Figure 75. Predicted year-round mean density and total abundance (right column) and coefficient of variation (left column) for the third (top row) and forth (bottom row) best Cymene dolphin models, with sightings overlaid.

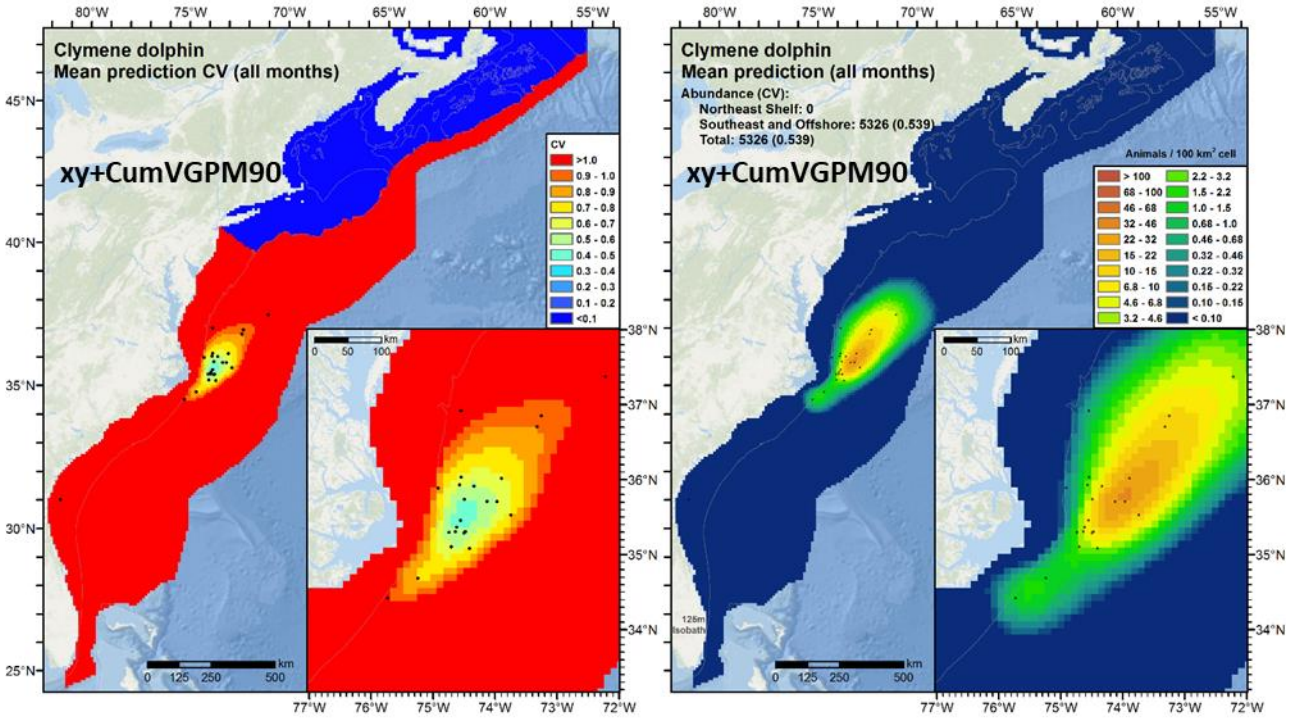

Figure 76. Predicted year-round mean density and total abundance (right) and coefficient of variation (left) for the fifth best Cymene dolphin model, with sightings overlaid.

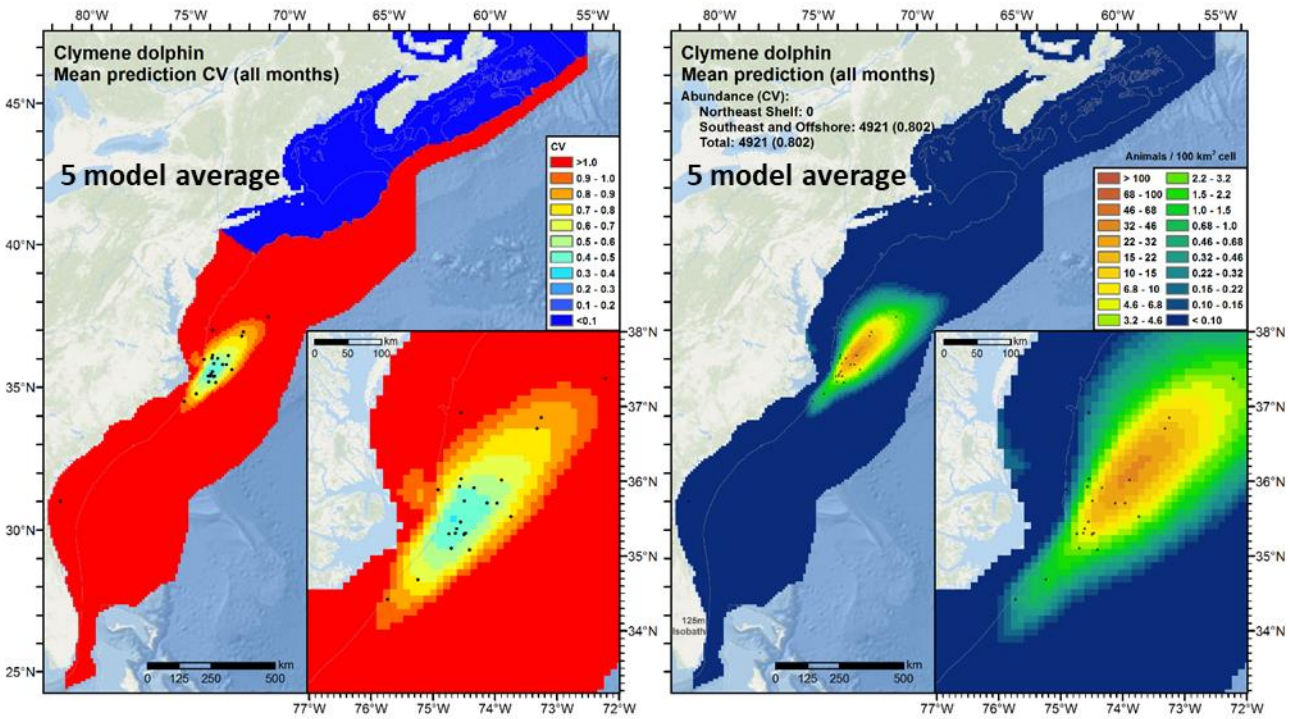

Figure 77. Predicted year-round mean density and total abundance (right) and coefficient of variation (left) for the Akaike-weighted average of the five best Clymene dolphin models.

The top model (TKE) had an AIC that was four less than the second best model, giving it 72% of the weight in the 5-model average (Table 37). The 5-model average concentrated density in the vicinity of the sightings near Cape Hatteras, as requested by the species experts (Figure 77). However, we urge caution for several reasons. First, the prediction of near zero density except at the Cape Hatteras area might not be correct. Fertl et al. (2003) reported three sightings in more distant, less surveyed waters to the south that were still relatively close to North America. These authors also reported several mass strandings in Florida. In August 2002, a SEFSC aerial survey sighted Clymene dolphins relatively near the Florida coast at 31 °N (Figure 71), far removed from the cluster of sightings off Cape Hatteras, but near the northernmost strandings reported by Fertl et al. (2003). This sighting occurred at 850 m perpendicular distance from the survey trackline, which was beyond the right-truncation distance of the detection function used for this survey, so it was removed from the analysis during detection modeling and not used in the spatial model. This sighting appears extralimital, given the apparent preference of the species for offshore waters, but accords with the strandings reported by Fertl et al. (2003).

A second reason for caution is that the 5-model average predicted a small patch of very low density along the coast south of Chesapeake Bay (Figure 77) which may be spurious. This prediction originated in the TKE model, which was the best of all candidates according to AIC. The other four best models did not predict any density close to shore, but because the TKE model carried 72% of the weight in the final prediction, the other models' predictions of negligible density did not reduce the TKE model's prediction by very much. Nevertheless, we are reluctant to manually "zero out" this prediction, both out of a desire to keep our methodology parsimonious and also because the sighting near Florida raised the possibility that the species may very occasionally occur close to shore.

Finally, this model was based on a low number of sightings, the majority of which were made far offshore during summer, the season to which offshore effort was heavily biased. To better characterize the species' distribution throughout the year, we recommend additional surveying of offshore waters in other seasons (acknowledging the logistical difficulties and safety risks of performing distant offshore surveys in seasons with poor weather).

Year-round total abundance predicted by the updated model was about 40% that predicted by the Roberts et al. (2016a) model used for Phase III (Table 38). We attribute this difference to two changes. First, in Phase III we lacked sufficient sightings to fit a spatial model and instead estimated a uniform density for the region within and south of the Gulf Stream. Sampling was heterogeneous and biased towards areas where the species was sighted, potentially biasing predictions higher in areas where it was not sighted. By using a density surface model, the updated model avoided this problem. Second, the updated model utilized the new SEFSC shipboard detection function that addressed the "spike" in detections close to the trackline (see Section 2.3.1 above). Clymene dolphin was one of the problematic species, and 12 of 26 sightings were from SEFSC shipboard surveys that exhibited the problem. The new detection function resulted in a much smaller correction for dolphins that were "missed" by observers, pushing abundance down in the updated model. CV in the updated model was higher than the Phase III model, owing to the use of a bivariate smooth of spatial location, a complex predictor.

The only other abundance estimate available for Clymene dolphin was from Mullin and Fulling (2003), which was based on a shipboard survey (also used in our model) conducted in summer 1998 from mid-Florida to Maryland, from shore to the outer limit of the U.S. EEZ. That survey reported only four sightings of Clymene dolphin and yielded an abundance estimate with CV=0.93 (Table 38). Despite that estimate's relatively high uncertainty, our updated prediction of mean abundance was much closer to it than our Phase III model's prediction (Table 38).

Table 38. Comparison of available abundance estimates (with CV in parentheses) for Clymene dolphin. "Updated model" refers to the Akaike-weighted average model described above (Figure 77).

	Years	Dec-Feb	Mar-May	Jun-Aug	Sep-Nov	Year-round
Mullin and Fulling (2003) [1]	1998			6,086 (0.93)		
Roberts et al. (2016) [2]	1992-2013					12,524 (0.56)
Updated model [2]	1998-2016					4,921 (0.802)

[1] Did not correct for perception bias (assumed that $g(0)=1$).

[2] CV is underestimated; it only accounts for uncertainty in spatial model parameters, not detection functions or $g(0)$.

2.3.5.11. Dwarf and pygmy sperm whales (Kogia) model

The two extant species of *Kogia*, the dwarf sperm whale (*Kogia sima*) and the pygmy sperm whale (*Kogia breviceps*), occur worldwide in tropical to temperate seas, generally in oceanic waters (Willis & Baird 1998; Bloodworth & Odell 2008; Waring et al. 2014). Although pygmy sperm whales are considered a more temperate species, the habitats and diets of the two species overlap substantially; they are often found over the continental slope, possibly to feed on cephalopods, a staple of their diet (Bloodworth & Odell 2008). An analysis of stomach contents and ratios of stable isotopes in muscle tissue samples of dwarf and pygmy sperm whales that stranded in North Carolina and Virginia concluded that the feeding ecologies of the two species were similar and that they occupied equivalent trophic niches in the region (Staudinger et al. 2014).

The two species are very difficult for observers to distinguish at sea and the majority of sightings reported by surveys contributed by our collaborators had ambiguous identifications. Given this, and that the two species occupy the same habitats in our study area, classification of the ambiguous sightings was intractable (see Section 2.3.4.3), so we again modeled the *Kogia* genus as a guild, incorporating both the definitive and ambiguous sightings, as we did in Phase III (Roberts et al. 2016a). Surveys added after the Phase III models more than tripled the number of *Kogia* sightings available (Table 9). When we discussed this with NMFS survey leaders, they expressed doubt that this was due to population growth. During AMAPPS I, NEFSC undertook a special effort to fully identify all *Kogia* using new techniques (D. Palka, pers. comm.), resulting in a large number of fully identified sightings that previously would have been reported as "*Kogia spp.*", or even "unidentified small whale". SEFSC did not undertake such an effort, but instead maintained the same protocol they used prior to AMAPPS I (L. Garrison, pers. comm.), resulting in mostly ambiguous "*Kogia spp.*" sightings during the AMAPPS I surveys.

Based on advice from NMFS survey leaders, and given the large number of sightings added after Phase III, we retained all of the SEFSC shipboard surveys but only the AMAPPS NEFSC shipboard surveys, on the basis that the pre-AMAPPS NEFSC shipboard surveys misclassified many *Kogia* as "unidentified small whale". (As an alternative, we explored retaining the pre-AMAPPS surveys and correcting for the problem during detection modeling, but the NEFSC only reported 11 *Kogia* sightings (fully identified and ambiguous together) during those surveys, making this intractable.) From the aerial surveys, we retained only the UNCW surveys of Navy OPAREAs, which were the only aerial surveys to substantially overlap *Kogia* habitat. (Among all of the other aerial surveys, only one Kogia sighting was ever reported (Table 9), by an NEFSC marine mammal abundance survey in August 2008 at the shelf break off New York, an area heavily covered by NEFSC shipboard surveys.) As with the models updated in Option Year 1, we reviewed the available literature and data to assess the feasibility of excluding surveys from 1992-1997 from the updated spatial model, as this period predated the launch of the SeaWiFS ocean color sensor needed for contemporaneous biological covariates. The only survey from 1992-1997 that was not excluded by the approach described above was the SEFSC shipboard survey of the Blake Plateau in winter of 1992 by R/V Oregon II (Figure 78). This survey reported the only five sightings we had during winter so we retained it for the updated model. After the exclusions noted above, the updated model was based on 100 sightings (Table 39), nearly 3 times what used in the Phase III model (31 sightings).

For the updated model, we applied $g(0)$ estimates (Table 40) derived from availability and perception bias corrections developed by Palka et al. (2017) and in the Phase III analysis (Roberts et al. 2016a).

Table 39. Dwarf and pygmy whale sightings from 1992-2016, available for the Option Year 2 spatial model. NEFSC shipboard sightings prior to the AMAPPS I program were excluded (see text). "Extant" sightings were used in the Phase III regional model (Roberts et al. 2016a). "Added" sightings were incorporated during the Base Year and Option Year 1 for the updated model.

			Dwarf sperm whale			Pygmy sperm whale			Ambiguous		
Platform	Provider	Program	Extant	Added	Total	Extant	Added	Total	Extant	Added	Total
Aerial	UNCW	Cape Hatteras Navy Surveys							1	3	4
		Jacksonville Navy Surveys							1		1
	All								2	3	5
Shipboard	NEFSC	Marine mammal abundance surveys		19	19		20	20		8	8
	SEFSC	Marine mammal abundance surveys	3	2	5				14	29	43
	All		3	21	24		20	20	14	37	51

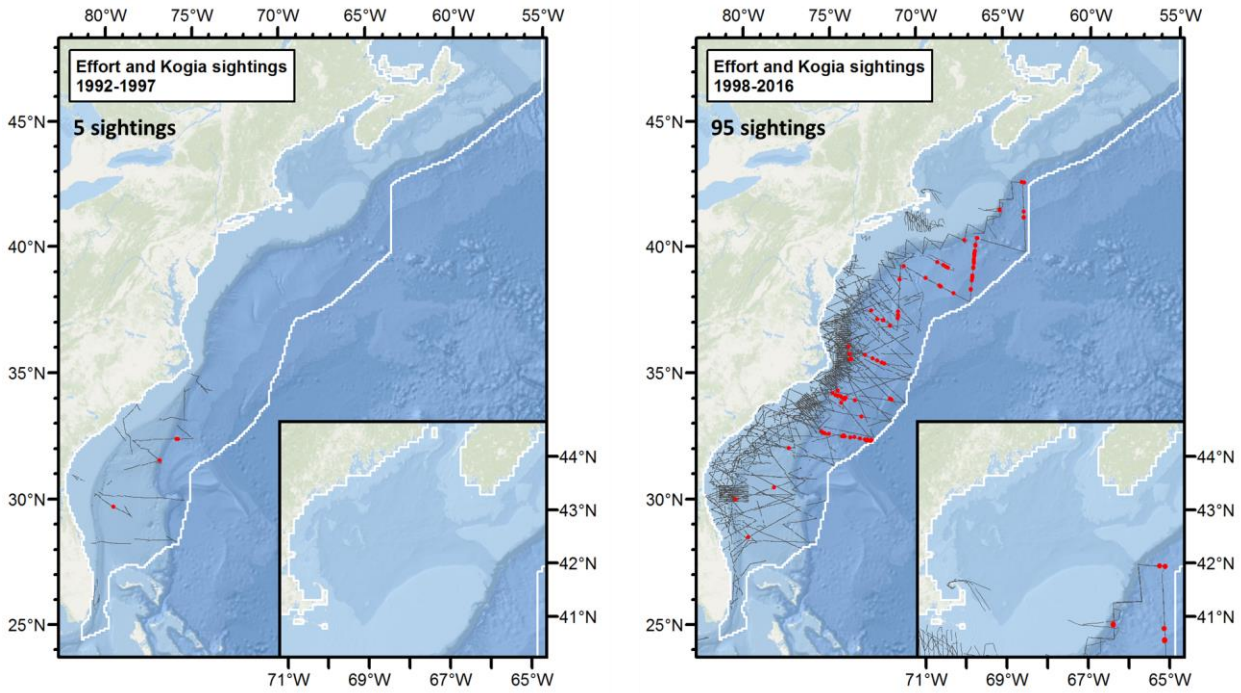

Figure 78. Survey effort and dwarf and pygmy sperm whale sightings available for the updated model. Unlike several other models, we did not exclude surveys from 1992-1997, in order to retain sightings reported by a SEFSC shipboard survey in winter 1992.

Table 40. *g*(0) estimates used in the updated dwarf and pygmy sperm whale model.

Platform	Region	Perception Bias	Availability Bias	*g*(0)	Source
Shipboard	Northeast	0.554	0.539	0.299	Palka et al. 2017
	Southeast	0.355	0.539	0.191	Palka et al. 2017
Aerial	Southeast	1	0.120	0.120	Roberts et al. 2016a

Given the absence of sightings over the continental shelf, the predominance of sightings over the lower continental slope and abyssal plain, and the multiple lines of evidence indicating that *Kogia* inhabit offshore waters, we split the study area at the shelf break (represented by the 125 m isobath), fit a model to survey segments collected over the slope and abyss, and assumed the species was absent over the shelf (Figure 79). Lacking evidence that *Kogia* would exhibit distinctly different behaviors in different seasons, we grouped all of the off-shelf segments into a single model.

Candidate models fitted to climatological environmental covariates yielded better REML scores and explained more deviance than models fitted to contemporaneous environmental covariates, so we selected the climatological-covariates model fitted to all survey segments as the best (Figure 79, Figure 81). The resulting model was relatively simple, retaining as the only covariates the depth of the seafloor and the distance to the closest geostrophic eddy at least four weeks old (Figure 81). Functional relationships indicated density increased as depth increased, and also in the vicinity of eddies but with the peak of that relationship occurring 100 km from eddy edges. Density was predicted to be relatively high and uniform over the deeper waters of the continental slope and the abyssal plain, to diminish over the mid-slope and across the Blake Plateau, then to rapidly approach zero ascending the upper slope to the shelf break.

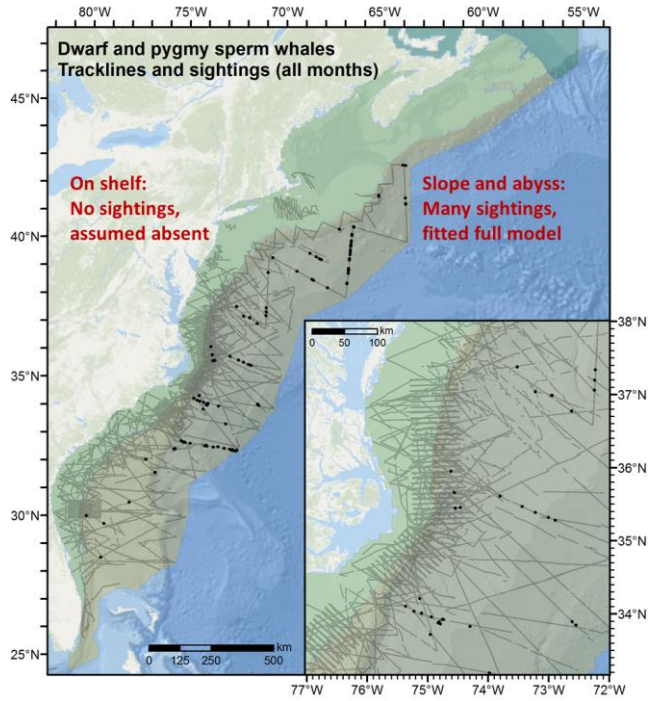

Figure 79. Dwarf and pygmy sperm whale model's tracklines, sightings, and prediction areas. For the continental shelf (light green), defined here as waters on the shallow side of the 125 m isobath plus all waters of the Gulf of Maine, there were no sightings and we assumed the species was absent. For the continental slope and abyss (brown), we fitted a spatial model.

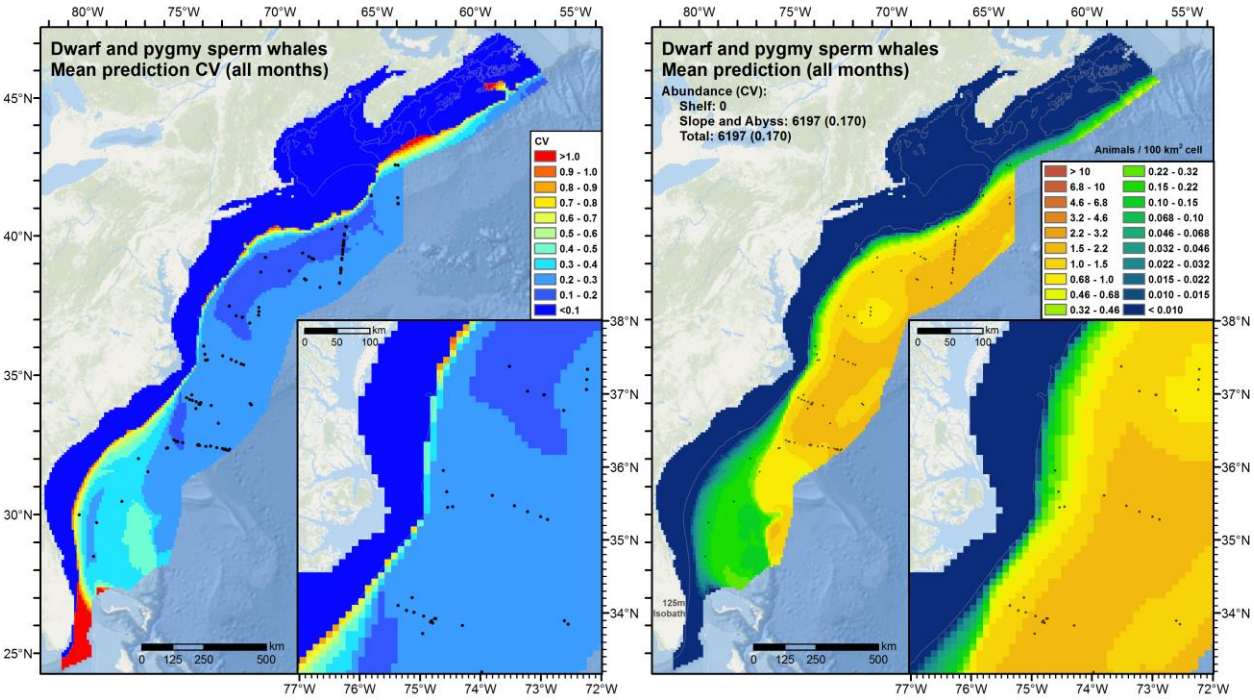

Figure 80. Predicted year-round mean density and total abundance (right) and coefficient of variation (left) for dwarf and pygmy sperm whales, with sightings overlaid.

```
Family: Tweedie(p=1.317)
Link function: log

Formula:
Abundance ~ offset(log(Area)) + s(log10(Depth), bs = "ts") + s(I(ClimDistToEddy4/1000), bs = "ts")

Parametric coefficients:
            Estimate Std. Error t value Pr(>|t|)
(Intercept)   -8.498      0.476  -17.85   <2e-16 ***
---
Signif. codes:  0 '***' 0.001 '**' 0.01 '*' 0.05 '.' 0.1 ' ' 1

Approximate significance of smooth terms:
                              edf Ref.df     F  p-value
s(log10(Depth))             1.129      9 3.861 1.95e-09 ***
s(I(ClimDistToEddy4/1000)) 2.980      9 2.278 2.58e-05 ***
---
Signif. codes:  0 '***' 0.001 '**' 0.01 '*' 0.05 '.' 0.1 ' ' 1

R-sq.(adj) =  0.0189   Deviance explained = 46.2%
-REML = 753.56  Scale est. = 52.238    n = 21447
```

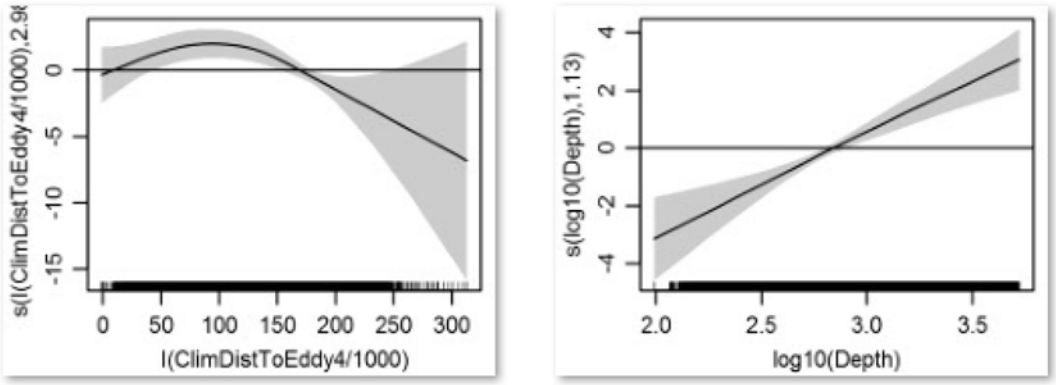

Figure 81. Dwarf and pygmy sperm whale model's statistical output and covariate functional plots.

Year-round total abundance predicted by the updated model was nearly 10 times higher than that predicted by the Roberts et al. (2016a) model used for Phase III (Table 41). As we noted in the supplementary report for the Phase III *Kogia* density model (version 3.2), we believed the Phase III model underestimated abundance. We attribute the abundance differences between the two models to several factors. First, as noted above, the Phase III model was based in part on NEFSC shipboard surveys that appeared to have misidentified many more Kogia than the more recent AMAPPS I surveys contributed to us after the Phase III models were completed. This resulted in lower densities on NEFSC's pre-AMAPPS transects than should have been the case.

Second, the Phase III model utilized all of the aerial surveys, while the updated model only used those from UNCW Navy OPAREAs. Like the updated model, the Phase III model excluded survey segments shoreward of the 125 m isobath. This eliminated most of the aerial transects, but there was still a significant number of them covering the upper continental slope that were retained in the Phase III model. In principle, this would not be a problem if density was distributed uniformly, as was assumed with the Phase III model. But according to the new model, density is lower on the upper slope than in areas farther off-shelf. By including so many upper-slope segments in the Phase III model, we biased its density estimate low; by then applying that low density estimate across the off-shelf areas, we biased the total abundance estimate low.

Finally, the updated model used $g(0)$ estimates (Table 40) that for SEFSC shipboard surveys was about half of that used for the Phase III model, and for NEFSC shipboard AMAPPS I surveys was about two-thirds of that for the NEFSC Abel-J surveys used in Phase III. All else being equal, density and abundance scale inversely with $g(0)$, so halving $g(0)$ typically causes density and abundance to double. We believe the multiplicative combination of this effect with the two other factors above explains much of the difference between the abundance estimate of Phase III and of the updated model.

The updated model's year-round and June-August abundance estimates were higher than the 2011 SAR but lower than Palka et al.'s (2017) density surface model (Table 41). Methodologically, our model was more similar to Palka et al.'s (2017) model than the 2011 SAR. The predicted density maps were similar in most areas, but Palka et al.'s (2017) model predicted substantially higher density in deeper waters off Cape Hatteras, extending south and east to the edge of the study area. These differences are an item for future investigation between the modeling teams.

Table 41. Comparison of abundance estimates (with CV in parentheses) for dwarf and pygmy sperm whales, obtained from recent NMFS Stock Assessment Reports (SARs) and density surface models. "Updated model" refers to the model presented here. For this, we recommend a single, year-round density surface for management purposes but show seasonal estimates (brown text) to facilitate more granular comparison to the SARs and Palka et al. (2017) estimates, which were made only for the June-August season. The Roberts et al. (2016) model, for which few sightings were available, did not retain any spatial covariates and thus yielded a uniform density estimate, with constant abundance for all seasons.

	Years	Dec-Feb	Mar-May	Jun-Aug	Sep-Nov	Year-round
NMFS SARs	2004			395 (0.40)		
	2011			3,785 (0.47)		
Roberts et al. (2016) [1]	1992-2013					678 (0.23)
Palka et al. (2017) [1]	2010-2013			9,951 (0.207)		
Updated model [1,2]	1992-2016	6,366	6,135	5,797	6,454	6,197 (0.170)

[1] CV is underestimated; it only accounts for uncertainty in spatial model parameters, not detection functions or $g(0)$.
[2] 3-month mean abundance shown for comparison, but we recommend the year-round average be used for management.

2.3.5.12. Phocid seals model

The harbor seal (*Phoca vitulina*) and the gray seal (*Halichoerus grypus*) occur year-round in the northern half of our East Coast study area and are the only abundant pinnipeds there. In winter, harp seals (*Pagophilus groenlandicus*) and hooded seals (*Cystophora cristata*) are reported to visit the Gulf of Maine regularly, while ringed seals (*Pusa hispida*) and bearded seals (*Erignathus barbatus*) visit rarely (Gilbert et al. 2005).

Harbor seals and gray seals were hunted in the United States from colonial times until the passage of the MMPA in 1972 (Gilbert et al. 2005). Hunting in Canada was curtailed around the same time and populations of both species have rebounded in the decades since (Gilbert et al. 2005; Moxley et al. 2017). This trend may be changing for harbor seals: NEFSC's population estimate for U.S. waters for 2012 (75,834, CV=0.153) was lower although not significantly different from the 2001 estimate (99,340, CV=0.091), possibly indicating a halt in growth or beginning of a decline (Waring et al. 2015). In contrast, the gray seal population has continued to expand, and since the 1980s gray seals have been recolonizing U.S. pupping sites where they were considered locally extinct (Wood et al. 2011; Johnston et al. 2015).

Typically, abundance estimates for seal populations are derived from visual surveys of seasonal haul-out sites, e.g. during pupping season. However, the Navy requested under our Cooperative Agreement that we model the density of seals in the water, not seals hauled out, and that we produce density surfaces comparable with what we had done for cetaceans. Although the two-stage density surface modeling methodology we used for cetaceans had been previously applied to model seals in the water (e.g., Herr et al. 2009), such studies were comparatively rare, and seals raised complications not present with cetaceans. Nevertheless, we endeavored to produce density surface models for seals using the same approach. The results should be viewed with considerable caution, for reasons we highlight throughout the rest of this section.

Harbor seals and gray seals are very difficult for aerial observers to differentiate when the seals are in the water. The majority of seal sightings contributed by collaborators were from aerial surveys by NEFSC (Table 10), and nearly all of these were reported as "unidentified seal". The in-water habitats of harbor seals and gray seals are not well described but quite likely overlap, and they haul out in similar locations throughout our study area. Given that, and

the few full identifications available, we did not attempt to classify the ambiguous "unidentified seal" sightings into one species or the other, but instead modeled all seals together as a guild.

Like harbor porpoises, seals at sea are difficult to detect in rough waters. In the Phase III analysis, we found total abundance nearly doubled when we fitted models to survey segments collected in Beaufort sea state 2 or less rather than to all segments, even when detection functions included Beaufort sea state as a covariate. These models assumed that perception bias directly on the trackline was constant in all conditions. It has since been shown that this assumption does not hold for cetaceans: the $g(0)$ parameter decreases as sea state increases, indicating increasing bias as seas get rougher, and the effect is most pronounced for the least conspicuous species (Barlow 2015). We lacked the data needed to develop sea-state-specific $g(0)$ corrections, so we restricted the updated seals model to survey segments collected in Beaufort 2 or less, as we did with the Phase III model (Roberts et al. 2016a). We also excluded surveys conducted at 1000 ft altitude, on advice of our collaborators, as well as offshore shipboard surveys that did not traverse the continental shelf to any substantial degree (none of the excluded surveys reported any seal sightings). Finally, as with other updated models, we reviewed the available literature and data to assess the feasibility of excluding surveys from 1992-1997 from the updated spatial model, as this period predated the launch of the SeaWiFS ocean color sensor needed for contemporaneous biological covariates.

Surveys from the 1992-1997 period reported only three seal sightings, while those from the 1998-2016 period reported over 1000 (Figure 82), so we dropped the 1992-1997 surveys from the updated model. After removing these, the other surveys noted above, and effort segments conducted in high sea states, 1147 sightings remained. We removed a further 13 sightings reported by the NARWSS right whale aerial surveys that we determined were hauled out seals. (We discovered these after the Phase III analysis; they likely biased the Phase III seal model's density and abundance high, as we discuss later in this section.) This left 1134 sightings for the updated model (Table 42), an increase of 43% over what was available to the Phase III model given the same constraints.

For the updated model, for aerial surveys we applied $g(0)$ estimates (Table 43) derived from perception bias corrections developed by Palka et al. (2017), replacing the estimate from Carretta et al. (2000) that we used for the Phase III analysis. Although Carretta's correction accounted for both perception and availability biases while Palka's only accounted for perception bias, we used Palka's because it was derived from the surveys used in our analysis, while Carretta's was derived from surveys off California, and because Palka's was lower, indicating that perception bias alone was higher for our surveys than the combined biases for Carretta's surveys.

For shipboard surveys, we used Reay's (2005) $g(0)$ estimate for gray seals (Table 43) sighted by naked eye from small research vessels with observer heights of approximately 3 m. In the surveys contributed by our collaborators, much larger vessels were used, however less than 10% of the sightings in our analysis were reported by shipboard surveys, so the bias introduced by an error in the shipboard $g(0)$ correction was likely similarly small.

Table 42. Seal sightings from 1998-2016, used in the Option Year 2 spatial model. "Extant" sightings were used in the Phase III regional model (Roberts et al. 2016a). "Added" sightings were incorporated during the Base Year and Option Year 1 for the updated model.

			Harbor seal			Gray seal			Unidentified seal		
Platform	Provider	Program	Extant	Added	Total	Extant	Added	Total	Extant	Added	Total
Aerial	NEFSC	Marine mammal abundance surveys	114	2	116		1	1	7	94	101
		NARWSS harbor porpoise survey							18		18
		NARWSS right whale surveys				2	2	4	587	235	822
	All		114	2	116	2	3	5	612	329	941
Shipboard	NEFSC	Marine mammal abundance surveys	48	2	50	15	3	18		1	1
	NJDEP	New Jersey Ecological Baseline Study	1		1				2		2
	All		49	2	51	15	3	18	2	1	3

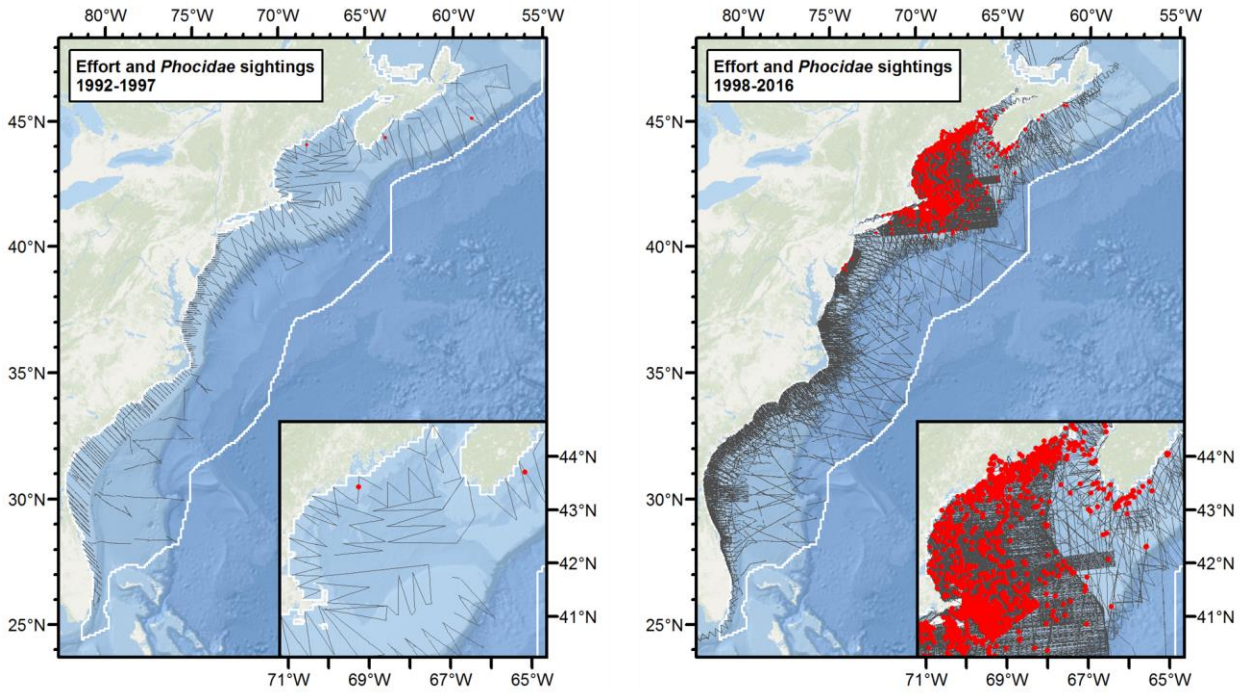

Figure 82. Survey effort and seal sightings from the 1992-1997 period (left), excluded from the updated model, and the 1998-2016 period (right), available for the updated model. Note that only we only utilized some of the data from the 1998-2016 period, excluding effort conducted when Beaufort sea state exceeded 2. Please see the text for details. **Table** 42 summarizes the sightings actually used, and Figure 83 shows the effort segments and sightings actually used.

Table 43. *g*(0) estimates used in the updated seals model.

Platform	Group size	Perception Bias	Availability Bias	*g*(0)	Source
Shipboard	Any	0.843	1	0.843	Reay (2005); gray seals from small boats
Aerial	1-12	0.181	1	0.181	Palka et al. (2017); max group size was 12
	>12	1	1	1	Assumed groups of 12 or more seals would always be available and perceived

Harbor seals and gray seals exhibit complex seasonal behaviors, including extended haul-outs to pup and molt, and extended trips to sea to forage. The timing and other dynamics of these behaviors vary by species, which complicated our effort to model them as a single guild. In general, both species move north in spring to northern shores of the Gulf of Maine and Nova Scotia, remain there through summer, and return in fall and early winter. In the past few decades, in the U.S., harbor seals have typically been seen in southern New England (south of Maine) from late September through May, and in Maine during summer months, where they pup (Payne & Selzer 1989; Gilbert et al. 2005). Moxley et al. (2017) reported much higher abundance of gray seals at Cape Cod haul out sites in the months of March and May than in June, and that 7 seals tagged at Chatham, MA and tracked by satellite were hauled out more frequently in the June-October period than the November-March period.

To account for the likelihood that seals change species-habitat relationships during parts of the year where they spend more time hauled out (e.g. to pup or molt) or at sea (e.g. to forage), we split our model into two seasons and modeled them independently. Based on the timings reported in the literature, we defined the "winter" season as November-May and the "summer" season as June-October. For both seasons, we assumed that species would not inhabit waters deeper than 1500m (Figure 83), nor shallower waters far in the southeast. For the winter season, we set this southernmost extent of the model at Cape Fear, based on reports that in winter and early spring, harbor seals regularly haul-out at rock-armored islands along the Chesapeake Bay Bridge Tunnel and periodically strand in North

Carolina (Byrd et al. 2014; Rees et al. 2016). In summer, we set the southernmost extent of the model at Cape Hatteras. In both seasons we fixed the northernmost limit of predictions to the areas that had been surveyed, excluding most of Canada in winter and the northern part of the Scotian Shelf in summer.

In both seasons, candidate models fitted to climatological environmental covariates yielded better REML scores and explained more deviance than models fitted to contemporaneous environmental covariates, so we selected the climatological-covariates models fitted to all survey segments as the best (Figures 84-87). The resulting models were moderately complex, with six covariates retained. Both models retained distance to shore and depth, indicating higher density close to shore and in shallower waters, as expected for shore-associated pinnipeds. Both models retained SST, indicating higher density in colder waters, consistent with the species' migration patterns. In winter, when seals may be ranging more widely to forage, the model indicated higher density in elevated levels of zooplankton biomass, a potential proxy for prey. By contrast, in summer, when seals may be more shore-associated and foraging trips more constrained, the model indicated a weak relationship of higher density at lower levels of primary productivity.

When predictions were summarized at a monthly time step, predictions for the middle of the "winter" season showed seals concentrated in southern New England (Figure 88). As the season ended, seal density retreated north, concentrating in southern Massachusetts, and moved up into the Gulf of Maine. At the beginning of the "summer" season, seal density was predicted highest close to shore around Maine and Nova Scotia. As this season ended (in October) density began increasing around Cape Cod again. These patterns resembled those described in the literature and collaborators expressed approval of the density predictions. Accordingly, we cautiously recommend the monthly mean density surfaces be used for management of these species, while bearing in mind the many caveats to these models.

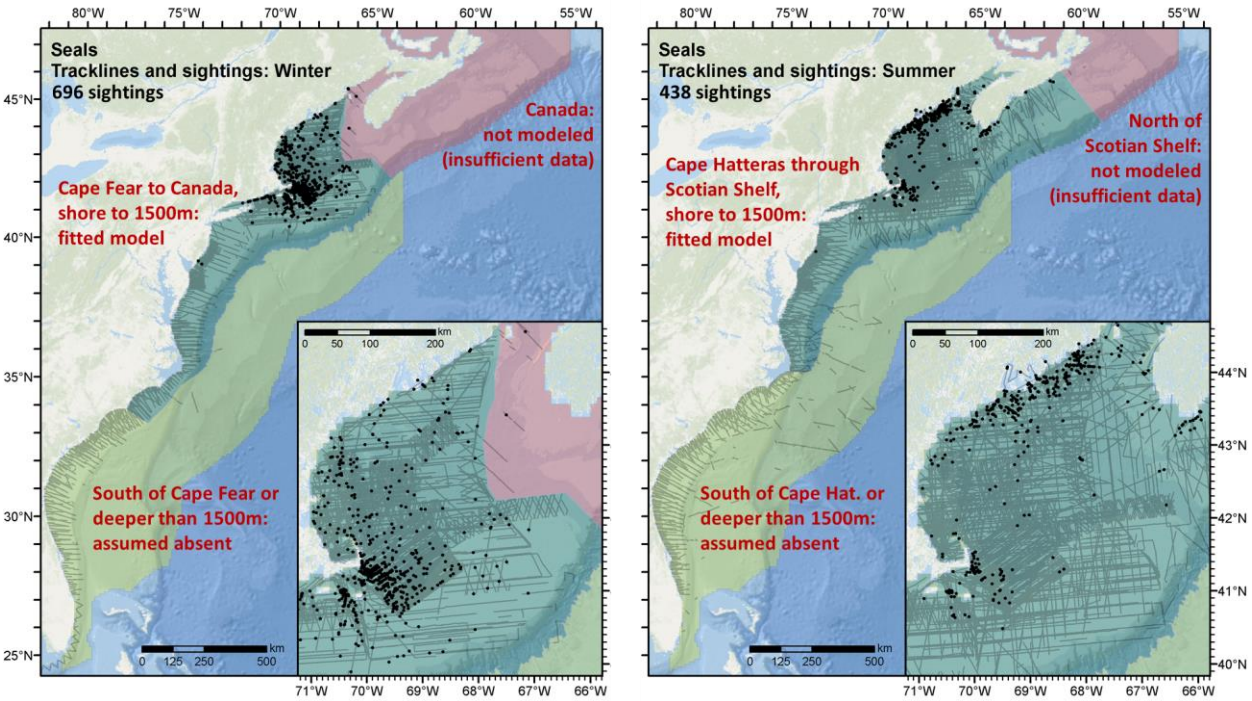

Figure 83. Seal models for winter (November-May, left) and summer (June-October, right). We fitted and predicted density surface models for the dark green areas. In the light green areas, we assumed seals were absent and set density to zero. We did not model the red areas.

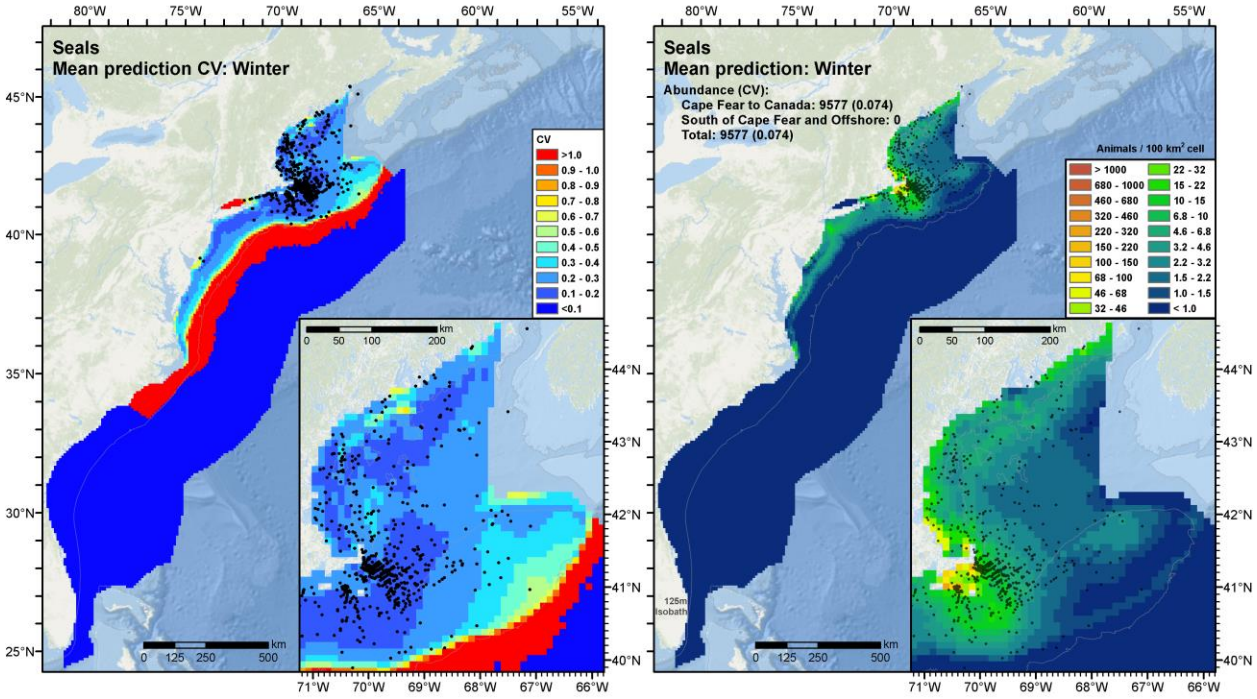

Figure 84. Predicted winter (November-May) seasonal mean density and total abundance (right) and coefficient of variation (left) for seals, with sightings overlaid. Note: We recommend that monthly mean predictions be used for management purposes (see text).

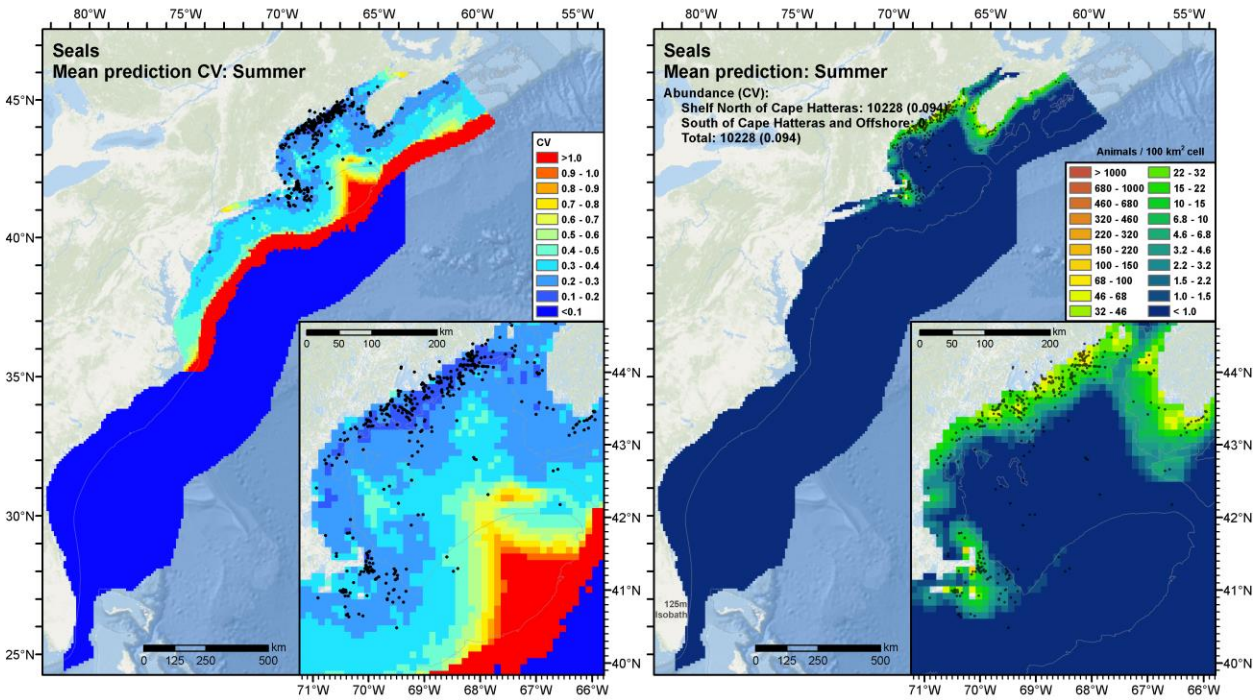

Figure 85. Predicted summer (June-October) seasonal mean density and total abundance (right) and coefficient of variation (left) for seals, with sightings overlaid. Note: We recommend that monthly mean predictions be used for management purposes (see text).

```
Family: Tweedie(p=1.292)
Link function: log

Formula:
Abundance ~ offset(log(Area)) + s(log10(Depth), bs = "ts") +
    s(sqrt(DistToShore/1000), bs = "ts") + s(ClimSST, bs = "ts") + s(pmax(ClimSalinity, 31), bs = "ts") +
    s(I(ClimDistToSSTFront1^(1/3)), bs = "ts") + s(log10(pmax(ClimPkPB1, 0.01)), bs = "ts")

Parametric coefficients:
            Estimate Std. Error t value Pr(>|t|)
(Intercept)  -4.4275     0.5971  -7.415 1.32e-13 ***
---
Signif. codes:  0 '***' 0.001 '**' 0.01 '*' 0.05 '.' 0.1 ' ' 1

Approximate significance of smooth terms:
                                  edf Ref.df      F  p-value
s(log10(Depth))                 5.799      9  5.682 9.33e-11 ***
s(sqrt(DistToShore/1000))       2.427      9  5.864 9.22e-14 ***
s(ClimSST)                      5.522      9  8.404 2.64e-16 ***
s(pmax(ClimSalinity, 31))       5.388      9  5.043 2.84e-09 ***
s(I(ClimDistToSSTFront1^(1/3))) 5.824      9  9.254  < 2e-16 ***
s(log10(pmax(ClimPkPB1, 0.01))) 5.964      9 17.119  < 2e-16 ***
---
Signif. codes:  0 '***' 0.001 '**' 0.01 '*' 0.05 '.' 0.1 ' ' 1

R-sq.(adj) =  0.0882   Deviance explained =   36%
-REML = 3289.6  Scale est. = 22.527    n = 9298
```

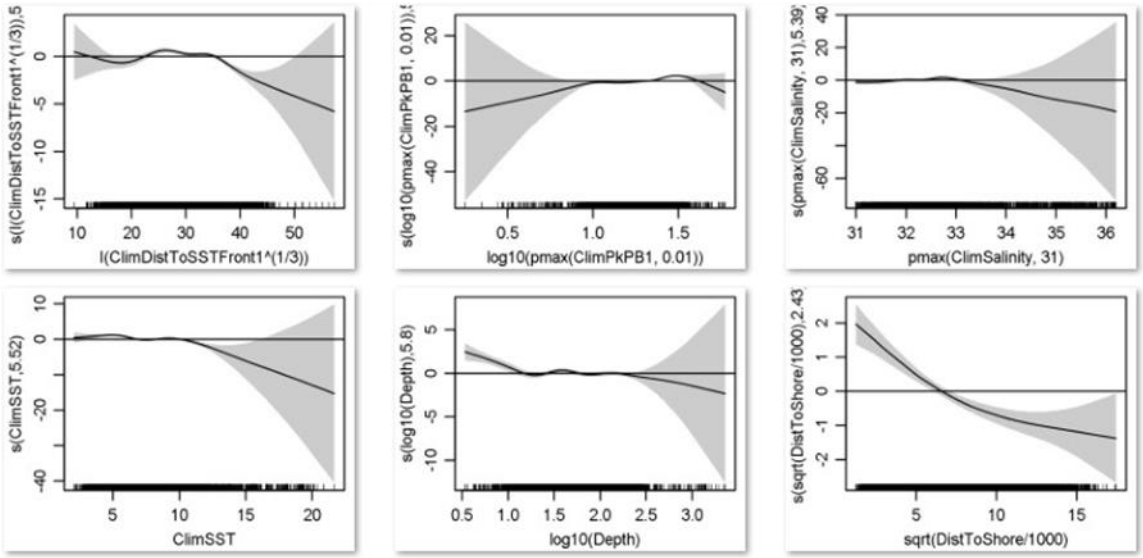

Figure 86. Winter (November-May) seal model's statistical output and covariate functional plots.

```
Family: Tweedie(p=1.291)
Link function: log

Formula:
Abundance ~ offset(log(Area)) + s(log10(Depth), bs = "ts") + s(sqrt(DistToShore/1000), bs = "ts") +
    s(log10(Slope), bs = "ts") + s(ClimSST, bs = "ts") + s(I(ClimDistToSSTFront2^(1/3)), bs = "ts") +
    s(I(ClimCumVGPM45^(1/3)), bs = "ts")

Parametric coefficients:
            Estimate Std. Error t value Pr(>|t|)
(Intercept)  -5.9891     0.2706  -22.13   <2e-16 ***
---
Signif. codes:  0 '***' 0.001 '**' 0.01 '*' 0.05 '.' 0.1 ' ' 1

Approximate significance of smooth terms:
                                   edf Ref.df      F  p-value
s(log10(Depth))                 5.4105      9  6.192 2.07e-12 ***
s(sqrt(DistToShore/1000))       4.4862      9 18.330  < 2e-16 ***
s(log10(Slope))                 0.8722      9  0.665  0.00716 **
s(ClimSST)                      5.2979      9  9.565  < 2e-16 ***
s(I(ClimDistToSSTFront2^(1/3))) 1.3564      9 13.139  < 2e-16 ***
s(I(ClimCumVGPM45^(1/3)))       0.8753      9  0.676  0.00732 **
---
Signif. codes:  0 '***' 0.001 '**' 0.01 '*' 0.05 '.' 0.1 ' ' 1

R-sq.(adj) =  0.0639   Deviance explained = 47.2%
-REML = 2042.9  Scale est. = 22.764    n = 11898
```

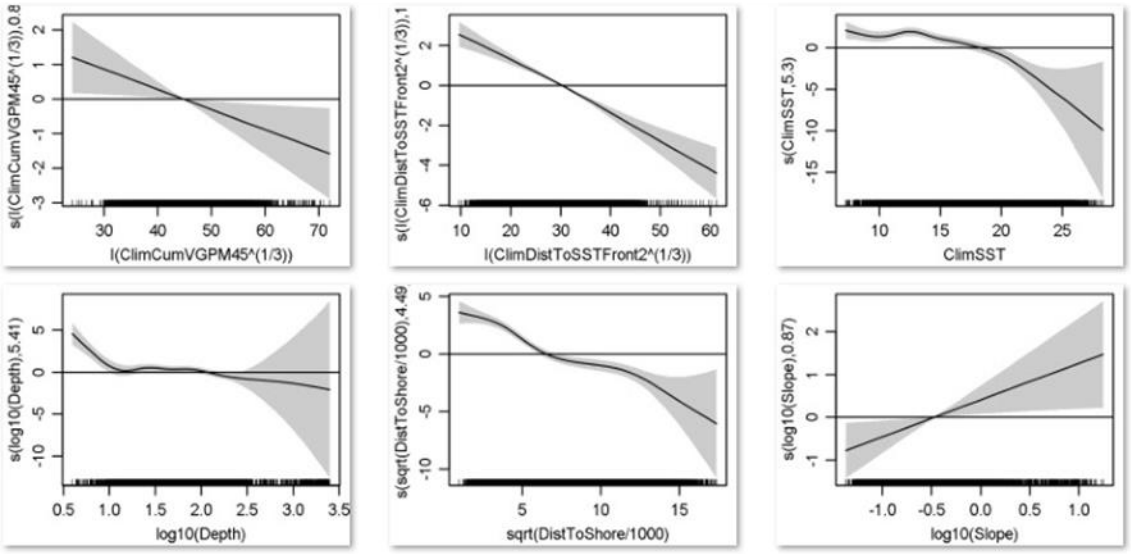

Figure 87. Summer (June-October) seal model's statistical output and covariate functional plots.

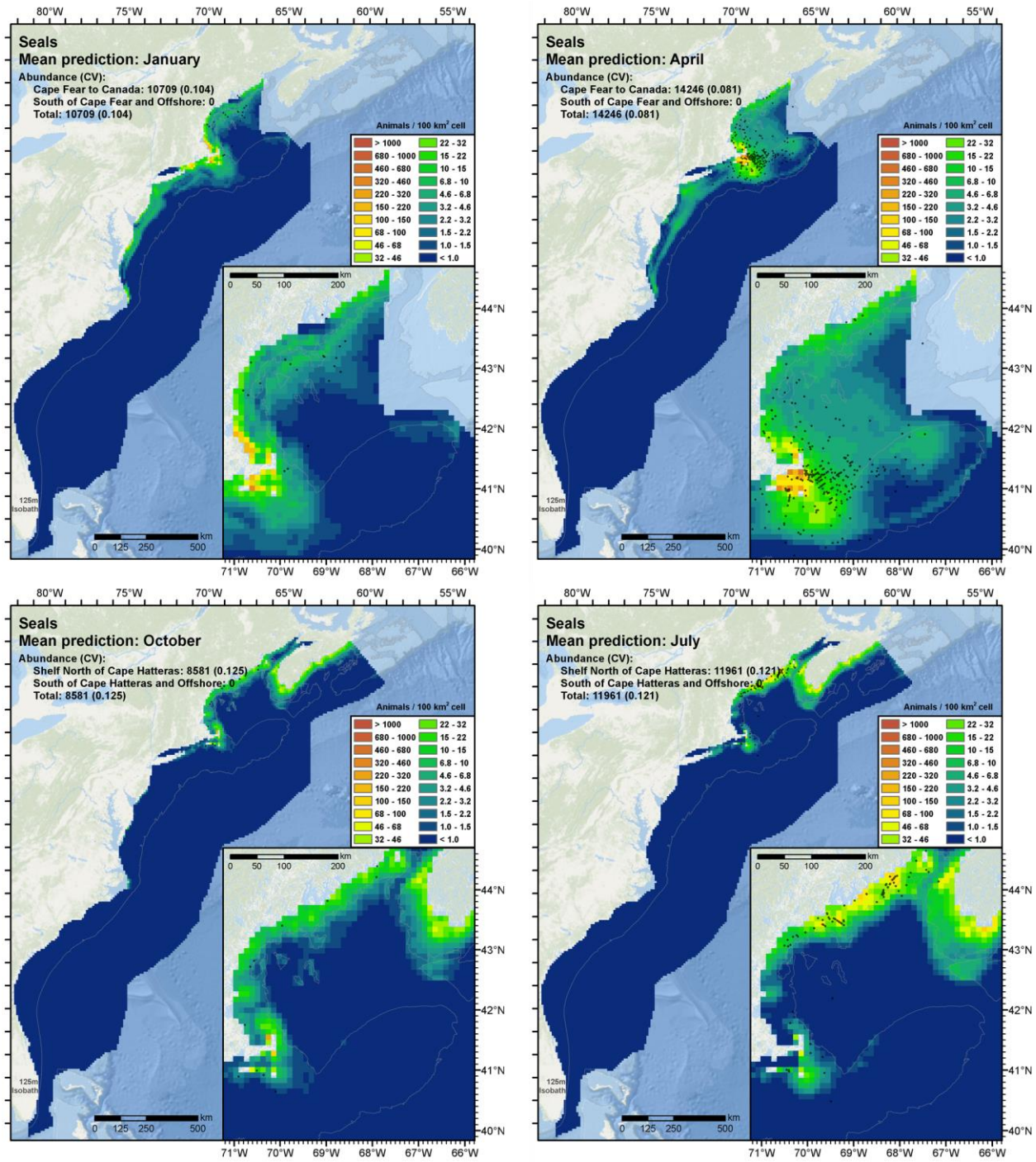

Figure 88. Four monthly predictions for the middle month of each calendrical season, with sightings overlaid. Clockwise from upper-left: winter (January), spring (April), summer (July), fall (October). Note that because survey effort was not uniform across months, a lack of sightings in an area should not be taken as evidence that the species was absent (there might have been no surveying done there during that month).

NOAA does not publish estimates of abundance for seals at sea, so there is no easy source of baseline abundance information against which we can assess the models. It might be possible to first obtain estimates of total population size (derived from surveys of hauled out seals), then apply corrections to estimate the counts of seals in the water during certain months or seasons. But this is a complex exercise that was beyond the scope of work we planned for Option Year 2.

The only at-sea abundance models that we are aware of are our own Phase III analysis and the AMAPPS model by Palka et al. (2017) (Table 44). For the Phase III model, we recommended that seasonal predictions be used, and defined the "winter" season as September-May and "summer" as June-August. Total abundance predicted by our updated model was lower in both modeled seasons, as well as the December-February and March-May calendrical seasons, but somewhat higher in the September-November calendrical season. The biggest difference was in June-August, when abundance of the new model was predicted to be 9x lower than for the old model. We believe there are three main reasons for the updated models' lower predictions.

First, while preparing data for the updated model we discovered 13 sightings reported by the NARWSS aerial survey that were of hauled out seals. These sightings comprised 8616 seals in total, with a mean group size of 664. Observer notes contained comments such as "hauled out on sand bar" but the sightings had been left as on effort. These group sizes are *much* larger than those of seals in open water; for example, the largest group size utilized in Palka et al.'s (2017) model of seals at sea was 12. Although few, these extreme sightings were reported essentially a distance of 0 from shore and at very shallow depths, biased our Phase III model and caused it to predict very large densities close to shore.

The second problem with the Phase III model that we discovered concerns the extreme summer prediction. Follow-on experiments we conducted during Option Year 2 revealed that this model was very sensitive to whether or not the 1992-1997 surveys were included. When we refitted the model without those surveys, abundance for the June-August period dropped from 98,757 (CV=0.55) to 31,201 (CV=0.33)—and this was before excluding the hauled out sightings from NARWSS.

The final factor we believe was responsible for the large decrease in abundance was that in Phase III, we predicted the model all the way up the Scotian Shelf and included Sable Island, the most abundant gray seal haul out site in the world. This provided additional shoreline around which high density was predicted and accumulated into the total abundance estimate. Together, we believe these three factors explain much of the difference between the Phase III model and the updated model. Although we do not have much external quantitative data against which to validate our updated model, we believe it provides a better estimate, insofar as it improves on the problems noted above.

The updated model predicted much lower abundance than Palka et al. (2017) in spring (March-May), much higher in summer (June-August), and about the same in fall (September-November). One reason for the large difference in spring is that Palka's model extends into Canada, halfway up the Scotian Shelf, and predicts high densities there, while our model stops at the U.S.-Canada border in the Gulf of Maine. If Palka's model is summed over our study area, total abundance will be substantially lower, although probably still higher than our prediction. These differences are an item for future investigation between the modeling teams.

Table 44. Comparison of seal abundance estimates (with CV in parentheses) for various density surface models. "Updated model" refers to the model presented here.

	Years	Dec-Feb	Mar-May	Jun-Aug	Sep-Nov	Sep-May
Roberts et al. (2016) [1,2]	1995-2014	16,330	24,197	98,747 (0.55)	4,574	15,002 (0.17)
Palka et al. (2017) [1]	2010-2013		43,781 (0.265)	5,721 (0.204)	6,279 (0.273)	
Updated model [1,2]	1998-2016	9,731	12,190	11,640	6,179	9,367

[1] CV is underestimated; it only accounts for uncertainty in spatial model parameters, not detection functions or $g(0)$.
[2] CV not estimated for 3-month averages (only 1-month), but could be if necessary.

3. [Omitted]

[This section contains information unrelated to the updated density models.]

4. Acknowledgements

Above all, we thank the observers, scientists, engineers, pilots, captains, and crews who collected and shared line transect surveys and environmental covariates with us; thank you for the opportunity to analyze the data you produced. We also thank the funding agencies and program managers for making these surveys possible. Beth Josephson, Debi Palka, Lance Garrison, Keith Mullin and their teams preprocessed the AMAPPS data and prepared it for our use. Lance Garrison also contributed the pre-AMAPPS GU-06-03 survey. Tim Cole and Christian Khan contributed the additional NARWSS surveys. Bill McLellan and his team contributed the additional UNC Wilmington surveys. Sarah Mallette, Gwen Lockhart, and Susan Barco contributed the VAMSC surveys of the Maryland and Virginia Wind Energy Areas, in collaboration with Rob DiGiovanni, Jr. Please see Roberts et al. (2016a) for additional specific acknowledgements.

5. References

Albertson GR, Baird RW, Oremus M, Poole MM, Martien KK, Baker CS. 2017. Staying close to home? Genetic differentiation of rough-toothed dolphins near oceanic islands in the central Pacific Ocean. Conservation Genetics **18**:33–51.

Amaral AR, Lovewell G, Coelho MM, Amato G, Rosenbaum HC. 2014. Hybrid Speciation in a Marine Mammal: The Clymene Dolphin (Stenella clymene). PLoS ONE **9**:e83645.

Archer FI. 2009. Striped dolphin. Pages 1127–1129 Encyclopedia of marine mammals 2nd Edition. Academic Press.

Atlas R, Hoffman RN, Ardizzone J, Leidner SM, Jusem JC, Smith DK, Gombos D. 2011. A Cross-calibrated, Multiplatform Ocean Surface Wind Velocity Product for Meteorological and Oceanographic Applications. Bulletin of the American Meteorological Society **92**:157–174.

Baird RW, Walters EL, Stacey PJ. 1993. Status of the bottlenose dolphin, Tursiops truncatus, with special reference to Canada. Canadian Field-Naturalist **107**:466–480.

Baird RW, Webster DL, Mahaffy SD, McSweeney DJ, Schorr GS, Ligon AD. 2008. Site fidelity and association patterns in a deep-water dolphin: Rough-toothed dolphins (*Steno bredanensis*) in the Hawaiian Archipelago. Marine Mammal Science **24**:535–553.

Baird RW, Webster DL, Swaim ZT, Foley HJ, Anderson DB, Read AJ. 2017. Spatial Use by Odontocetes Satellite Tagged off Cape Hatteras, North Carolina in 2016. Final Report. Prepared for U.S. Fleet Forces Command. Submitted to Naval Facilities Engineering Command Atlantic, Norfolk, Virginia, under Contract No. N62470-15-D-8006, Task Order 28. Page 54. HDR, Inc., Virginia Beach, Virginia.

Barlow J. 2015. Inferring trackline detection probabilities, g(0), for cetaceans from apparent densities in different survey conditions. Marine Mammal Science **31**:923–943.

Barlow J, Forney KA. 2007. Abundance and population density of cetaceans in the California Current ecosystem. Fishery Bulletin **105**:509–526.

Barlow J, Sexton S. 1996. The effect of diving and searching behavior on the probability of detecting track-line groups, go, of long-diving whales during linetransect surveys. Page 21. Administrative Report LJ-96-14. NOAA National Marine Fisheries Service, Southwest Fisheries Center.

Baron SC, Martinez A, Garrison LP, Keith EO. 2008. Differences in acoustic signals from Delphinids in the western North Atlantic and northern Gulf of Mexico. Marine Mammal Science **24**:42–56.

Becker JJ et al. 2009. Global Bathymetry and Elevation Data at 30 Arc Seconds Resolution: SRTM30_PLUS. Marine Geodesy **32**:355–371.

Behrenfeld MJ, Falkowski PG. 1997. Photosynthetic rates derived from satellite-based chlorophyll concentration. Limnology and oceanography **42**:1–20.

Bleck R. 2002. An oceanic general circulation model framed in hybrid isopycnic-Cartesian coordinates. Ocean Modelling **4**:55–88.

Bloodworth BE, Odell DK. 2008. Kogia breviceps (Cetacea: Kogiidae). Mammalian Species **819**:1–12.

Borchers DL, Zucchini W, Fewster RM. 1998. Mark-Recapture Models for Line Transect Surveys. Biometrics **54**:1207.

Brasnett B. 2008. The impact of satellite retrievals in a global sea-surface-temperature analysis. Quarterly Journal of the Royal Meteorological Society **134**:1745–1760.

Burnham KP, Anderson DR. 2002. Model Selection and Multimodel Inference: A Practical Information-Theoretic Approach. Springer Science & Business Media.

Burt ML, Borchers DL, Jenkins KJ, Marques TA. 2014. Using mark-recapture distance sampling methods on line transect surveys. Methods in Ecology and Evolution **5**:1180–1191.

Byrd BL et al. 2014. Strandings as indicators of marine mammal biodiversity and human interactions off the coast of North Carolina. Fishery Bulletin **112**:1–23.

Canny JF. 1986. A computational approach to edge detection. IEEE Transactions on Pattern Analysis and Machine Intelligence **8**:679–698.

Carretta JV, Lowry MS, Stinchcomb CE, Lynn MS, Cosgrove R. E. 2000. Distribution and abundance of marine mammals at San Clemente Island and surrounding offshore waters: results from aerial and ground surveys in 1998 and1999. NOAA ADMINISTRATIVE REPORT LJ-00-02.

Chelton DB, Schlax MG, Samelson RM. 2011. Global observations of nonlinear mesoscale eddies. Progress in Oceanography **91**:167–216.

d'Ovidio F, Fernández V, Hernández-García E, López C. 2004. Mixing structures in the Mediterranean Sea from finite-size Lyapunov exponents. Geophysical Research Letters **31**:n/a-n/a.

Duignan PJ, House C, Odell DK, Wells RS, Hansen LJ, Walsh MT, Aubin DJS, Rima BK, Geraci JR. 2006. Morbillivirus Infection in Bottlenose Dolphins: Evidence for Recurrent Epizootics in the Western Atlantic and Gulf of Mexico. Marine Mammal Science **12**:499–515.

Fertl D, Jefferson TA, Moreno IB, Zerbini AN, Mullin KD. 2003. Distribution of the Clymene dolphin Stenella clymene. Mammal Review **33**:253–271.

Garrison LP. 2007. Interactions between marine mammals and pelagic longline fishing gear in the U.S. Atlantic Ocean between 1992 and 2004. Fishery Bulletin **105**:408–417.

Gilbert JR, Waring GT, Wynne KM, Guldager N. 2005. Changes in Abundance of Harbor Seals in Maine, 1981–2001. Marine Mammal Science **21**:519–535.

Gowans S, Whitehead H. 1995. Distribution and habitat partitioning by small odontocetes in the Gully, a submarine canyon on the Scotian Shelf. Canadian Journal of Zoology **73**:1599–1608.

Harris PT, Macmillan-Lawler M, Rupp J, Baker EK. 2014. Geomorphology of the oceans. Marine Geology **352**:4–24.

Hayes SA, Josephson E, Maze-Foley K, Rosel PE. 2018. U.S. Atlantic and Gulf of Mexico Marine Mammal Stock Assessments - 2017. NMFS-NE-245, NOAA Technical Memorandum. National Marine Fisheries Service, Woods Hole, MA.

Hedley SL, Buckland ST. 2004. Spatial models for line transect sampling. Journal of Agricultural, Biological, and Environmental Statistics **9**:181–199.

Herr H, Scheidat M, Lehnert K, Siebert U. 2009. Seals at sea: modelling seal distribution in the German bight based on aerial survey data. Marine Biology **156**:811–820.

Jefferson TA, Curry BE. 2003. Stenella clymene. Mammalian Species:1–5.

Jefferson TA, Fertl D, Bolaños-Jiménez J, Zerbini AN. 2009. Distribution of common dolphins (Delphinus spp.) in the western Atlantic Ocean: a critical re-examination. Marine Biology **156**:1109–1124.

Jefferson TA, Schiro AJ. 1997. Distribution of cetaceans in the offshore Gulf of Mexico. Mammal Review **27**:27–50.

Jefferson TA, Weir CR, Anderson RC, Ballance LT, Kenney RD, Kiszka JJ. 2014. Global distribution of Risso's dolphin Grampus griseus: a review and critical evaluation. Mammal Review **44**:56–68.

Johnston DW, Frungillo J, Smith A, Moore K, Sharp B, Schuh J, Read AJ. 2015. Trends in Stranding and By-Catch Rates of Gray and Harbor Seals along the Northeastern Coast of the United States: Evidence of Divergence in the Abundance of Two Sympatric Phocid Species? PLOS ONE **10**:e0131660.

Keenan-Bateman TF et al. 2016. Prevalence and anatomic site of *Crassicauda* sp. infection, and its use in species identification, in kogiid whales from the mid-Atlantic United States. Marine Mammal Science **32**:868–883.

Kerem D, Goffman O, Elasar M, Hadar N, Scheinin A, Lewis T. 2016. The Rough-Toothed Dolphin, Steno bredanensis, in the Eastern Mediterranean Sea. Pages 233–258 Advances in Marine Biology, Vol. 75. Elsevier. Available from http://linkinghub.elsevier.com/retrieve/pii/S0065288116300098 (accessed June 20, 2018).

Laake JL, Borchers DL. 2004. Methods for incomplete detection at distance zero. Pages 108–189 Advanced Distance Sampling. Oxford University Press, Oxford.

Lawson JW, Gosselin J-F. 2009. Distribution and preliminary abundance estimates for cetaceans seen during Canada's Marine Megafauna Survey-A component of the 2007 TNASS. Canadian Science Advisory Secretariat= Secrétariat canadien de consultation scientifique. Available from http://biblio.uqar.qc.ca/archives/30125408.pdf (accessed March 25, 2014).

Lawson JW, Gosselin J-F. 2011. Fully-corrected cetacean abundance estimates from the Canadian TNASS survey. Page 28. Ottawa, Canada.

Lehodey P, Murtugudde R, Senina I. 2010. Bridging the gap from ocean models to population dynamics of large marine predators: a model of mid-trophic functional groups. Progress in Oceanography **84**:69–84.

Mannocci L et al. 2018. Assessing cetacean surveys throughout the Mediterranean Sea: a gap analysis in environmental space. Scientific Reports **8**. Available from http://www.nature.com/articles/s41598-018-19842-9 (accessed August 1, 2018).

Mannocci L, Roberts JJ, Miller DL, Halpin PN. 2017. Extrapolating cetacean densities to quantitatively assess human impacts on populations in the high seas. Conservation Biology **31**:601–614.

Maritorena S, d'Andon OHF, Mangin A, Siegel DA. 2010. Merged satellite ocean color data products using a bio-optical model: Characteristics, benefits and issues. Remote Sensing of Environment **114**:1791–1804.

Miller DL, Burt ML, Rexstad EA, Thomas L. 2013. Spatial models for distance sampling data: recent developments and future directions. Methods in Ecology and Evolution **4**:1001–1010.

Moxley JH et al. 2017. Google Haul Out: Earth Observation Imagery and Digital Aerial Surveys in Coastal Wildlife Management and Abundance Estimation. BioScience **67**:760–768.

Mullin KD, Fulling GL. 2003. Abundance of cetaceans in the southern US North Atlantic Ocean during summer 1998. Fishery Bulletin **101**:603–613.

Oremus M, Poole MM, Albertson GR, Baker CS. 2012. Pelagic or insular? Genetic differentiation of rough-toothed dolphins in the Society Islands, French Polynesia. Journal of Experimental Marine Biology and Ecology **432**–**433**:37–46.

Palka D, Read A, Potter C. 1997. Summary of knowledge of white-sided dolphins (Lagenorhynchus acutus) from US and Canadian Atlantic Waters. Rep. Int. Whal. Commn **47**:729–734.

Palka DL. 2006. Summer abundance estimates of cetaceans in US North Atlantic navy operating areas. 06–03, Northeast Fish Sci Cent Ref Doc. U.S. Department of Commerce, Woods Hole, MA. Available from http://www.nefsc.noaa.gov/publications/crd/crd0603/crd0603.pdf (accessed March 5, 2014).

Palka DL et al. 2017. Atlantic Marine Assessment Program for Protected Species: 2010-2014 (OCS Study BOEM 2017-071). US Dept. of the Interior, Bureau of Ocean Energy Management, Washington, DC. Available from https://www.boem.gov/espis/5/5638.pdf.

Payne PM, Selzer LA. 1989. The Distribution, Abundance and Selected Prey of the Harbor Seal, Phoca Vitulina Concolor, in Southern New England. Marine Mammal Science **5**:173–192.

Perrin WF. 2001. Stenella attenuata. Mammalian Species **683**:1–8.

Powell JWB, Rotstein DS, McFee WE. 2012. First Records of the Melon-Headed Whale (Peponocephala electra) and the Atlantic White-Sided Dolphin (Lagenorhynchus acutus) in South Carolina. Southeastern Naturalist **11**:23–34.

Read AJ et al. 2014. Occurrence, distribution and abundance of cetaceans in Onslow Bay, North Carolina, USA. Journal of Cetacean Research and Management **14**:23–35.

Reay N. 2005. Estimation of g(0) for bottlenose dolphin, grey seal, and harbour porpoise in Cardigan Bay SAC. Master's Thesis. University of Wales, Bangor.

Rees DR, Jones DV, Bartlett BA. 2016. Haul-out Counts and Photo-Identification of Pinnipeds in Chesapeake Bay, Virginia: 2015/16 Annual Progress Report. Prepared for U.S. Fleet Forces Command, Norfolk, VA.

Roberts JJ. 2015. Estimates of bottlenose dolphin density for estuaries in the AFTT area for the Phase III NMSDD, Document version 1.2. Duke University Marine Geospatial Ecology Lab, Durham, NC.

Roberts JJ et al. 2016a. Habitat-based cetacean density models for the U.S. Atlantic and Gulf of Mexico. Scientific Reports **6**:22615.

Roberts JJ, Mannocci L, Halpin PN. 2015. Marine mammal density models for the U.S. Navy Atlantic Fleet Training and Testing (AFTT) study area for the Phase III Navy Marine Species Density Database (NMSDD), Document Version 1.1. Duke University Marine Geospatial Ecology Lab, Durham, NC.

Roberts JJ, Mannocci L, Halpin PN. 2016b. Final Project Report: Marine Species Density Data Gap Assessments and Update for the AFTT Study Area, 2015-2016 (Base Year), Document Version 1.0. Page 21. Duke University Marine Geospatial Ecology Lab, Durham, NC.

Roberts JJ, Mannocci L, Halpin PN. 2017. Final Project Report: Marine Species Density Data Gap Assessments and Update for the AFTT Study Area, 2016-2017 (Opt. Year 1), Document Version 1.4. Page 87. Duke University Marine Geospatial Ecology Lab, Durham, NC.

Selzer LA, Payne PM. 1988. The Distribution of White-Sided (Lagenorhynchus acutus) and Common Dolphins (Delphinus delphis) vs. Environmental Features of the Continental Shelf of the Northeastern United States. Marine Mammal Science **4**:141–153.

Staudinger MD, McAlarney RJ, McLellan WA, Ann Pabst D. 2014. Foraging ecology and niche overlap in pygmy (*Kogia breviceps*) and dwarf (*Kogia sima*) sperm whales from waters of the U.S. mid-Atlantic coast. Marine Mammal Science **30**:626–655.

Taubenberger JK, Tsai M, Krafft AE, Lichy JH, Reid AH, Schulman Y, Lipscomb TP. 1996. Two Morbilliviruses Implicated in Bottlenose Dolphin Epizootics. Emerging Infectious Diseases **2**:213–216.

Thomas L, Buckland ST, Rexstad EA, Laake JL, Strindberg S, Hedley SL, Bishop JRB, Marques TA, Burnham KP. 2010. Distance software: design and analysis of distance sampling surveys for estimating population size. Journal of Applied Ecology **47**:5–14.

Torres LG, Rosel PE, D'Agrosa C, Read AJ. 2003. Improving management of overlapping bottlenose dolphin ecotypes through spatial analysis and genetics. Marine Mammal Science **19**:502–514.

U.S. Department of the Navy. 2017. U.S. Navy Marine Species Density Database Phase III for the Atlantic Fleet Training and Testing Area: Final Technical Report. Page 293. Naval Facilities Engineering Command Atlantic, Norfolk, VA.

Viricel A, Rosel PE. 2014. Hierarchical population structure and habitat differences in a highly mobile marine species: the Atlantic spotted dolphin. Molecular Ecology **23**:5018–5035.

Wagenmakers E-J, Farrell S. 2004. AIC model selection using Akaike weights. Psychonomic Bulletin & Review **11**:192–196.

Waring GT, DiGiovanni RA, Josephson E, Wood S, Gilbert JR. 2015. 2012 Population Estimate for the Harbor Seal (Phoca vitulina concolor) in New England Waters. Page 22. NMFS-NE-235, NOAA Technical Memorandum. NOAA/National Marine Fisheries Service, Northeast Fisheries Science Center.

Waring GT, Josephson E, Maze-Foley K, Rosel PE. 2014. U.S. Atlantic and Gulf of Mexico Marine Mammal Stock Assessments - 2013. NMFS-NE-228, NOAA Technical Memorandum. National Marine Fisheries Service, Woods Hole, MA.

Waring GT, Josephson E, Maze-Foley K, Rosel PE. 2016. U.S. Atlantic and Gulf of Mexico Marine Mammal Stock Assessments - 2015. NMFS-NE-238, NOAA Technical Memorandum. National Marine Fisheries Service, Woods Hole, MA.

Watwood SL, Miller PJ, Johnson M, Madsen PT, Tyack PL. 2006. Deep-diving foraging behaviour of sperm whales (Physeter macrocephalus). Journal of Animal Ecology **75**:814–825.

Wells RS, Manire CA, Byrd L, Smith DR, Gannon JG, Fauquier D, Mullin KD. 2009. Movements and dive patterns of a rehabilitated Risso's dolphin, Grampus griseus, in the Gulf of Mexico and Atlantic Ocean. Marine Mammal Science **25**:420–429.

West KL, Mead JG, White W. 2011. Steno bredanensis (Cetacea: Delphinidae). Mammalian Species **43**:177–189.

Willis PM, Baird RW. 1998. Status of the dwarf sperm whale, Kogia simus, with special reference to Canada. Canadian Field-Naturalist **112**:114–125.

Winn HE. 1982. CeTAP: A Characterization of Marine Mammals and Turtles in the Mid- and North Atlantic Areas of the U.S. Outer Continental Shelf: Final Report. University of Rhode Island Graduate School of Oceanography, Kingston, RI.

Wood SA, Frasier TR, McLeod BA, Gilbert JR, White BN, Bowen WD, Hammill MO, Waring GT, Brault S. 2011. The genetics of recolonization: an analysis of the stock structure of grey seals (*Halichoerus grypus*) in the northwest Atlantic. Canadian Journal of Zoology **89**:490–497.

Würsig B, Lynn SK, Jefferson TA, Mullin KD. 1998. Behaviour of cetaceans in the northern Gulf of Mexico relative to survey ships and aircraft. Aquatic Mammals **24**:41–50.